AD/A-003 123

STEEL FIBROUS CONCRETE FOR AIRPORT PAVEMENT APPLICATIONS

Frazier Parker, Jr.

Army Engineer Waterways Experiment Station

Prepared for:

Federal Aviation Administration

November 1974

NOTICES

This document is disseminated under the sponsorship of the Department of Transportation in the interest of information exchange. The United States Government assumes no liability for its contents or use thereof.

The United States Government does not endorse products or manufacturers. Trade or manufacturers' names appear herein solely because they are considered essential to the object of this report.

ia

Technical Report Documentation Page

1. Report No.	2. Government Accession No.	3. Recipient's Catalog No.
FAA-RD-74-31		AD/A-003 123

4. Title and Subtitle	5. Report Date
STEEL FIBROUS CONCRETE FOR AIRPORT PAVEMENT APPLICATIONS	November 1974
	6. Performing Organization Code
7. Author(s)	8. Performing Organization Report No.
Frazier Parker, Jr.	
9. Performing Organization Name and Address	10. Work Unit No. (TRAIS)
U. S. Army Engineer Waterways Experiment Station Soils and Pavements Laboratory Vicksburg, Miss. 39180	11. Contract or Grant No. FA71WAI-218
	13. Type of Report and Period Covered
12. Sponsoring Agency Name and Address	Final report
Office, Chief of Engineers, U. S. Army, and Federal Aviation Administration Systems Research and Development Service Washington, D. C. 20590	14. Sponsoring Agency Code FAA/ARD-430

15. Supplementary Notes

16. Abstract

This report describes a study conducted to develop criteria for the design and construction of steel fibrous concrete airport pavements. Controlled, accelerated traffic tests and field tests conducted as a part of this study and similar tests conducted by other agencies are described and the results from these tests compiled. The results from all tests were analyzed and used in the formulation of criteria for designing steel fibrous concrete pavements and overlays. Recommended practices and procedures for batching, mixing, and placing fibrous concrete were formulated. Conclusions based on this study indicate that fibrous concrete pavements will perform better than plain concrete pavements, will result in thinner pavements, and can be produced and placed with conventional paving equipment and techniques.

17. Key Words	18. Distribution Statement
Design criteria, Steel fibrous concrete, Fibrous concrete, Airfields, Pavements, Overlays	Document is available to the public through the National Technical Information Service, Springfield, Va. 22151

19. Security Classif. (of this report)	20. Security Classif. (of this page)	21. No. of Pages	22. Price
Unclassified	Unclassified	204	$7.25

Form DOT F 1700.7 (8-72) Reproduction of completed page authorized

PREFACE

The study reported herein was jointly sponsored by the Federal Aviation Administration as part of Inter-Agency Agreement FA71WAI-218, "Development of Airport Pavement Criteria," and by the Office, Chief of Engineers, U. S. Army, as part of the Military Engineering Design for Expedient Airfields and Heliports Study and the Short-Range Airfield Pavement Research Program. Portions of the information used in this study were obtained from tests conducted by the U. S. Army Construction Engineering Research Laboratory with support provided by the U. S. Army Engineer Waterways Experiment Station (WES) for the Office, Chief of Engineers, U. S. Army. The study was conducted during the period July 1971-December 1973, under the general supervision of Mr. James P. Sale, Chief of the Soils and Pavements Laboratory, WES. This report was prepared by Dr. Frazier Parker, Jr.

Directors of WES during the conduct of this study were BG E. D. Peixotto, CE, and COL G. H. Hilt, CE. Technical Director was Mr. F. R. Brown.

TABLE OF CONTENTS

Preceding page blank

CONVERSION FACTORS, U. S. CUSTOMARY TO METRIC (SI) UNITS OF MEASUREMENT

U. S. customary units of measurement used in this report can be converted to metric (SI) units as follows:

Multiply	By	To Obtain
mils	0.0254	millimeters
inches	2.54	centimeters
feet	0.3048	meters
square inches	6.4516	square centimeters
cubic yards	0.7645549	cubic meters
pounds	0.45359237	kilograms
kips	0.45359237	metric tons
pounds per cubic inch	0.0276799	kilograms per cubic centimeter
pounds per cubic foot	16.01849	kilograms per cubic meter
pounds per square inch	6894.757	pascals
Fahrenheit degrees	5/9	Celsius degrees or Kelvins*

* To obtain Celsius (C) temperature readings from Fahrenheit (F) readings, use the following formula: $C = (5/9)(F - 32)$. To obtain Kelvin (K) readings, use: $K = (5/9)(F - 32) + 273.15$.

INTRODUCTION AND SUMMARY

INTRODUCTION

In the past several years, considerable interest has been generated in the use of concrete containing discrete, randomly dispersed steel fibers for pavement applications. The introduction of fibers into the concrete matrix imparts to the concrete certain characteristics, such as resistance to spalling and the ability to sustain load and keep cracks tightly closed after cracking, which improve the performance of fibrous concrete pavement when compared with plain or conventionally reinforced concrete pavement. Thus, a reduction in required thickness can be realized by using fibrous concrete in place of plain or conventionally reinforced concrete. In areas where there is a shortage of quality aggregate or where a reduction in required pavement thickness is essential because of such factors as grade or drainage considerations, it may be advantageous to use fibrous concrete pavement in lieu of conventional types of pavement. Fibers can be used with available aggregate to improve the quality of the concrete or it may become feasible to import higher quality aggregate since the addition of fibers will permit thinner sections and therefore require less aggregate. Cost will be the controlling factor in the use of fibrous concrete, but unfortunately the state-of-the-art has not progressed to the point at which reliable guidance can be given concerning the economic aspects of the use of fibrous concrete. This report contains the results of an investigation conducted by the U. S. Army Engineer Waterways Experiment Station (WES) for the purpose of developing criteria for the design of fibrous concrete airport pavements and guidance for constructing these pavements.

SUMMARY

This report contains a discussion of the behavioral properties of fibrous concrete and the possible effects of these properties on the performance of pavements constructed with the material. Comparisons of various characteristics of fibrous concrete and material characteristics desirable for airport pavement applications indicate that use of

Preceding page blank

fibrous concrete would be desirable. Pavements constructed and tested by WES and by other agencies are described, and the results from these tests are presented and analyzed. From these test results, recommended criteria for selecting slab thickness and joint requirements are formulated and guidance for constructing fibrous concrete pavements is developed. The recommended criteria are compatible with current Federal Aviation Administration (FAA) and Corps of Engineers design systems. Specific recommendations are provided, as required, to reflect observed differences between the performance of fibrous and plain or conventionally reinforced concrete pavement. The recommended criteria will result in thinner pavements with larger permissible joint spacings. Construction of fibrous concrete pavement can be accomplished using conventional batching, mixing, and paving equipment. Developing procedures and equipment for bulk handling of fibers is the primary area in which additional work is needed.

BACKGROUND

DEFINITION OF FIBROUS CONCRETE

Fibrous concrete is a composite material consisting of a concrete matrix containing a random dispersion of small fibers. Numerous types of fiber material have been used including steel, fiberglass, nylon, asbestos, rayon, cotton, polypropylene, and polyethylene. Attention, particularly in the United States, is currently focused on use of steel and fiberglass fibers. For pavement applications, only steel fibers have been seriously considered. Only the use of steel fibers has been considered in this study; therefore, the recommended criteria should only be considered applicable to concrete containing steel fibers.

MECHANICS OF FIBER STRENGTHENING

The inclusion of fibers in the concrete matrix alters the properties of the resulting composite material. The ductile, high-tensile-strength fibers compensate for the low tensile strength and low ductility of the concrete and enhance the mechanical and physical properties of the composite. Properties such as fatigue endurance, impact resistance, and toughness are improved.

The response of the composite can be explained by considering the manner in which brittle materials such as concrete fail. Hsu et al.[1] attribute the low tensile strengh of concrete to the propagation of cracks originating from internal flaws within the matrix. The internal flaws consist of air voids, deleterious material particles, or microcracks formed during curing. The ductile, high-tensile-strength fibers compensate for the low tensile strength and brittle character of the concrete by acting as arrestors which restrict the growth of the flaws. Mechanisms for explaining fiber strengthening were proposed and experimentally verified by Romualdi and Batson.[2,3]

The fiber strengthening mechanism may be explained by considering Figure 1. This figure is a schematic load-deflection curve for a fibrous concrete beam. Up to point A, the response of the beam is linear, but beyond this point it becomes nonlinear and reaches a maximum at

point B. The stress at point A is defined as the first crack strength and that at point B as the ultimate strength. The fiber strengthening mechanism considered in the following paragraphs explains the behavior up to the first crack strength. After the development of the first crack, a different mechanism is used to explain the continued ability of the material to sustain load.

The fiber strengthening mechanism may be developed by considering Figure 2, which shows a side view of an internal crack between two fibers. The material in the vicinity of the crack is subjected to a tensile stress σ . As the crack begins to grow, the strains at the tip of the crack become larger than the average strains because of the stress concentration at the tips. The fibers being stiffer than the concrete resist the displacement at the crack tip. Bond stresses between the concrete and fibers are developed that act to reduce the stress concentration at the crack tip, thereby permitting a higher level of gross stress to exist before the crack propagates. The ability of the fibers to resist crack propagation is dependent primarily on the bond between the fibers and concrete and the fiber spacing. The bond between the concrete and fibers is the mechanism whereby the stress is transferred from the concrete to the fibers. A schematic distribution of the bond stresses along the fibers is also shown in Figure 2. The ability of the fibers to develop sufficient bond is dependent on the fiber geometry (length and cross section). Assuming that the geometry of the fibers is sufficient to develop the necessary bond, it has been shown by Romualdi and Batson[3] that the theoretical first crack strength is inversely proportional to the fiber spacing, as shown in Figure 3. Romualdi and Mandel[4] have shown that the expected ratio of first crack strength of mortar with short fibers to first crack strength of plain mortar is a function of fiber spacing, as shown in Figure 4. Also shown in Figure 4 are experimental data verifying this relationship.

For realistic conditions of fiber size and percentage of fibers, sufficient bond may not be developed to significantly increase first crack strength. For certain sizes of fibers, it may not be possible to mix adequately enough fibers to increase first crack strength. The

problem of mixing will be considered later. The combined effects of spacing and fiber geometry are illustrated in Figure 5, which shows the results of tests conducted by Snyder and Lankard.[5] General trends indicated in this figure are as follows:

a. Fibers increase the strength of the material.

b. Increasing fiber content or conversely decreasing fiber spacing results in higher strength. (Two points for 0.5- and 1.0-in.* fibers for smaller spacings are discounted because of poor workability.)

c. Strength increases as the fiber length increases. (This trend illustrates the importance of bond development since bond development varies directly with fiber length.)

Thus far, only the first crack strength has been considered. However, at this point, the ultimate load-carrying capacity of fibrous concrete will be considered since it is the postcracking response which accounts for the improvements in mechanical properties and the resulting performance of fibrous concrete pavements.

Fibrous concrete still has considerable load-carrying capacity after initial cracking, as illustrated in Figure 1. For plain concrete, the first crack and ultimate strength are synonymous, but for fibrous concrete the cracks cannot extend without stretching or debonding the fibers. Consequently, additional energy is required before the ultimate stress and complete fracture occur.

Before the discussion of the mechanical properties of fibrous concrete and the response of fibrous concrete pavement slabs to load is presented, the relationships between strength (first crack and ultimate) and fiber geometry will be examined further by considering Equation 1 developed by Romualdi and Mandel[4] for average fiber spacing and experimental results presented by Waterhouse and Luke.[6] The equation developed by Romualdi and Mandel for the average fiber spacing is

$$s = 13.8\, d\sqrt{l/p} \qquad (1)$$

* A table of factors for converting U. S. customary units of measurement to metric (SI) units is presented on page 5.

where

s = spacing between centroids of fibers, in.

d = fiber diameter, in.

p = percent fiber reinforcement by volume

Figure 6 illustrates the effect of fiber volume on the first crack and ultimate flexural strength. This figure verifies previous conclusions that the flexural strength varies inversely with fiber spacing. In Equation 1, if d remains constant, the spacing will decrease as the volume of fibers increases.

Figure 7 illustrates the effect of fiber length and fiber diameter (or equivalent diameter). In Equation 1, if p and d remain constant, the spacing will remain constant; thus, the improvement in strength can be attributed to the better bond developed by the longer and smaller diameter fibers. Another interesting aspect of fibrous concrete is illustrated in Figures 6 and 7. This is the problem of mixing fibers, which will be mentioned briefly here and discussed in more detail later. Based on Figures 6 and 7, the ideal situation would be to have long fibers with small cross-sectional areas. However, as the aspect ratio (length to diameter or equivalent diameter for fibers with cross-sectional shapes other than round) increases, the mixability decreases. As an example, for the study conducted by Waterhouse and Luke,[6] the maximum length of fibers with a 0.010-in. diameter which could be mixed was about 1-1/4 in., while for the 0.020-in. diameter fibers, longer lengths could be adequately mixed. This factor should be kept in mind when interpreting data presented in these curves.

Figure 8 illustrates the effect of fiber diameter. As the diameter decreases, the flexural strength increases for a constant length and volume. The effect of fiber diameter can also be illustrated by considering Equation 1. In this equation, if p remains constant, the spacing should decrease as fiber diameter decreases. Therefore, the strength should increase as the diameter decreases.

In summary, the following conclusions can be drawn:

a. The inclusion of fibers increases the first crack and ultimate flexural and tensile strength.

b. The inclusion of fibers in a concrete matrix increases the ductility of the composite.

c. The efficiency of the fibers as crack arrestors is dependent on the spacing of the fibers (or volume of fibers), providing the necessary bond is developed between the fibers and the concrete matrix.

d. The ability of the fibers to develop bond varies directly with the length and inversely with the diameter, i.e., for a given volume percentage and length of fibers, the smaller the fiber diameter the larger will be the bond area.

MATERIAL CHARACTERISTICS

In addition to increasing the tensile (flexural) strength of concrete, the addition of fibers enhances certain other properties which are important from the standpoint of pavement performance. Among these are increased ductility and toughness, increased dynamic strength, increased resistance to spalling, and increased fatigue strength. Limited available data indicate that abrasion resistance and thermal conductivity may be somewhat increased. Compressive strength is only slightly increased and the modulus of elasticity remains essentially unchanged.

As illustrated in the previous section, the tensile and flexural strength of the resulting composite (fibrous concrete) is increased when fibers are added to concrete. Batson[7] reports increases in first crack flexural strength of fibrous concrete of up to 2.5 times the strength of plain concrete with fiber contents up to 4 percent by volume. Gray and Rice[8] indicate that increases of 150 and 200 percent can be expected for first crack and ultimate flexural strength, respectively. Comparisons such as these are rather meaningless because of the variations which occur between fiber types, test procedures, and methods for comparing data. There is also no basis for selecting comparable plain and fibrous concrete mixtures. The difficulties in comparing strengths are summarized below by Dixon and Mayfield.[9]

> Associated with this ambiguity of definition is the consideration of the control mix necessary for a datum with which to compare mixes containing added chopped wire. If chopped wire is merely added to given constant mix proportions, the workability will obviously decrease, due to particle interference and the increase in surface area to be covered by the paste. The apparent increase in strength shown could have been more easily and cheaply produced by either a reduction of water or an increase in cement. If the chosen criterion is constant workability extra water must be added with a possible reduction in comparable strength.

In order for results to be meaningful, the mix used and specific conditions for batching, mixing, curing, and testing must be considered. Much of the data reported has been for concrete that has a high fiber content (in many cases, higher than can be used in the field) and that has been batched, mixed, and cured in the laboratory and tested in small beams (less than 6- by 6- by 36-in. beams). Under these conditions, higher strengths have been obtained than can be obtained under field conditions. Under field conditions, mixtures which can be mixed and placed will yield ultimate flexural strengths of about 1000 psi at 90 days as measured with 6- by 6- by 36-in. beams tested according to American Society for Testing and Materials (ASTM) Designation: C 78-64.[10] An expected range would be from 900 to 1300 psi depending on the workability required for proper placement. Results reported by Parker,[11] Grambling,[12] and Arnold and Brown[13] and of tests conducted as part of this study verify this range of expected strength.

The ductility of fibrous concrete is greater than that of plain concrete. Figure 9 illustrates typical load-deflection curves for plain and fibrous concrete beams. The initial straight-line portion for both curves is essentially the same, so values of the modulus of elasticity for fibrous concrete will be essentially the same as those for plain concrete made from the same materials. The ultimate load for plain concrete corresponds to the first crack load for fibrous concrete inasmuch as the ultimate load for the plain beam is the load at which the first crack propagates through the specimen. For fibrous concrete, the

first crack load does not result in a catastrophic failure as it does for plain concrete, and the specimen will withstand additional load before an ultimate is reached. After the ultimate load is reached, the load begins to decrease but catastrophic failure does not occur at this point either. The behavior of the beam after the first crack condition is reached is a result of the debonding and stretching of the fibers across the cracks in the beam.

"Toughness" is the energy required to completely separate the specimen. The area under the stress-strain curve (in this case, the load-deflection curve) is a measure of the toughness of a material. From Figure 9, it can be seen that fibrous concrete offers a significant improvement in this respect over plain concrete.

Tests reported for the Ohio River Division Laboratories (ORDL) by Williamson[14,15] and Birkimer and Hossley[16] indicate that the dynamic strength of fibrous concrete is greater than that of plain concrete. Dynamic flexural and compressive tests, impact tests, and tests with explosive loading conducted during the studies reported in References 14-16 all showed that fibrous concrete resists these types of loadings better than plain concrete. Figure 10a shows a plain concrete cylinder after dynamic compressive loading, and Figure 10b shows a fi brous concrete cylinder subjected to the same loading. The plain concrete shattered, while the fibrous concrete remained intact. Figure 11a shows a plain concrete slab after being subjected to an explosive loading, and Figure 11b shows a fibrous concrete slab after being subjected to the same loading. The plain concrete slab completely disintegrated, while the fibrous concrete slab held together. The explosive loading tests indicate that for fibrous concrete the number of fragments resulting from explosion can be reduced in excess of 80 percent.

Airport pavements receive impact loadings during landings and rather rapid loadings during takeoffs and landings. Presently, it is felt that dynamic loading conditions are not as severe in terms of pavement performance as static or slow moving loading conditions. It would appear therefore that improvements in the response of fibrous concrete to dynamic loading should enhance the performance of fibrous concrete

pavements subjected to slow moving loads. However, no experimental data exist nor have any theoretical studies been conducted to substantiate or disprove this effect.

Another property of fibrous concrete which makes it superior to plain concrete is its resistance to spalling. There is no quantitative measure for spall resistance, but qualitatively this property can be determined from results of dynamic and explosive loading tests as shown in Figures 10 and 11. In both of these figures, it can be seen that the fibrous concrete specimens do not disintegrate upon loading but are held together by the fibers. Although the loadings on pavements will be different, the ability of fibrous concrete to remain intact after cracking will result in much less spalling.

Forrest et al.[17] report that the fatigue flexural strength of plain concrete (2×10^6 to 10×10^6 load repetitions) ranges from about 50 to 60 percent of the static strength. Batson et al.[18] speculate that the fatigue strength of fibrous concrete would be increased because "...the propagation of a flaw in fibrous concrete subject to cyclic loading would be retarded by the use of closely spaced steel fibers...."

Experimental data presented by Batson et al.[18] and Ball[19] indicate that the expected increases in fatigue strength occur only for materials with 2.98 percent of fibers, a greater percentage than can be mixed and placed under field conditions. One series of tests with 2.98 percent fibers and two series of tests with 2.00 percent fibers reported by Ball[19] showed that the fatigue strengths of the resulting materials were comparable to that of plain concrete. It should be noted that some of the tests reported were for complete reversal of loading and others were for loading from zero to the maximum value.

Another complicating factor to be considered when processing the results of fatigue tests is the definition of the strength used to compute the stress to strength ratio. For the tests reported, the first crack static strength was used and fatigue failure defined as the repetition level at which deflections become large. The use of the ultimate static strengths would have resulted in smaller stress ratios and thereby reduced the apparent influence of the fibers. Because of the limited

data available and because of the ambiguity which exists in defining strength ratios, it is concluded that the addition of fibers in quantities which can be mixed and placed in the field has little or no effect on the fatigue strength of concrete.

Tests conducted by Mikkelmeni[20] indicate that the resistance to abrasion of concrete may be somewhat increased by the addition of fibers. This conclusion, however, is based on qualitative data and is limited to a specific set of materials and test conditions.

Dixon and Mayfield[9] report that the inclusion of wire fibers increases the thermal conductivity of the concrete. Increased thermal conductivity results in more uniform temperature distributions through slabs. This should theoretically reduce warping stresses in the slabs caused by nonuniform temperature distributions.

The rather severe environmental conditions to which a pavement is subjected may result in corrosion of the steel fibers and loss of the beneficial effects of the fibers. The large surface area to volume ratio of the fibers makes them more susceptible to corrosion than conventional reinforcement. However, no data exist which show conclusively either the nature of the effect of fiber corrosion on pavement performance or even if it does have a significant effect.

Some qualitative information on fiber corrosion has been accumulated from experimental pavements which have been in place for a number of years. This information is based on limited visual observations, but it does permit some preliminary conclusions to be drawn. The corrosion of fibers on the surface, within the pavement, across open cracks, and across cracks that are held closed are considered separately.

Based on observations of pavements constructed to date, the fibers on exposed surfaces oxidize and deteriorate rather rapidly. However, the deterioration appears to be limited to the surface and, as a result, should not affect pavement performance.

There is no indication that fibers within pavement slabs deteriorate. Cores taken in 1972 from fibrous concrete slabs constructed at ORDL in 1967 and at Lockbourne AFB, Ohio, in 1970 showed no evidence of fiber deterioration within the concrete. Figure 12a shows a core taken

from one of the slabs with no apparent deterioration of the fibers. A study by Shroff[21] indicated that no change in flexural strength occurred when mortar with fibers was alternately submerged in salt water and dried for 90 days. All the data accumulated thus far indicate that the performance of fibrous concrete pavements should not be adversely affected by the corrosion of fibers within the concrete.

When considering deterioration or corrosion of fibers at a crack, two distinct types of cracks must be considered. Cracks which occur due to shrinkage or volume change of the concrete or reflective cracks in overlays due to volume change in the base pavement constitute the first type. It has been observed that such cracks are sufficiently wide to admit water and air and that corrosion of the fibers occurs rapidly. However, the width of this type crack will be such that unbonding or breaking of the fibers across the crack will have occurred, and as a consequence, any deterioration of the fibers due to corrosion will have little if any effect on the pavement performance. In a number of the experimental pavements built thus far, insufficient or, in some cases, no joints were provided. As a result, cracks occurred which opened up rather wide and the fibers deteriorated rapidly. Figure 12b shows a core taken across such a crack which occurred in one of the slabs constructed at ORDL in 1967. The fibers across this crack were completely deteriorated.

Load-induced cracks are the other type which must be considered. These are cracks which occur upon application of loads to the pavement. In most cases, these cracks are not continuous and are initially held tightly closed by the fibers. They propagate, open up, and become working cracks only with the continued application of loads. If the fibers across such cracks deteriorate because of corrosion, then the performance of the pavement will be adversely affected. Sufficient data are not available to draw any definite conclusions concerning the deterioration of fibers across such cracks. As a result, the design criteria which are presented later in this report were developed based on a failure condition in which only a minimum amount of cracking had occurred.

RESPONSE OF FIBROUS
CONCRETE PAVEMENT SLABS TO LOAD

The response of fibrous concrete slabs to repeated applications of load will be influenced by the material properties discussed in the previous section. One of these is the high energy-absorbing characteristic or toughness of fibrous concrete.

When pavement slabs are loaded, the critical stress in the slab is assumed to be the tensile stress at the bottom of the slab. There are conditions such as loading at corners for which the maximum tensile stress occurs at the top of a slab. When the tensile strength of the concrete is exceeded, a crack will occur. For plain concrete pavements, this crack will not immediately propagate to the surface as it does with a beam but requires additional energy before this propagation will occur. The required energy is supplied by additional repetitions of load and changes in temperature.

For fibrous concrete pavements, the energy requirements or load applications required for the crack to propagate to the surface will be higher than those for plain concrete because of the higher energy-absorbing characteristic of fibrous concrete. The load-deflection diagrams for both plain and fibrous concrete beams shown in Figure 9 illustrate that, even after the ultimate load is reached for the fibrous concrete beam, considerable energy is required before complete fracture occurs. This characteristic is also illustrated by the response of a fibrous concrete beam during loading. A crack forms at the bottom of the beam but does not immediately propagate to the surface and cause failure of the beam. The load must be sustained in order to debond or stretch the fibers across the crack before the crack will reach the top of the beam. This requirement means that for comparable fibrous concrete and plain concrete pavements having the same strength concrete, surface cracking should occur earlier in the plain concrete pavement than in the fibrous concrete pavement.

After the cracks reach the surface, the fibers will prevent the cracks from propagating horizontally to a free edge. In the previous section, the mechanism by which fibers resist the propagation of small

cracks or flaws within the concrete was discussed. On a macroscopic scale, the same phenomenon occurs. Figures 13 and 14 show cracked fibrous concrete slabs. From these figures, it can be seen that visible cracks are discrete and discontinuous. The cracks shown in Figure 13 probably developed because of tensile stresses in the bottom of the slab, while those shown in Figure 14 probably developed because of tensile stresses in the top of the slab. However, it should be noted that the latter cracks are also discontinuous. The formation of discontinuous cracks is contrary to the behavior of plain concrete slabs, in which cracks propagate to a free edge when they form. As traffic continues, cracks in fibrous concrete slabs will continue to propagate until a free edge or another crack is encountered.

The mechanism by which fibers restrict the growth of cracks is similar to that discussed in the preceding section for internal microcracks and flaws. When cracks first occur in fibrous concrete pavement, they are held tightly closed by the fibers. They can only be seen by very careful examination, and at times wetting of the slab is necessary to find them. The fibers across the cracks being stiffer than the concrete reduce the stress concentrations at the ends of the crack and prevent it from propagating. Additional load applications are necessary to produce the energy required for the crack to open up and propagate further. Therefore, for identical conditions of strength, thickness, and applied stress, a fibrous concrete slab should carry more repetitions of load before the crack reaches the surface and propagates to a free edge.

Figure 15 illustrates three cracks at various stages of their development. Crack 1 is in the early stages of development and is not visible through the layer of paint. Crack 2 has developed to the point at which it is visible through the paint at several locations, and crack 3 has opened up considerably and is easy to see. Crack 3 is in an advanced stage of development, and from the standpoint of performance of the pavement, it would be as detrimental as a crack in plain concrete which had just formed. This crack has opened up sufficiently to permit infiltration of moisture and cause a reduction in load transfer across

the crack. If it is assumed that crack 3 initially occurred at some lower traffic level and required additional traffic to propagate and open up, it is apparent that the occurrence of the first crack in a fibrous concrete slab is not comparable to the occurrence of the first crack in a plain concrete slab from the standpoint of pavement performance. This conclusion leads to a rather arbitrary definition of first crack failure for fibrous concrete pavement.

In plain concrete pavements, the first crack that develops propagates to a free edge so that first crack failure is reached when a slab is broken into two to three pieces. For fibrous concrete pavements, the first crack that develops does not propagate to a free edge and is really not detrimental to the load-carrying capability of the pavement. As a result, the definition used to describe the first crack or initial failure condition for fibrous concrete pavement is only an attempt to describe a condition of fibrous concrete pavement which would be comparable to the condition of plain concrete pavement at first crack or initial failure. For the accelerated traffic tests, the first crack failure condition was selected by visually examining the condition of the slabs and determining when a crack or cracks similar to crack 3 in Figure 15 had developed to the point at which it would be as detrimental to the performance of the fibrous concrete pavement as a crack in a plain concrete pavement.

Although design is usually based on the initial crack failure condition, the slabs can safely carry additional traffic after this condition has been reached. According to Hutchinson,[22] condition surveys and accelerated test track studies have indicated that pavements constructed on high-strength foundations (having modulus of subgrade reaction values of 300 pci or greater) will continue to carry traffic without undue displacements and maintenance problems even after the slabs have cracked. This phenomenon leads to the definition of two additional failure conditions described by Hutchinson.[23] These are the shattered slab and complete failure conditions. The ability of the pavement to carry traffic will depend (a) on the ability of the underlying material to resist the effects of water without pumping or

permanent deformation, (b) on the ability of the slabs to resist further cracking, and (c) on the spall resistance of the concrete adjacent to cracks and joints.

In previous paragraphs, the development of cracks in fibrous concrete has been discussed, and it has been shown that the performance of fibrous concrete should be better than that of plain concrete. Dynamic, impact, and explosive loading tests indicate qualitatively that the spall resistance of fibrous concrete should also be better than that of plain concrete. This characteristic has been verified by accelerated traffic tests. Figure 16 shows a severely spalled crack in a plain concrete test pavement at complete failure. Spalling at cracks and joints is usually associated with failure of plain concrete pavements. Figure 17 shows the condition of typical cracks in fibrous concrete pavement at complete failure. The absence of deep spalls and the resulting debris has been observed in all of the fibrous concrete pavements tested. The deterioration of cracks in fibrous concrete pavements is characterized as raveling rather than spalling since the edges appear to wear away rather than break off in large pieces. The ability of fibrous concrete to resist spalling is clearly demonstrated in Figure 18. The circular-shaped crack about 5 in. in diameter located near the center of the slab developed soon after traffic was started. Figure 18 shows the condition of the slab after considerable traffic (4500 coverages). The interior of the circle was still in place even though some deterioration had occurred around the perimeter. The fact that the concrete between the cracks remained in place can be attributed to the spall-resistant properties of fibrous concrete. While not contributing significantly to the first crack performance of fibrous concrete pavements, the high spall resistance should improve the postcracking performance of the pavement.

DESCRIPTION OF EXPERIMENTAL INSTALLATIONS

The experimental fibrous concrete pavement installations can be divided into two categories: accelerated traffic test sections and field test pavements. The accelerated traffic test sections were constructed under controlled conditions and subjected to simulated aircraft traffic to determine the response of the pavements to repeated loads. Results from these tests were used to establish joint and thickness design criteria. The field test pavements were constructed using conventional construction procedures, and their behavior was observed under actual environmental and traffic conditions. Results from these tests were used to establish construction procedures and techniques and joint requirements and to determine the effects of environmental conditions.

In this section of the report, the test installations will be described, construction of the pavements discussed, and properties of the materials used in the pavements presented. The tests conducted for this study are presented in chronological order, and this presentation is followed by a summary of the work conducted by other agencies.

KEYED LONGITUDINAL JOINT TEST SECTION

The U. S. Army Construction Engineering Research Laboratory sponsored the construction and testing of two fibrous concrete test pavements during June 1971-March 1972. These pavements were constructed at WES as a part of a test section designed to study the effects of multiple-wheel heavy gear load (MWHGL) aircraft (C-5A and Boeing 747) on keyed longitudinal construction joints. Results from this study are reported by Grau.[24] The layout of the test section is shown in Figure 19. A 6-in. fibrous concrete slab (item 5 of the test section) was constructed along with the other pavements. The two south slabs in item 3, which was a 10-in. plain portland cement concrete (PCC) pavement, failed after a limited number of load applications were applied. At this time, traffic was stopped and a 4-in. fibrous concrete overlay constructed over all four slabs in item 3. The two north slabs had received no traffic prior to overlaying.

CONSTRUCTION

The existing heavy clay subgrade at the test site was constructed previously for another test section. The top 6 in. of the subgrade was reprocessed to produce a strength of about 4 CBR and then fine-graded. Figure 20 shows the finished surface of the subgrade. A 4-in. sand filter course was placed on the finished subgrade. Figure 21 shows the finished surface of the 4-in. sand filter course with the side forms and supports for the movable vibrator supports in place for item 5.

Round fibers, 0.016 in. in diameter and 1 in. long, as shown in Figure 22 were used in item 5. Concrete was batched at a ready-mix facility by emptying the boxes of fibers onto a belt charging the aggregate to the transit-mix truck. The concrete was mixed and hauled to the site by the transit-mix truck. The concrete was deposited in the forms, struck off, vibrated, and finished as shown in Figures 23-25. The supports and pipes were removed after consolidation with the vibrating screed was completed, and the voids left by the removal of the supports and pipe were filled by hand. The concrete was moist-cured for 7 days. Wet burlap was placed on the fresh concrete and kept wet for 24 hr. The burlap was then thoroughly wetted and covered with plastic sheeting which was maintained in place for the remainder of the 7-day curing period.

Some balling of fibers such as that shown in Figures 26 and 27 occurred. The balls contained fibers and fine aggregate and were coated with mortar indicating that the balling occurred in the truck after the aggregate and fiber were charged but before the cement and water were added. Some fiber balls were found which contained no fine aggregate indicating that some clumps of fibers were never broken up before the cement and water were added.

After the two south slabs of item 3 had reached a failure condition, as illustrated in Figure 28, the entire item was overlaid with a 4-in. partially bonded fibrous concrete slab. The surface of the existing plain PCC slab was prepared by removing all loose material from the spalled cracks (see Figure 16), removing joint sealant which protruded

above the surface, and sweeping and washing the surface free of debris. The surface of the existing pavement was moistened prior to placing the overlay. Concrete was batched, mixed, and placed in the same manner as it was for item 5. Rectangular fibers, 0.010 by 0.022 in. in cross section and 1 in. long, as shown in Figure 29 were used. The concrete was practically free from balling, and the few balls that were found were small. Although the base pavement consisted of four 25- by 25-ft slabs, no joints were constructed in the overlay.

MATERIAL PROPERTIES

The subgrade for both items consisted of a heavy clay (CH, E-11*) that had a liquid limit (LL) of 73, a plastic limit (PL) of 25, and a plasticity index (PI) of 48. Classification data for this soil are shown in Figure 30. The sand filter course placed over the heavy clay subgrade consisted of a clean sand (SP, E-2). Classification data for this soil are also shown in Figure 30. The results of CBR, water content, density, and plate bearing tests on the subgrade and the sand filter course are summarized in Table 1. These tests were conducted as the pavement was constructed and after the completion of all traffic.

Six- by 6- by 36-in. beams and 6- by 12-in. cylinders were cast during placement of the fibrous concrete according to ASTM C 192-69[27] (CRD-C 10[28]). These beams and cylinders were tested for strength and modulus of elasticity at the initiation and completion of traffic. The results of these tests are presented in Table 2 and summarized in Table 3. Cores and beams were removed from the slabs after completion of traffic and strength tested according to ASTM C 42-68[34] (CRD-C 27[28]). Results of these tests are presented in Table 4. The average tensile strength of the fibrous concrete in item 5 was 788 psi, with a standard deviation of 112 psi. For the overlay of item 3, the average tensile strength was 795 psi, with a standard deviation of 161 psi.

---

* Soil classifications given in parentheses are according to the Unified Soil Classification System (USCS)[25] and the FAA soil classification system,[26] respectively.

Table 1

Results of CBR, Water Content, Density, and Plate Bearing Tests for Items 3 and 5 of the Keyed Longitudinal Joint Test Section

Item No.	Material	Water Content percent	Dry Density pcf	CBR	Modulus of Soil Reaction pci
		As Constructed			
3	Sand filter (SP, E-2)	--	--	--	--
	Subgrade (CH, E-11)	33.4	84.0	3.2	89
5	Sand filter (SP, E-2)	--	--	--	--
	Subgrade (CH, E-11)	36.6	80.7	2.1	50
		After Traffic			
3	Sand filter (SP, E-2)	--	--	--	104
	Subgrade (CH, E-11)	32.1	85.4	--	--
5	Sand filter (SP, E-2)	--	--	--	92
	Subgrade (CH, E-11)	--	--	--	--

TRAFFIC

Test traffic was applied with the 12-wheel and twin-tandem assemblies shown in Figures 31 and 32, respectively, both of which were equipped with 49x17 tires with a ply rating of 26. The tire pressure was checked and adjusted, as needed, each morning prior to testing.

The 12-wheel assembly and test wheel configuration represented one main gear of the C-5A aircraft. The 12-wheel assembly consisted of two load boxes, each carried by six load wheels which resulted in the wheel arrangement shown in Figure 33a. The boxes were loaded to produce a net weight of 360 kips distributed equally over the 12 wheels. Each tire was inflated to 100 psi, which resulted in a tire contact area of 285 sq in. per tire and a contact pressure of about 106 psi.

The twin-tandem assembly and wheel spacing shown in Figure 33b represented one twin-tandem component of the Boeing 747 assembly. The

Table 2

Material Properties of Fibrous Concrete Used in Items 3 and 5 of the Keyed Longitudinal Joint Test Section

Item No.	Specimen No.	Age at Testing days	Compressive Strength* psi	Flexural Strength** psi	Tensile Strength† psi	Modulus of Elasticity in Flexure†† 10^6 psi	Dynamic Modulus of Elasticity‡ 10^6 psi	Slump‡‡ in.	Air Content§ percent
				Initiation of Traffic					
5	1-1	73	4490					9	
	1-2	73	4490					9	
	1-A	73		650		3.64	4.21	9	
	2-1	73	5870					5	5.3
	2-2	73	5760					5	5.3
	2-5	73			745			5	5.3
	2-A	73		860		5.67	5.49	5	5.3
	2-B	73		1040				5	5.3
	4-1	73	5590					3-1/2	5.8
	4-2	73						3-1/2	5.8
	4-5	73			770			3-1/2	5.8
	4-A	73		1120		5.68	5.16	3-1/2	5.8
	4-B	73		730				3-1/2	5.8
	5-1	73	6170					3	
	5-2	73	6310					3	
	5-A	73		940		5.69	5.39	3	
3	B1-1	40	7190					3-1/4	5.8
	B1-2	40	7240					3-1/4	5.8
	B1-A	40		1090		5.66	5.55	3-1/4	5.8
	B2-1	40	7200					3-1/4	6.5
	B2-2	40	6790					3-1/4	6.5
	B2-5	40			930			3-1/4	6.5
	B2-A	40		1180		5.38	5.76	3-1/4	6.5
	B2-B	40		1195				3-1/4	6.5
	B3-1	40	6770					3	5.9
	B3-2	40	7040					3	5.9
	B3-A	40		1130		6.17	5.65	3	5.9
	B4-1	40	6720					3-1/2	5.7
	B4-2	40	7070					3-1/2	5.7
	B4-5	40			810			3-1/2	5.7
	B4-A	40		1095		6.23	5.13	3-1/2	5.7
	B4-B	40		1115				3-1/2	5.7
	B5-1	40	6840					3-1/4	5.6
	B5-2	40	6770					3-1/4	5.6
	B5-A	40		1160		6.87	5.56	3-1/4	5.6
				Completion of Traffic					
5	1-3	255	5420					9	
	1-4	255	5680					9	
	1-B	255		865		4.50	4.74	9	
	2-3	255	6980					5	5.3
	2-4	255	6690					5	5.3
	2-6	255			740			5	5.3
	2-C	255		755		5.39	5.43	5	5.3
	2-D	255		1065				5	5.3
	4-3	255	6730					3-1/2	5.8
	4-4	255	6570					3-1/2	5.8
	4-6	255			810			3-1/2	5.8
	4-C	255		790		5.50	5.75	3-1/2	5.8
	4-D			1160				3-1/2	5.8
	5-3	255	7410					3	
	5-4	255	8000					3	
	5-B	255		1025		5.81	6.05	3	
3	B1-3	137	8380					3-1/4	5.8
	B1-4	137	8320					3-1/4	5.8
	B1-B	137		1240		5.94	6.12	3-1/4	5.8
	B2-3	137	8110					3-1/4	6.5
	B2-4	137	8380					3-1/4	6.5
	B2-6	137			885			3-1/4	6.5
	B2-C	137		1140		5.54	5.84	3-1/4	6.4
	B2-D	137		1410				3-1/4	6.5
	B3-3	137	8130					3	5.9
	B3-4	137	8390					3	5.9
	B3-B	137		1260		6.48	6.13	3	5.9
	B4-3	137	8040					3-1/2	5.7
	B4-4	137	8250		970			3-1/2	5.7
	B4-6	137						3-1/2	5.7
	B4-C	137		1280		5.62	5.26	3-1/2	5.7
	B4-D	137		1330				3-1/2	5.7
	B5-3	137	8160					3-1/4	5.6
	B5-4	137	8450					3-1/4	5.6
	B5-B	137		1160			6.01	3-1/4	5.6

* Tested according to ASTM C 39-71[29] (CRD-C 14[28]).
** Tested according to ASTM C 78-64[10] (CRD-C 16[28]).
† Tested according to ASTM C 496-71[30] (CRD-C 77[28]).
†† Tested according to CRD-C 21[28].
‡ Tested according to ASTM C 215-60[31] (CRD-C 18[28]).
‡‡ Tested according to ASTM C 143-71[32] (CRD-C 5[28]).
§ Tested according to ASTM C 231-72T[33] (CRD-C 41[28]).

Table 3

Summary of Material Properties of Fibrous Concrete Used in Items 3 and 5 of the Keyed Longitudinal Joint Test Section

Property	Average	Standard Deviation	Coefficient of Variation
Flexural strength, psi			
40 days (item 3 overlay)	1138	38	0.03
73 days (item 5)	890	164	0.18
137 days (item 3 overlay)	1260	75	0.06
255 days (item 5)	943	133	0.14
Compressive strength, psi			
40 days (item 3 overlay)	6963	195	0.03
73 days (item 5)	5540	698	0.13
137 days (item 3 overlay)	8261	135	0.02
255 days (item 5)	6683	791	0.12
Modulus of elasticity,* 10^6 psi			
40 days (item 3 overlay)	5.80	0.47	0.08
73 days (item 5)	5.12	0.72	0.14
137 days (item 3 overlay)	5.88	0.35	0.05
255 days (item 5)	5.40	0.50	0.09
Slump, in.			
Item 3 overlay	3-1/4	--	--
Item 5	5-1/8	--	--
Air content, percent			
Item 3 overlay	5.9	--	--
Item 5	5.5	--	--

Note: Test methods used are presented in Table 2.
* Represents results from flexural and compression tests combined.

Table 4

Results of Strength Tests on Cores and Beams from Items 3 and 5 of the Keyed Longitudinal Joint Test Section

Item No.	Specimen Type and No.	Core Length in.	Beam Width and Depth in.	Tensile Strength* psi	Flexural Strength** psi
5	Core 1	6.0		720	970†
	Core 2	6.0		725	975†
	Core 3	6.0		710	960†
	Core 4	6.0		685	935†
	Core 5	6.6		975	1225†
	Core 6	6.6		910	1160†
	Beam 1		6.1		1175
	Beam 2††		6.0		760
3	Core 7	4.5		720	
	Core 8	4.7		530	970†
	Core 9	4.4		1065	780†
	Core 10	4.3		805	1055†
	Core 11	4.25		875	1125†
	Core 12	4.45		775	1025†
	Beam 3		4.4		985
	Beam 4		4.4		1010

* Tested according to ASTM C 496-71 (CRD-C 77).
** Tested according to ASTM C 78-64 (CRD-C 16).
† Computed from correlation between tensile and flexural strength.
†† Fracture observed in specimen prior to test.

twin-tandem assembly was loaded to a net weight of 166 kips (41.5 kips per wheel) and was equipped with four tires which were inflated to a tire pressure of 200 psi and a contact area of about 207 sq in.

The layout shown in Figure 19 indicates the location, width, and length of the traffic lanes. Traffic was applied over selected portions of the pavement. Traffic lane 1 was 200 in. wide and was subjected to the 12-wheel assembly traffic. The south edge of the traffic lane was located 132 in. north of the south edge of the test section, and the north edge of the 200-in.-wide traffic lane was positioned 32 in. north of the longitudinal construction joints in items 1-4 (center line of the test section).

The traffic lane for the twin-tandem assembly traffic (lane 2) was 120 in. wide and was located in the middle of the north paving lane (Figure 19) to minimize the effects that the 12-wheel assembly traffic might have had on the structural condition of the pavement. The north edge of this lane was located 90 in. south of the north edge of the test section, and the south edge was located 90 in. north of the longitudinal construction joints in items 1-5 (center line of the test section).

The traffic patterns (the distribution of traffic applied over the width of the traffic lanes) are shown in Figure 34. The coverage levels* referred to in this report are the total number of coverages applied in the central portion of the traffic pattern.

Traffic was applied in the 12-wheel assembly traffic lane (lane 1) by repetitions of the traffic pattern shown in Figure 34a. The traffic pattern consisted of 22 passes of the load cart distributed over the traffic lane by following five guidelines painted on the pavement surface on 16-in. centers (approximately one tire print width). The

---

* For rigid pavements, coverages are a measure of the number of maximum stress repetitions that occur in the pavement due to the applied traffic. One coverage occurs when each point of the pavement within the traffic lane has been subjected to a maximum stress, assuming that the stress is equal under the full tire print width. For the 12-wheel assembly, separate and distinct maximum stresses occur under the front and rear 6-wheel arrays. For the twin-tandem assembly, the front and rear twin wheels are close enough together so that only one maximum stress repetition occurs for each pass of the assembly.

22 passes resulted in 16 coverages in the center 60 in. of the traffic lane and a lesser number along the edges of the traffic lane. The distribution of passes and coverages in lane 1 is also shown in Figure 34a. To apply the traffic shown, the load cart traveled for the full length of the traffic lane along guideline 1 (south edge of the traffic lane) and back along the same line; then the cart was shifted laterally to guidelines 2, 3, 4, and 5 in succession for one pass in each direction on each guideline. After tracking guideline 5 (north edge of the traffic lane), the guidelines were run in reverse order commencing with guideline 5. One pass in each direction was made on each of the five guidelines except for guideline 3, along which two passes were made in each direction to produce a uniform traffic pattern in the center of the traffic lane.

Traffic with the twin-tandem assembly load cart was applied to lane 2 in the pattern shown in Figure 34b using five guidelines, each 15 in. apart. The load cart was operated forward and backward along guideline 1 and then was shifted laterally to guidelines 2, 3, 4, and 5 in succession for one pass in each direction on each guideline. The load cart then made one pass in each direction along guidelines 4, 3, 2, 3, 4, 4, 3, 2, and 3, in that order, to produce the pattern shown in Figure 34b. This traffic pattern required 30 passes and resulted in 10 coverages in the central portion of the traffic lane.

All traffic patterns were started from the east maneuver area, and the forward direction of traffic was with the load cart moving from east to west.

TAMPA OVERLAYS

During February 1972, two fibrous concrete overlay test pavements were constructed at Tampa International Airport, Florida. The construction of these pavements and the early performance are reported by Parker[11] and are summarized below.

The pavements were constructed on a taxiway parallel to one of the primary runways. The layout for the pavements is shown in Figure 35. Item 1, a 4-in. overlay of an existing PCC pavement, was situated in the

center of the taxiway. The section was formed by construction of two 25-ft-wide paving lanes. The paving lanes were constructed so that the center of the paving lanes coincided with the longitudinal construction joints in the base pavement. The longitudinal construction joint was a butt-type joint without load-transfer capabilities. No transverse joints were formed in the overlay. The ends of the section coincided with transverse contraction joints so that one transverse contraction joint and one longitudinal construction joint in the base pavement were spanned by each lane of the overlay. Bituminous transition overlays were constructed around the overlay.

Item 2, a 6-in. overlay of an existing PCC pavement, spanned the entire width of the taxiway. The section was formed by constructing three 25-ft-wide paving lanes. The longitudinal construction joints in the overlay matched the longitudinal construction joints in the base pavement. Vertical faces were formed along the edges of the paving lanes with no provisions for load transfer. No transverse joints were formed in the overlay; therefore, all transverse contraction joints in the base pavement were spanned by the overlay. One expansion joint in the base pavement located 75 ft from the south end of the section was spanned by the overlay. The ends of the overlay coincided with transverse contraction joints in the base pavement. Bituminous transition sections were constructed on each end of the overlay.

CONSTRUCTION

A Rex central-mix plant was used for the production of 8-cu-yd batches of the fibrous concrete. The basic components of the plant and batching are illustrated in Figure 36.

Aggregate was fed into the aggregate charging hopper on conveyor belts, weighed in the aggregate weigh hoppers, and discharged onto the charging belt, which discharged into the horizontal mixing drum. For the fibers, a conveyor belt was located so that fibers could be discharged directly onto the charging belt, as shown in Figure 36. Forty-pound boxes of fibers were emptied by hand onto the conveyor belt (Figure 37). A hopper and pipe arrangement (Figure 36) was used for

weighing and charging the fly ash. Compressed air was used to move the fly ash up the pipe and into the horizontal drum. Cement, water, and additives were measured and charged directly into the horizontal drum where the ingredients were mixed and then transferred to the tilting drum for additional mixing and discharge. Very few fiber balls were observed in the concrete.

A minimum of surface preparation was performed, and no attempt was made either to bond the fibrous concrete to the base pavement or to completely eliminate bond between the overlay and the base pavement. The surface preparation consisted of first chipping to remove all loose material from the cracks, removing all joint sealer that protruded above the surface, brooming to remove all loose material, and wetting the surface prior to placing the concrete.

Concrete was hauled to the paving site in side-dump trucks and was either spread with a spreader for the slip-formed lanes or dumped directly onto the old pavement for fill-in lanes. The slip-form paver shown in Figure 38 was used to form the 25-ft-wide paving lanes. Surface texture was applied with a wire comb or a stiff bristle brush moving transversely across the paving lanes. After texturing, the surface was sprayed with a membrane curing compound. Longitudinal construction joints were sawed and sealed, and asphaltic concrete transition sections were constructed at the ends of the overlays.

MATERIAL PROPERTIES

The existing taxiway pavement was constructed in 1965 and was opened to traffic in January 1966. The pavement system was composed of 12 in. of PCC surfacing and 3 in. of limerock base over a sand subgrade (E-3) with a minimum thickness of 28 in. The limerock base was a compacted mixture of 50 percent crushed limerock and 50 percent in-situ sand.

Based on plate bearing tests run at other locations at the airport, the subgrade modulus k at the time of construction of the test section was between 150 and 200 pci. A k value of 165 pci had been used for design and analysis of the airport pavements.

The design flexural strengths of the PCC were 650 and 715 psi at 28 and 90 days, respectively. The pavement was constructed in three 25-ft-wide paving lanes. The longitudinal construction joints between the paving lanes were keyed and tied with 30-in.-long No. 5 deformed bars placed at 30-in. centers. Transverse contraction joints were spaced at 25-ft intervals and were dowelled with 1-1/4-in.-diam, 20-in.-long smooth bars placed at 15-in. centers. The expansion joints contained 1-1/4-in.-diam, 20-in.-long dowels that were placed at 15-in. centers and were equipped with expansion caps. The expansion joints were filled with 3/4 in. of nonextruding, premolded compressible material topped with 3/4 in. of hot-poured seal.

An inspection was made in February 1972 prior to placement of the overlay test items, and the crack pattern in the base pavement was as shown in Figure 39. All slabs in the test area contained either longitudinal or transverse cracks or both. A longitudinal weakened-plane (contraction) joint had been sawed in one of the exterior slabs in an attempt to control the longitudinal cracking. The cracks in the exterior slabs were similar to those in the center slabs in that they meandered within a band approximately 2 to 4 ft wide on either side of the longitudinal center line of the slabs.

Tests for slump and entrained air of the fibrous concrete were performed at the batch plant and at the paving site. An attempt was made to provide concrete at the paving site that would have a slump ranging from 1 to 2 in. and an entrained air content of 4 to 5 percent.

One set of six 6- by 6- by 36-in. beams and two 6- by 12-in. cylinders were made from a batch that was placed in each of the five paving lanes. The beams were tested for flexural strength at 5, 7, 28, and 90 days. The cylinders were tested in compression for compressive strength and modulus of elasticity. The results of these tests are presented in Table 5 and summarized in Table 6.

TRAFFIC

Construction of the overlays was completed on 28 February 1972, and the taxiway was opened to traffic on 6 March 1972. Traffic has

Table 5

Material Properties of Fibrous Concrete Used in the Tampa International Airport Overlays

Item No.	Paving Lane	Slump in.	Entrained Air Content percent	Ultimate Flexural Strength, psi, at Indicated Curing Time				Compressive Strength, psi		Initial Tangent Modulus at 90 Days, 10^6 psi
				5 Days	7 Days	28 Days	90 Days	28-Day	90-Day	
1	West	4-1/2	5.3	569*	658	646	842	4102	4860	3.75
						713	990			
	East	2	4.2	--	779	915	912	5115	6130	4.23
					725	808	1050	5168		
2	East	1-1/2	4.5	658	812	787	952	5447	5940	4.33
						783	1060			
	West	3/4	3.0	819	875	1054	1025	7021	8800	5.05
						950	1350			
	Center	2-3/4	5.0	--	750	752	812	5113	6150	4.20
					758	860	1075	5008		

* Tested after 4 days.

Table 6

Summary of Material Properties of Fibrous Concrete Used in the Tampa International Airport Overlays

Property	Average	Standard Deviation	Coefficient of Variation
Slump, in.	2.3	--	--
Entrained air content, percent	4.3	--	--
Flexural strength, psi			
5 days	682	--	--
7 days	765	63	0.08
28 days	827	114	0.14
90 days	1007	140	0.14
Compressive strength, psi			
28 days	5282	810	0.15
90 days	6376	1302	0.20
Modulus of elasticity, 10^6 psi	4.31	--	--

consisted of taxiing aircraft landing from the north or departing to the north on runway 18R-36L. The traffic is composed primarily of DC-9 and Boeing 727 aircraft, with a few wide-bodied jet (Boeing 747 and DC-10-10) operations.

STRUCTURAL LAYERS TEST SECTION

Two fibrous concrete test items were constructed and tested as a part of full-scale pavement tests designed to study the effects of chemical stabilization, insulating materials, and fibrous concrete on pavement performance. The test sections were constructed and tested at WES during the period March 1972-May 1973. The design, construction, and behavior under traffic of the pavements in two test sections, one rigid and one flexible, are reported by Burns et al.[35] The construction, material properties, and traffic applied to the two fibrous concrete test items, which were part of the rigid test section, are described below.

A layout of the rigid pavement test section is shown in Figure 40.

Item 1 consisted of 7 in. of fibrous concrete on a 20-in. layer of lean clay encased in a waterproof membrane over a heavy clay subgrade. Item 2 consisted of 4 in. of fibrous concrete on a 17-in. layer of clay gravel stabilized with 6 percent portland cement over a heavy clay subgrade. Each item was composed of two 25- by 50-ft slabs divided by a construction joint. Details of the longitudinal construction joints are shown in Figure 41.

CONSTRUCTION

The heavy clay subgrade on which the structural layers test section was constructed had been used previously for the MWHGL test section and more recently for the keyed longitudinal joint test section. The old pavement was broken up and removed to expose the subgrade. The top 6 to 12 in. of the subgrade was reprocessed and then compacted and graded, as necessary, to achieve a subgrade with a CBR of about 4 and the proper elevation. A view of the finished subgrade in item 1 is shown in Figure 42.

A 20-in.-thick membrane encapsulated soil layer (MESL) was placed over the subgrade for item 1. Figures 43-45 illustrate the construction procedures. The lean clay was placed and compacted in one 8-in. and two 6-in. lifts after the bottom membrane was in place. The surface was then fine-graded to the desired elevation, and the top membrane was constructed.

A 17-in.-thick cement-stabilized base was placed over the subgrade for item 2. Figures 46 and 47 illustrate the construction. The cement-treated gravel was placed in three lifts of approximately the same thickness. The cement for each lift was spread by hand and mixed with a pulvimixer, and then the lift was compacted.

Concrete for both items was batched at a ready-mix facility, mixed and hauled in transit-mix trucks, and placed and cured using the same procedures and techniques as were used for the keyed longitudinal joint test items. The three types of fibers shown in Figure 48 were used for the two test items. Round fibers, 0.016 in. in diameter and 1 in. long, were used in item 1. The 3/4-in.-long deformed fibers formed from

0.016-in.-diam wire were used for the north slab of item 2. The flat fibers, which were 3/4 in. long and 0.010 by 0.014 in. in cross section, were used for the south slab. Some balling of the fibers was noted, especially with the 1-in.-long fibers. The larger balls usually consisted of only fibers, whereas some of the smaller balls were composed of both fibers and mortar (Figure 49).

MATERIAL PROPERTIES

The subgrade consisted of a heavy clay (CH, E-11) that had an LL of 73, a PL of 25, and a PI of 48. The MESL in item 1 consisted of a lean clay (CL, E-7) that had an LL of 43, a PL of 22, and a PI of 21. The cement-treated base in item 2 consisted of a clay gravel (SP-SC, E-5) stabilized with 6 percent portland cement by weight. Classification data for each soil are shown in Figure 50. Results of CBR, water content, density, and plate bearing tests conducted on the subgrade, MESL, and cement-treated base after construction and after traffic are presented in Table 7.

Six- by 6- by 36-in. beams and 6- by 12-in. cylinders were cast during placement of the fibrous concrete according to ASTM C 192-69 (CRD-C 10). These beams and cylinders were tested for strength and modulus of elasticity at 28 days, at the initiation of traffic, and at the completion of traffic. The results of these tests are presented in Table 8 and summarized in Table 9. Cores and beams were removed from the slabs after completion of traffic and tested for strength and modulus of elasticity according to ASTM C 42-68 (CRD-C 27). Results of these tests are presented in Table 10 and are summarized in Table 11.

TRAFFIC

Test traffic was applied with a twin-tandem assembly equipped with 49x17 tires with a ply rating of 26. The tire pressure was checked and adjusted, as needed, each morning prior to testing.

The load cart used is shown in Figure 32. The wheel arrangement and spacing used are shown in Figure 33b. This arrangement represented one twin-tandem component of a Boeing 747 assembly. The load cart was

Table 7

Results of CBR, Water Content, Density, and Plate Bearing Tests for Items 1 and 2 of the Structural Layers Test Section

Item No.	Material	Slab	Average Water Content percent	Average Dry Density pcf	CBR	Modulus of Soil Reaction pci
			As Constructed			
1	Lean clay MESL (CL, E-7)		13.6	99.8	23	175
	Subgrade (CH, E-11)		31.7	86.4	2.7	47
2	Cement-treated base		5.8	135.1	150+	545
	Subgrade (CH, E-11)		34.2	84.5	3.4	85
			After Traffic			
1	Lean clay MESL (CL, E-7)	S	15.2	99.2	--	230
		N	12.5	100.1	--	250
	Subgrade (CH, E-11)	S	--	--	--	180
		N	27.7	92.1	--	200
2	Cement-treated base	S	--	--	--	490
		N	--	--	--	375
	Subgrade (CH, E-11)	S	33.1	85.5	--	118
		N	--	--	--	--

Table 8

Material Properties of Fibrous Concrete Used in Items 1 and 2 of the Structural Layers Test Section

Item No.	Slab	Specimen No.	Age at Testing days	Compressive Strength* psi	Flexural Strength** psi	Modulus of Elasticity in Compression† 10^6 psi	Modulus of Elasticity in Flexure†† 10^6 psi	Slump‡ in.
				28-Day Tests				
1	N	47-C	28	5860				6
	N	49-B	28		805			6
	S	51-C	28	4790				5
	S	53-C	28	4290				6
	S	55-B	28		765			5
	S	58-B	28		700			6
2	N	43-C	28	6080				4
	N	46-C	28	6120				4
	N	43-B	28		770			4
	N	46-B	28		850			4
	S	49-C	28	4660				5
	S	52-B	28		695			5
				Initiation of Traffic				
1	N	48-C	150	6770				6
	N	50-B	150		1145		6.93	6
	S	52-C	150	6150				5
	S	54-C	150	6160				6
	S	56-B	150		965		5.43	5
	S	59-B	150		900		5.13	6
2	N	44-C	150	8040		4.37		4
	N	46-C	150	8210		4.37		4
	N	44-B	150		875		6.24	4
	N	47-B	150		790		6.91	4
	S	50-C	150	6140				5
	S	53-B	150		900		6.34	5
				Completion of Traffic				
1	N	51-B	330		1390		6.33	6
	S	57-B	330		1090		6.98	5
	S	60-B	330		1225		6.98	6
2	N	45-B	330		815		6.38	4
	N	48-B	330		1070		6.38	4
	S	54-B	330		1115		6.31	5

* Tested according to ASTM C 39-71 (CRD-C 14).
** Tested according to ASTM C 78-64 (CRD-C 16).
† Tested according to ASTM C 469-65[36] (CRD-C 19).
†† Tested according to CRD-C 21.
‡ Tested according to ASTM C 143-71 (CRD-C 5).

Table 9

Summary of Material Properties of Fibrous Concrete Used in Items 1 and 2 of the Structural Layers Test Section

Age days	Average Flexural Strength psi		Average Compressive Strength psi		Modulus of Elasticity* 10^6 psi	
	Item 1	Item 2	Item 1	Item 2	Item 1	Item 2
28	757	772	4980	5620	--	--
150	1003	855	6360	7463	5.83	5.65
330	1235	1000	--	--	6.76	6.36

Note: Test methods ured are presented in Table 8. Average slump for item 1 = 5.7 in.; average slump for item 2 = 4.3 in.
* Represents results from flexural and compression tests combined.

Table 10

Results of Strength and Modulus of Elasticity Tests on Beams and Cores from Items 1 and 2 of the Structural Layers Test Section

Item No.	Specimen Type and No.	Core Diameter in.	Core Length in.	Beam Width in.	Beam Depth in.	Beam Length in.	Compressive Strength psi	Tensile Strength psi	Modulus of Elasticity in Compression 10^6 psi	Flexural Strength psi	Modulus of Elasticity in Flexure 10^6 psi
1	Core 1	3.89	6.90				5840*		4.34		
	Core 2	3.89	7.05				7610		5.25		
	Core 3	3.89	6.50				6690		4.75		
	Core 4	3.89	6.50				6840		5.00		
	Beam 1			7.70	7.80	24.0				1330	4.50
	Beam 2			7.80	7.80	24.0				1110	5.49
	Beam 3			7.80	7.80	24.0				850	4.06
	Beam 4			7.10	7.00	21.0				905	4.86
	Beam 5			6.95	7.00	21.0				940	5.12
	Beam 6			7.00	7.00	21.0				1130	6.02
2	Core 5	5.90	4.50					830			
	Core 6	5.90	4.50					860			
	Core 7	5.90	4.00					880			
	Core 8	5.90	4.50					905			
	Beam 7			4.30	4.00					1100	6.63
	Beam 8			4.00	3.90					1140	6.50
	Beam 9			4.30	4.00					1120	6.12
	Beam 10			4.00	4.00					1010	4.22
	Beam 11			4.00	3.80					1120	3.82
	Beam 12			4.00	4.15					1400	5.76

Note: Test methods, except that for tensile strength (ASTM C 496-71, CRD-C 77), are presented in Table 8.
* Fracture observed in specimen prior to test.

Table 11

Summary of Results of Strength and Modulus of Elasticity Tests on Beams and Cores from Items 1 and 2 of the Structural Layers Test Section

Property	Average	Standard Deviation	Coefficient of Variation
Item 1 compressive strength, psi	6745	--	--
Item 2 tensile strength, psi	869	--	--
Flexural strength, psi			
Item 1	1044	164	0.15
Item 2	1148	120	0.10
Modulus of elasticity, 10^6 psi			
Item 1*	4.94	0.52	0.10
Item 2	5.51	1.09	0.20

* Represents results from flexural and compression tests combined.

loaded to a net weight of 200 kips for trafficking lane 1 and to 240 kips for trafficking lane 2. For both loadings, the tire contact area was maintained at 267 sq in. by using inflation pressures of 190 and 250 psi for the 200- and the 240-kip loads, respectively.

The layout shown in Figure 40 indicates the locations of the traffic lanes. Both lanes were 10 ft wide. Lane 1 was laid out so that the longitudinal construction joint coincided with the edge of the area that received 100 percent of the traffic. Lane 2 was laid out approximately at the center of the north slabs.

Traffic was applied in the same manner as that used during the twin-tandem assembly traffic for the keyed longitudinal joint test section described earlier. The distribution of traffic applied over the widths of the traffic lanes was the same as that shown in Figure 34b, although the loading intensity was different.

WES ROADWAY

On 19 July 1973, a fibrous concrete roadway was constructed on a street at WES. The pavement was 1000 ft long, 24 ft wide, and 4 in. thick. The layout for the pavement is shown in Figure 51. The pavement was formed by constructing a 24-ft-wide lane without any joints. The pavement was permitted to crack where necessary to reduce tensile stresses induced during curing. The ends of the slab adjacent to an existing 5-in. fibrous concrete slab and a new 6-in. plain PCC pavement were thickened to 6 in. A 1-in. expansion joint was provided at both ends of the pavement.

CONSTRUCTION

The site where the pavement was constructed had previously been graded and used for some time as an unsurfaced roadway during construction of WES Building 6006 (Figure 51). Before the fibrous concrete was placed, the site was regraded and a 6-in. clay gravel (SP-SC, E-5) subbase was constructed to the required cross section and elevation as shown in Figure 51.

Fibrous concrete for the roadway was batched at a ready-mix

facility. Fibers were fed onto a belt which transported the aggregate from the weigh hoppers to the transit-mix trucks. Figure 52a shows the arrangement at the ready-mix facility, and Figure 52b shows the fibers being hand-dumped from 40-lb boxes onto the aggregate charging belt. After the aggregate and fibers (5-cu-yd batches) had been fed into the truck, water, cement, and an air-entraining additive were added and the ingredients were mixed in transit-mix trucks (7-cu-yd capacity). Very few fiber balls were observed in the mix, and the few that were observed were small and created no problems in placing.

The concrete was spread directly in front of the paver (Figure 53). The subbase was moistened prior to placing the concrete. The concrete was consolidated and formed to the desired cross section with a slip-form paver (Figure 54). No difficulties were experienced in forming the cross section. The surface and edges finished with no undertearing or sagging. However, some problems were experienced in the area where the grade was steepest (approximately 12 percent). In this area, the paver was moving downhill and upon vibration some of the mortar tended to move down the hill. This problem was accentuated by the fact that the concrete had a higher slump than is desirable for slip-form operations. A relatively high slump was required in order to discharge the concrete from the transit-mix trucks.

Very little hand-finishing was required. A garden hose attached to the paver as shown in Figure 54b provided adequate finishing. The surface of the pavement was sprayed with a membrane curing compound. Some problems were experienced in applying the curing compound. The curing compound was applied by hand and initially not enough sprayers were provided to keep up with the paver. Some shrinkage cracking or crazing was observed and additional sprayers were added. The problem was accentuated by the high temperature (approximately 95°F), the high cement content (9 bags per cubic yard), the use of the garden hose behind the paver, which removed the free moisture from the surface, and by the fact that the paver was moving downhill.

MATERIAL PROPERTIES

No tests were conducted on the loess subgrade or the clay gravel subbase. Testing and precise control of the subbase construction were not necessary since such construction with a thin bituminous surfacing has been used extensively for streets at WES and has proven adequate for the light traffic. It should also be noted that the primary purpose of this construction was not to evaluate the pavement for structural adequacy but rather to study the cracking pattern which would develop and the behavior of the cracks.

One set of six 6- by 6- by 36-in. beams and seven 6- by 12-in. cylinders were cast, according to ASTM C 31-69[37] (CRD-C 11), from a batch of concrete placed near each end of the roadway and from a batch placed near the center of the roadway. Beams were sprayed with curing compound and stored at the paving site for curing. Beams were tested in flexure for strength and modulus of elasticity and cylinders were tested for splitting tensile strength at ages of 1, 2, 7, and 28 days in order to assess the early strength. The early strength data were used for analyzing the cracking which occurred. The results of the tests are shown in Table 12 and summarized in Table 13.

TRAFFIC

Traffic on this pavement has been light. The pavement should be adequate to withstand the applied traffic indefinitely, and no attempt will be made to assess the structural performance of the pavement. Primary emphasis will be placed on evaluating the cracking, the behavior of the cracks, and qualitatively the susceptibility of the fibers to corrosion.

TESTS CONDUCTED BY OTHER AGENCIES

Fibrous concrete has been used for overlays on bridge decks, floor slabs in industrial buildings, such as warehouses, foundries, and parking garages which are subjected to large static as well as impact loads and extreme temperatures, large dolos for erosion control, hydraulic structures where cavitation occurs, burial vaults, and pavements.

Table 12

Material Properties of Fibrous Concrete Used in the WES Roadway

Specimen Type and No.	Age days	Flexural Strength* psi	Tensile Strength** psi	Compressive Strength† psi	Modulus of Elasticity in Flexure†† 10^6 psi	Slump‡ in.	Air Content‡‡ percent
Beam 1	1	565			4.44	4-3/4	4.2
Beam 2	1	430			3.44	4-3/4	4.2
Beam 7	1	555			4.02	4	3.6
Beam 8	1	770			5.05	4	3.6
Beam 13	1	510			3.62	3-3/4	3.8
Beam 14	1	445			3.42	3-3/4	3.8
Cylinder core 1	1		305			4-3/4	4.2
Cylinder core 2	1		315			4-3/4	4.2
Cylinder core 7	1		315			4	3.6
Cylinder core 8	1		330			4	3.6
Cylinder core 13	1		310			3-3/4	3.8
Cylinder core 14	1		275			3-3/4	3.8
Beam 3	2	655			4.23	4-3/4	4.2
Beam 4	2	685			4.32	4-3/4	4.2
Beam 9	2	580			4.38	4	3.6
Beam 10	2	585			4.19	4	3.6
Beam 15	2	665			4.75	3-3/4	3.8
Beam 16	2	640			3.99	3-3/4	3.8
Cylinder core 3	2		455			3-3/4	4.2
Cylinder core 4	2		445			4-3/4	4.2
Cylinder core 9	2		505			4	3.6
Cylinder core 10	2		510			4	3.6
Cylinder core 15	2		485			3-3/4	3.8
Cylinder core 16	2		400			3-3/4	3.8
Beam 5	7	670			5.13	4-3/4	4.2
Beam 11	7	765			5.93	4	3.6
Beam 17	7	770			5.52	3-3/4	3.8
Cylinder core 5	7		590			4-3/4	4.2
Cylinder core 11	7		655			4	3.6
Cylinder core 17	7		580			3-3/9	3.8
Beam 6	28	985			4.63	4-3/4	4.2
Beam 12	28	905			5.51	4	3.6
Beam 18	28	910			4.71	3-3/4	3.8
Cylinder core 6	28		650			4-3/4	4.2
Cylinder core 12	28		705			4	3.6
Cylinder core 18	28		620			3-3/4	3.8
Cylinder core 19	28			5640		4-3/4	4.2
Cylinder core 20	28			5640		4	3.6
Cylinder core 21	28			5980		3-3/4	3.8

* Tested according to ASTM C 78-64 (CRD-C 16).
** Tested according to ASTM C 496-71 (CRD-C 77).
† Tested according to ASTM C 39-71 (CRD-D 14).
†† Tested according to CRD-C 21.
‡ Tested according to ASTM C 143-71 (CRD-C 5).
‡‡ Tested according to ASTM C 231-72T (CRD-C 41).

Table 13

Summary of Material Properties of Fibrous Concrete Used in the WES Roadway

Property	Average	Standard Deviation	Coefficient of Variation
Flexural strength, psi			
1 day	546	112	0.21
2 days	635	39	0.06
7 days	735	--	--
28 days	933	--	--
Tensile strength, psi			
1 day	308	17	0.05
2 days	467	38	0.08
7 days	608	--	--
28 days	658	--	--
Modulus of elasticity, 10^6 psi			
1 day	4.00	0.59	0.15
2 days	4.31	0.23	0.05
7 days	5.53	--	--
28 days	4.95	--	--
Slump, in.	4-1/8	--	--
Air content, percent	3.8	--	--

Note: Test methods used are presented in Table 12.

Appendix A contains a list of nine additional pavement placements with a brief summary of the features of each. These placement were, in general, small and were placed by personnel who had never worked with fibrous concrete and with limited financial resources and equipment. A great deal has been learned from these placements, but all these factors should be considered by the reader before drawing any conclusions regarding the use of fibrous concrete as a paving material. Placement 9 in Green County, Iowa, is an exception. This is a large project, and a great deal of planning and effort went into its construction. The variables incorporated in the project should begin to answer a number of questions concerning the use of fibrous concrete as a paving material. However, the project was only completed in October 1973, and it will be several years before any real conclusions can be drawn.

Experience gained from these placements has been mainly qualitative and is concerned primarily with construction practices and the response of fibrous concrete slabs to conditions other than vehicular traffic. Results from these placements, as well as other placements discussed in this section, will be summarized in the following section.

RESULTS AND ANALYSIS OF TESTS

In this part of the report, the results of the various fibrous concrete pavement tests will be presented and analyzed. The analysis of the accelerated traffic tests consists basically of a comparison of the structural performance of the fibrous concrete with the performance of plain concrete. The tests of the structural layers test section provide some information on joint performance. Results from the field tests pertain primarily to construction, joint requirements, and general behavior.

RESULTS FROM CONTROLLED, ACCELERATED TRAFFIC TESTS

The conditions of the fibrous concrete pavements in the keyed longitudinal joint test section and in the structural layers test section as traffic was applied are shown in Figures 55-76 and 77-95, respectively. The coverage levels at failure for each pavement with each type load for the initial crack, shattered slab, and complete failure conditions are presented in Table 14.

ITEM 5, KEYED LONGITUDINAL JOINT TEST SECTION

Figure 55 shows the pavement prior to initiation of traffic with the 360-kip, 12-wheel simulated C-5A assembly. Figures 56-63 illustrate the progressive deterioration of the pavement under traffic. Initial failure was assigned at 350 coverages. This was the level of traffic at which the transverse crack illustrated in Figure 57 first appeared. The condition of the slab at this time was between the conditions illustrated in Figures 56 and 57. The pavement reached the shattered slab condition at 2400 coverages (Figure 59) and complete failure at 6000 coverages (Figure 63). The arc-shaped cracks that developed at the edge of the slabs were attributed to high deflections at the pavement edge which produced pumping (Figure 59) along the edge. The edges of the slabs were thickened to 9 in., which resulted in an increased stiffness parallel to the edge. However, at some distance from the edge, the stiffness perpendicular to the edge was for a 6-in. slab. The thin slab,

Table 14

Coverages at Failure for Controlled, Accelerated Traffic Tests

Failure Condition	Keyed Longitudinal Joint Test Section: Item 5: 360-kip 12-Wheel Assembly	Item 5: 166-kip Dual-Tandem Assembly	Item 3: 360-kip 12-Wheel Assembly	Item 3: 166-kip Dual-Tandem Assembly	Item 3: 240-kip Dual-Tandem Assembly
Initial (2-3 pieces)	350	80	2800	950	--
Shattered slab (6 pieces)	2400	150	5000	--	265
Complete (35 pieces)	6000	320	Did not fail	--	415

Failure Condition	Structural Layers Test Section: Item 1: 200-kip Dual-Tandem Assembly	Item 1: 240-kip Dual-Tandem Assembly	Item 2: 200-kip Dual-Tandem Assembly	Item 2: 240-kip Dual-Tandem Assembly
Initial (2-3 pieces)	1000	200	500	150
Shattered slab (6 pieces)	1800	650	1200	400
Complete (35 pieces)	3000	1010	1770	740

weak subgrade, and large assembly load resulted in large edge deflections, high vertical pressures on the soil, and large tensile stresses at the slab surface. The effects of these parameters are indicated by the transverse cracking, pumping as illustrated in Figure 59, and large permanent deformations as illustrated by the cross sections shown in Figure 96.

Figures 64-67 illustrate the progressive deterioration of item 5 as traffic with the 166-kip, dual-tandem assembly was applied. Initial failure was assigned at 80 coverages. This was the level of traffic at which the longitudinal crack shown in Figure 65 reached the transverse crack shown in Figure 64. The pavement was considered to have reached the shattered slab condition at 150 coverages (prior to the condition shown in Figure 66) and complete failure at 320 coverages. Complete failure was assigned before the pavement reached the condition shown in Figure 67, at which time the pavement was untrafficable. Deterioration under the 166-kip, dual-tandem assembly was much like that occurring under the 360-kip, 12-wheel assembly in that it was characterized by arc-shaped cracking at the slab edges, pumping, and large permanent deformations (especially along the slab edges).

The lack of spalling was evident for traffic with both the 12-wheel and the dual-tandem assemblies. Even at complete failure, Figures 63 and 66 show no evidence of large spalls.

ITEM 3 OVERLAY, KEYED LONGITUDINAL JOINT TEST SECTION

Figure 68 shows the condition of the pavement prior to initiation of traffic with the 360-kip, 12-wheel simulated C-5A assembly. Figures 69-72 show the progressive deterioration of the pavement as traffic was applied. Initial failure was assigned at 2800 coverages. This was the level of traffic at which the condition of the slab was as illustrated in Figure 70. Although the slab had not been completely bisected by a crack, it was felt that the multiple short cracks which existed would be as detrimental to performance as a continuous crack in the slab. Evidence of edge effects are illustrated by the arc-shaped cracks at both

ends of the slab. These were discounted in assigning failure since it was felt that they were caused primarily by construction procedures. The pavement was considered to have reached the shattered slab condition at 5000 coverages. This condition is illustrated in Figure 72.

The cracks in the overlay tended to match the cracks in the old pavement. The overlay was partially bonded to the base pavement, but there was no evidence of reflection cracking prior to traffic. However, as traffic was applied, the cracks which formed were directly over the cracks in the base pavement. The short transverse crack in the foreground in Figure 69 was directly over the first transverse crack from the end in the base pavement as shown in Figure 28. The longitudinal cracking beginning to show in Figure 70 matched the longitudinal joint and two fairly distinct longitudinal cracks in the base pavement shown in Figure 28. As cracking progressed, the pattern of matching cracks became more apparent, as can be seen by comparing Figure 28 with Figures 71 and 72.

The condition of lane 2 of the item 3 overlay prior to initiation of traffic with the 166-kip, dual-tandem assembly is shown in Figure 73. The cracks were caused by the outrigger wheels from the prime mover for the 12-wheel assembly. The cracks were hairline and were held tightly closed. The longitudinal crack corresponded to a crack in the base pavement, and the short transverse cracks corresponded to the transverse contraction joint in the base pavement. This cracking was not considered as representative of the initial failure condition.

Figures 74-76 show the progressive deterioration of the pavement as traffic was applied. Initial failure was assigned at 950 coverages with the 166-kip assembly load. The condition of the slab at this coverage level is illustrated in Figure 74. The transverse crack had progressed to the edge of the slab, and the longitudinal crack ran from the edge to the transverse crack. The load on the dual-tandem assembly was increased to 240 kips after 950 coverages had been applied with the 166-kip assembly load. The pavement was considered to have reached the shattered slab condition after 250 coverages and complete failure after 400 coverages of the 240-kip load. The 950 coverages with the 166-kip

load were converted to 15 equivalent coverages of the 240-kip load with the relative loading index procedure as outlined by Hutchinson.[23] The values shown in Table 14 reflect these additional 15 coverages. The pavement at the shattered slab condition was essentially as shown in Figure 75. Complete failure was assigned before the pavement reached the condition shown in Figure 76.

ITEM 1, STRUCTURAL LAYERS TEST SECTION

Figure 77 shows the condition of the pavement in item 1, lane 1, prior to initiation of traffic with the 200-kip, dual-tandem assembly. Figures 78-81 show the progressive deterioration of the pavement as traffic was applied. Initial failure was assigned at 1000 coverages. This was the level of traffic at which the condition of the slab was as illustrated in Figure 79. Although the slab was not completely bisected by a crack, it was felt the transverse crack and permanent deformation along the longitudinal construction joint would be as detrimental as a continuous crack across the slab. The arc-shaped cracking occurring at the ends of the slab was discounted in determining failure of the slabs. It was felt that this premature cracking was caused by construction procedures. Sufficient compaction of the lean clay in the MESL was not obtained at the ends of the section because of the inability of compaction equipment to operate in this area. The pavement was considered to have reached the shattered slab condition at 1800 coverages. This condition is illustrated in Figure 80. Discounting the arc-shaped cracks at either end, it was felt that the multiple cracking in the interior would represent a structural deterioration of the pavement which would be similar to the slab breaking into 5 or 6 distinct pieces. Complete failure was assigned at 3000 coverages, as illustrated in Figure 81.

Figure 82 shows the condition of the pavement in lane 2 of item 1 prior to initiation of traffic with the 240-kip, dual-tandem assembly. Initial failure was assigned at 200 coverages. This condition is illustrated in Figure 83. Shattered slab failure was assigned at 650 coverages and complete failure at 1010 coverages. The condition at complete failure is shown in Figure 84.

Failure of the pavement under both 200- and 240-kip traffic was characterized by multiple cracking. The cracks did not spall but did ravel around the edges and widen as traffic was applied. The pavements also experienced a maximum permanent deformation of about 0.7 in. in both lane 1 and lane 2. Typical cross sections are shown in Figure 97. The permanent deformations were caused primarily by densification in the lean clay MESL and in the clay subgrade. Density measurements (Table 7) showed only minor increases in average density, but measurements of the modulus of soil reaction showed significant increases, indicating the densification of the lean clay in the MESL and of the subgrade.

The cross sections of permanent deformations in lane 2 (Figure 97b) indicate some upheaval outside the traffic lane. Test pits dug across both lanes failed to reveal any major shear failures in the MESL. Therefore, it is believed that the permanent deformations and upheavals outside lanes 1 and 2 were caused by densification of the lean clay MESL with shear failure in the subgrade. This conclusion, however, does not preclude the possibility of shear having occurred in the MESL. The application of traffic probably caused a kneading or remolding of the lean clay which resulted in its densification. The action may be very similar to that of a sheepsfoot or rubber-tired roller.

ITEM 2, STRUCTURAL LAYERS TEST SECTION

Figure 85 shows the condition of the pavement in item 2, lane 1, prior to initiation of traffic with the 200-kip, dual-tandem assembly. Figures 86-89 shows the progressive deterioration of the pavement as traffic was applied. Initial failure was assigned at 500 coverages. At this coverage level, the longitudinal cracking was more extensive than that shown in Figure 86, but the cracks had not begun to widen as shown in Figure 87. The pavement was considered to have reached the shattered slab condition at 1200 coverages. At this coverage level, some of the longitudinal cracks were beginning to widen, and transverse cracks connecting the longitudinal cracks were beginning to occur. Complete failure was assigned at 1770 coverages. This condition is illustrated in Figure 88. Multiple cracking had occurred and some of the cracks had

widened. Although traffic was continued up to 3000 coverages after repairing the ends of the slab, it was felt that the condition illustrated in Figure 88 constituted complete failure.

Figure 90 shows the condition of the pavement in item 2, lane 2, prior to initiation of traffic with the 240-kip, dual-tandem assembly. Initial failure was assigned at 150 coverages. The cracking at 150 coverages was not quite as extensive as that shown in Figure 91. The cracking was not considered sufficient to consider the pavement failed, but permanent deformations of about 0.5 in. had occurred. Evidence of upheaval was also noted. The shattered slab condition was assigned at 400 coverages and complete failure at 740 coverages. The condition of the slab after 950 coverages is shown in Figure 92. From Figures 91 and 92, it can be seen that cracking and permanent deformation progressed rapidly after 200 coverages.

Deterioration of the pavement in lanes 1 and 2 was characterized by multiple cracking and large permanent deformations. The pavements behaved more like flexible than rigid pavements. Traffic was continued after the slabs were considered completely failed, and permanent deformations of up to 2.1 in. were experienced in lane 1 and up to 3.2 in. in lane 2. Such large permanent deformations are typical of failure in flexible rather than rigid pavement. Typical cross sections of permanent deformations from both lanes are illustrated in Figure 98. The cross sections in Figure 98 show that considerable differential deformation occurred along the longitudinal construction joint in lane 1 and that considerable upheaval occurred outside lane 2. The differential movement in lane 1 indicates that the joint was inadequate, and the upheaval in lane 2 indicates that shear failure occurred in the underlying material.

The failure of the thickened-edge longitudinal construction joint was evident from the differential movements shown in Figure 98 and illustrated in Figures 93 and 94. As traffic was applied along the joint, the north edge of the south slab moved downward relative to the north slab. The thickened edge stiffened the slab parallel to the joint and prevented cracking perpendicular to the joint. However, since there was no load transferred to the adjacent slab, high vertical pressures on the base

and subgrade resulted. This development caused some shearing in the cement-treated base and some densification in the subgrade. The results in Table 7 show that the modulus of soil reaction for the subgrade increased from 85 to 118 pci and for the cement-treated base decreased from 545 to 490 pci. Although the magnitude of the changes is small, their directions indicate densification in the subgrade and shear in the cement-treated base. The test pit shown in Figure 95 confirmed that densification probably occurred.

As traffic was applied in lane 1, the deformation along the joint increased, resulting in longitudinal cracking as shown in Figures 86 and 87. The pavement appeared to behave as if it were cantilevered, with the point of fixity located near the edge of the traffic lane.

Failure of the pavement in lane 2 was caused by shear failures in the cement-treated base and in the subgrade as indicated by the large upheavals occurring outside the traffic lane (Figure 98). Upheavals of up to 2.1 in. occurred along the north edge of the pavement. Modulus of soil reaction tests (Table 7) on the cement-treated base showed a decrease from 545 to 375 pci. This decrease indicates that shear failure occurred in the base course. The magnitude of the upheavals and the fact that upward movement occurred for a considerable distance outside the traffic lane indicate that shear failure occurred in the subgrade. The large deformation initially caused longitudinal cracking in the slab.

ANALYSIS OF RESULTS FROM CONTROLLED, ACCELERATED TRAFFIC TESTS

The performances of the four test items are analyzed in the following paragraphs. Material properties (primarily flexural strength and modulus of soil reaction) were selected to represent average conditions during the period traffic was applied. This selection was necessary since the material properties are affected by both age and the repeated application of load.

The procedure for evaluating the performance of the fibrous concrete pavement consisted of using present criteria and computing an

unreinforced concrete pavement thickness for the test conditions that would have been required for the volume of traffic applied. The methods used in evaluating the test results follow the Corps of Engineers procedure, but the results are compatible with FAA procedure because of the common basis for both procedures.

The required thickness was selected by first computing the standard thickness. The standard thickness is the thickness required for 5000 coverages of the design load based on the initial or, as often referred to, first crack failure criterion. The standard thickness is selected by determining the thickness which will result in a stress σ equal to the design flexural strength R divided by a design factor of 1.3 when the design loading is applied, i.e.,

$$\sigma = \frac{R}{1.3} \tag{2}$$

The selection of a design factor of 1.3 is based on the results of accelerated traffic tests and condition surveys and is explained by Hutchinson.[22] The stress is computed for the edge load and dense liquid foundation condition as developed by Westergaard[38-42] from the influence charts developed by Pickett et al.[43] and Pickett and Ray.[44] The thickness required for the applied traffic was computed by multiplying the standard thickness by the appropriate thickness ratio for the applied coverage level determined from Figures 10-12 presented by Hutchinson.[23]

For the overlay of item 3 from the keyed longitudinal joint test section, the required overlay thickness for 5000 coverages of the required load was computed using the equation

$$h_o = \sqrt[1.4]{h_d^{1.4} - C\left[\left(\frac{h_d}{h_{db}}\right)h_e\right]^{1.4}} \tag{3}$$

where

h_o = overlay thickness for 5000 coverages, in.

h_d = standard thickness of plain concrete pavement determined using the modulus of subgrade reaction of the underlying material, in.

C = condition coefficient for the base pavement depending on its structural condition and the design flexural strength for the overlay

h_e = thickness of the existing pavement, in.

h_{db} = standard thickness of plain concrete determined using the subgrade modulus of the underlying material and the flexural strength of the base pavement, in.

This equation was recommended by Hutchinson[22] for cases in which the flexural strength of the overlay differs from the flexural strength of the base pavement by more than 100 psi. This will usually be the case when fibrous concrete is used to overlay a plain concrete pavement. The standard thickness was modified by multiplying by the appropriate thickness ratios for the applied traffic level. The computed thickness was then compared with the actual thickness of the fibrous concrete, and the comparison was used in modifying present criteria to reflect the performance of the fibrous concrete pavement. Recommended criteria will be presented in the next section of this report.

The deflection of the pavement was also considered. Since the fibrous concrete slabs were relatively thin, they experienced rather large deflections before the flexural strength of the concrete was exceeded. The magnitudes of the deflections and other response parameters were more characteristic of flexible pavement than of rigid pavement. Shear and densification in the underlying material were evident in several of the test pavements. If premature failure in the underlying material was to be minimized, it was felt that, in addition to stress in the slab, some other parameter such as deflection would have to be considered in design.

ITEM 5 AND ITEM 3 OVERLAY, KEYED LONGITUDINAL JOINT TEST SECTION

From the material properties presented in Tables 1-4, the properties presented in Table 15 were selected for analyzing the performance of the pavements.

The concrete modulus of elasticity value used for both items is the average of the values from all tests, both flexural and compressive.

Table 15

Selected Material Properties for Item 5 and the Item 3 Overlay of the Keyed Longitudinal Joint Test Section

Property	Item 5	Item 3 Overlay	Item 3 Base Pavement
Modulus of elasticity of concrete E_c, 10^6 psi	5.6	5.6	6.4
Modulus of soil reaction k, pci	75		100
Nominal slab thickness h, in.	6.0	4.4	9.5
Poisson's ratio of concrete ν_c	0.2	0.2	0.2
Flexural strength of concrete R_c, psi	940	1050	750

The modulus of soil reaction values were selected somewhat on the high side. The foundation became stiffer with traffic, and the values selected were closer to the after-traffic measurements than to the as-constructed measurements.

Average measured thickness values were used, and a value for Poisson's ratio of 0.2 was assumed. A condition coefficient of 0.35 was assigned the base pavement in lane 1 of item 3, and 1.00 was assigned in lane 2. The fibrous concrete flexural strength used in the analysis was selected with the aid of Figure 99. This figure shows flexural strength as a function of age for the beams molded during construction, the strength of beams sawed from the pavement slabs, and the time periods during which traffic was applied.

A value of 940 psi was chosen as the flexural strength for both lane 1 and lane 2 of item 5. The concrete showed relatively little strength gain from the time traffic was started until completion of traffic, and the strengths from the beams and cores taken from the slabs were consistent with the strengths from the molded beams. There was also considerable scatter in the results indicating nonuniform concrete in the slabs. Therefore, the selection of one value was considered

sufficiently accurate for the analysis.

A value of 1050 psi was chosen as the flexural strength for both lane 1 and lane 2 of the item 3 overlay. The molded beams showed a strength gain of about 100 psi from the time traffic was started until traffic was completed. The beams and cores taken from the pavement slabs indicated lower strengths than did the molded beams. This result was not consistent with what was expected since the sawed beams were smaller (4 by 4 in.), a characteristic which should have resulted in higher strengths than those of the 6- by 6-in. molded beams. However, differences in curing conditions could have caused the differences in strengths. This item was an overlay and did not have access to moisture from the subgrade as do slabs on grade. Therefore, both surfaces were usually dry, with only the top surface subjected to moisture during precipitation. On the other hand, a slab on grade is exposed to the moisture in the underlying material. Because of the erratic nature of the values from strength measurements, the strength used in the analysis was chosen as slightly higher than the average strength obtained for the specimens from the slabs. It was felt that this value would be more representative of the strength of the concrete in the pavement than a higher value based on the molded and laboratory cured specimens.

With the material properties presented in Table 15, thickness requirements were computed for the applied traffic levels using the procedure outlined previously. The computed thickness values are presented in Table 16. The next to the last column in Table 16 shows ratios of the computed thickness of plain PCC to the actual thickness of fibrous concrete. For all failure modes, the ratio indicates that the fibrous concrete pavement performed better than current criteria would have predicted plain concrete pavement to perform. The average ratio for both items, both loads, and all failure conditions is 1.58 and the standard deviation is 0.123. The ratios suggest that the required thickness of fibrous concrete is about two-thirds of that required for plain concrete.

The last column in Table 16 shows the ratios of the actual fibrous concrete thickness to the computed standard thickness of plain PCC.

Table 16

Comparative Performance of Item 5 and the Item 3 Overlay of the Keyed Longitudinal Joint Test Section

Failure Condition	Assembly	Coverage Level	Required Percent Standard Thickness	Standard PCC Thickness in.	Required PCC Thickness in.	Ratio of Required PCC to Actual Fibrous Concrete Thickness	Ratio of Actual Fibrous Concrete to Standard PCC Thickness
			Item 5				
Initial	360-kip, 12-wheel	350	92	10.2	9.4	1.56	0.59
Initial	166-kip, dual-tandem	80	88	12.7	11.1	1.85	0.47
Shattered slab	360-kip, 12-wheel	2400	92	10.2	9.4	1.56	0.59
Shattered slab	166-kip, dual-tandem	150	76	12.7	9.7	1.61	0.47
Complete	360-kip, 12-wheel	6000	94	10.2	9.6	1.60	0.59
Complete	166-kip, dual-tandem	320	71	12.7	9.0	1.50	0.47
			Item 3 Overlay				
Initial	360-kip, 12-wheel	2800	98	7.4	7.3	1.66	0.59
Initial	166-kip, dual-tandem	950	95	6.2	5.9	1.34	0.71
Shattered slab	360-kip, 12-wheel	5000	95	7.4	7.1	1.61	0.59
Shattered slab	240-kip, dual-tandem	265	76	9.6	7.3	1.66	0.46
Complete	240-kip, dual-tandem	415	68	9.6	6.5	1.46	0.46

These ratios are approximately one-half. The ratios are plotted versus the applied coverage levels in Figures 100 and 101. Also shown in Figures 100 and 101 are curves for plain PCC as presented by Hutchinson.[23] The locations of the points illustrate the improved performance of the fibrous concrete pavements.

Maximum static elastic deflections measured before traffic was applied are plotted versus the coverage levels in Figure 102. Although there are not enough points to draw any definite conclusions, the trend seems to be, as would be expected, that the allowable traffic volume increases as elastic deflection decreases. No reliable measurements were available for the 360-kip, 12-wheel assembly on the item 3 overlay or for the 240-kip, dual-tandem assembly.

ITEMS 1 AND 2, STRUCTURAL LAYERS TEST SECTION

From the material properties presented in Tables 7-11, the properties presented in Table 17 were selected for analyzing the performance

Table 17

Selected Material Properties for Items 1 and 2 of the Structural Layers Test Section

Property	Item 1		Item 2	
	Lane 1	Lane 2	Lane 1	Lane 2
Modulus of elasticity of concrete E_c , 10^6 psi	5.6	5.6	5.6	5.6
Modulus of soil reaction k , pci	225	225	500	500
Slab thickness h , in.	7.0	7.0	4.0	4.0
Poisson's ratio of concrete ν_c	0.2	0.2	0.2	0.2
Flexural strength of concrete R_c , psi	1000	1200	1000	1050

of the pavements. The concrete modulus of elasticity used for both lanes of both items is the average of all flexural and compressive values. Nominal values of thickness were used, and Poisson's ratio of 0.2 was assumed.

The modulus of soil reaction values were selected on the high

side. The MESL and subgrade in item 1 underwent considerable densification during traffic, which resulted in increased stiffness. The value of 225 pci selected represents the after-traffic conditions more closely than it does as-constructed conditions.

The cement-treated base in item 2 experienced shear failure during traffic, which resulted in a decrease in the stiffness. A value of 500 pci was selected for the modulus of soil reaction to represent both lanes. For lane 1, this value may be unconservative, and for lane 2, it may be too conservative. However, the effects of such errors on the analysis will be small.

Figure 103 was used in selecting the flexural strength to use in the analysis. This figure shows flexural strength as a function of age for beams molded during construction, the strength of beams sawed from the pavement slabs, and the time periods during which traffic was applied.

A value of 1000 psi was chosen as the flexural strength for lane 1 of item 1, and a value of 1200 psi was chosen for lane 2 of item 1. The field-molded specimens showed a considerable increase in flexural strength with time. However, the specimens sawed from the slabs indicated a smaller strength gain than the molded specimens. The difference in the molded beams and sawed beams can be explained by a difference in molding and curing conditions as well as beam size. As with the overlay of item 3 of the keyed longitudinal joint test section, the slab did not have access to moisture in the underlying material because of the impervious membrane. This may have affected the strength gain and caused the flexural strength values to be lower than those of the molded beams which were moist-cured. The beams sawed from the slabs were also larger than the molded beams, a characteristic which could have caused a reduction in measured strength. The value of 1000 psi selected for lane 1 is consistent with results from the molded specimens and is approximately equal to the average of the values from the sawed beams. The value of 1200 psi selected for lane 2 is lower than that obtained in the after-traffic tests on the molded beams but higher than the average of the values for the sawed beams. It was felt that the beams sawed from the

slabs better represented the strength of the concrete in the slabs.

A value of 1000 psi was chosen for the flexural strength for lane 1 of item 2, and a value of 1050 psi was chosen for lane 2 of item 2. The molded beams and the beams sawed from the slabs showed a consistent gain in strength with age. The results obtained from lane 1 were very consistent. The beams sawed from lane 2 showed a larger increase than was indicated by the molded beams. The value of 1000 psi selected for lane 1 is consistent with results from both the molded and sawed specimens. The value of 1050 psi selected for lane 2 is higher than the results from the after-traffic tests on the molded beams but lower (60 psi) than the results from tests of the sawed beams. This difference is somewhat inconsistent with the criterion used in the selection of the strength for the other items since the usual procedure was to select values which were larger than or approximately equal to the values for the sawed beams. However, in this case, some weight was given to the fact that the molded beams showed an increase in strength, which was consistent with results for the sawed beams.

With the material properties tabulated in Table 17, thickness requirements were computed for the applied traffic levels using the procedure outlined previously. The computed thickness values are presented in Table 18. The next to last column in Table 18 shows ratios of the computed thickness of plain PCC to the actual thickness of fibrous concrete. For the initial (or first crack) failure mode, the ratios show that the fibrous concrete pavement performed better than current criteria would have predicted for plain PCC pavement. However, the ratios are not as large as they were for the two items from the keyed longitudinal joint test section previously considered. For the shattered slab and complete failure modes, the ratios decrease. This development reflects the failure of the underlying material. The criterion used for the calculations is for plain PCC pavement in which failure of the underlying material is not a factor in the performance, i.e., pressure on the underlying material is insufficient to cause shear or densification. However, for these two test items, the slabs were thin enough so that the pressures on the underlying material were sufficient to cause densification

Table 18

Comparative Performance of Items 1 and 2 of the Structural Layers Test Section

Failure Condition	Assembly	Coverage Level	Required Percent Standard Thickness	Standard PCC Thickness in.	Required PCC Thickness in.	Ratio of Required PCC to Actual Fibrous Concrete Thickness	Ratio of Actual Fibrous Concrete to Standard PCC Thickness
			Item 1				
Initial	200-kip, dual-tandem	1000	94	10.3	9.7	1.38	0.68
Initial	240-kip, dual-tandem	200	89	10.3	9.2	1.31	0.68
Shattered slab	200-kip, dual-tandem	1800	83	10.3	8.6	1.22	0.68
Shattered slab	240-kip, dual-tandem	650	76	10.3	7.8	1.11	0.68
Complete	200-kip, dual-tandem	3000	76	10.3	7.8	1.12	0.68
Complete	240-kip, dual-tandem	1010	66	10.3	6.8	0.97	0.68
			Item 2				
Initial	200-kip, dual-tandem	500	75	8.3	6.2	1.56 (1.93)	0.48
Initial	240-kip, dual-tandem	150	72	9.4	6.8	1.70 (2.10)	0.43
Shattered slab	200-kip, dual-tandem	1200	59	8.3	4.9	1.22	0.48
Shattered slab	240-kip, dual-tandem	400	51	9.4	4.8	1.20	0.43
Complete	200-kip, dual-tandem	1770	48	8.3	4.0	1.00	0.48
Complete	240-kip, dual-tandem	740	37	9.4	3.5	0.88	0.43

in the MESL and underlying subgrade in item 1 and shear failure in the cement-treated base and shear failure and densification in the underlying material in item 2. It is believed that the failure of the underlying material accelerated the deterioration of the slabs. It should be noted that the computed values for initial failure are based on a criterion which permits a reduction in thickness for high-strength foundations (modulus of soil reaction of 300 pci or greater). The numbers in parentheses in Table 18 (for item 2) reflect no reduction in required thickness for high-strength foundations and are in agreement with the performance observed in the previously discussed tests, i.e., the required thickness of fibrous concrete is about two-thirds of the required thickness of plain PCC. Recommended criteria reflecting no decrease in thickness for high-strength foundations are presented in the following section of this report.

The last column in Table 18 presents ratios of actual fibrous concrete thickness to the computed standard thickness of PCC. The ratios are plotted versus the applied coverage levels in Figures 104 and 105. Also shown in these figures are curves for plain concrete as presented by Hutchinson.[23] The locations of the points indicate that the fibrous concrete performed better than plain PCC for most cases. One exception was for the complete failure mode for item 1 with the 240-kip, dual-tandem loading. Complete failure of item 2 with the 240-kip, dual-tandem loading would also be an exception since the ratio is less than one. However, this is not apparent from Figure 105 since a curve for complete failure with a modulus of soil reaction k of 500 pci is not shown.

Maximum static elastic deflections measured before traffic was applied are plotted versus the coverage levels in Figure 106. The general trend appears to be, as would be expected, that the allowable traffic volume increases as the elastic deflection decreases. The points for the 200-kip, dual-tandem loading were along the longitudinal joint and would be expected to be somewhat different even though load transfer was adequate. The measurements fail to show any definite trends in this respect, and the scatter shown is inherent in this type testing.

RESULTS FROM FIELD INSTALLATIONS

The results from the field installations are presented in the following paragraphs. Results from these installations deal primarily with the construction and behavior of fibrous concrete pavements under field conditions.

TAMPA OVERLAYS

The construction of these pavements illustrated that fibrous concrete can be produced and placed with conventional paving equipment. The construction also demonstrated that with proper batching and mixing techniques balling of the fibers can be essentially eliminated and that with proper equipment low-slump (1 to 2 in.) fibrous concrete can be placed. The manual techniques used for introducing the fibers emphasized the need for bulk-handling of fibers. This problem is being studied and will be considered later.

The overlays were partially bonded, but no reflection cracking was observed prior to opening for traffic. However, as traffic has been applied, cracking has developed in the overlays as illustrated in Figure 107. The cracks in the overlay coincide with joints or cracks in the base pavement. The cracks in the overlay which correspond to joints in the base pavement have widened sufficiently to cause failure (bond or fracture) of the fibers across the cracks. The condition of these cracks illustrates that, for partially bonded fibrous concrete overlays, as with plain or reinforced concrete, joints in the overlay and base pavement should be matched. The cracks in the overlays corresponding to the cracks in the base pavement have not widened significantly, indicating that the fibers across the crack are still effective.

WES ROADWAY

This pavement was constructed primarily to study the crack pattern which would develop in a fibrous concrete pavement and the nature of the cracks that would form. The crack pattern that developed is shown in Figure 108. The slab lengths ranged from 63 to 240 ft. The average slab length was 126.4 ft, and the standard deviation of the

slab length was 56.3 ft. All seven cracks in the pavement occurred during the first night following concrete placement. The cracks widened considerably, i.e., they were not hairline cracks held tightly closed by the fibers such as have been noticed for load-induced cracks. No additional cracking has been observed to this date even though the concrete temperature has dropped from a high of 120° F on the day the pavement was constructed to a low of about 35° F.

A plot of crack width versus slab temperature for a typical crack is shown in Figure 109. This figure shows, as expected, that the crack width increased as the temperature decreased. Also, if the data points are examined carefully, it will be noted that the width increased with age for several days after construction until a stable condition was reached in which the crack width was basically a function of only temperature. The slopes of the lines between two points for a particular day are consistent, and, with the exception of the measurements made on 28 February 1974, the magnitudes of the crack widths appear to follow a definite trend. The measurements made on 28 February 1974 indicate that a gradual noncyclic or permanent opening of the crack was occurring.

Maximum crack widths (measured at a slab temperature of 36° F) are shown plotted in Figure 110 versus the length of slab contributing to movement at the crack (one-half of the sum of the lengths of slabs on either side of the crack). This figure illustrates the problem of long slabs, i.e., the crack opening will be proportional to the slab length. This problem indicates that the number of joints should be reduced, but such a reduction will increase difficulties involved in providing adequate load transfer and keeping the joints sealed. Because of the probability of large joint openings, it may be advisable to maintain a joint spacing consistent with current practices (15 to 25 ft) with say 50 ft as a maximum if steps are taken to provide adequate load transfer (dowels) and proper seal (preformed compression seals).

The magnitudes of the joint openings which occurred were magnified by the conditions under which the pavement was constructed. The air temperature during placement reached a high of 95° F. This combined with the high cement content (9 sacks per cubic yard) resulted in high slab

temperatures (up to 120° F measured) during hydration. Therefore, the measured crack widths shown in Figure 110 correspond to a temperature drop in the slab of about 84° F. The dashed curve shown in Figure 110 is computed from the formula

$$\Delta X = Xe\Delta t \tag{4}$$

where

ΔX = slab movement, ft

X = slab length, ft

e = thermal coefficient for concrete (assumed equal to 0.000006 per degree Fahrenheit)

Δt = temperature drop (84° F)

The correlation between the measured values and the computed relationship indicates that the large measured values are reasonable.

The fact that all the cracks occurred during the night after the pavement was placed points out another factor which must be considered in the construction of fibrous concrete pavement. The high cement contents normally used will accelerate hydration, and therefore the temperature rise should be higher. When fibrous concrete is placed during warm weather, the sawing of contraction joints must be closely coordinated in order to avoid shrinkage cracking.

TESTS CONDUCTED BY OTHER AGENCIES

Visual examination of cores taken from the slab constructed at ORDL in 1967 (Placement 1 in Appendix A) showed no evidence of fiber corrosion in the uncracked concrete. Cores taken across a shrinkage crack showed that the exposed fibers were completely deteriorated. The crack was about 1/2 in. wide, and the fibers were completely exposed to air and moisture.

Placements 3 and 4 were slabs which contained leave-outs for the installation of outlets for utilities or drainage structures. Normally, reinforcement is placed around such openings to hold the cracks that form tightly closed. In the fibrous concrete slabs, the cracking around

the openings has been contained, and the short cracks that have formed are being held tightly closed.

Placement 5 illustrates, as did the WES roadway, that shrinkage cracking will occur in long fibrous concrete slabs, that the resulting slabs are longer than can be obtained with conventional PCC, and that the crack widths will be larger since they are proportional to the slab lengths. The 500-ft-long slab was placed on 9 August 1971 (air temperature from 78° to 85° F). On 10 August, a crack occurred approximately 265 ft from one end of the pavement. This crack was about 1/2 in. wide when it was observed on 19 April 1972 (temperature of approximately 45° F). During December 1971, a crack formed about 95 ft from the north end. This crack was about 3/8 in. wide when observed on 19 April 1972.

Placement 8 illustrated several construction problems and several response problems. The overlay was placed directly on the base pavement. Proper grade control was not exercised and in several areas the thickness was only about 1 to 2 in. thick, whereas the design thickness was 3 in. A deficiency of 1 or 2 in. would not be as severe for a 6- or 8-in. PCC overlay as it is for say a 3- or 4-in. fibrous concrete overlay.

The air temperature during construction of Placement 8 ranged from about 40° to 55° F. Because of the thinness of the slabs, the lower temperatures affected the strength gain of the concrete much more than they would have affected that in a thicker slab. The slow strength gain with time combined with the necessity to open the pavement to traffic at the earliest possible date led to early failure of parts of the pavement having a low fiber content.

The bond between the overlay and the base pavement was lost over most of the area after about 6 months. After bond was lost, temperature and moisture gradients through the slabs caused warping or curling of the thin slabs. The warping of the thin slabs resulted in high flexural stresses with traffic and a subsequent rapid deterioration of the overlays. Deterioration was more rapid in those areas which had 120 lb of fiber per cubic yard than in those containing 200 lb of fiber per cubic yard. The deterioration was accentuated by deficiencies in thickness at certain locations. Those areas with 120 lb of fiber per cubic yard

which were only 1 to 2 in. thick were severely deteriorated after only 3 months. Approximately three-fourths of the pavement was removed after about 10 months. A complete discussion of the performance of the overlays is given by Arnold and Brown[13] and Arnold.[45]

The Greene County, Iowa, project was completed in October 1973. This project incorporated a number of variables, and study of it should begin to answer a number of questions concerning the use of fibrous concrete for pavements.

Several important questions were answered during construction. This placement constituted the first time that mechanical means were used to introduce the fibers into the batching sequence. A vibrating hopper with a screen for the bottom was used to disperse the fibers and dispense them onto a conveyor belt which fed them onto the aggregate charging belt of the central-mix plant. Fibers for a batch were hand-dumped from boxes into the bucket of a front-end loader. The front-end loader then dumped the fibers into the hopper. The equipment still requires a great deal of refinement, but it did illustrate that such a procedure is feasible and necessary for the production of large quantities of fibrous concrete.

It was demonstrated that it is possible to place thin (as small as 2-in.) bonded, partially bonded, or unbonded fibrous concrete with slip-form paving equipment. Adjustments must be made to equipment and concrete workability, but placement is possible.

An inspection of the pavements after service of about 8 months revealed several aspects concerning the performance of the fibrous concrete pavement. The 3-in. sections performed significantly better than the 2-in. sections. The 2-in. sections tended to begin cracking along the edges and joints no matter what the bond condition. However, after 8 months, the deterioration was most serious in the unbonded sections and seemed to be associated with curling or warping of the slabs. The cracking that occurred in the bonded and partially bonded sections appeared to be reflections of cracks in the base pavement. Some of the cracks widened considerably, depending on the cracks in the base slab, but some remained closed. The 2-[illegible] in.-long fibers appear to be more

effective in holding the cracks closed than are the 1-in.-long fibers. The sections in which the concrete contained 160 lb of fiber per cubic yard performed better than the sections in which the concrete contained 60 or 100 lb of fiber per cubic yard.

RECOMMENDED DESIGN CRITERIA

PAVEMENT DESIGN

Requirements for an adequate soil investigation and evaluation and material requirements for bases and subbases for conventional plain and reinforced concrete pavements are applicable to fibrous concrete. Design procedures currently used where special soil and environmental conditions exist are also applicable to the design of fibrous concrete pavements. Currently used traffic area designations and traffic distribution procedures are applicable to fibrous concrete.

THICKNESS REQUIREMENTS

It is recommended that the required thickness be computed based on the limiting stress criterion. The maximum tensile stress computed at the slab edge acting parallel to the edge will be limited by the strength of the concrete.

Thickness requirements will be computed in terms of the thickness required for a specified volume of traffic. The Corps of Engineers concept of standard thickness was used in formulating the design methodology. The standard thickness for a particular loading or type aircraft is defined as the thickness required for 5000 coverages and is the thickness such that the induced stress in the slab (computed stress σ multiplied by 0.75 to account for 25 percent load transfer) is equal to the concrete flexural strength R_c divided by a design factor of 1.3. In order to determine the fibrous concrete thickness required for 5000 coverages or any other coverage level, the computed standard thickness for PCC is multiplied by the thickness ratios obtained from the curve for fibrous concrete in Figure 111.

The curve for fibrous concrete is based on the initial (first crack) failure criterion, with no allowance for reduced thickness with high-strength foundations. Current Corps of Engineers criteria permit a reduction in thickness of PCC pavements on foundations which have a modulus value of 300 pci or greater. The curves in Figures 104 and 105 which are labeled for subgrade modulus values of 300 pci or more reflect

the allowable thickness reduction for high-strength foundations. The points for item 2 of the structural layers test section plotted in Figure 105 also reflect this reduction. However, current FAA criteria for unreinforced concrete permit no reduction for high-strength foundations, and, after evaluating the performance of item 2, it was decided that such a reduction would not be in agreement with the conservative nature desired in the design criteria. Therefore, the points plotted in Figure 111 for item 2 are based on no reduction in thickness for high-strength foundations. These values are presented in Table 19.

Table 19

Comparative Performance Based on Initial Failure Criterion of Item 2 of the Structural Layers Test Section

Loading	Coverage Level	Required Percent Standard Thickness	Standard PCC Thickness in.	Required PCC Thickness in.	Ratio of Required PCC to Actual Fibrous Concrete Thickness	Ratio of Actual Fibrous Concrete to Standard PCC Thickness
200-kip dual-tandem	500	93	8.3	7.7	1.93	0.48
240-kip dual-tandem	150	89	9.4	8.4	2.10	0.43

The curve for fibrous concrete in Figure 111 is drawn through the upper range of the points obtained from the controlled, accelerated traffic tests and is parallel to the curve for plain PCC. It should be noted that the assigned definition of initial or first crack failure for the fibrous concrete pavement was rather arbitrary. For the fibrous concrete items, initial failure was assigned when the structural condition of the pavement was assumed to be comparable to that of plain concrete pavement when the slabs are broken into two or three pieces (definition of initial or first crack failure of plain concrete pavement).

Another factor which will influence the criteria is the relationship between the structural condition of the pavement and the functional condition of the pavement. For plain concrete pavement, the relationship between structural failure and functional failure has been

established by field observations. For fibrous concrete, it was assumed that the same relationship was valid, since only the structural condition of the fibrous concrete in the test sections could be evaluated and related to the comparable structural condition of plain concrete pavement. An additional limitation of the proposed criteria is the required extrapolation of the data for coverages greater than about 1000. It was assumed that the relationship between the performance of plain and fibrous concrete established for coverage levels less than 1000 was valid for coverage levels greater than 1000. These factors plus the unknown effects of long-term environmental factors on the performance of fibrous concrete pavement have led to conservative assumptions in the development of the criteria for estimating required thickness of fibrous concrete.

Design curves developed using the proposed criteria are presented in Appendix B. Curves for civil and military aircraft are provided in current FAA and Department of the Army format.

VERTICAL DEFLECTION LIMITATIONS

Since thickness requirements for fibrous concrete will be considerably less than those for plain PCC, the pavement structure will be more flexible. The deflections experienced by fibrous concrete pavements will be greater than those for equivalent plain PCC pavements and can lead to failure of the underlying material. Criteria are proposed for controlling fibrous concrete pavement deflection. These criteria are designed to minimize the possibility of pumping and densification of or shear in the underlying material or loss of load transfer across joints.

Elastic deflections measured from test sections reported by Grau,[24] Burns et al.,[35] ORDL,[46] Mellinger et al.,[47] and Ahlvin et al.[48] were used to establish limiting deflections. These values do not reflect limiting or maximum deflections which the foundation material could have withstood. Rather, they indicate deflections which proved to be acceptable for the entire pavement system.

Only a few data points are available for fibrous concrete. As a

consequence, it was necessary to use data from plain and reinforced pavement to develop relationships between elastic deflection and pavement performance. It was assumed that the trends shown by the data for the plain and reinforced pavements would hold for fibrous concrete pavement. As with the limiting stress criterion, it was necessary to extrapolate the relationships to large coverage levels since most of the data from the test section studies were for less than 10,000 coverages.

Measured values of elastic deflection are shown plotted in Figure 112 versus the coverage level at which the pavement for which the deflection was measured failed. The deflections were obtained by loading the pavement with the gear which was used to apply traffic and measuring the vertical deflection of the surface with a rod and level, or with electronic instruments for those test items where instrumentation was installed. There is a great deal of scatter in the data points which is caused by several factors. The most obvious is the inherent scatter or variation associated with experimental measurements such as these. Another is that there is probably no unique value of deflection which would be obtained for all pavements which provide the same performance. Rather, the limiting deflection would depend on the composition of the pavement, i.e., layer thickness, material strength, etc. Therefore, the curve drawn through the points for the plain and reinforced concrete pavement is probably an approximation of a family of curves.

The curve indicates that the limiting deflection becomes constant (0.05 in.) for coverage levels greater than about 30,000. No data are available to validate this trend, but it may be argued, based on a knowledge of material response to load, that there is a limiting coverage level such that if the underlying material has experienced a certain deflection the indicated number of times without failure then it will probably withstand an infinite number of load applications without failing. This limiting coverage level is probably less than 30,000 and is probably a function of material type. As a consequence, for those cases in which the pavement is designed for a large number of coverages, the performance of the pavement will be controlled exclusively by fatigue

of concrete in the slab. Conversely, for lower coverage levels, the thickness of the slabs may be such that the response of the underlying material may significantly affect the performance of the pavement, i.e., performance of the pavement (and therefore the design) may not be controlled exclusively by fatigue of the concrete. Therefore, the purpose of the limiting deflection criterion is to insure that pavements designed on the basis of the limiting stress (fatigue) criterion will perform as designed and not fail prematurely because of factors not considered in the design.

The measured elastic deflections for the fibrous concrete pavements are shown within the shaded area in Figure 112. It can be seen that the majority of these deflections are larger than deflections for comparable plain and reinforced concrete. The curve through these points was drawn parallel to the curve for plain and reinforced concrete and extrapolated for coverage levels greater than 1000.

If it were possible to compute pavement deflections accurately, the relationship between deflection and coverages shown in Figure 112 could be used directly in the design procedure. However, experience has shown that there are discrepancies between measured and computed values; thus, it will be necessary to establish a relationship between measured and computed values. In order to maintain consistency between analytical procedures for predicting pavement response, elastic deflections were computed based on slab theory as proposed by Westergaard[38-42] from influence charts developed by Pickett et al.[43] and Pickett and Ray.[44] Elastic deflections (interior load condition) for the test pavements were computed using measured slab and foundation properties. These computed elastic deflections, as well as measured deflections, are plotted versus initial failure coverage levels in Figure 113. From this figure, it can be seen that the computed defletions are all smaller than the measured deflections but that the same trend exists. The curve for computed elastic deflections was drawn through the points parallel to the curve for measured elastic deflections. This curve indicates that the limiting deflection computed for the pavement becomes constant (0.05 in.) for coverage levels greater than about 30,000. This

relationship between elastic deflection and traffic should be used in design for limiting deflections. The elastic deflection for pavements designed on the basis of the limiting stress criterion should be checked to insure that it does not exceed the limiting value determined from Figure 113.

Curves for computing elastic slab deflection for civil and military aircraft are provided in Appendix B. In addition, tables of limiting deflection obtained from Figure 113 are also provided. The curves and tables are in a format which is compatible with the format used for the design curves based on limiting stress.

JOINT REQUIREMENTS

Variations in temperature and moisture content cause volume changes in fibrous concrete just as they do in plain concrete. These volume changes cause stresses in the concrete which can produce uncontrolled cracking in the pavement if the pavement is not properly jointed. In addition, construction joints will occur as a result of construction operations.

As a result of the increased tensile strength of fibrous concrete, it may be possible to increase joint spacing, thereby reducing the number of joints and the problems associated with joints. It is recommended that the minimum spacing of longitudinal joints be increased to 25 ft for all slab thicknesses. This spacing will eliminate the need for constructing hinged or dummy contraction joints in the center of 25-ft paving lanes.

In order to provide adequate load transfer across longitudinal construction joints and to protect the underlying material against premature failure, it is recommended that longitudinal construction joints be either keyed-and-tied, doweled, or thickened edge with a key. The dimensions of the key and thickened edge should be as recommended in FAA Advisory Circular AC 150/5320-6A,[26] Department of the Army Technical Manual TM 5-823-3,[49] or TM 5-824-3,[50] except that the dimensions of the key should be based upon the thickness of the thickened edge. Because of construction problems that are associated with placement of dowels in

longitudinal construction joints during slip-form paving and with shaping stabilized materials to form the thickened edge, the keyed-and-tied joint appears to be the most satisfactory. However, some freedom of movement must be provided. It is recommended that a maximum pavement width of 100 ft be tied together. For taxiways, which are usually constructed in three or four 25-ft-wide lanes, all joints may be tied. For runways, which are usually constructed in six or eight 25-ft-wide lanes, the four center lanes may be tied together with the outside joints either doweled or thickened edge with a key. For apron pavements constructed in 25-ft-wide lanes, the jointing layout will have three adjacent joints keyed-and-tied with every fourth joint either doweled or thickened edge with a key.

Transverse joint spacing may also be increased for fibrous concrete without resulting in cracking caused by volume change in concrete. Experimental placements (Placement 5, Appendix A, and the WES roadway) indicate that lengths of around 100 ft can be attained with 4-in.-thick slabs. These placements also indicate that openings proportional to the slab lengths will occur at transverse cracks or joints and that for 100-ft-long slabs these can be considerable. Because of the large movements which will occur for 100-ft-long slabs, a maximum transverse joint spacing of 50 ft is recommended. For slabs greater than 6 in. in thickness, the spacing may be increased, but special precautions should be taken to insure adequate load transfer and proper sealing. It is recommended that dowels and preformed compression seals be provided at all transverse joints where the joint spacing is greater than 50 ft.

OVERLAY DESIGN

Requirements for an adequate evaluation of the existing pavement for conventional plain and reinforced overlays are also applicable for fibrous concrete overlays. Currently used procedures for preparing the surface of the old pavement are applicable for fibrous concrete. For overlays that are designed to restore the load-carrying capacity of existing pavements in poor structural condition or to increase the

load-carrying capacity of existing pavements by providing additional thickness, the minimum recommended thickness is 4 in.

THICKNESS REQUIREMENTS

Procedures are provided for determining thickness requirements for fibrous concrete overlays of flexible pavement and partially bonded or unbonded overlays of rigid pavement. While only partially bonded overlays have been tested, the procedure for unbonded overlays was extrapolated from this procedure by assuming that the performance of an unbonded fibrous concrete overlay will be similar to the performance of an unbonded plain concrete overlay.

It is recommended that fibrous concrete overlays of flexible pavement be designed as a slab on grade by considering the flexible pavement as a base course. The maximum value to be used as the design subgrade modulus should not exceed 500 pci.

The thickness of partially bonded overlays of rigid pavement will be determined from the equation

$$h_o = (0.75) \sqrt[1.4]{h_d^{1.4} - C\left[\left(\frac{h_d}{h_{db}}\right)h_e\right]^{1.4}} \qquad (5)$$

where

h_o = required thickness of the fibrous concrete overlay, in.

h_d = required thickness of an equivalent single slab of plain concrete having a flexural strength equal to the flexural strength of the fibrous concrete used for the overlay, in.

h_{db} = required thickness of an equivalent single slab of plain concrete having a flexural strength equal to the flexural strength of the concrete in the existing pavement, in.

h_e = thickness of the existing pavement, in.

C = coefficient describing the condition of the existing pavement as presented in AC 150/5320-6B or TM 5-823-3

It is recommended that the thickness of unbonded overlays be determined from the equation

$$h_o = (0.75)\sqrt{h_d^2 - C\left[\left(\frac{h_d}{h_{db}}\right)h_e\right]^2} \qquad (6)$$

where the variables are as identified above. The factor 0.75 in Equations 5 and 6 reflects the differences between thickness requirements for plain and fibrous concrete pavement as indicated by the vertical distance between the curves in Figure 111.

JOINT REQUIREMENTS

Joints in partially bonded fibrous concrete overlays should coincide with joints in the base pavement; however, when the transverse contraction joint spacing in the base pavement is 15 ft or less, every other joint in the overlay may be eliminated. It is not necessary for joints to be over similar joints. Longitudinal contraction joints in the base pavement may be spanned in partially bonded overlays. Longitudinal construction joints in partially bonded overlays should be matched with longitudinal construction joints in the base pavement.

For unbonded overlays, it is likewise unnecessary for the joints to coincide with joints in the base pavement. Longitudinal construction joints in unbonded fibrous concrete overlays should be either doweled or keyed-and-tied. Longitudinal construction joints in partially bonded overlays should be doweled.

RECOMMENDED CONSTRUCTION PRACTICES

The addition of fibers to concrete complicates the selection of a mix design. It is recommended that a rather extensive mix design be carried out using available materials in order to select a mix that will be economical, workable, and provide the required strength and durability. Guidelines for mix selection are outlined in the following section.

The addition of fibers to the concrete also requires some changes in batching, mixing, and placing procedures. The major differences will be in batching and mixing because the shape of the fibers requires that they be handled differently than aggregate, cement, or water because of the tendency of the fibers to form into balls. In the following paragraphs, batching, mixing, and placing procedures will be discussed.

MIX DESIGN CONSIDERATIONS

The large surface area to volume ratio of the steel fibers requires an increase in the paste necessary to insure that the fibers and aggregate are coated. The shape of the fibers also requires an increase in the paste necessary to insure that the fibers are properly dispersed in order to avoid harsh mixes which are difficult to place. Cement contents from 550 to 950 lb per cubic yard have been used with water-cement ratios between 0.4 and 0.6, as reported in an American Concrete Institute state-of-the-art paper.[51]

The size, type, and volume of fibers will influence other parameters in the mix. The following are two general rules regarding the influence of fibers:

a. An increase in fiber content results in increased strength and decreased workability. Experience has shown that fiber contents in excess of 2 percent by volume are difficult to mix.[51]

b. An increased fiber aspect ratio (length to diameter or equivalent diameter) results in increased strength and decreased workability. For proper mixing, the maximum aspect ratio should be about 100.[51]

There are presently only a few sizes of fiber commercially available. Therefore, the usual procedure is to select a type of fiber and

then trade off strength for economy and workability. The most commonly used fibers are 1 in. long and either have a round cross section (0.016 in. in diameter), as shown in Figure 22, or are rectangular in cross section (0.010 by 0.022 in.), as shown in Figure 29. A 0.025-in.-diam by 2-1/2-in.-long round fiber has had limited use, as have some of the more exotic types shown in Figure 48.

In addition to variations in fiber type, there are several other parameters which are unusual for fibrous concrete and can be varied in a mix design. The procedure for optimizing a fibrous concrete mix for preselected material is similar to that used for conventional concrete. A trial mix is selected based on experience, and then the constituents are adjusted to produce the desired properties. Typical mixes which have been used are shown in Table 20. Some of the other parameters are as follows:

<u>a</u>. For pavement applications, maximum-size coarse aggregate has varied between 3/8 and 3/4 in., with the 3/8-in. size used predominately.

<u>b</u>. The percentage of coarse aggregate (of the total aggregate content) can be varied. The percentage has been varied from 25 to 60 percent for pavement application.

<u>c</u>. The composition of the cementitious constituent can be varied. Specifically, fly ash or other pozzolans can be substituted for portland cement. The substitution of a pozzolan decreases the rate of strength gain and may increase workability.

<u>d</u>. Admixtures for air entrainment, water reduction, and set control have been used for fibrous concrete, and conventional procedures regarding their use should be followed.

The procedures and typical values outlined above should be considered only as guidelines, and before any construction is started, a thorough mix design survey should be conducted with available material in order to select a workable mix which will yield the required strength. It is recommended that a flexural strength be selected not greater than 1000 psi at 90 days measured according to ASTM C 78-64.[10] Higher strengths are readily attainable, but placement of such mixes will usually be difficult. The 1000-psi maximum value can usually be attained with mixes that can be placed with conventional equipment and procedures.

Table 20

Typical Fibrous Concrete Mixes

Material	Saturated Surface Dry Batch Weight lb
Mix I	
Cement (type 1)	846
Fine aggregate (natural sand)	1700 (70%)
Coarse aggregate (3/8-in. maximum-size natural peagravel)	728 (30%)
Fibers (round, 1 in. long by 16 mils in diameter)	250 (2%)
Water	390
Air-entraining agent (5% air)	--
Mix II	
Cement (type 1)	517
Fly ash	225
Fine aggregate (natural sand)	1525 (55%)
Coarse aggregate (3/4-in. maximum-size crushed limestone)	1200 (45%)
Fibers (rectangular, 1 in. by 10 by 22 mils)	200 (1-1/2%)
Water	275
Air-entraining agent (4% air)	--
Set-retarding admixture	--
Mix III	
Cement (1 - P)	822
Fine aggregate (natural sand)	1593 (60%)
Coarse aggregate (3/8-in. maximum-size natural peagravel)	1014 (40%)
Fibers	115 (1%)
Water	325
Air-entraining agent (5% air)	--

Mix I resulted in slumps of about 4 in. and was used for manually constructed test pavements.

Mix II resulted in slumps of about 2 in. and was used for slip-formed 4- and 6-in.-thick overlays.

Mix III resulted in slumps of about 4 in. and was used for manually constructed test pavements.

BATCHING

Bulk-handling techniques for introducing the fibers during the batching operation have not been developed. Fiber and equipment manufacturers are currently developing equipment and techniques for shipping and handling large quantities of fibers. The extent of this development will depend on the large-scale application of fibrous concrete, and vice versa the use of large quantities of fibrous concrete will depend on the ability to efficiently handle large volumes of fibers.

Manual procedures have been used for introducing the fibers into the batching operation. Fibers are presently shipped in 1-cu-ft boxes containing from 40 to 80 lb of fiber. This method is not an efficient way to ship the fibers since a cubic foot of steel weighs about 490 lb. With this packaging procedure, additional labor is required for handling because of the wasted space. However, the need for weighing is eliminated and not as much effort is required to dispense the fibers as would be required if they were packed more efficiently.

In the batching operation, fibers are generally handled as aggregate, but care must be taken when the fibers are required to pass through a constriction since they have a tendency to bridge over an opening and stop the flow. Efforts should also be made to disperse the fibers as much as possible and to achieve as much preblending of the fibers with the aggregate as possible prior to mixing.

Several procedures have been used successfully for ready-mix operations. The most successful method has been to dump the fibers onto a belt or through a chute carrying the aggregate to the mixing drum. With this procedure, the fibers and aggregate are preblended before entering the mixing drum, and this preblending helps to minimize balling. Then, cement and water are added after the fibers and aggregate have been charged. Another procedure that has been used is the introduction of the aggregate into the mixing drum followed by the introduction of the fibers and then the cement and water. When introducing the fibers, an effort should be made to achieve as much dispersal as possible.

For control batch operations, the most successful method that has been used is that of feeding the fibers onto a belt that deposits the

fibers onto the charging belt of the control-mix plant. A number of methods for placing the fibers onto the first belt have been tried. The most successful has been to manually dump the fibers directly onto the belt. The vibrating screen used during the construction of the overlays in Greene County, Iowa (Placement 9, Appendix A), dispersed the fibers as they dropped onto the belt. As with ready-mix operations, regulation of the flow of the aggregate so that the fibers and aggregate are preblended before entering the mixing drum minimizes the formation of fiber balls.

MIXING

Mixing action should be as vigorous as possible to break up any balls or clumps of fibers. Mixing time requirements are essentially the same for fibrous as for plain concrete, but overmixing should be avoided since the fibers tend to ball up and the balls tend to grow as mixing is continued. When transit-mix trucks are used, special precautions should be taken to prevent overmixing.

PLACING

Fibrous concrete can be placed with conventional paving equipment. Hand methods, bridge-deck machines, form-riding pavers, and slip-form pavers have been successfully used to place fibrous concrete pavement. Because of the harshness of fibrous concrete, it is more difficult to handle. This characteristic leads to the tendency to increase the water content in order to make the concrete easier to handle. However, as with plain concrete, the water content should be kept as low as possible. With central-mix facilities and modern slip-form paving trains, fibrous concrete with slumps as low as 1 in. has been placed successfully in thicknesses as small as 4 in. Slabs 2 and 3 in. thick have been successfully placed with slip-form pavers, but these placements have consisted of higher slump concrete. Thin slabs (2 to 3 in. thick) have been placed with manual procedures and bridge-deck finishing machines. For these placements, concrete with slumps ranging from 3 to 6 in. has been used. The slump required for proper placement will depend on the slab thickness and the equipment used. Thin slabs placed with manual

procedures will require higher slump concrete than thicker slabs placed with modern paving equipment. The equipment used for transporting and spreading the concrete will affect the slump required.

When transit-mix trucks are used, it will be necessary to use concrete with at least a 3-in. slump for proper discharge. Because of the harshness of fibrous concrete, it is difficult and sometimes impossible to discharge fibrous concrete with slumps less than about 3 in. When mechanical spreaders are used, lower slump concrete can be used than is possible when manual techniques are used.

For pavements thinner than 4 in. and relatively high-slump concrete, surface vibration is all that is necessary for proper placement. However, for thicker sections and low-slump concrete, internal vibration is recommended.

The surface of fibrous concrete pavement can be finished with conventional techniques. Because of the high cement content, the surface usually finishes easily. No problems have been encountered in finishing fibrous concrete that can be attributed to the presence of the fibers. A burlap drag cannot be used for surface texturing since the fibers stick in the burlap and cause tearing of the surface. Transverse texturing with a stiff bristle brush or a wire comb has been successful. The presence of the fibers cause no problems and the resulting texture appears to be no different from that obtained for plain concrete.

The sawing of grooves should not present any problems. Grooving has not been tried on any of the installations placed thus far, but no difficulties have been encountered in sawing joints.

CONCLUSIONS AND RECOMMENDATIONS

Conclusions regarding the use of fibrous concrete for airport pavements are summarized as follows:

a. Fibrous concrete pavements will perform better than comparable plain concrete pavements having identical thicknesses, foundation conditions, and concrete flexural strengths.

b. Fibrous concrete can be produced and placed with conventional batching, mixing, and paving equipment and techniques. Bulk-handling of fibers and a mechanical system for introducing the fibers during batching operations will be required to produce fibrous concrete in sufficient quantities for large airport paving jobs.

c. The recommended design criteria are based on limited performance data. In addition, the analysis of the data is based on several rather arbitrary, though conservative, decisions and assumptions. As a result, the criteria should be considered as tentative and subject to change as additional performance data are accumulated.

d. The use of fibrous concrete will result in thinner pavements and will offer an alternative design that has several advantages over conventional construction, especially for areas in which high-quality construction materials are scarce or in situations in which control of the pavement grade is critical.

In order to improve the reliability of the proposed criteria, it is recommended that the following areas receive further study:

a. Additional performance data are needed. In particular, performance data for overlays of flexible pavement and for unbonded and partially bonded overlays are needed.

b. Additional data are needed to substantiate and/or modify proposed limiting deflection requirements.

c. Additional information on permissible joint spacing and types of load-transfer mechanisms is needed for large joint openings and thin slabs.

d. Additional data are needed to determine the effects of corrosion of fibers on pavement performance.

e. A mix design study is needed in order to establish more specific guidelines for selecting a workable mix which will produce the desired properties.

f. The feasibility of using thin fibrous overlays for resurfacing should be investigated.

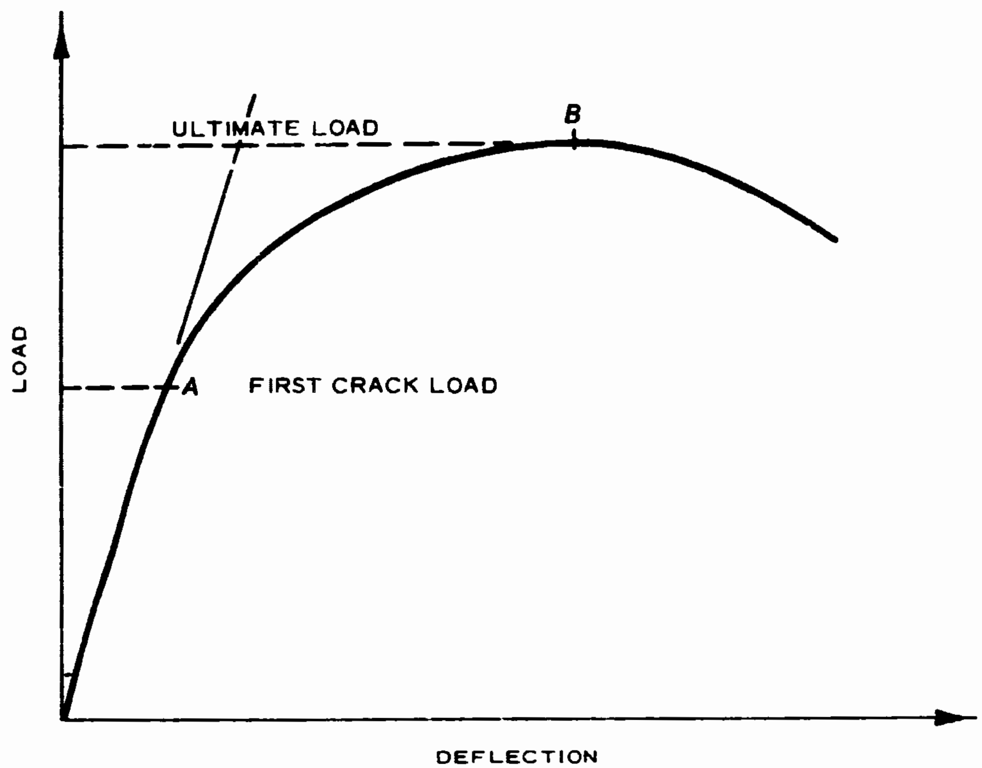

Figure 1. Schematic load-deflection diagram of a steel- or glass-reinforced beam (after Romualdi and Batson[3])

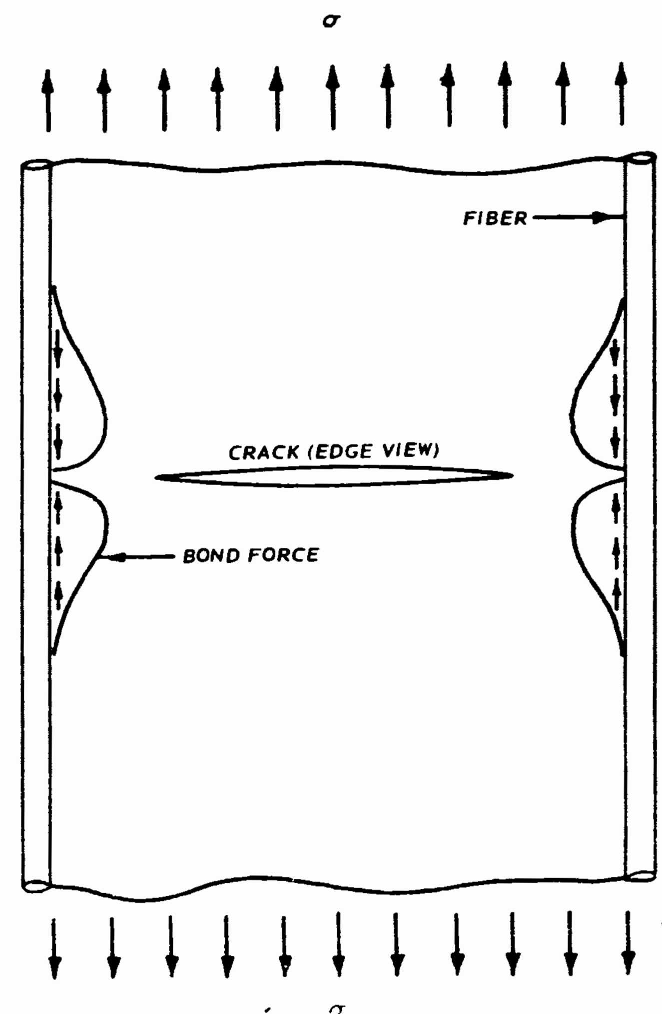

Figure 2. Section through a crack and adjacent fibers (after Romualdi and Batson[3])

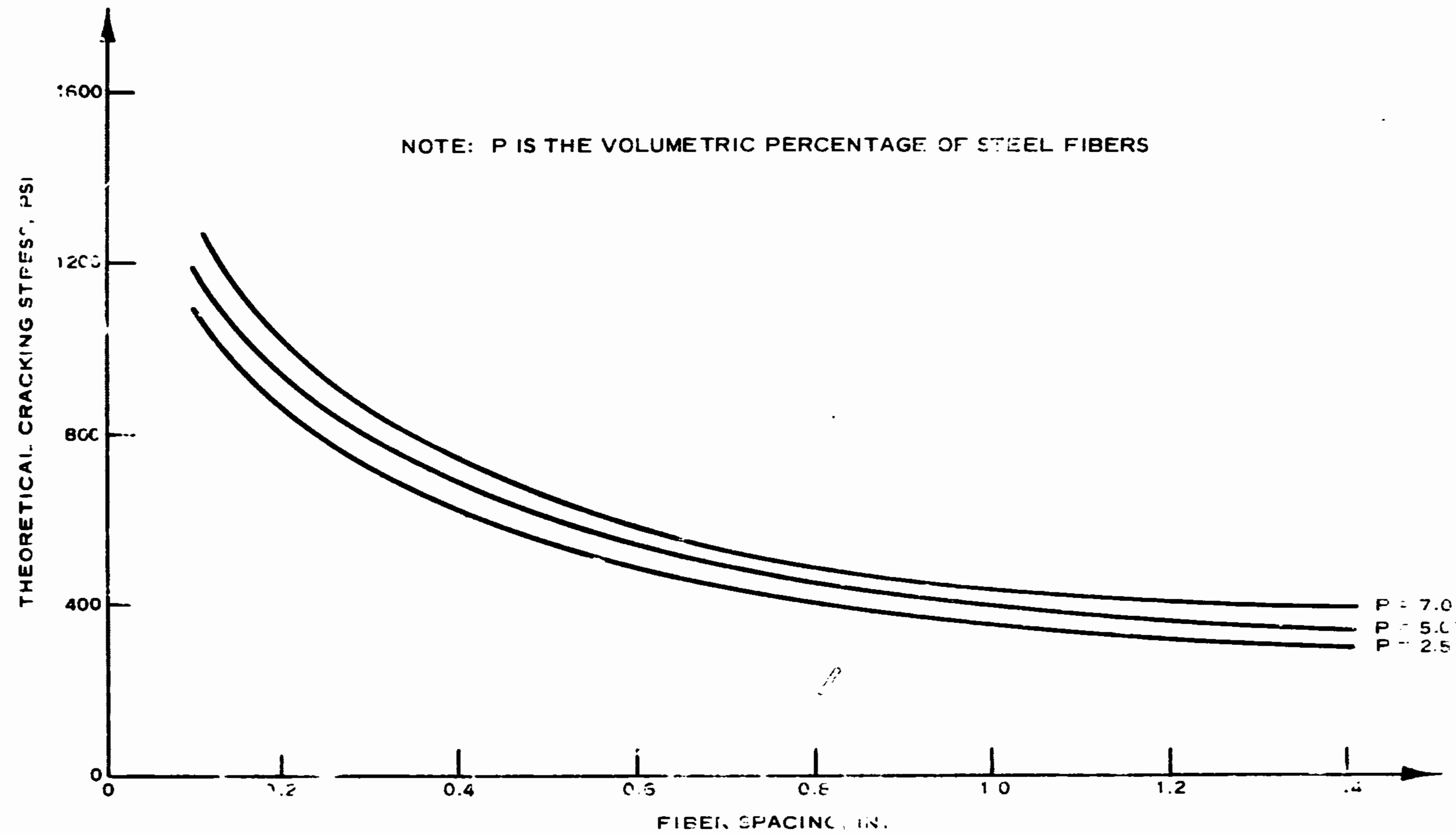

Figure 3. Theoretical cracking stress as a function of fiber spacing (after Romualdi and Batson[3])

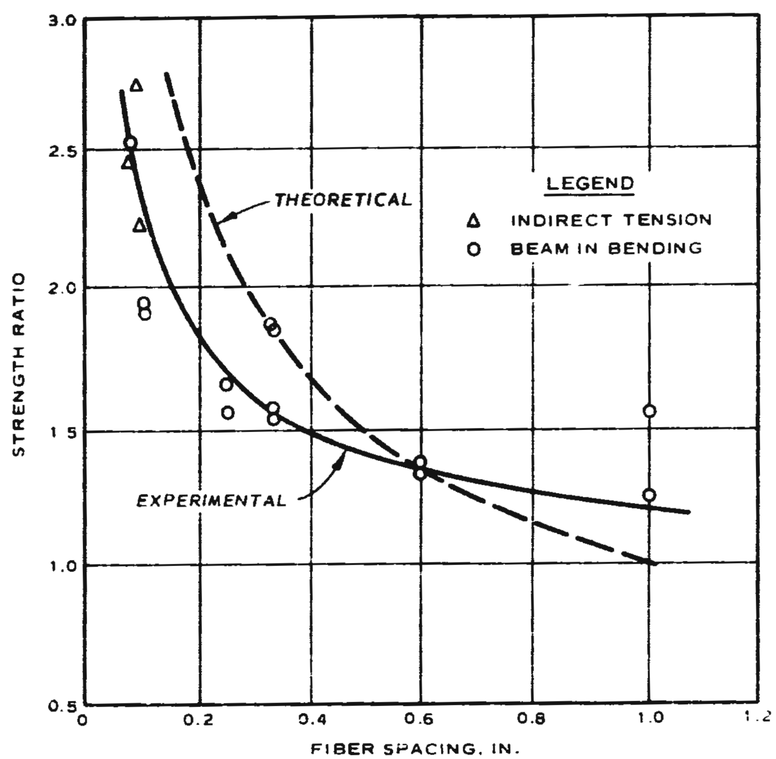

Figure 4. Theoretical and experimental strength ratio as a function of fiber spacing (after Romualdi and Mandel[4])

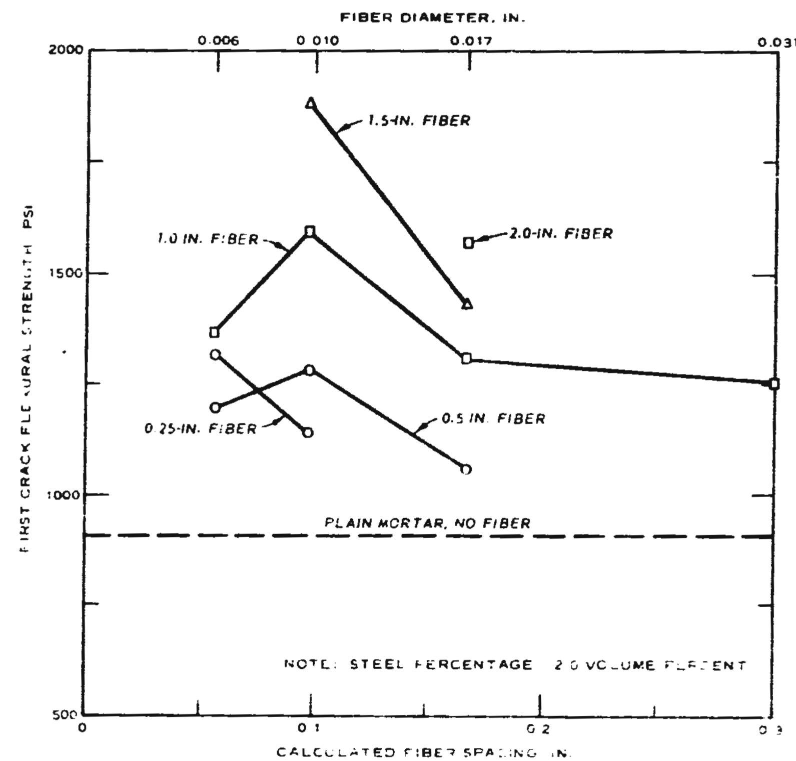

Figure 5. Effect of spacing on the first crack flexural strength of mortar containing fibers (after Snyder and Lankard[5])

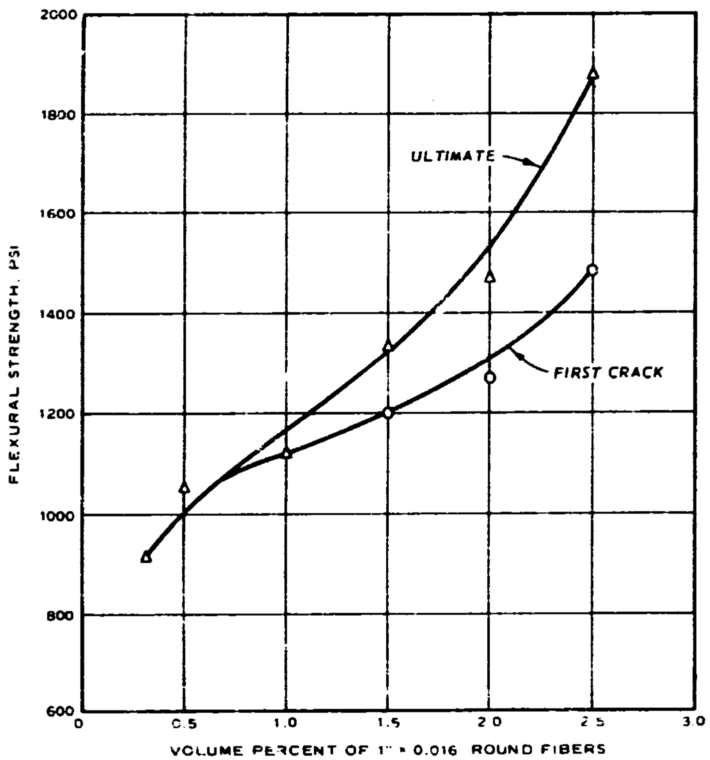

Figure 6. Flexural strength as a function of volume percent of 1- by 0.016-in. round fibers (after Waterhouse and Luke[6])

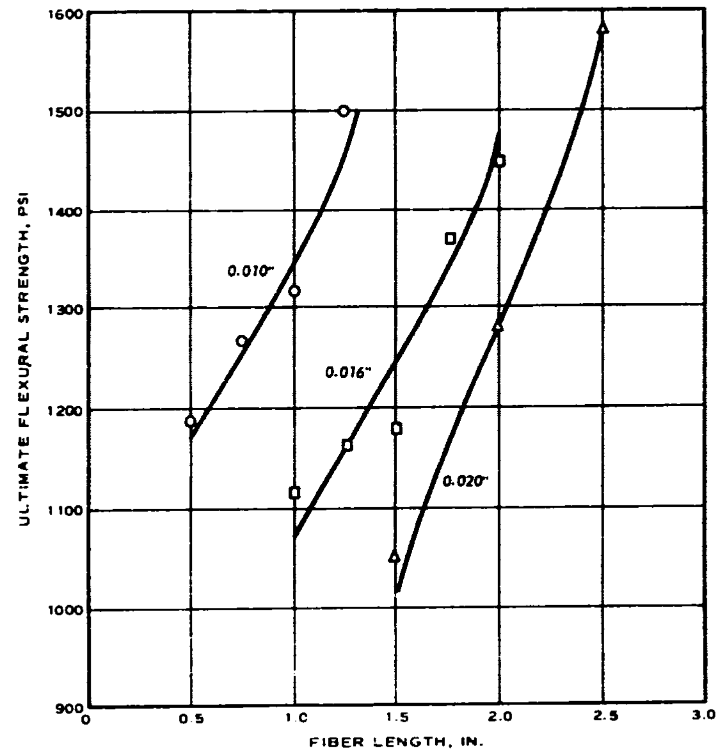

Figure 7. Ultimate flexural strength as a function of fiber length for 1 volume percent of round fibers (after Waterhouse and Luke[6])

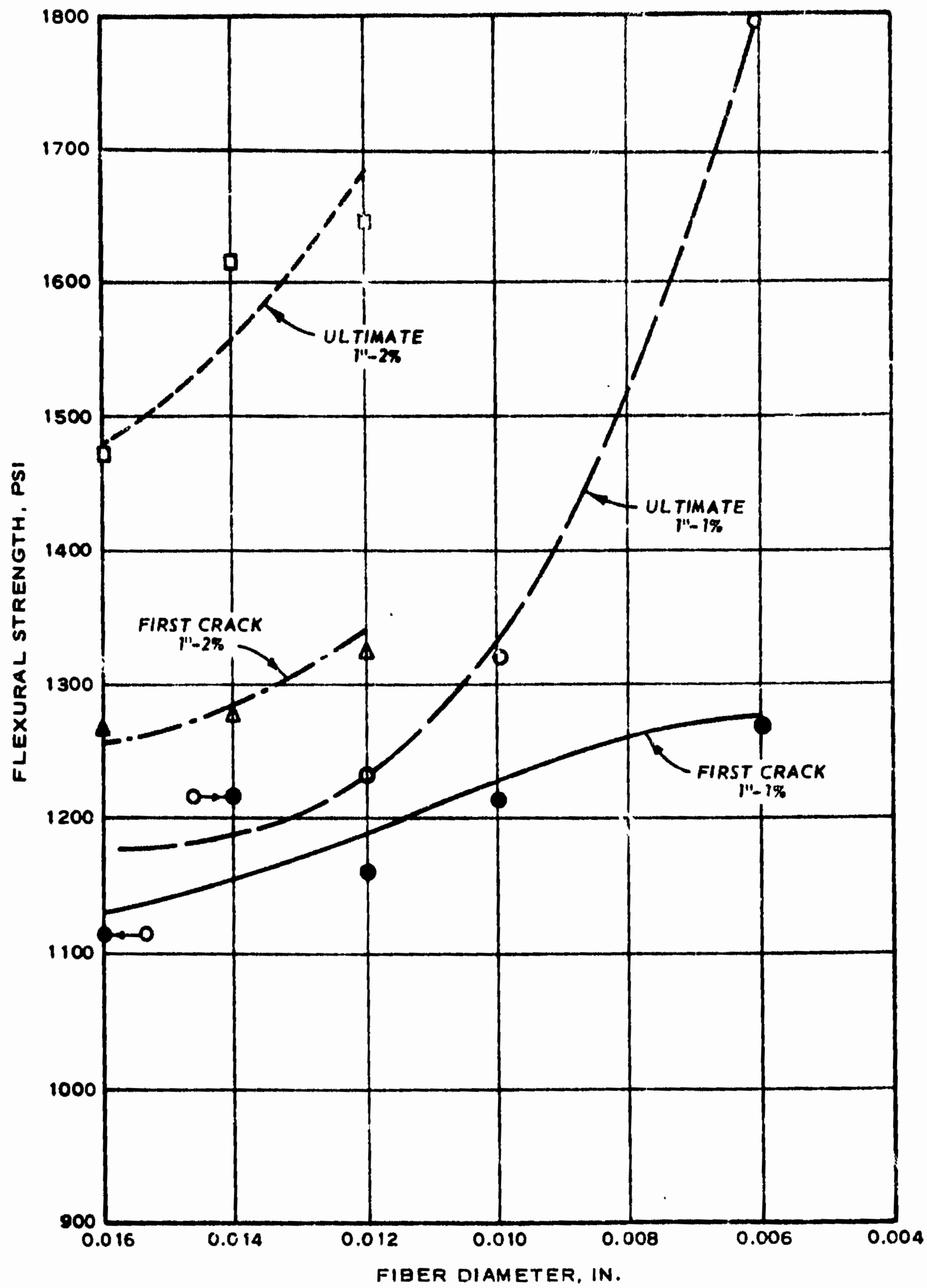

Figure 8. Flexural strength as a function of fiber diameter for 1 and 2 volume percents of 1-in. fibers (after Waterhouse and Luke[6])

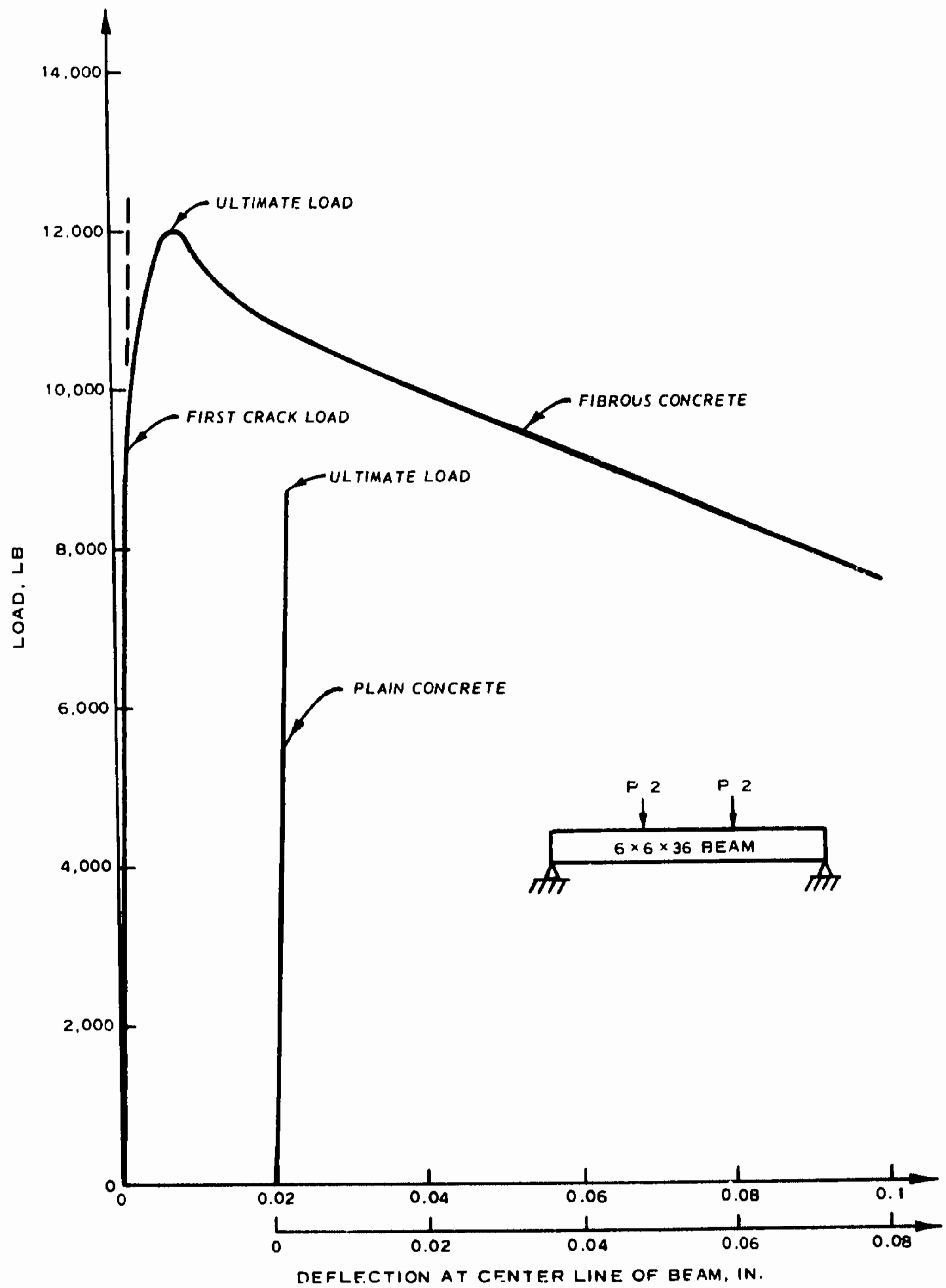

Figure 9. Typical load-deflection curves for a fibrous concrete beam and a plain concrete beam

a. Plain concrete

b. Fibrous concrete

Figure 10. Response of concrete cylinders to a dynamic compressive loading

a. Plain concrete

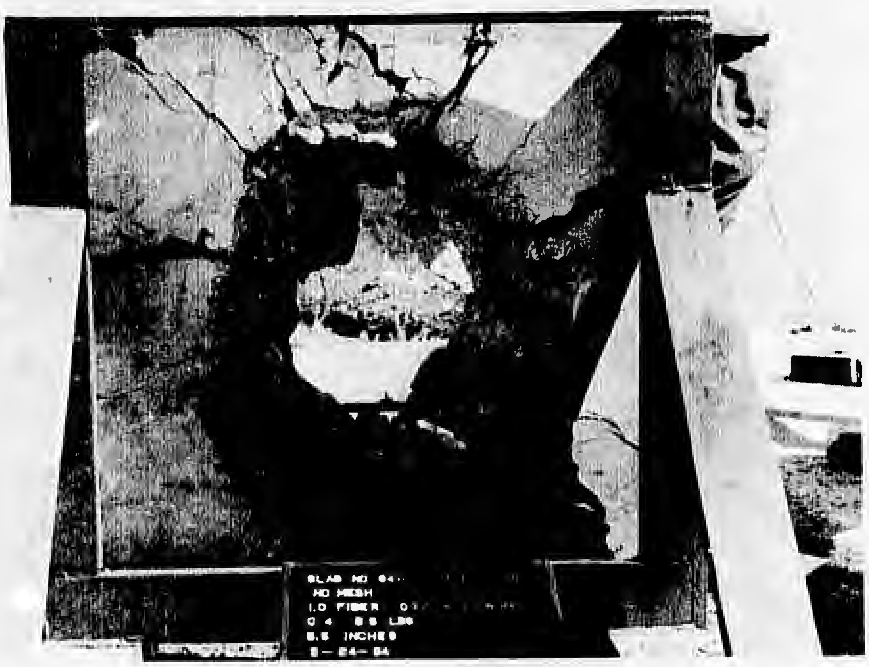

b. Fibrous concrete

Figure 11. Response of concrete slabs to an explosive loading

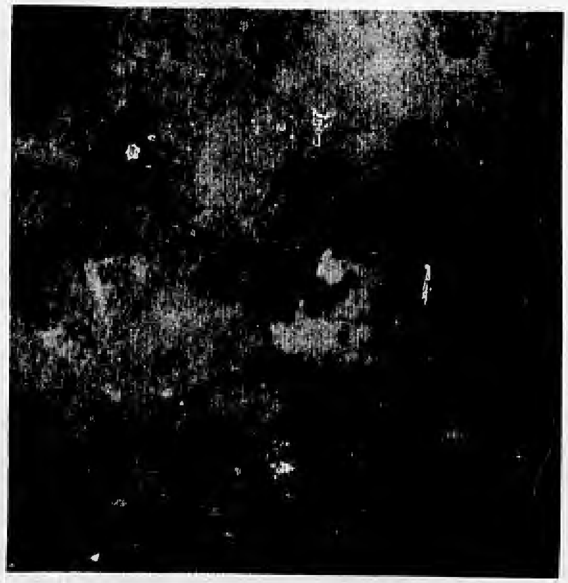

a. Core from an uncracked area

b. Core taken at a crack

Figure 12. Cores taken from a fibrous concrete slab at ORDL

Figure 13. Early cracking of a 6-in. fibrous concrete slab on a clay subgrade

Figure 14. Early cracking of a 4-in. fibrous concrete slab on a cement-treated gravel base

Figure 15. Typical cracks that develop in fibrous concrete slabs with traffic

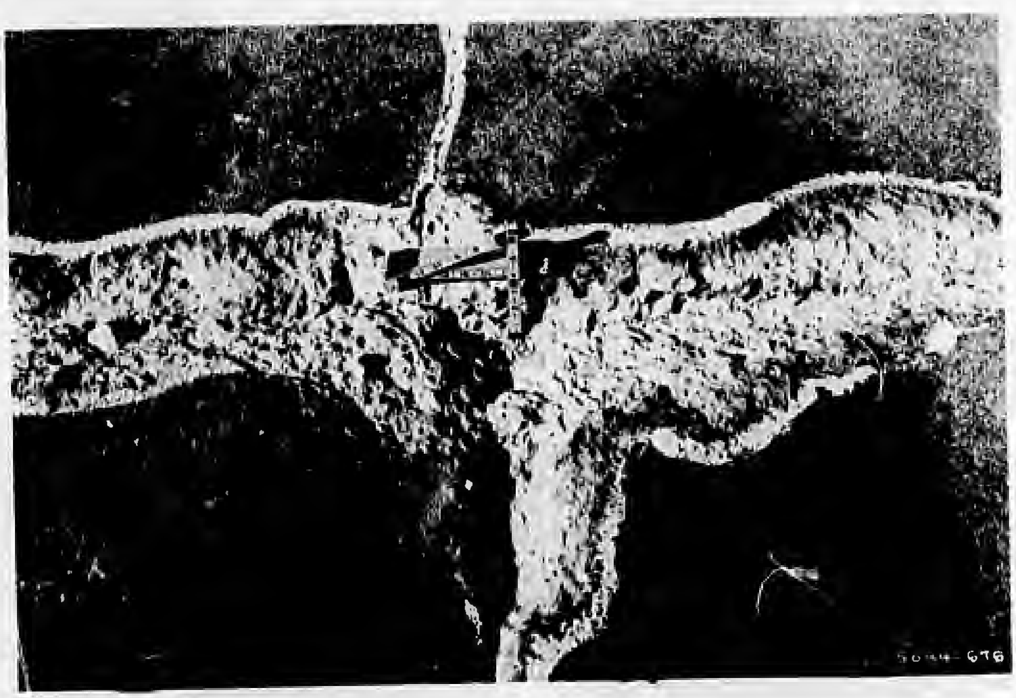

Figure 16. Severely spalled crack in a plain concrete test pavement at complete failure

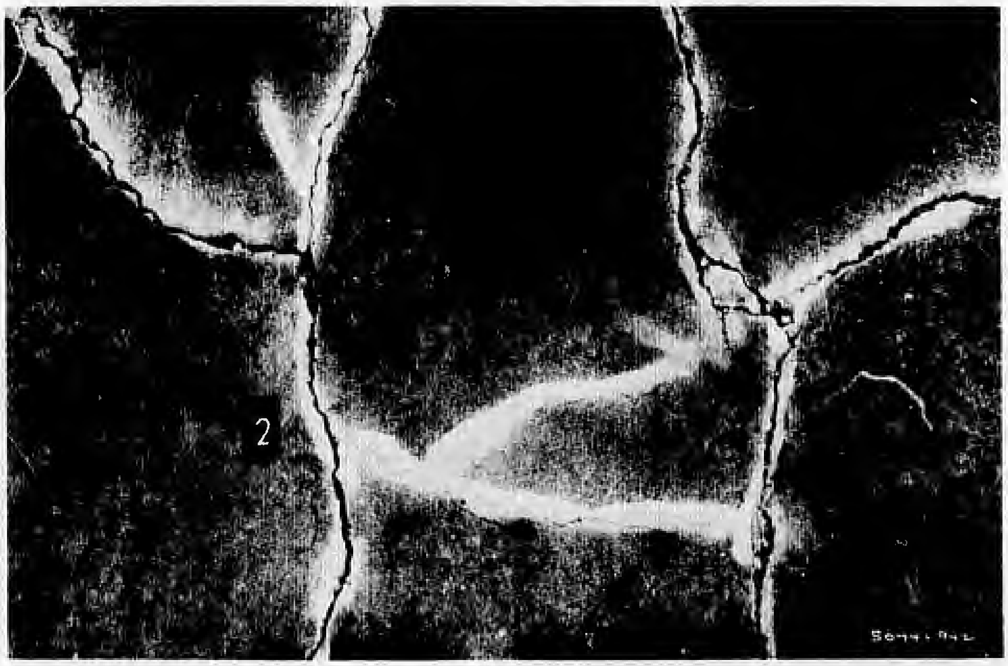

Figure 17. Cracks in a fibrous concrete test pavement at complete failure

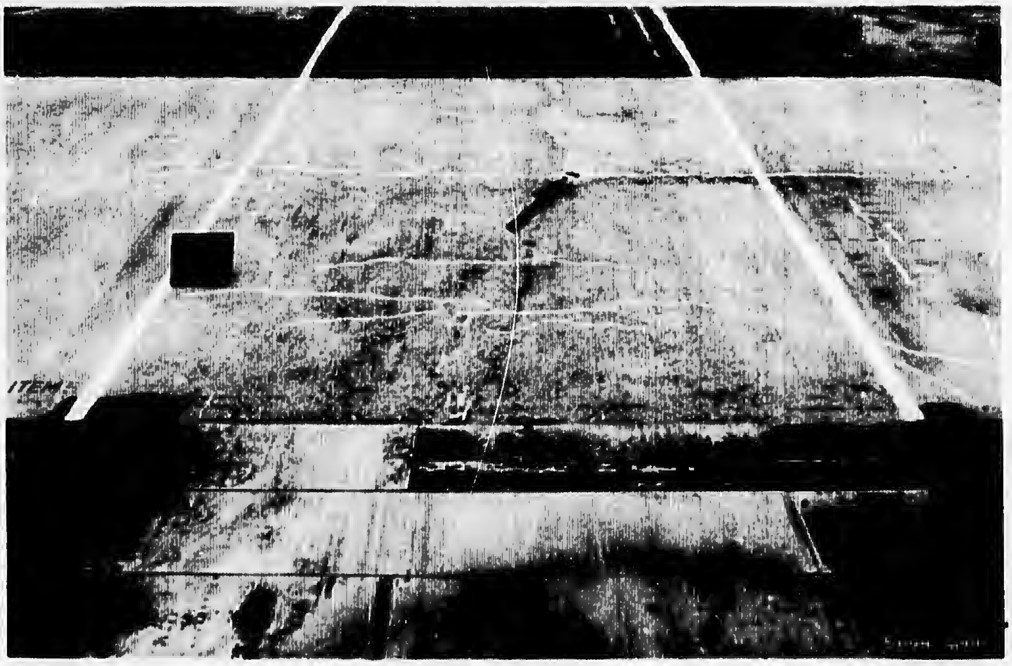

Figure 18. Fibrous concrete test pavement after 4500 coverages

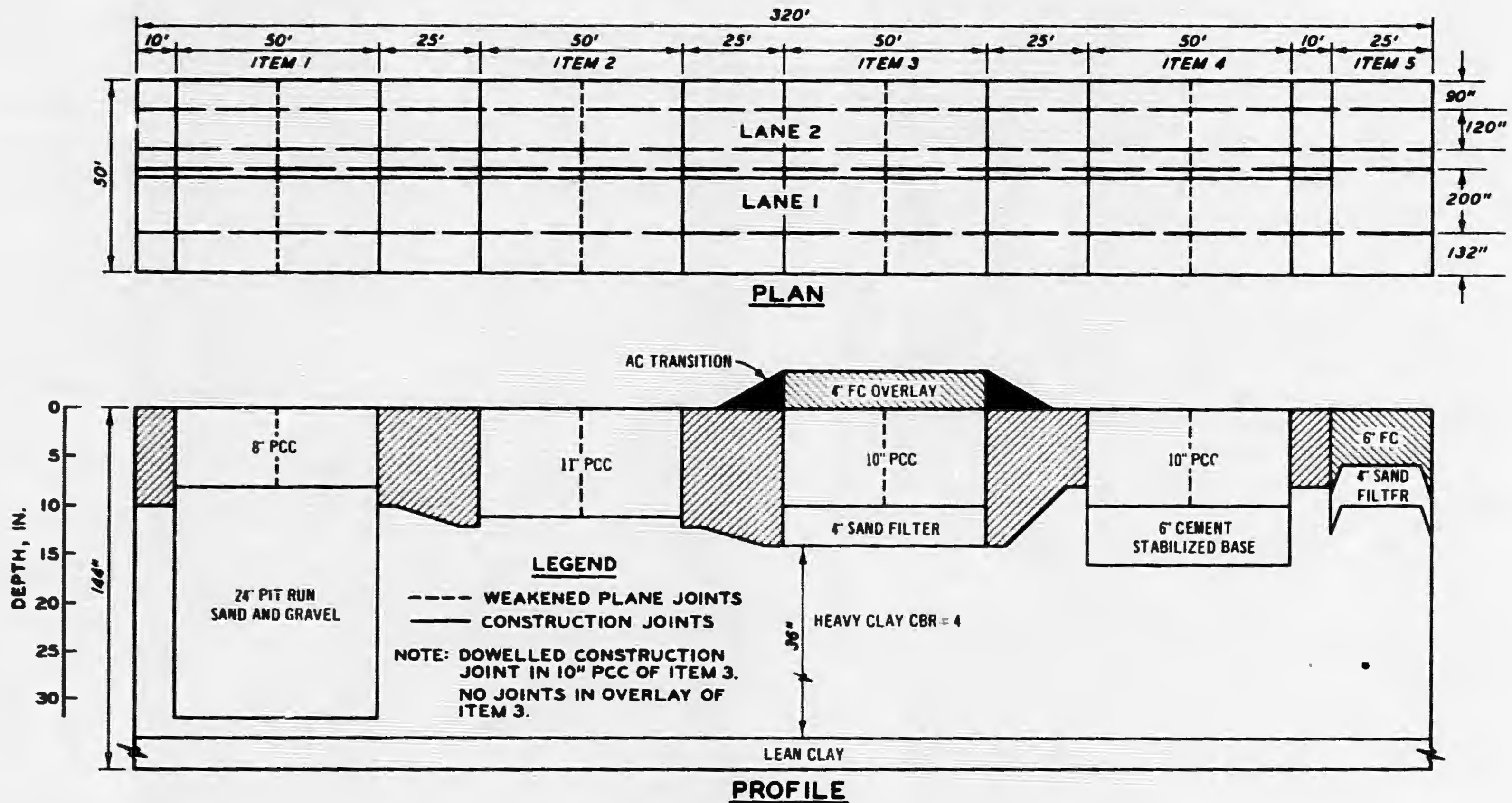

Figure 19. Plan and profile of the keyed longitudinal joint test section

Figure 20. Finished surface of the subgrade (item 5)

Figure 21. Finished surface of the sand filter course (item 5)

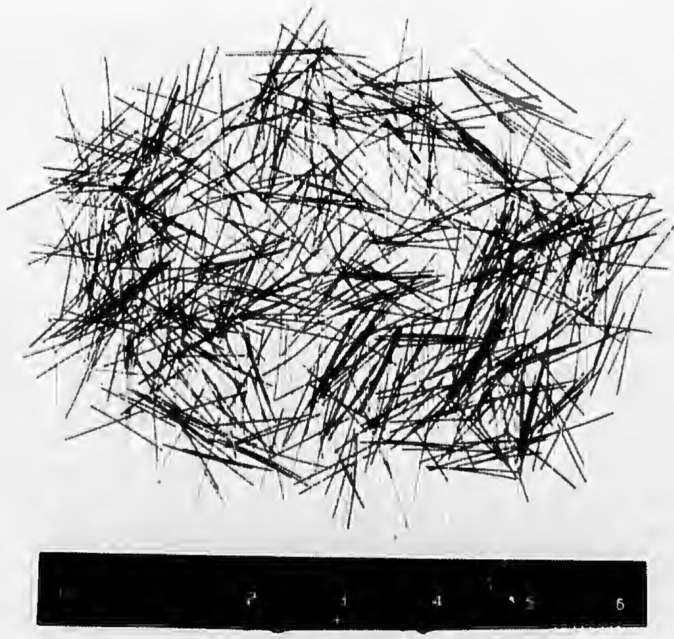

Figure 22. Round, 0.016-in.-diam, 1-in.-long steel fibers

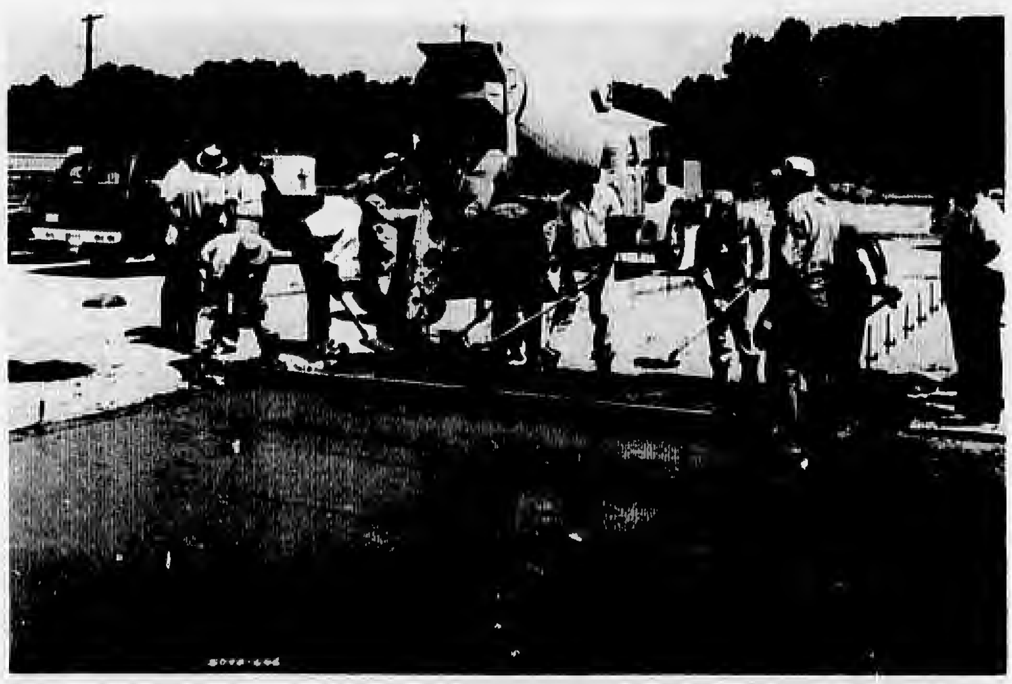

Figure 23. Placing and screeding fibrous concrete

Figure 24. Vibration of fibrous concrete with a surface vibrator

Figure 25. Finishing the surface of a fibrous concrete slab

Figure 26. Fiber ball coated with mortar

Figure 27. Inside of fiber ball consisting of fine aggregate and fibers

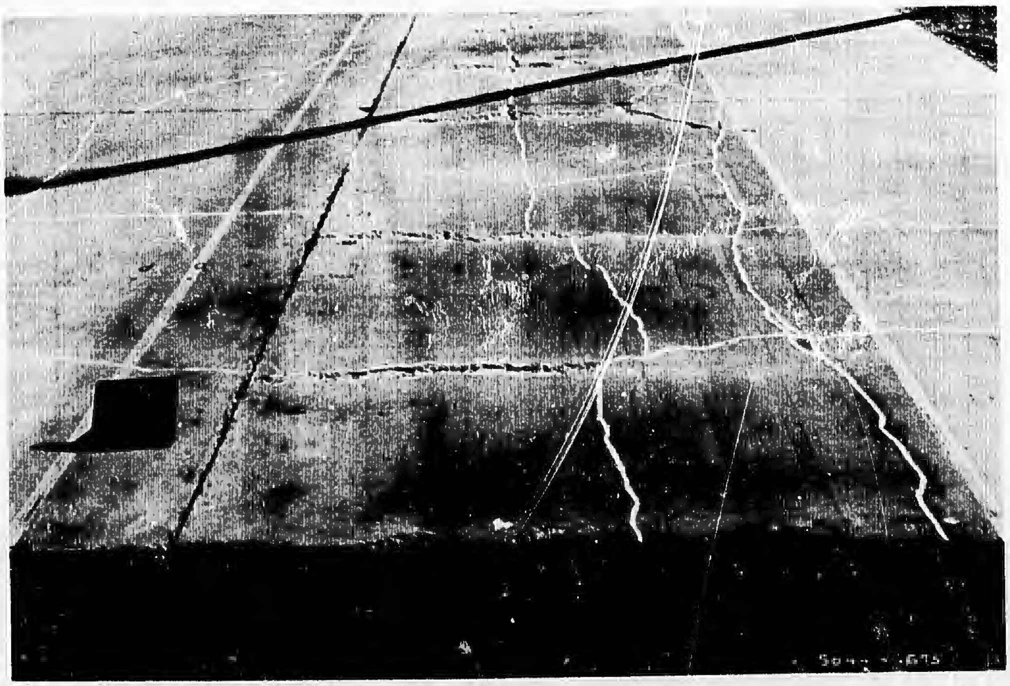

Figure 28. Item 3 prior to placement of the 4-in. fibrous concrete overlay

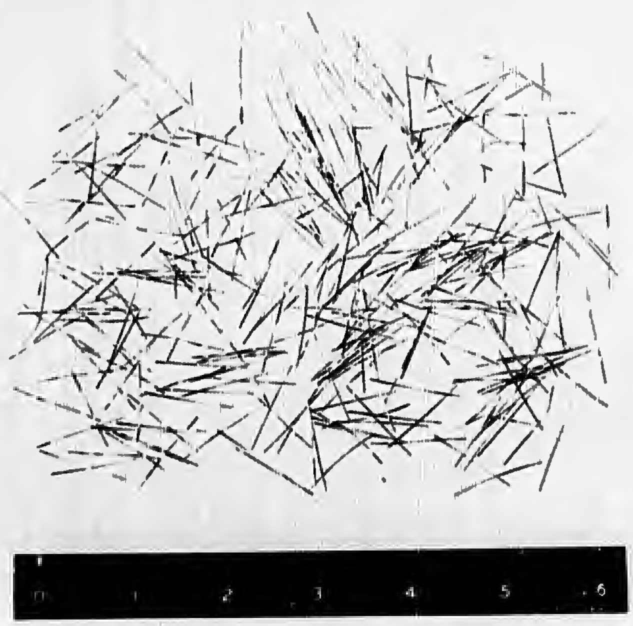

Figure 29. Rectangular 1-in.-long steel fibers, 0.010 by 0.022 in. in cross section

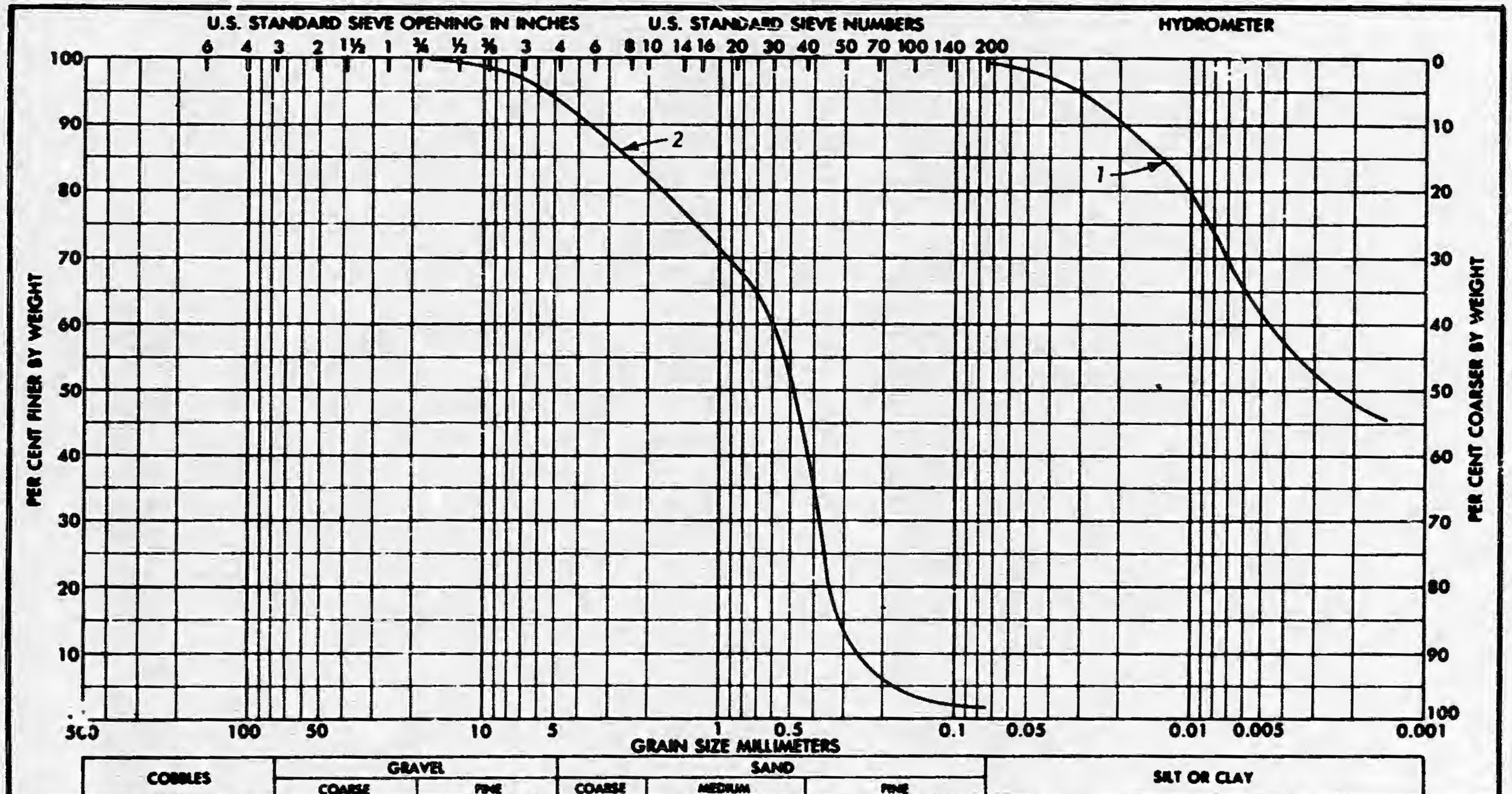

SAMPLE NO.	ELEV OR DEPTH	CLASSIFICATION	NAT W%	LL	PL	PI
1	SUBGRADE	HEAVY CLAY (CI E-11)		73	25	48
2	SAND FILTER	SAND (SP, E-2)		NONPLASTIC		

Figure 30. Classification data for the subgrade and sand filter course materials

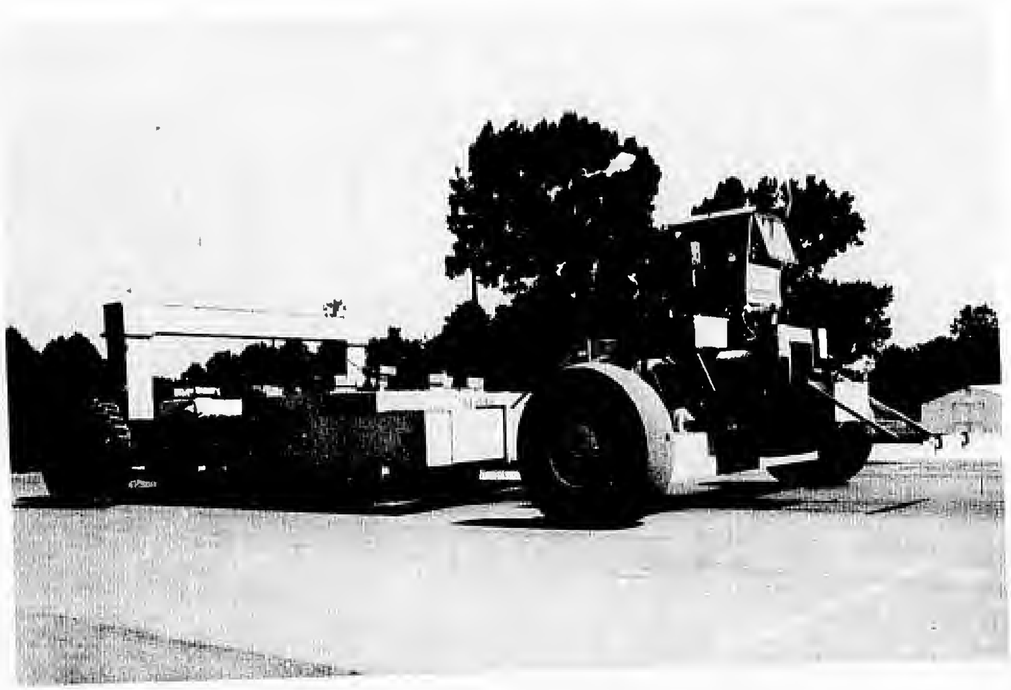

Figure 31. 360-kip, 12-wheel assembly load cart

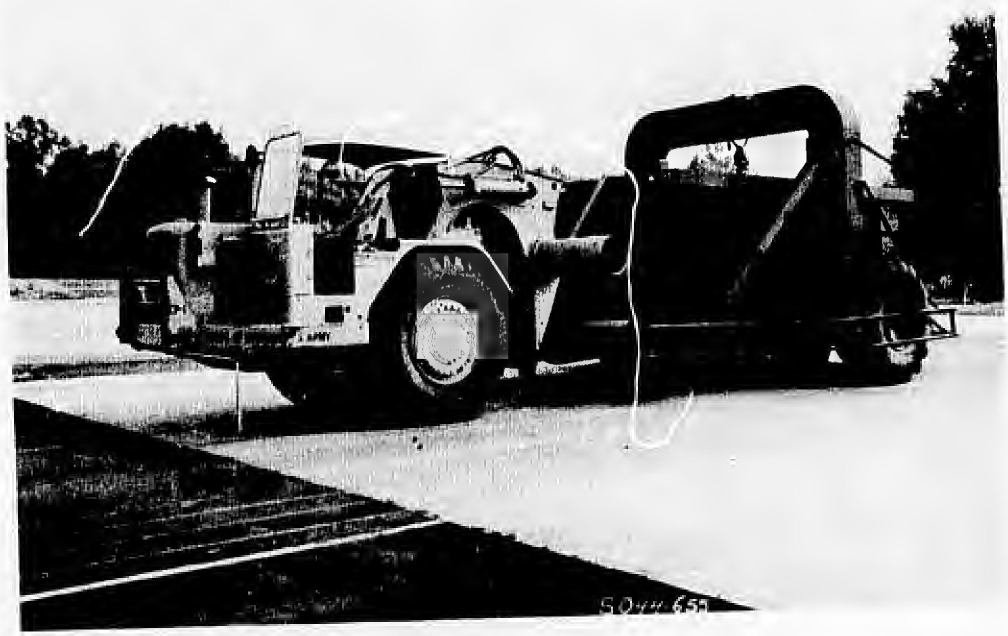

Figure 32. 166-kip, twin-tandem assembly load cart

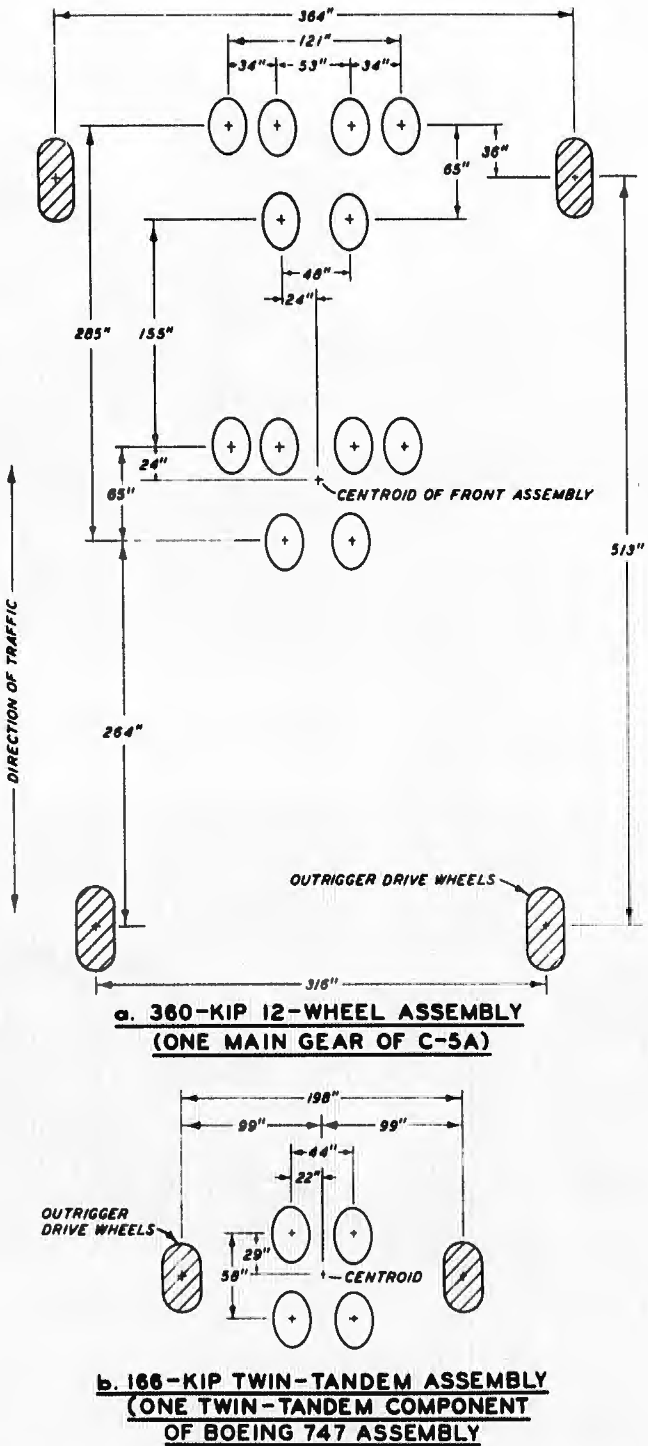

Figure 33. Wheel arrangements for the 12-wheel and twin-tandem assemblies

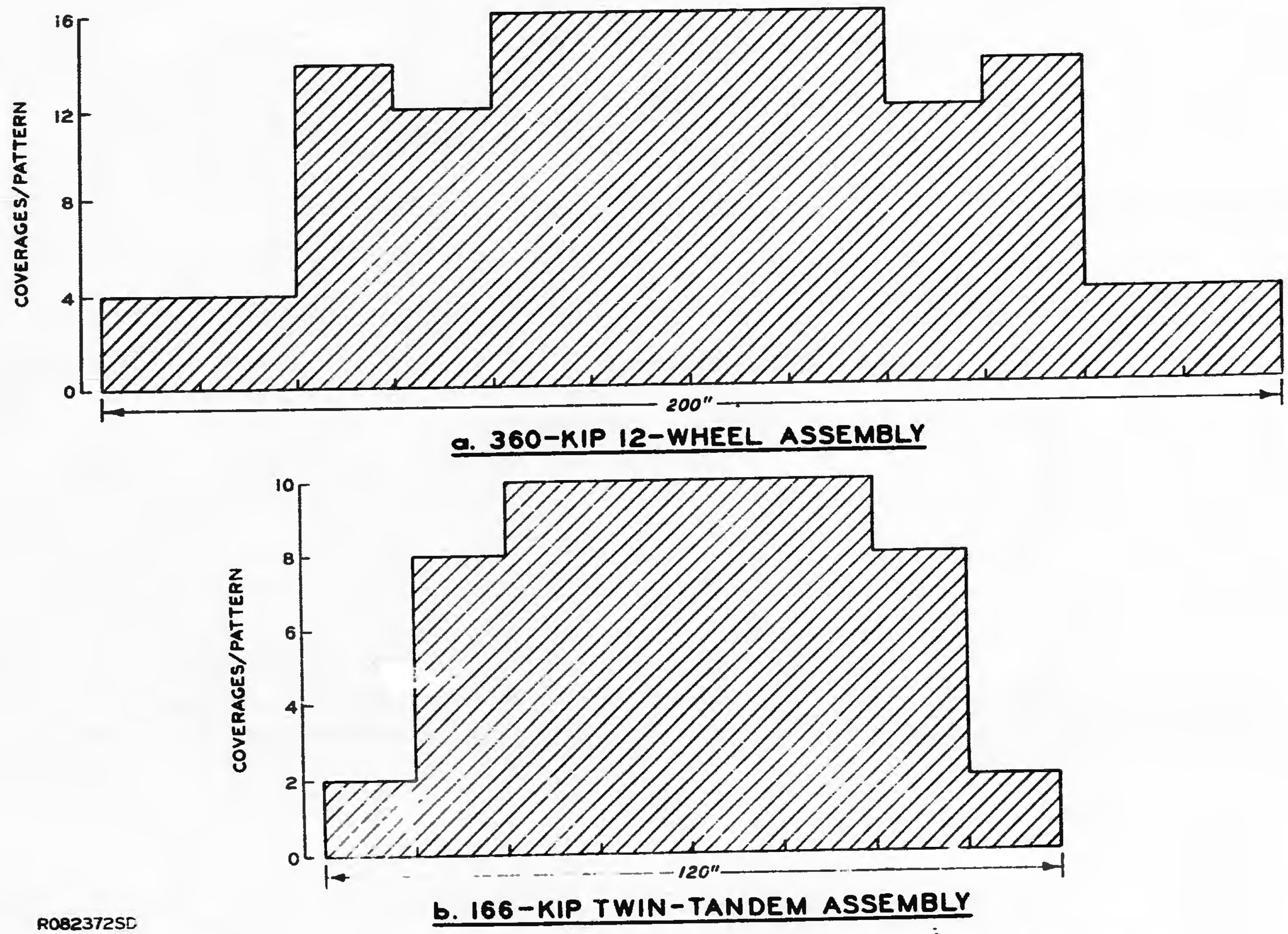

Figure 34. Traffic patterns for the 12-wheel and twin-tandem assemblies

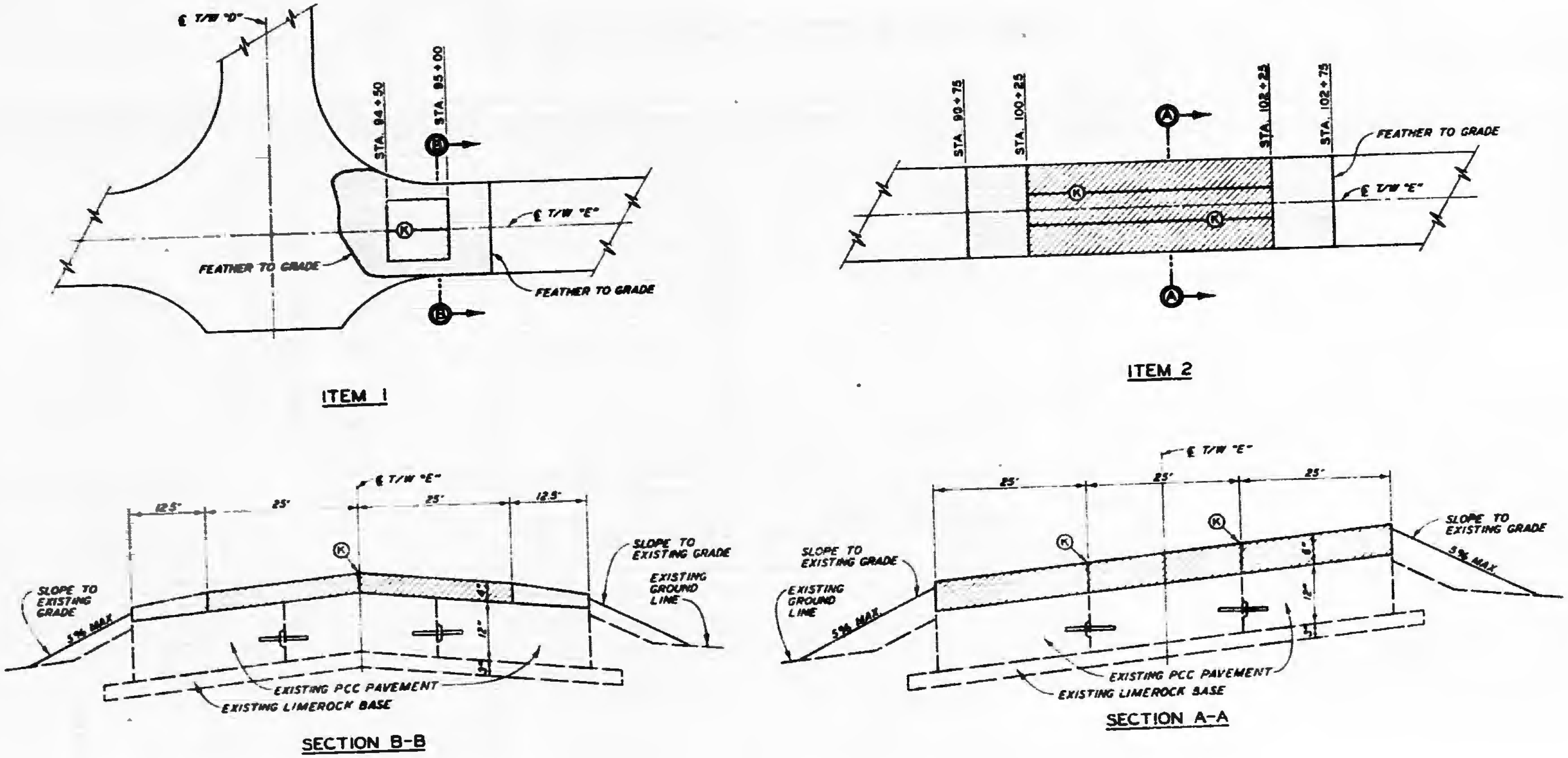

NOTE: THE SURFACES WILL BE CLEANED OF ALL LOOSE MATERIAL AND DIRT. JOINT SEALING MATERIAL EXTENDING ABOVE THE SLAB SURFACE WILL ALSO BE REMOVED

PRIOR TO PLACEMENT OF THE CONCRETE OVERLAY, THE EXISTING SURFACE SHALL BE IN A DAMP CONDITION. THIS SHALL BE ACHIEVED BY SOAKING THE SURFACE WITH WATER FOR A PERIOD OF AT LEAST 24 HOURS AT THE START OF THE OVERLAY OPERATIONS, ANY FREE STANDING WATER SHALL BE REMOVED

THE Ⓚ JOINT ON THE 4-IN-THICK CONCRETE OVERLAY WILL BE SAWED TO A DEPTH OF 1½ IN INSTEAD OF 2 IN

LEGEND

PCC OVERLAY (STEEL FIBER ADDITIVE)

BITUMINOUS OVERLAY TRANSITION

Figure 35. Layout and specifications for the Tampa overlay test items

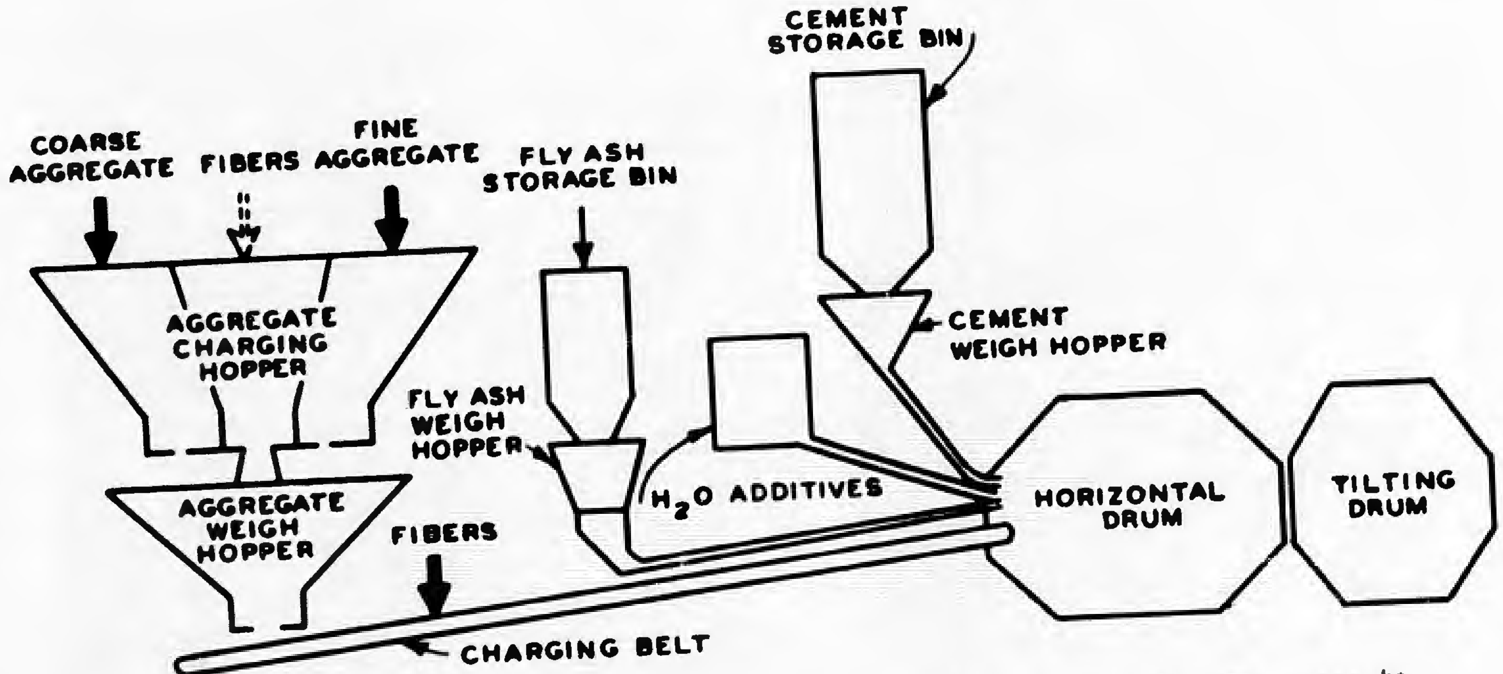

Figure 36. Components of the central-mix plant used to produce fibrous concrete

Figure 37. Emptying fibers onto a conveyor belt

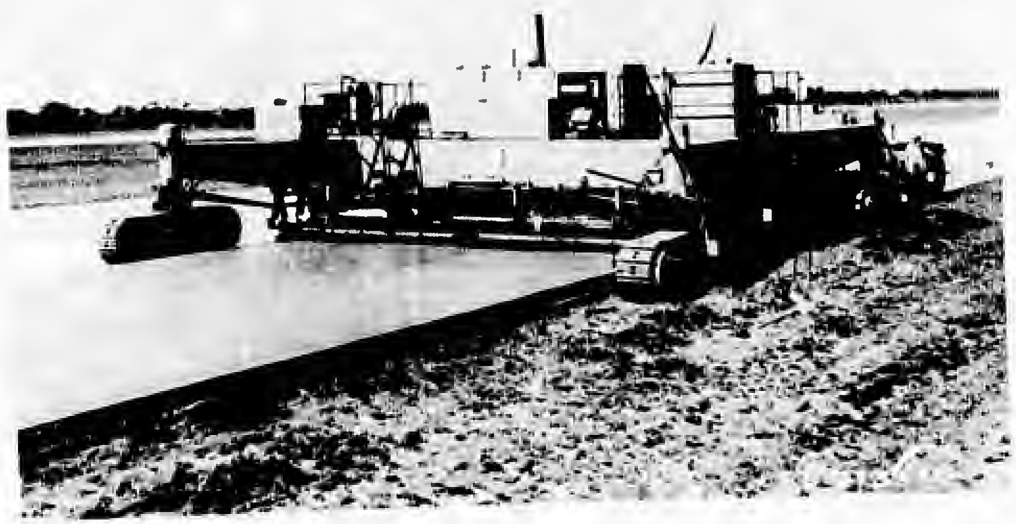

Figure 38. Slip-form paver placing a 6-in. overlay

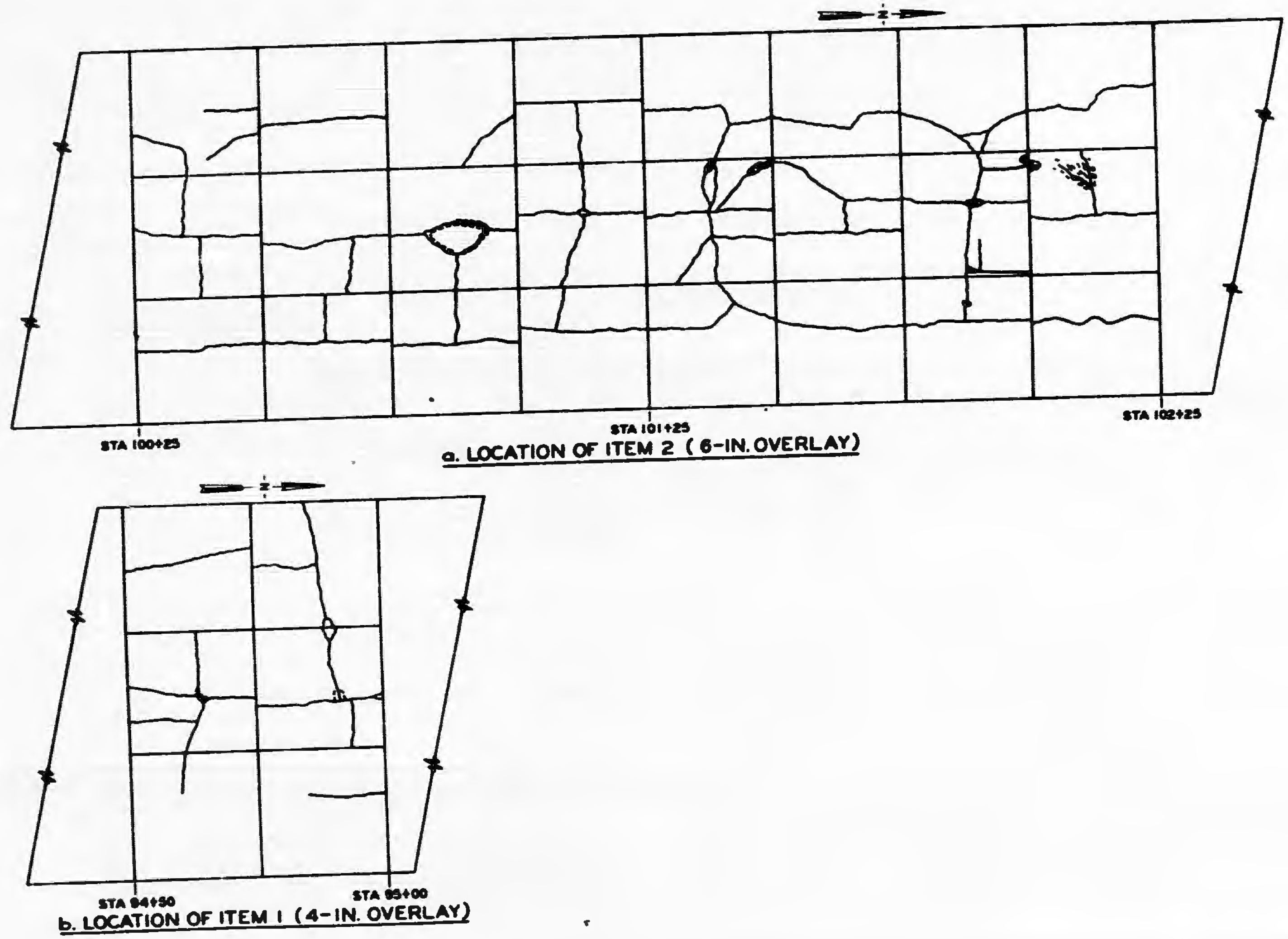

Figure 39. Crack patterns in the original pavements prior to placement of the overlays

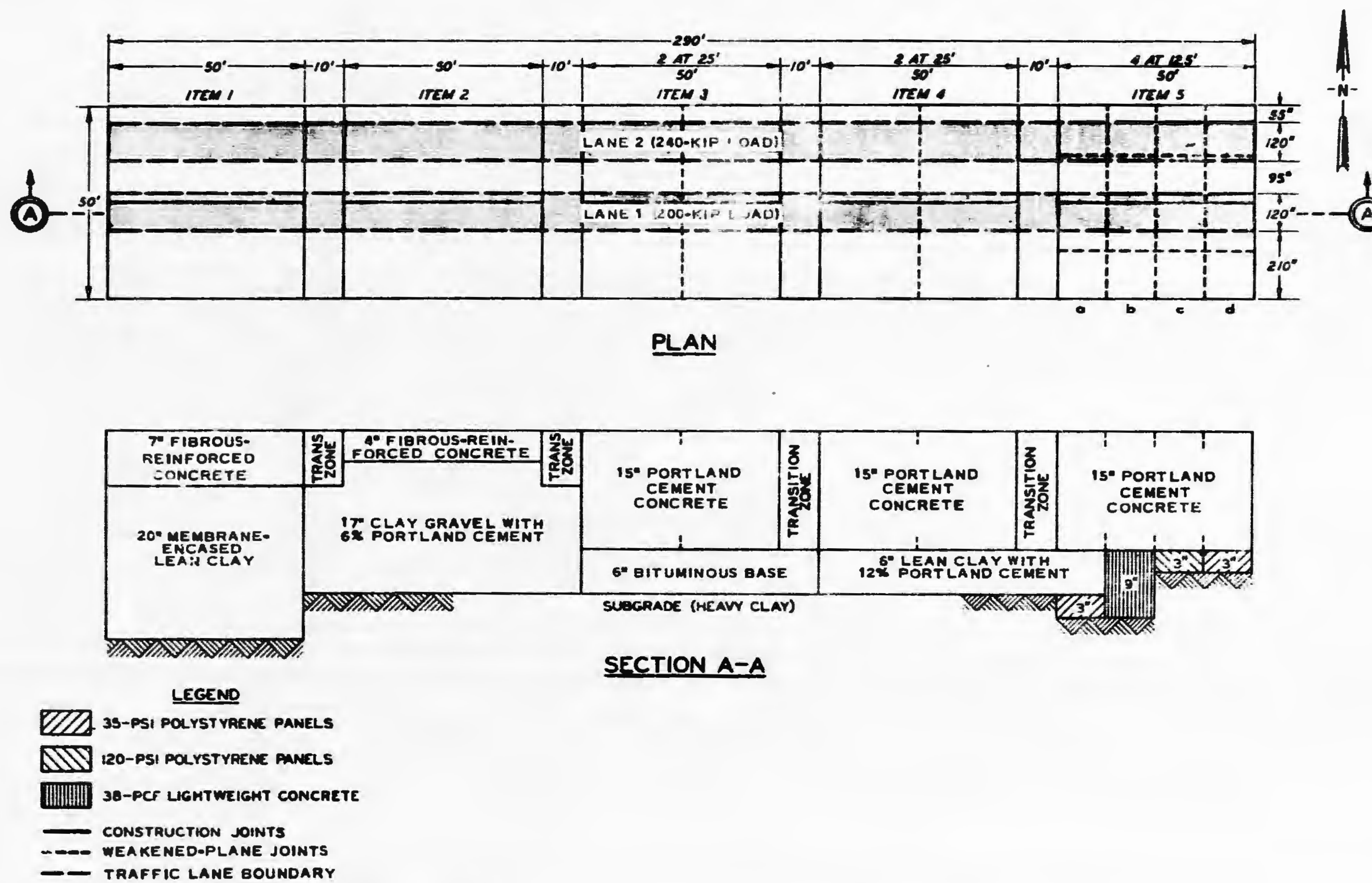

Figure 40. Plan and profile of the structural layers test section

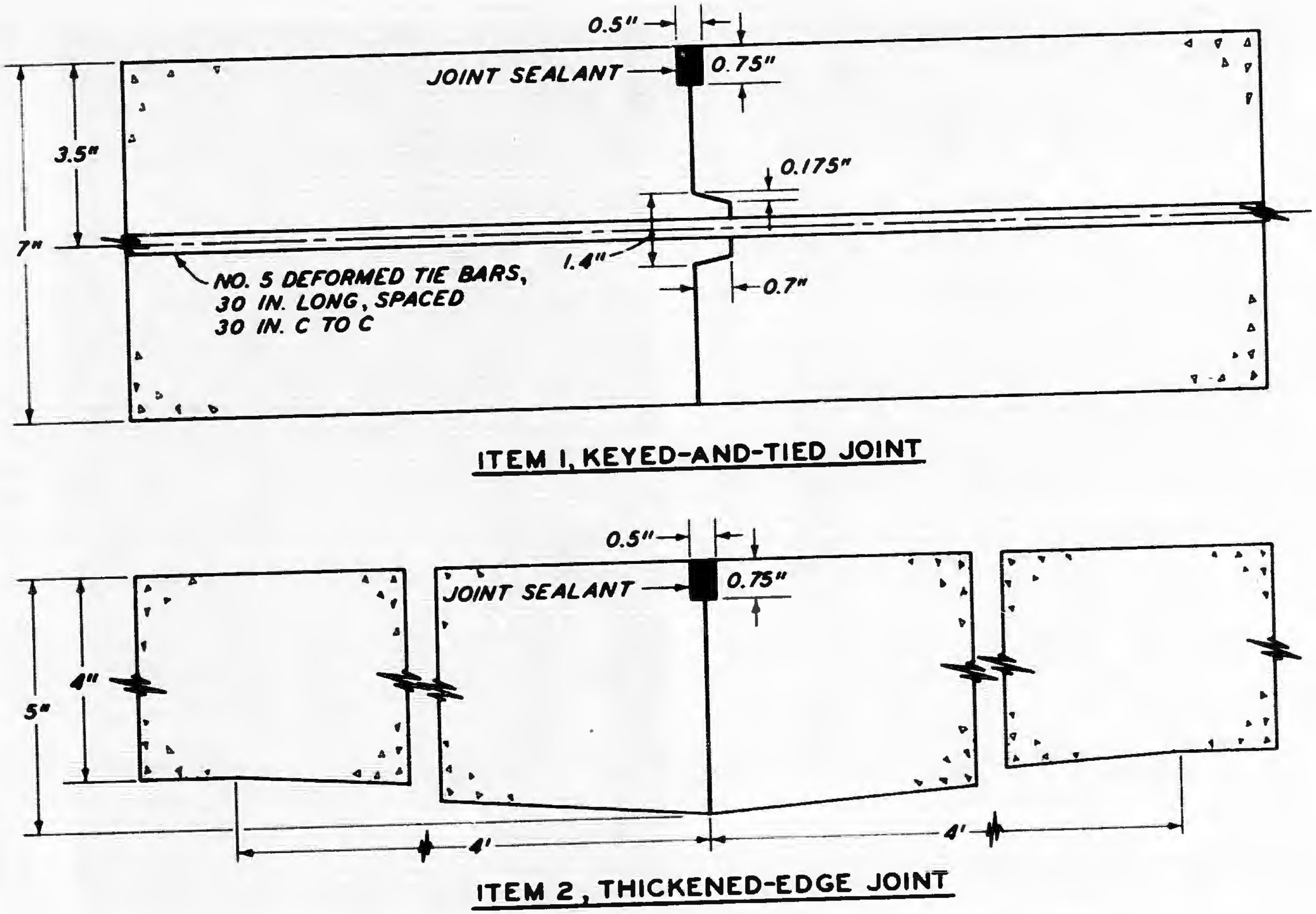

Figure 41. Details of the longitudinal construction joints

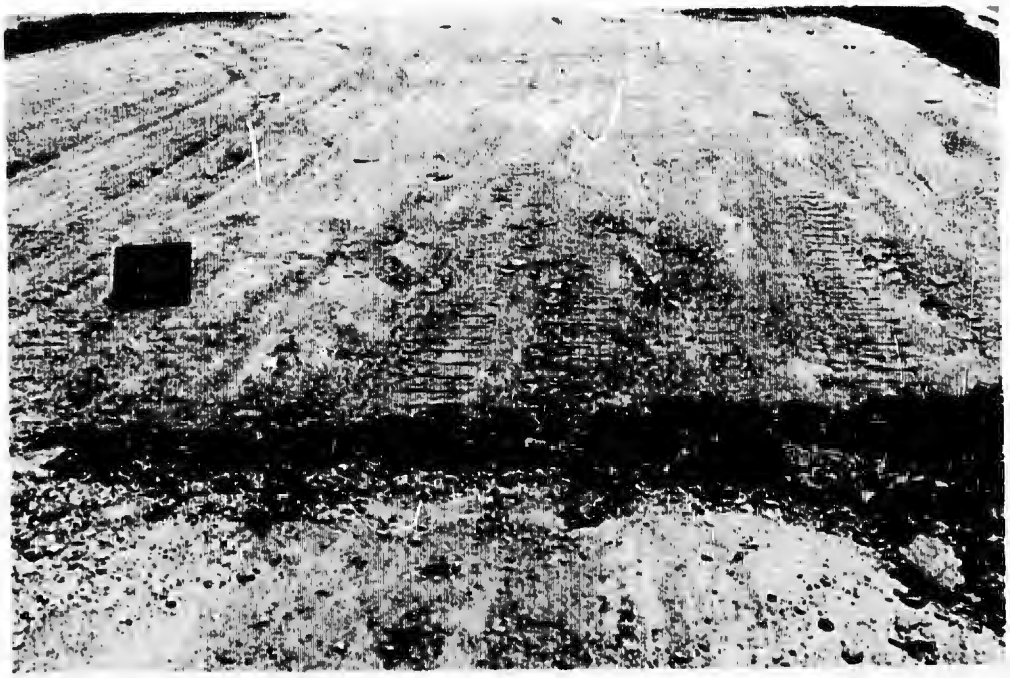

Figure 42. Finished surface of the subgrade (item 1)

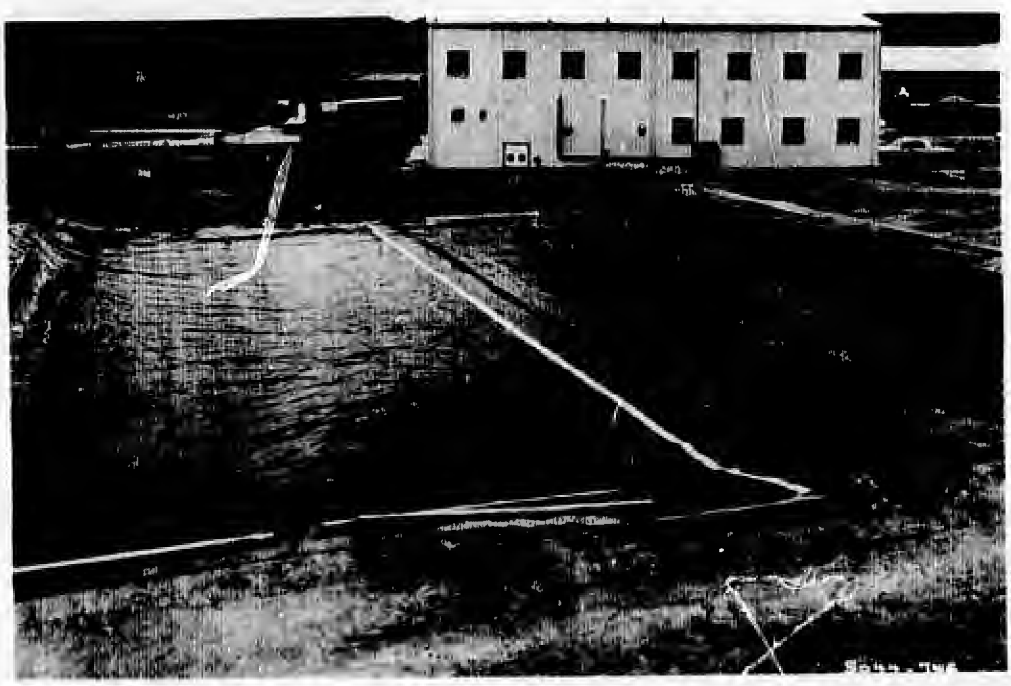

Figure 43. Bottom membrane in place over the prepared subgrade (item 1)

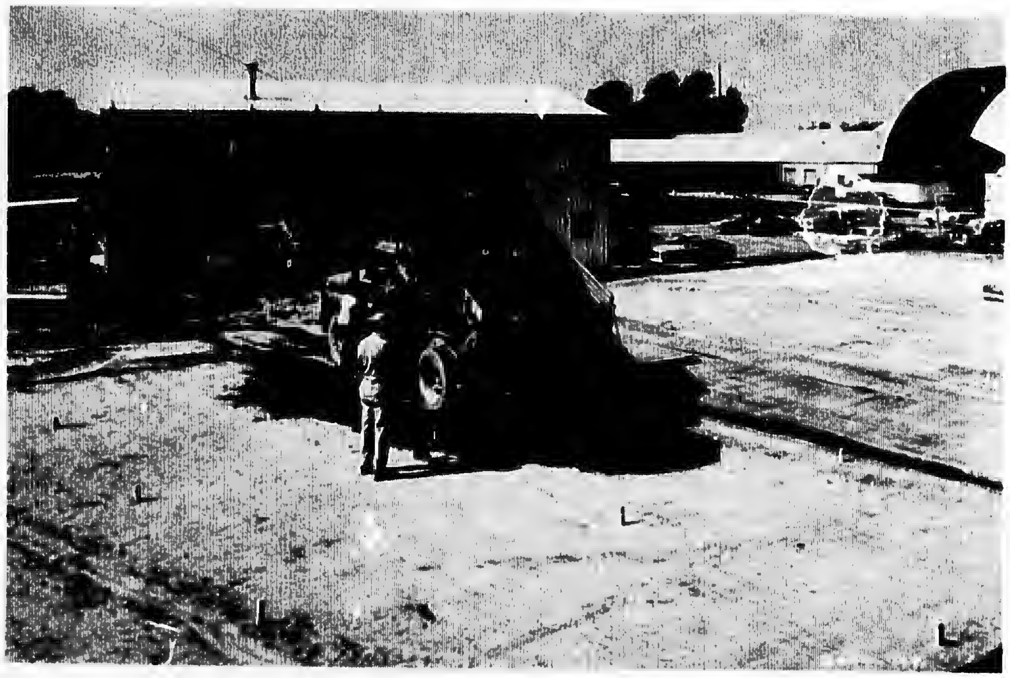

Figure 44. Processed lean clay being placed in the MESL (item 1)

Figure 45. Finished surface of the MESL (item 1)

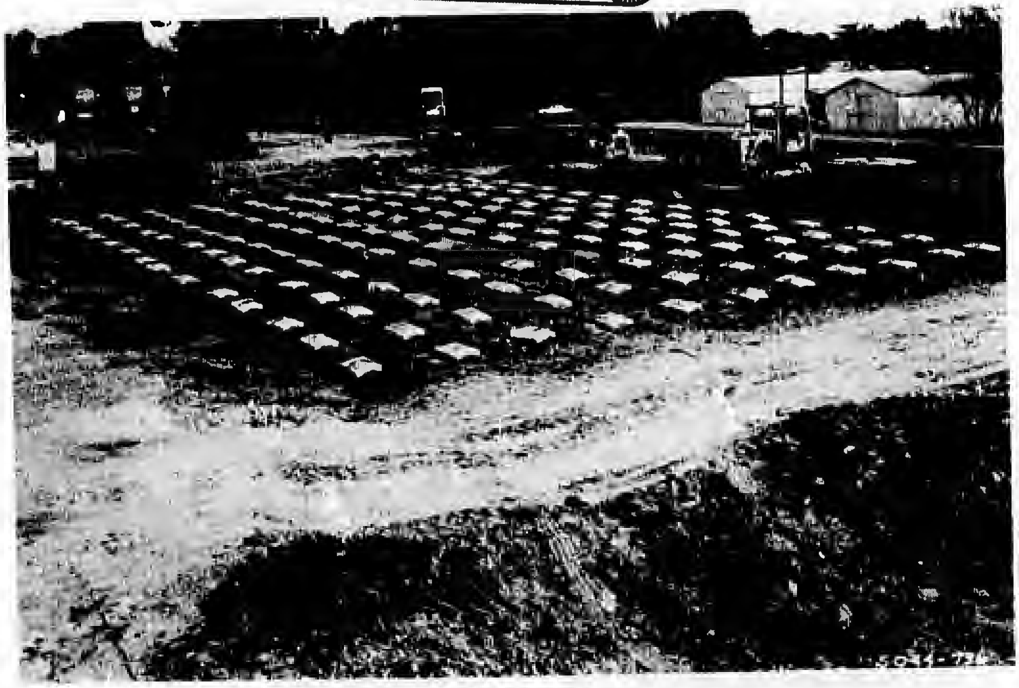

Figure 46. Cement ready for spreading (item 2)

Figure 47. Finished surface of the cement-treated base (item 2)

Figure 48. Types of steel fibers used in items 1 and 2

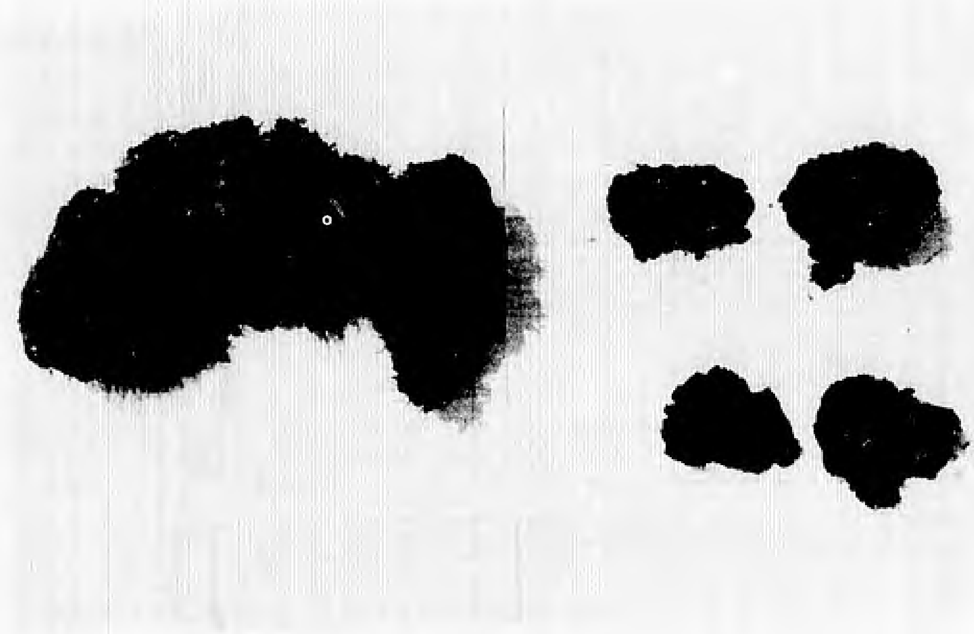

Figure 49. Typical fiber balls formed during mixing of the fibrous concrete, items 1 and 2

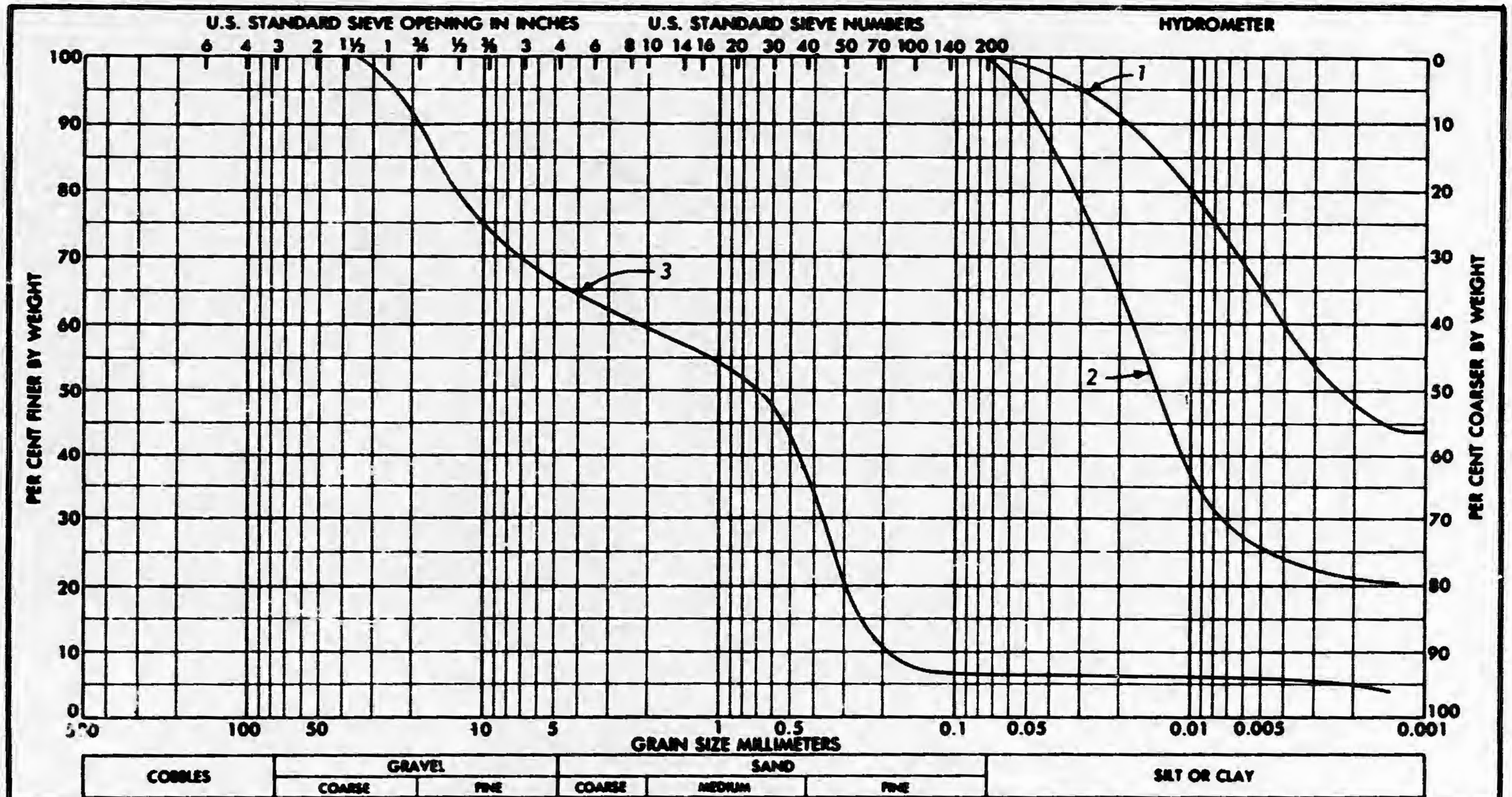

SAMPLE NO.	ELEV OR DEPTH	CLASSIFICATION	NAT W%	LL	PL	PI
1		HEAVY CLAY (CH, E-11)		73	25	48
2		LEAN CLAY (CL, E-7)		43	22	21
3		CLAY GRAVEL (SP-SC, E-5)		29	14	15

Figure 50. Classification data for subgrade, MESL, and cement-treated base materials

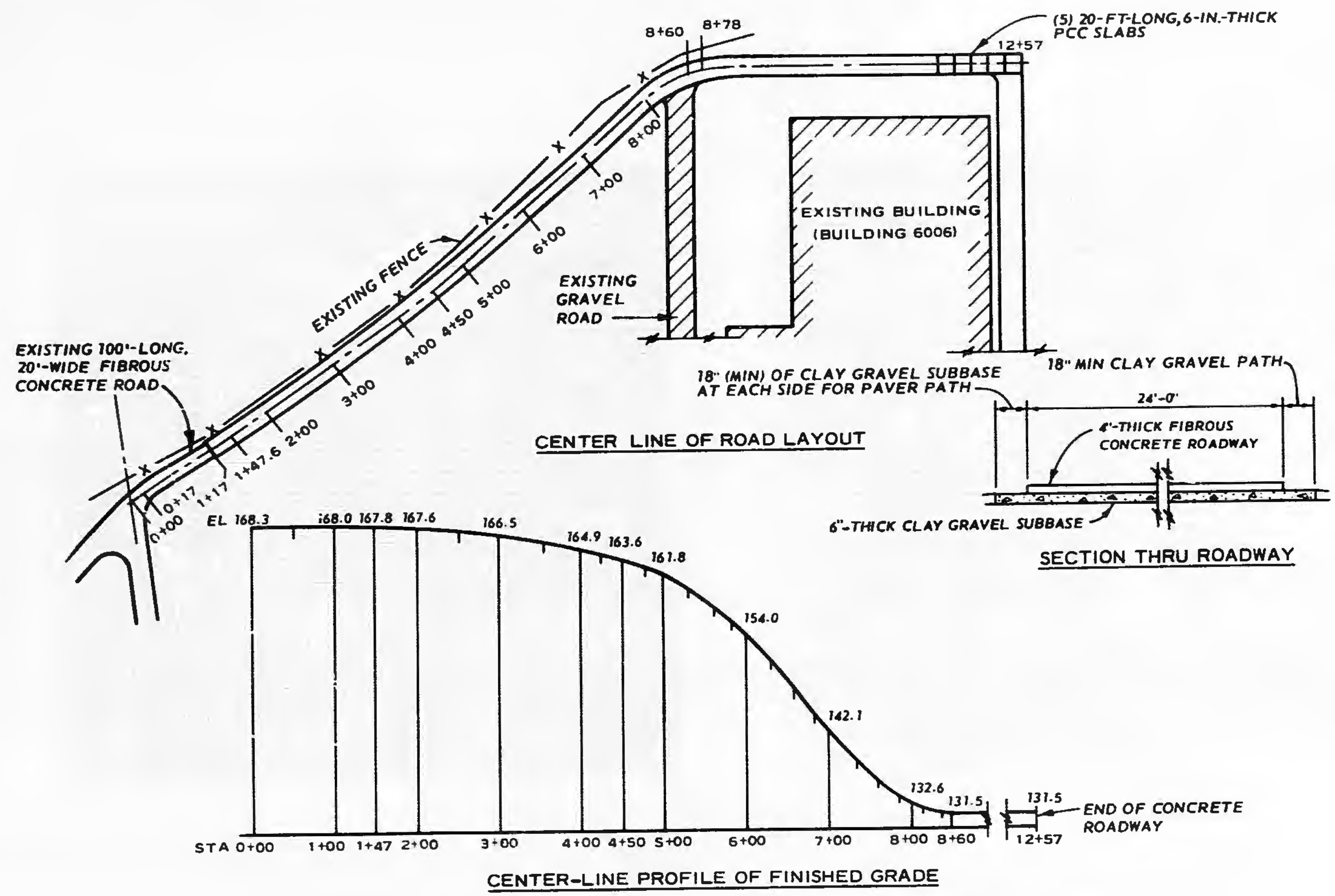

Figure 51. Layout for the WES fibrous concrete roadway

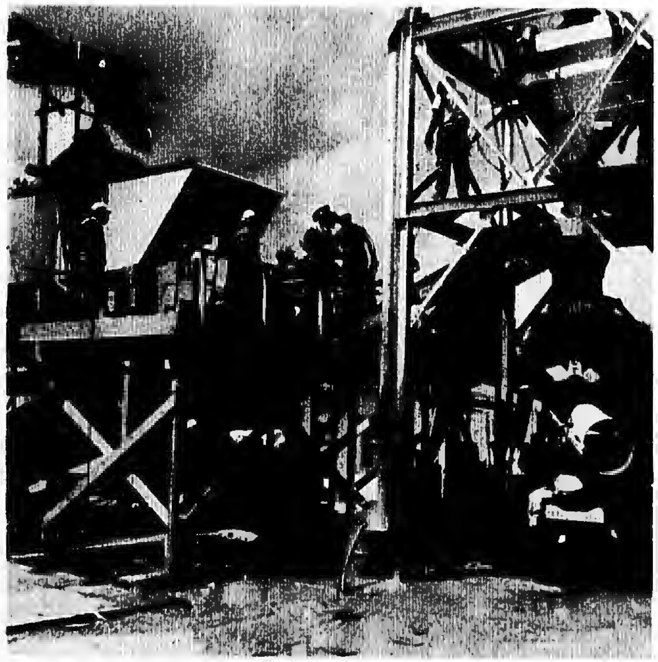

a. View of ready-mix facility

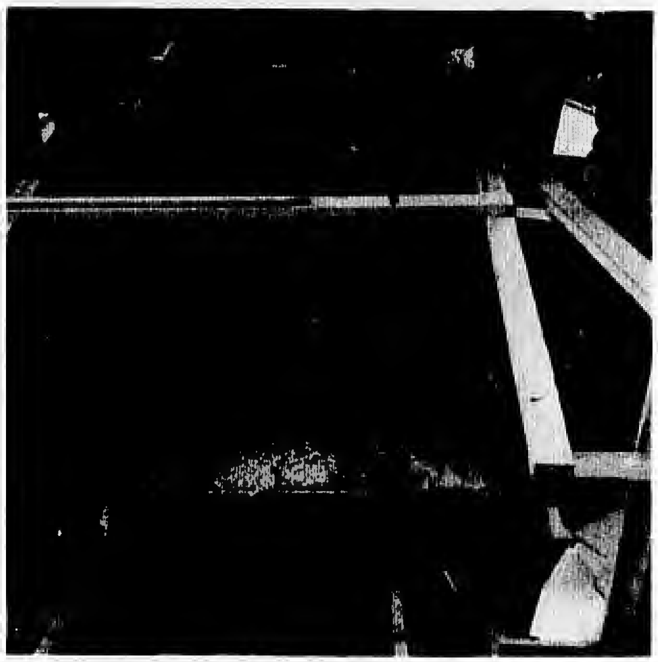

b. Charging fibers

Figure 52. Batching fibrous concrete for the WES roadway

a. Placing concrete in front of paver

b. Front view of paver

Figure 53. Placing fibrous concrete with a slip-form paver

a. Finished edge

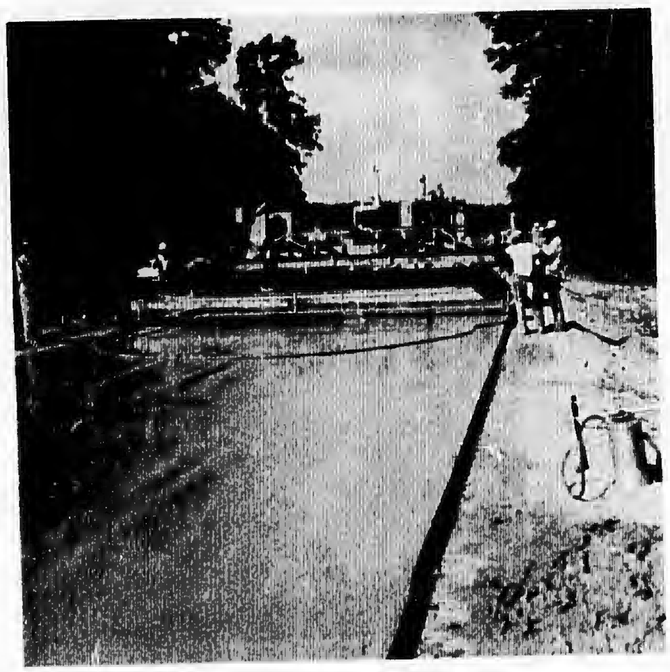

b. Rear view of paver

Figure 54. Finished pavement

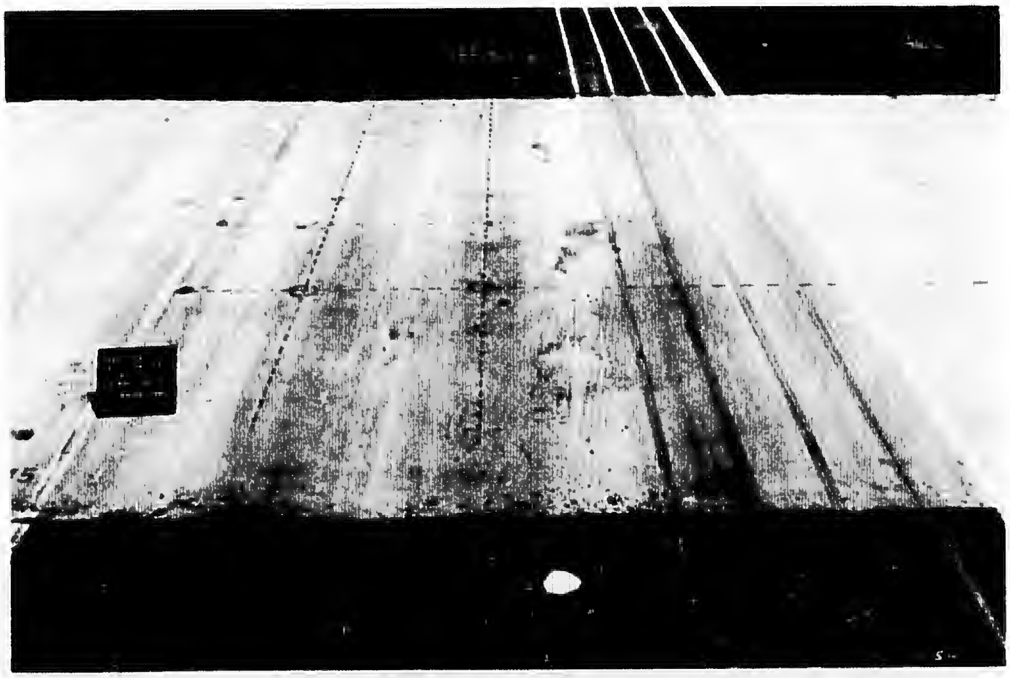

Figure 55. Item 5 prior to initiation of traffic with 360-kip, 12-wheel assembly

Figure 56. Item 5 after 144 coverages of 360-kip, 12-wheel assembly

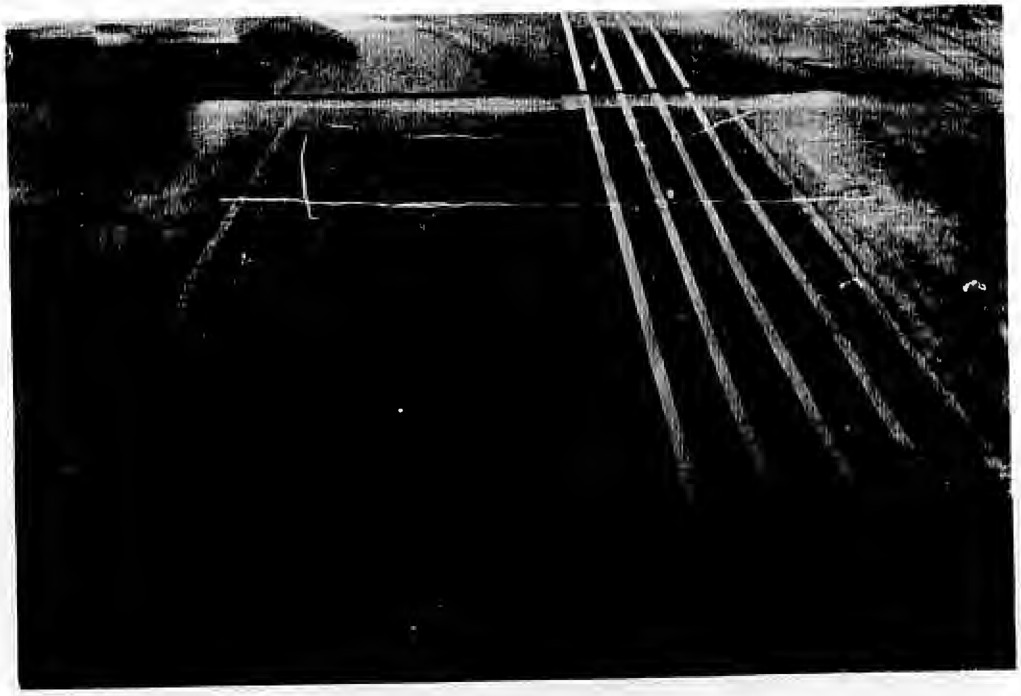

Figure 57. Item 5 after 504 coverages of 360-kip, 12-wheel assembly

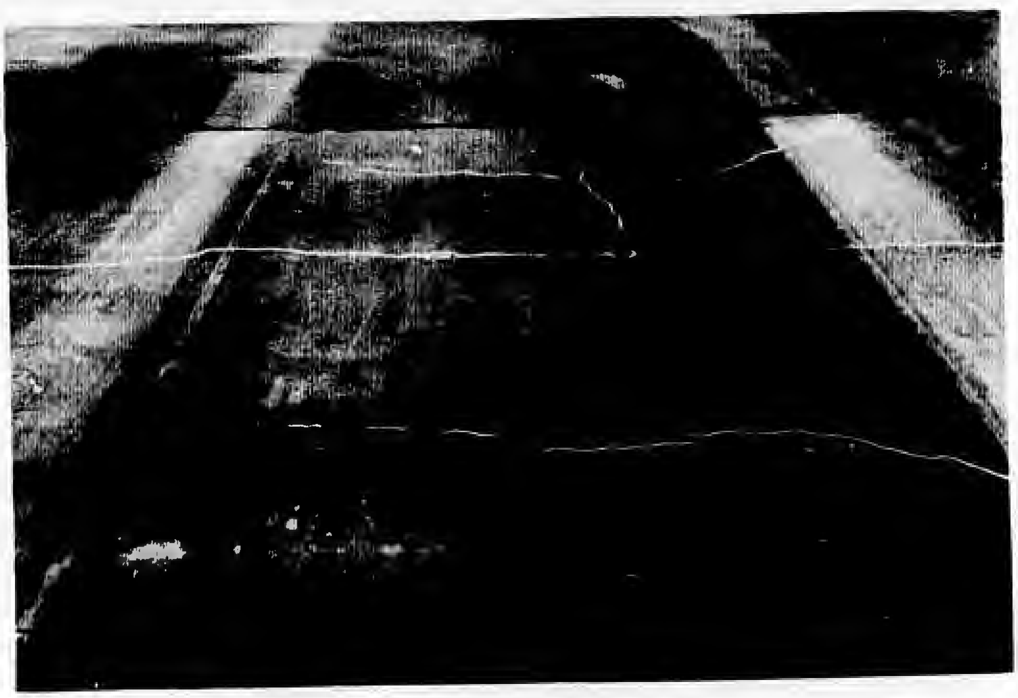

Figure 58. Item 5 after 1328 coverages of 360-kip, 12-wheel assembly

Figure 59. Item 5 after 2336 coverages of 360-kip, 12-wheel assembly

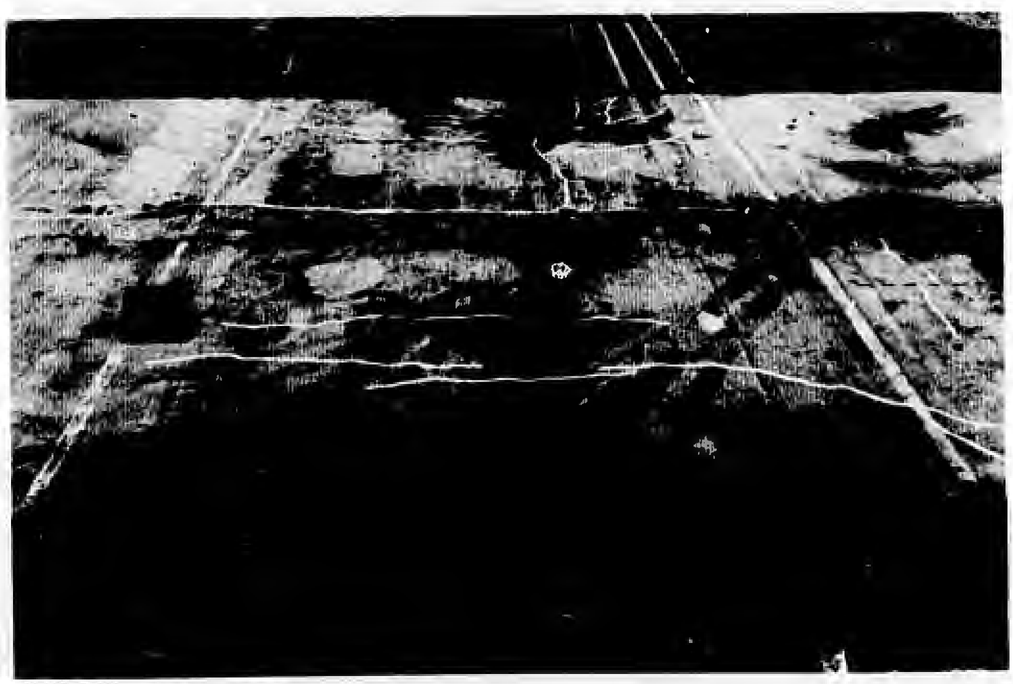

Figure 60. Item 5 after 3200 coverages of 360-kip, 12-wheel assembly

Figure 61. Item 5 after 4176 coverages of 360-kip, 12-wheel assembly

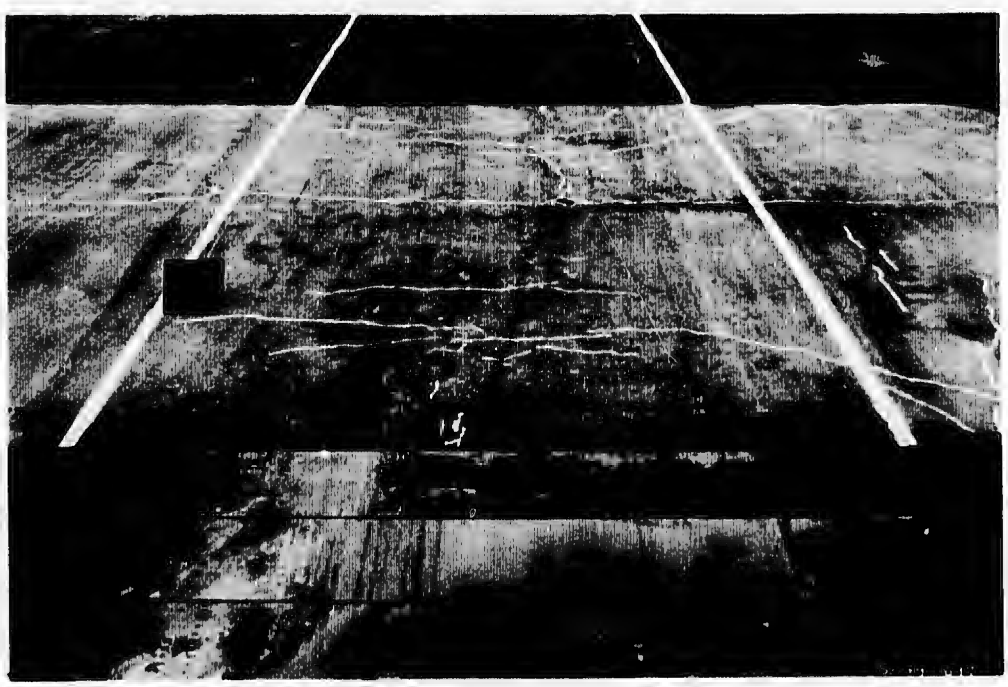

Figure 62. Item 5 after 4512 coverages of 360-kip, 12-wheel assembly

Figure 63. Item 5 after 6352 coverages of 360-kip, 12-wheel assembly

Figure 64. Item 5 after 35 coverages of 166-kip, dual-tandem assembly

Figure 65. Item 5 after 130 coverages of 166-kip, dual-tandem assembly

Figure 66. Item 5 after 170 coverages of 166-kip, dual-tandem assembly

Figure 67. Item 5 after 550 coverages of 166-kip, dual-tandem assembly

Figure 68. Item 3 overlay prior to initiation of traffic with 360-kip, 12-wheel assembly

Figure 69. Item 3 overlay after 1872 coverages of 360-kip, 12-wheel assembly

Figure 70. Item 3 overlay after 2848 coverages of 360-kip, 12-wheel assembly

Figure 71. Item 3 overlay after 3184 coverages of 360-kip, 12-wheel assembly

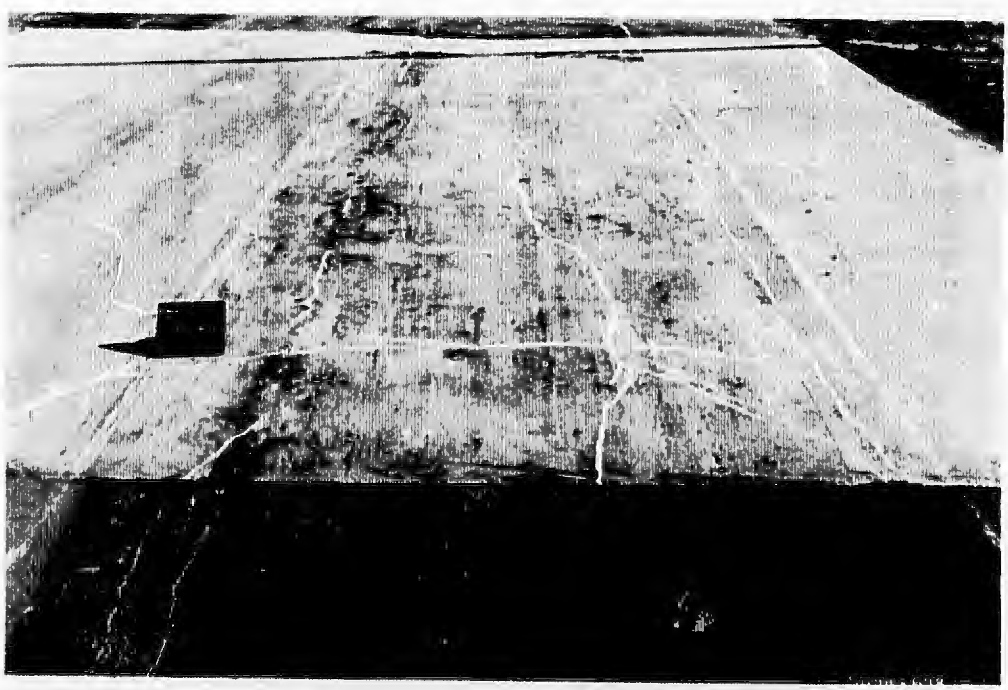

Figure 72. Item 3 overlay after 5024 coverages of 360-kip, 12-wheel assembly

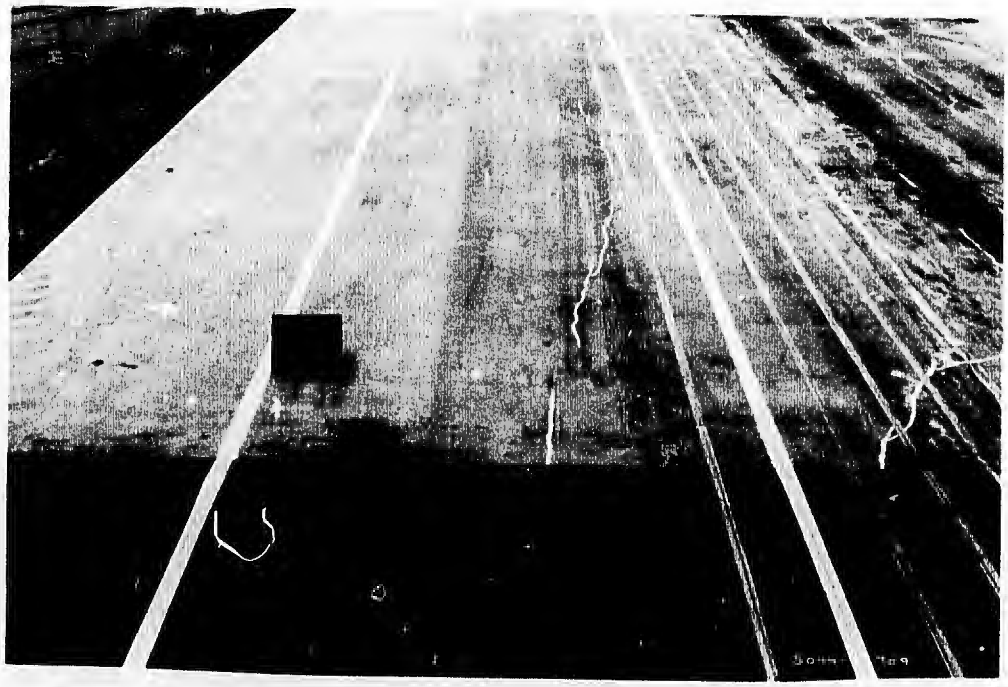

Figure 73. Item 3 overlay prior to initiation of traffic with 166-kip, dual-tandem assembly

Figure 74. Item 3 overlay after 950 coverages of 166-kip, dual-tandem assembly

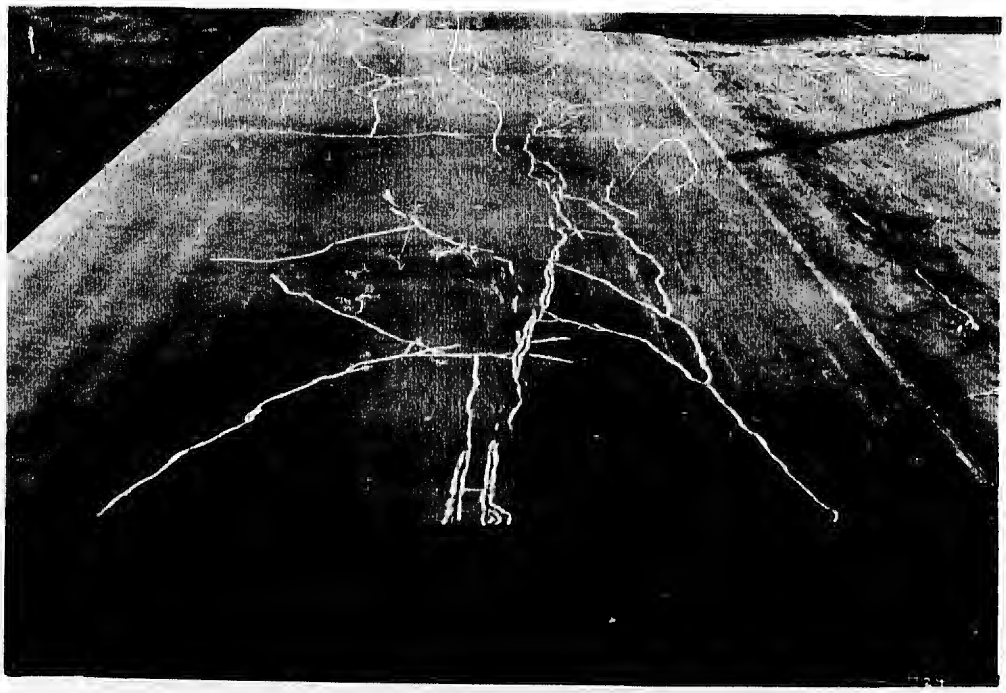

Figure 75. Item 3 overlay after 260 coverages of 240-kip, dual-tandem assembly

Figure 76. Item 3 overlay after 420 coverages of 240-kip, dual-tandem assembly

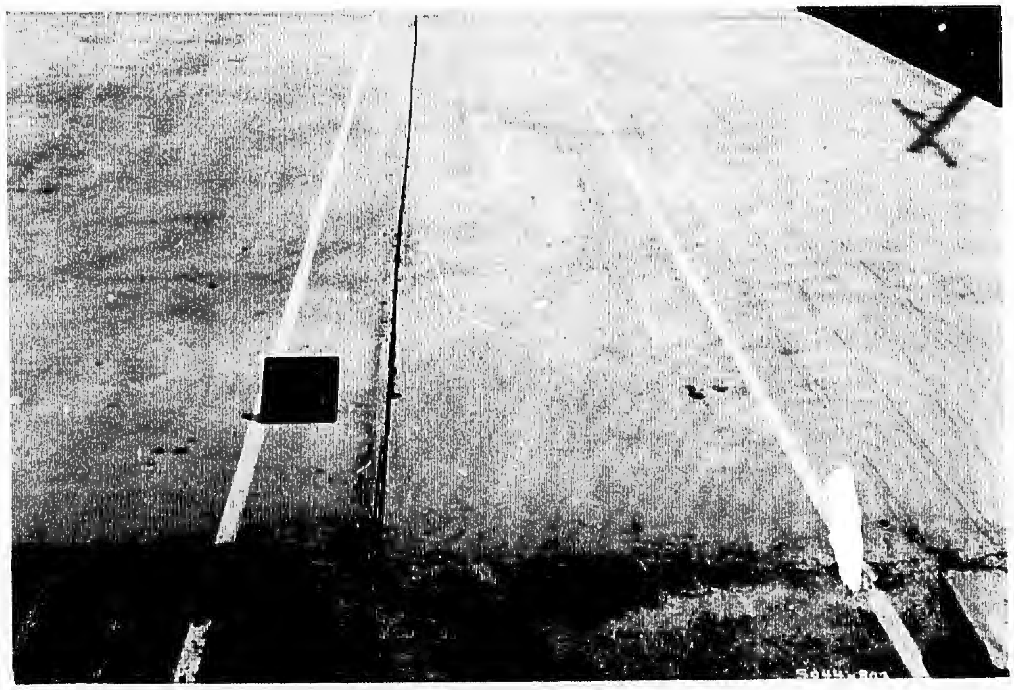

Figure 77. Item 1 prior to initiation of traffic with 200-kip, dual-tandem assembly

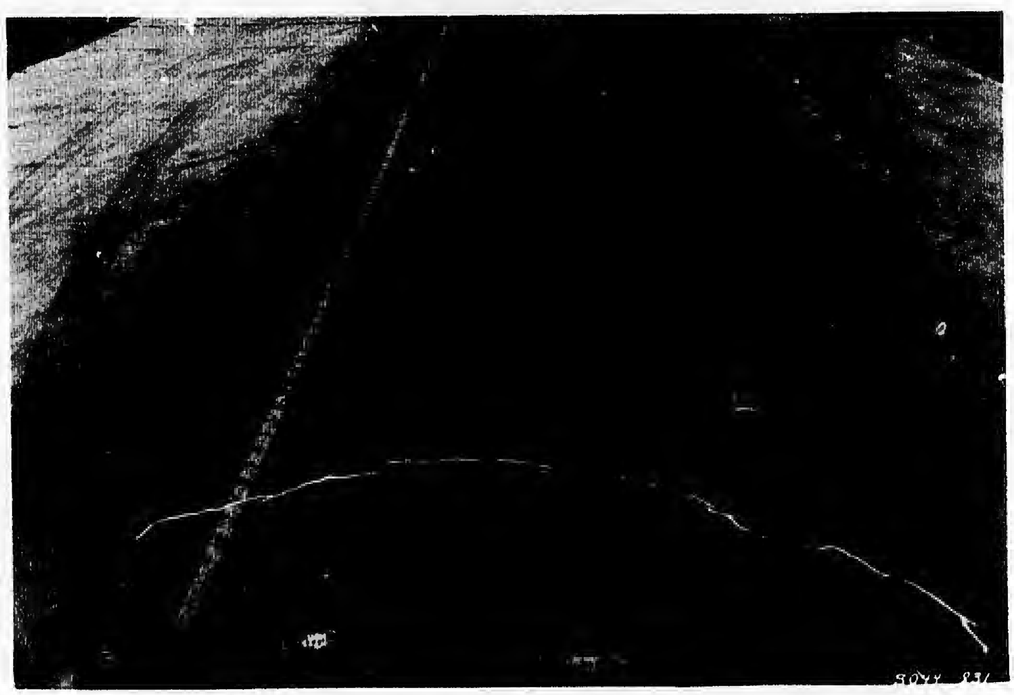

Figure 78. Item 1 after 200 coverages of 200-kip, dual-tandem assembly

Figure 79. Item 1 after 1000 coverages of 200-kip, dual-tandem assembly

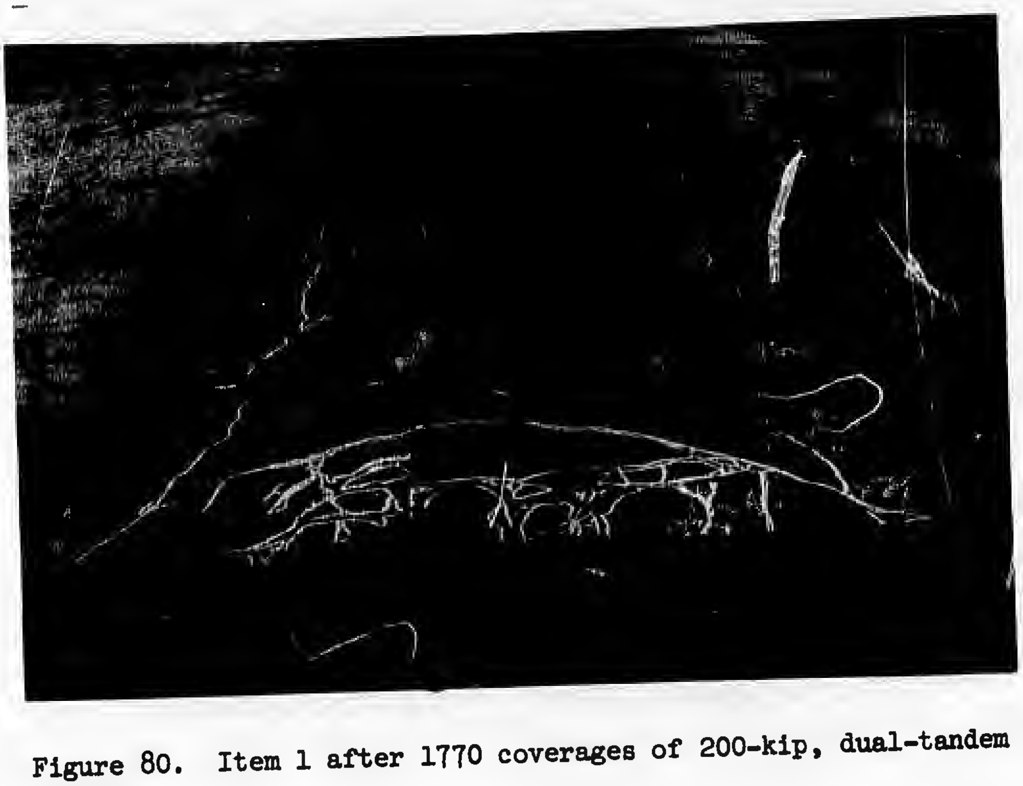

Figure 80. Item 1 after 1770 coverages of 200-kip, dual-tandem assembly

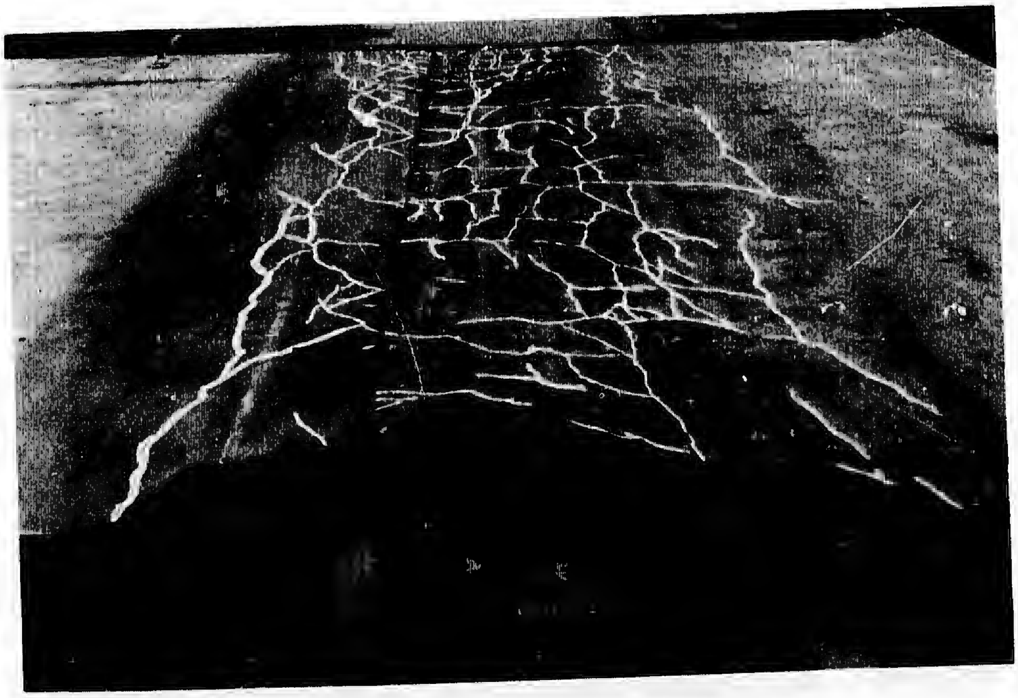

Figure 81. Item 1 after 3000 coverages of 200-kip, dual-tandem assembly

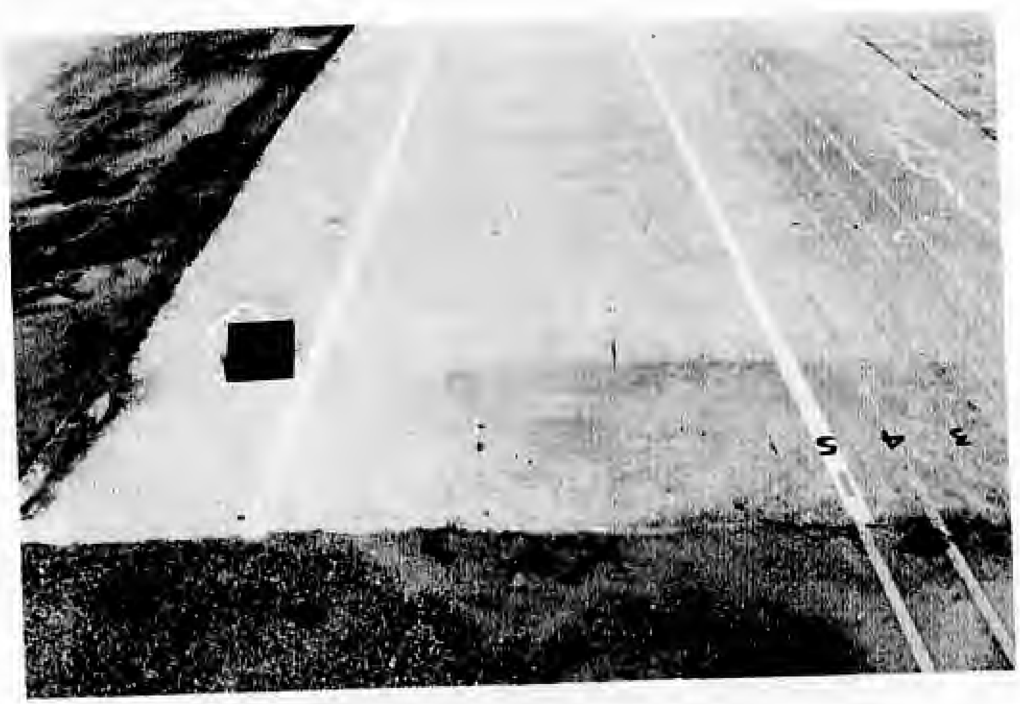

Figure 82. Item 1 prior to initiation of traffic with 240-kip, dual-tandem assembly

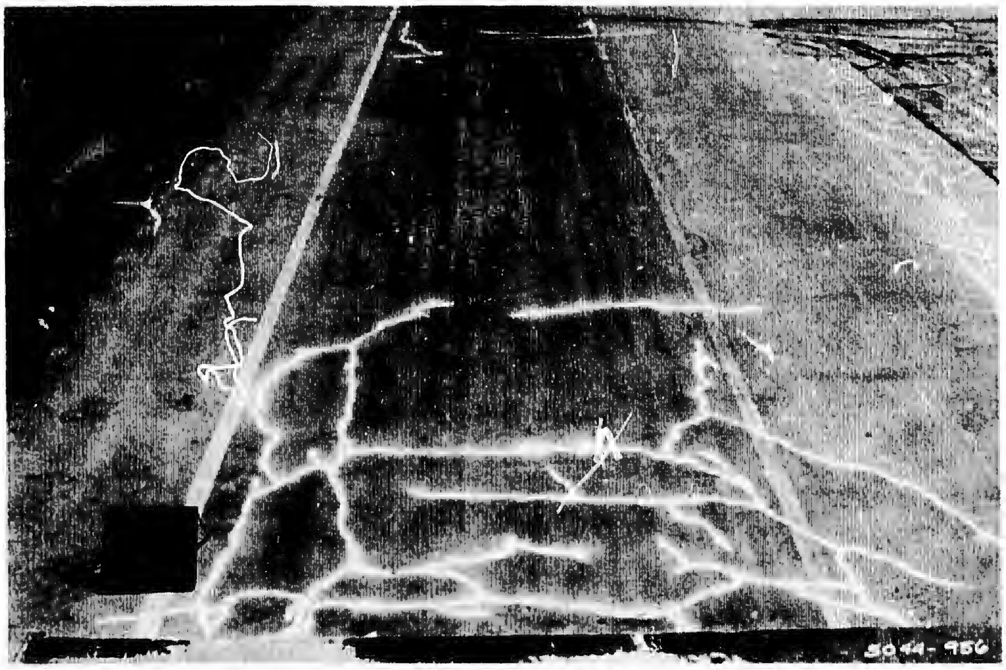

Figure 83. Item 1 after 200 coverages of 240-kip, dual-tandem assembly

Figure 84. Item 1 after 1010 coverages of 240-kip, dual-tandem assembly

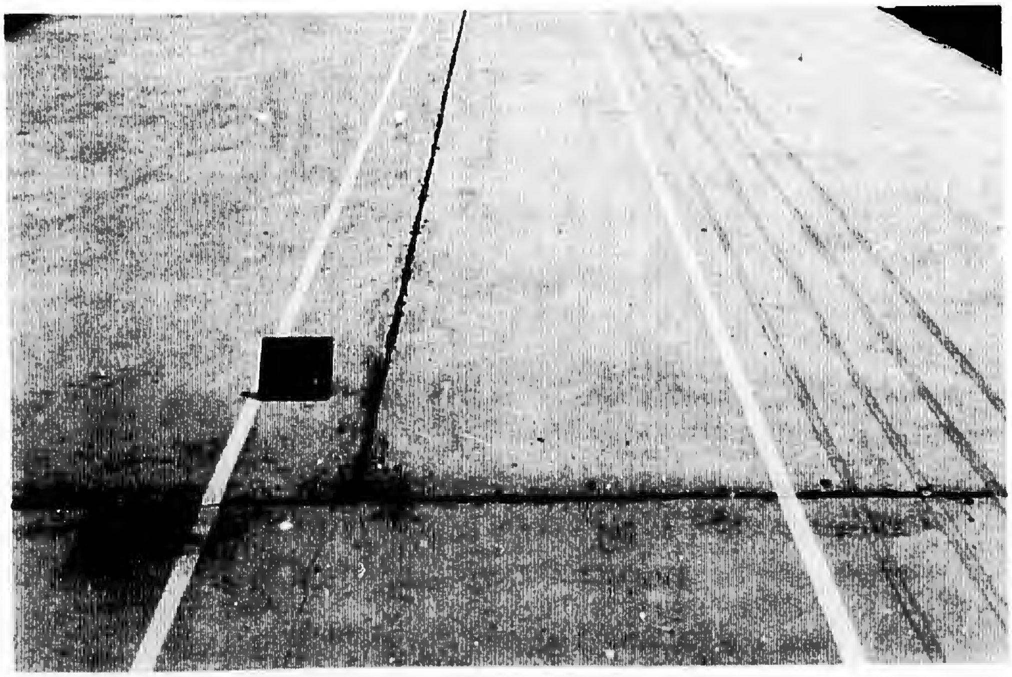

Figure 85. Item 2 prior to initiation of traffic with 200-kip, dual-tandem assembly

Figure 86. Item 2 after 200 coverages of 200-kip, dual-tandem assembly

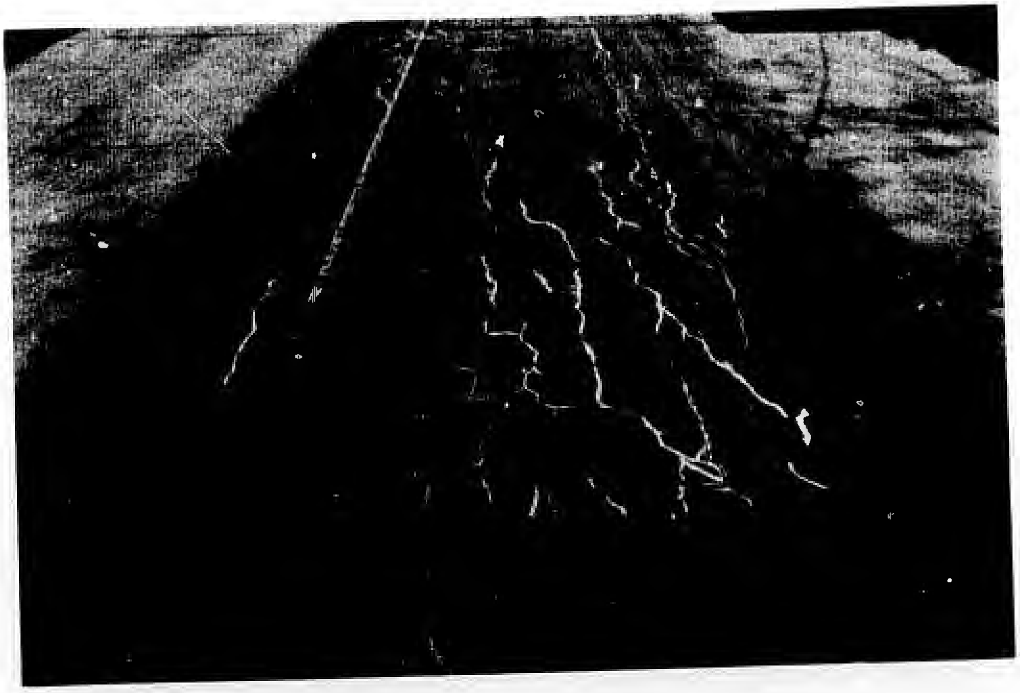

Figure 87. Item 2 after 1000 coverages of 200-kip, dual-tandem assembly

Figure 88. Item 2 after 1770 coverages of 200-kip, dual-tandem assembly

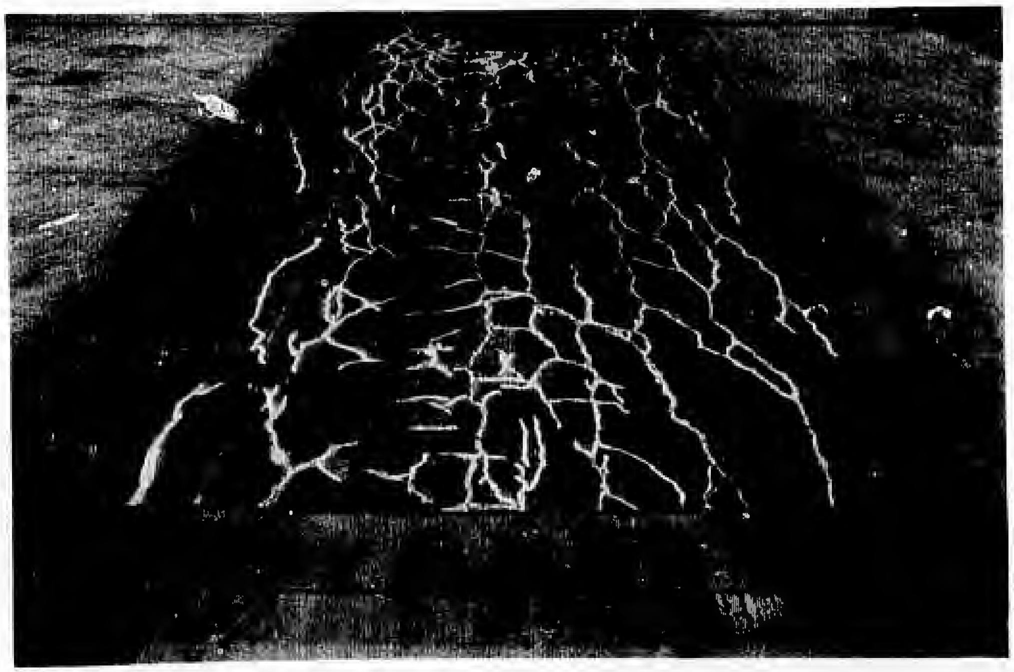

Figure 89. Item 2 after 3000 coverages of 200-kip, dual-tandem assembly

Figure 90. Item 2 prior to initiation of traffic with 240-kip, dual-tandem assembly

Figure 91. Item 2 after 200 coverages of 240-kip, dual-tandem assembly

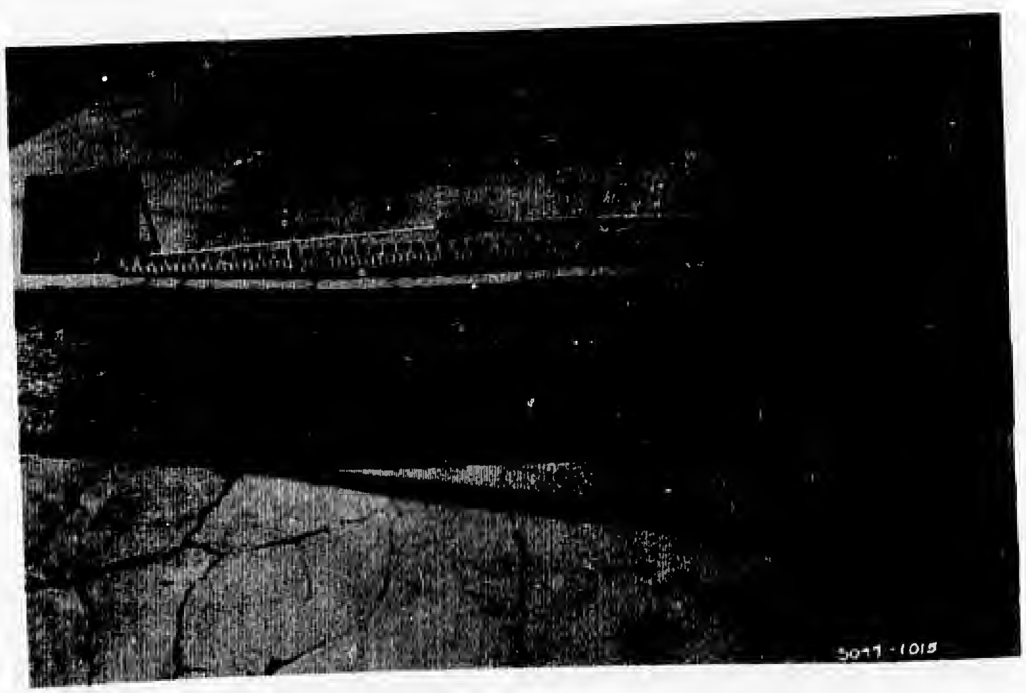

Figure 92. Item 2 after 950 coverages of 240-kip, dual-tandem assembly

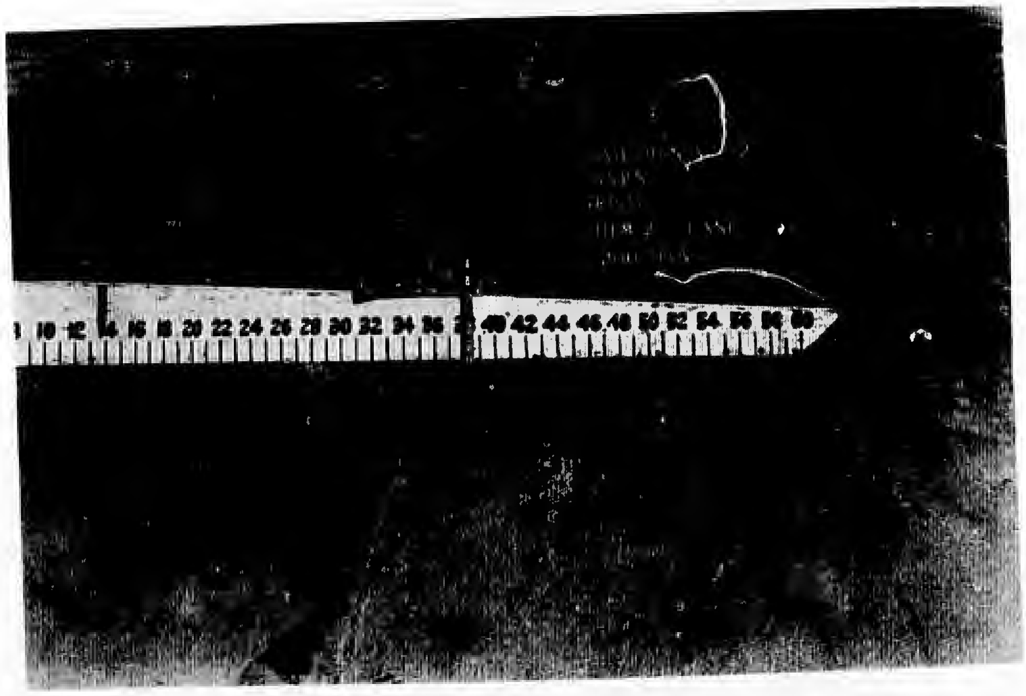

Figure 93. Condition of longitudinal construction joint in Item 2 after 200 coverages of 200-kip, dual-tandem assembly

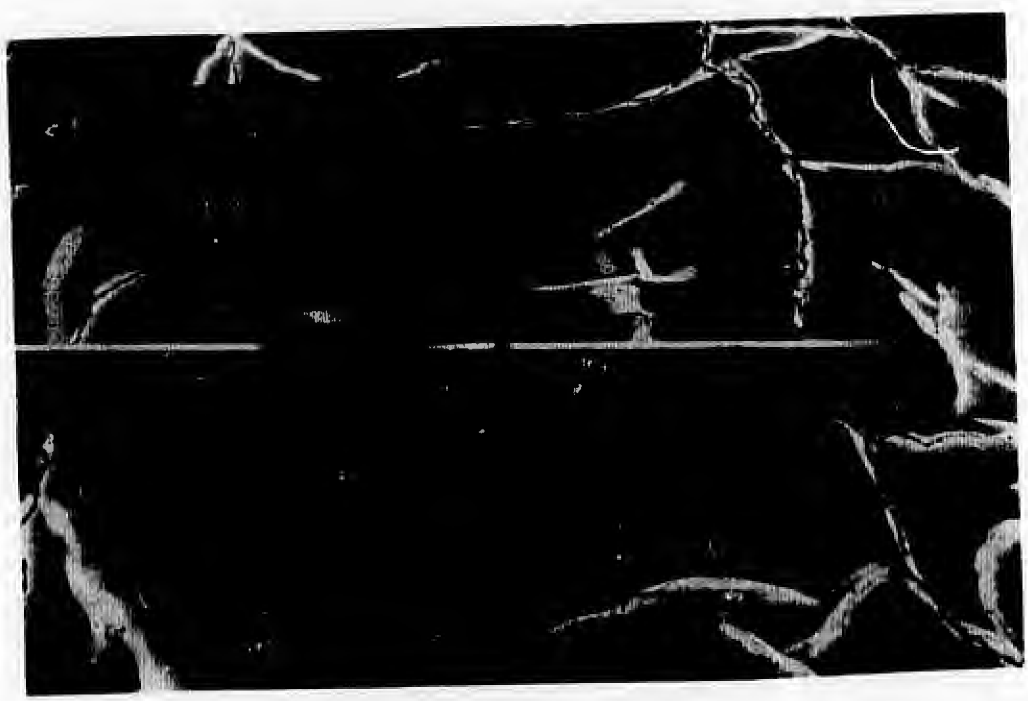

Figure 94. Condition of longitudinal construction joint in Item 2 after 3000 coverages of 200-kip, dual-tandem assembly

Figure 95. Test pit across longitudinal construction joint in Item 2 after 3000 coverages of 200-kip, dual-tandem assembly

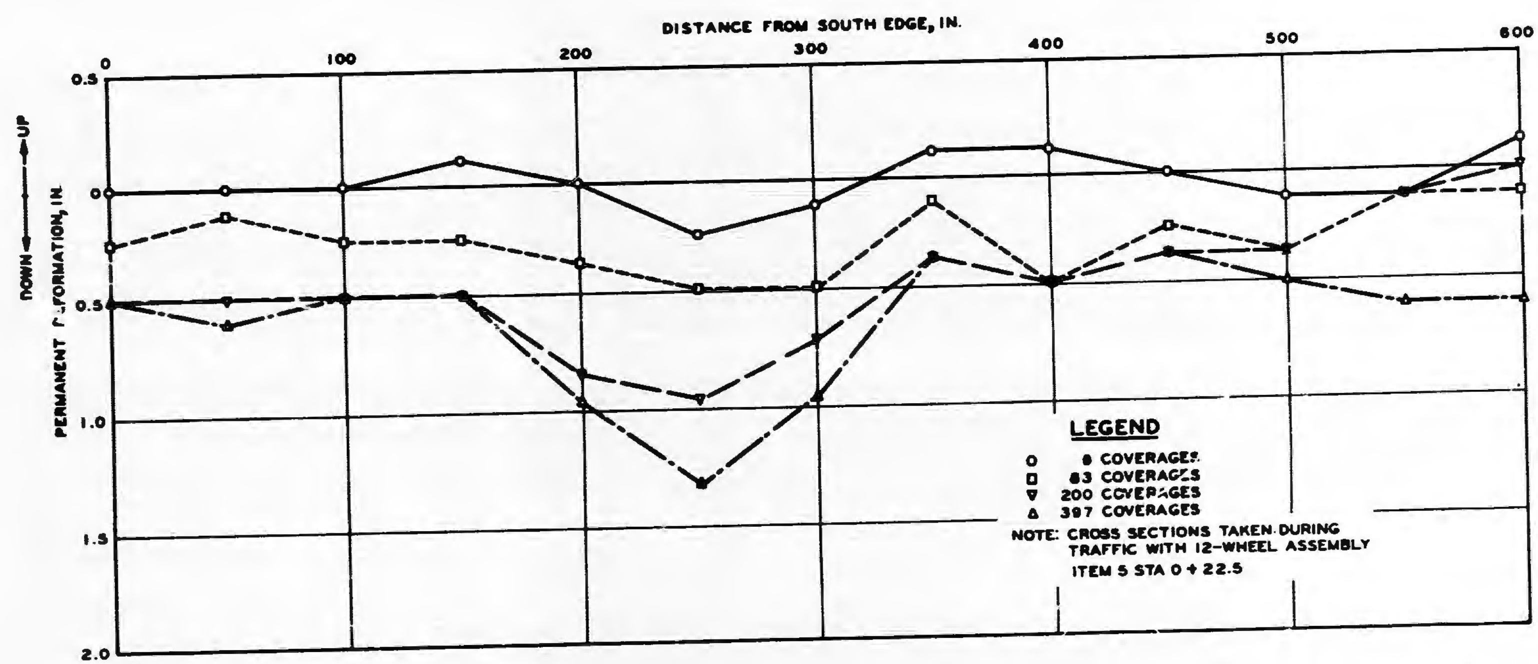

Figure 96. Permanent deformations under 360-kip, 12-wheel assembly, item 5 of the keyed longitudinal joint test section

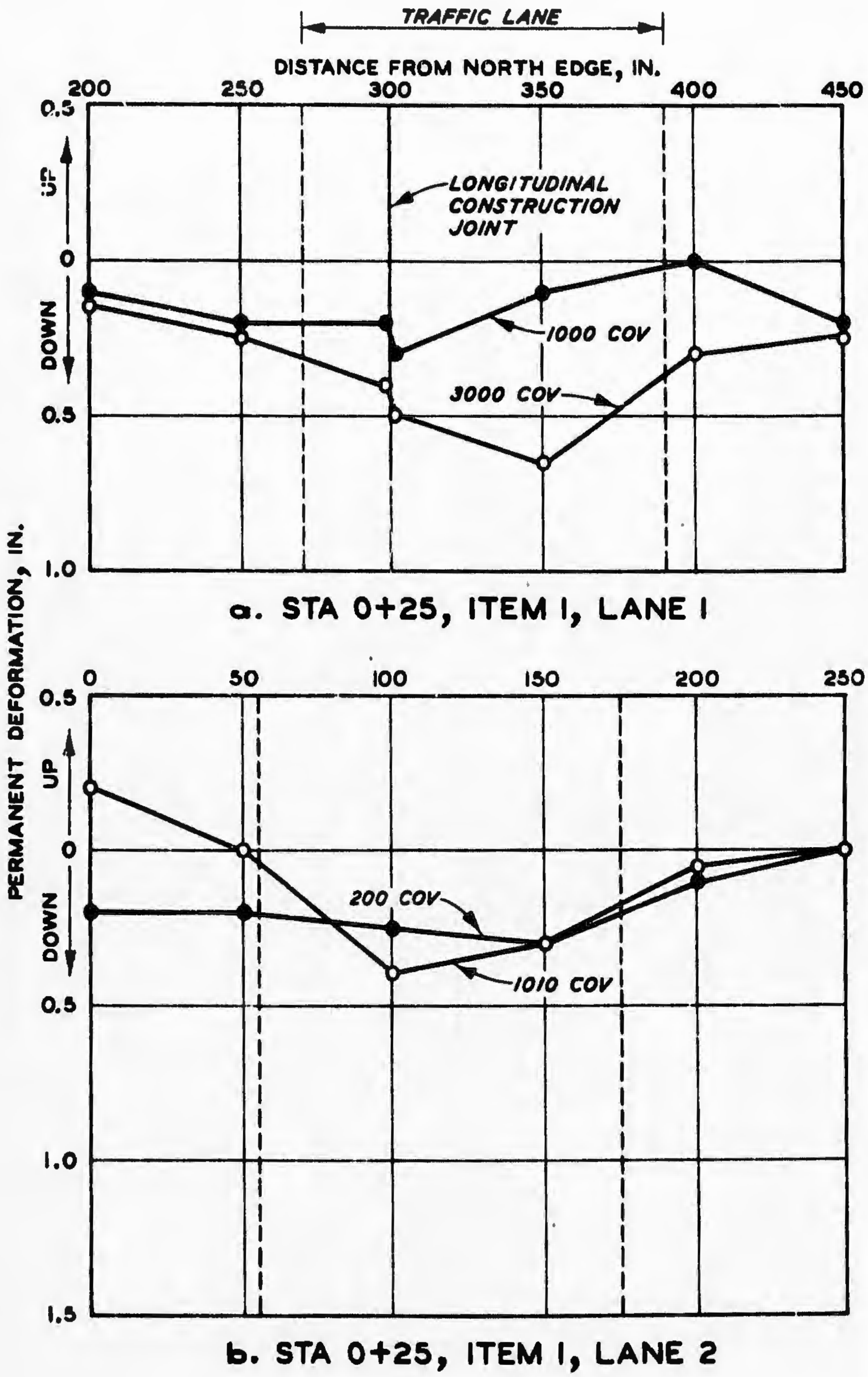

Figure 97. Permanent deformations, item 1, structural layers test section

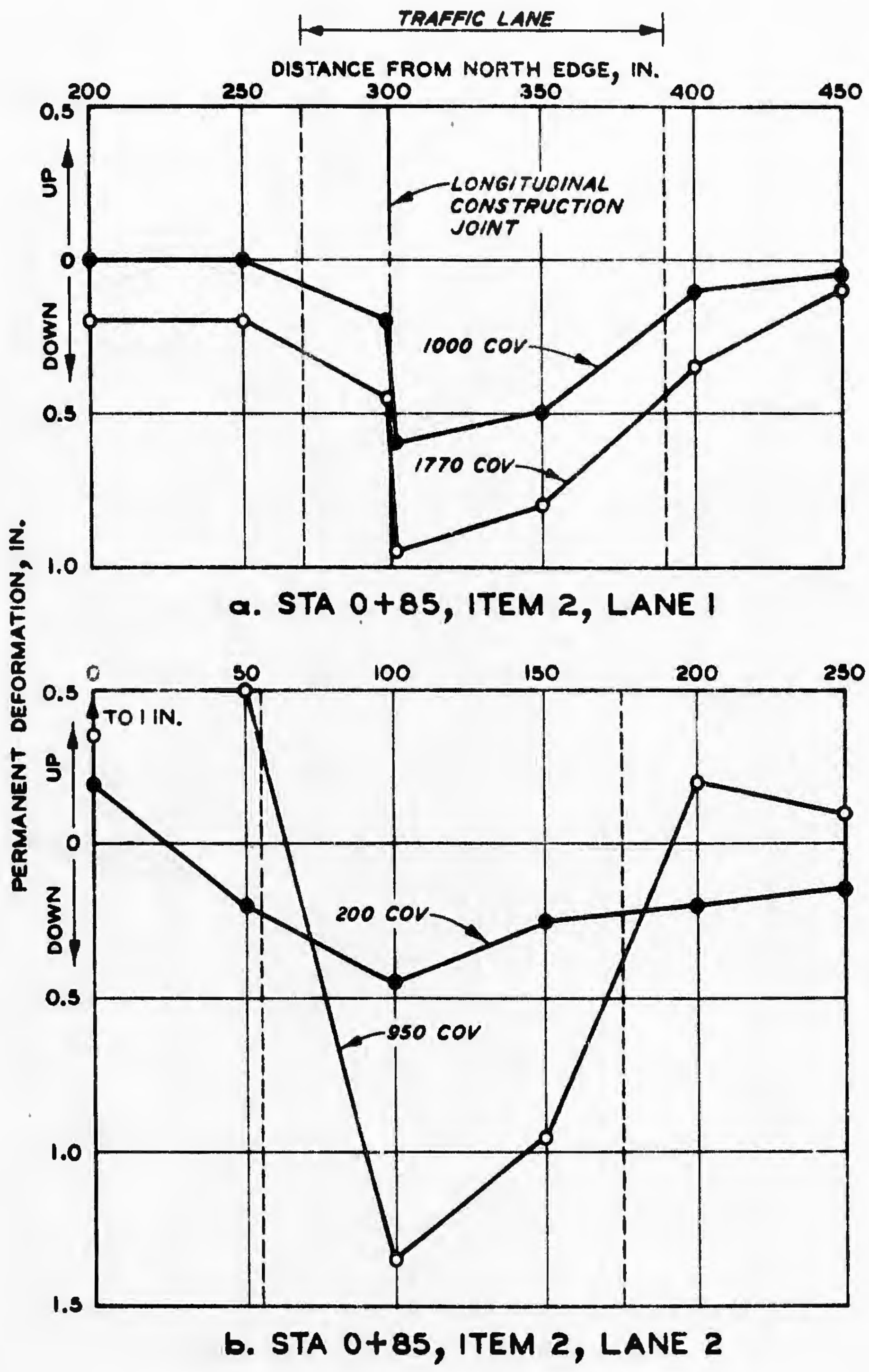

Figure 98. Permanent deformations, item 2, structural layers test section

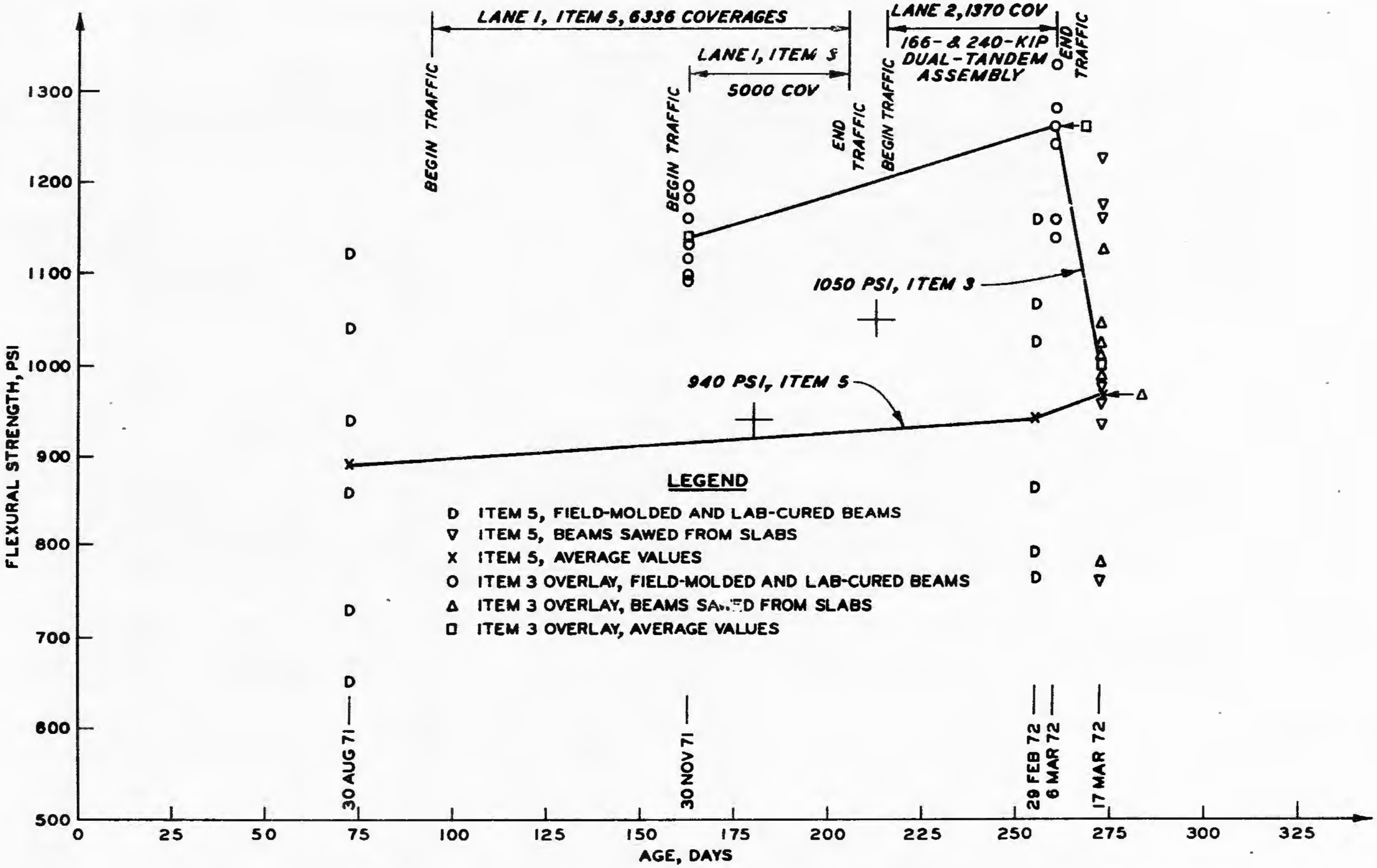

Figure 99. Flexural strength as a function of pavement age and traffic for the keyed longitudinal joint test section

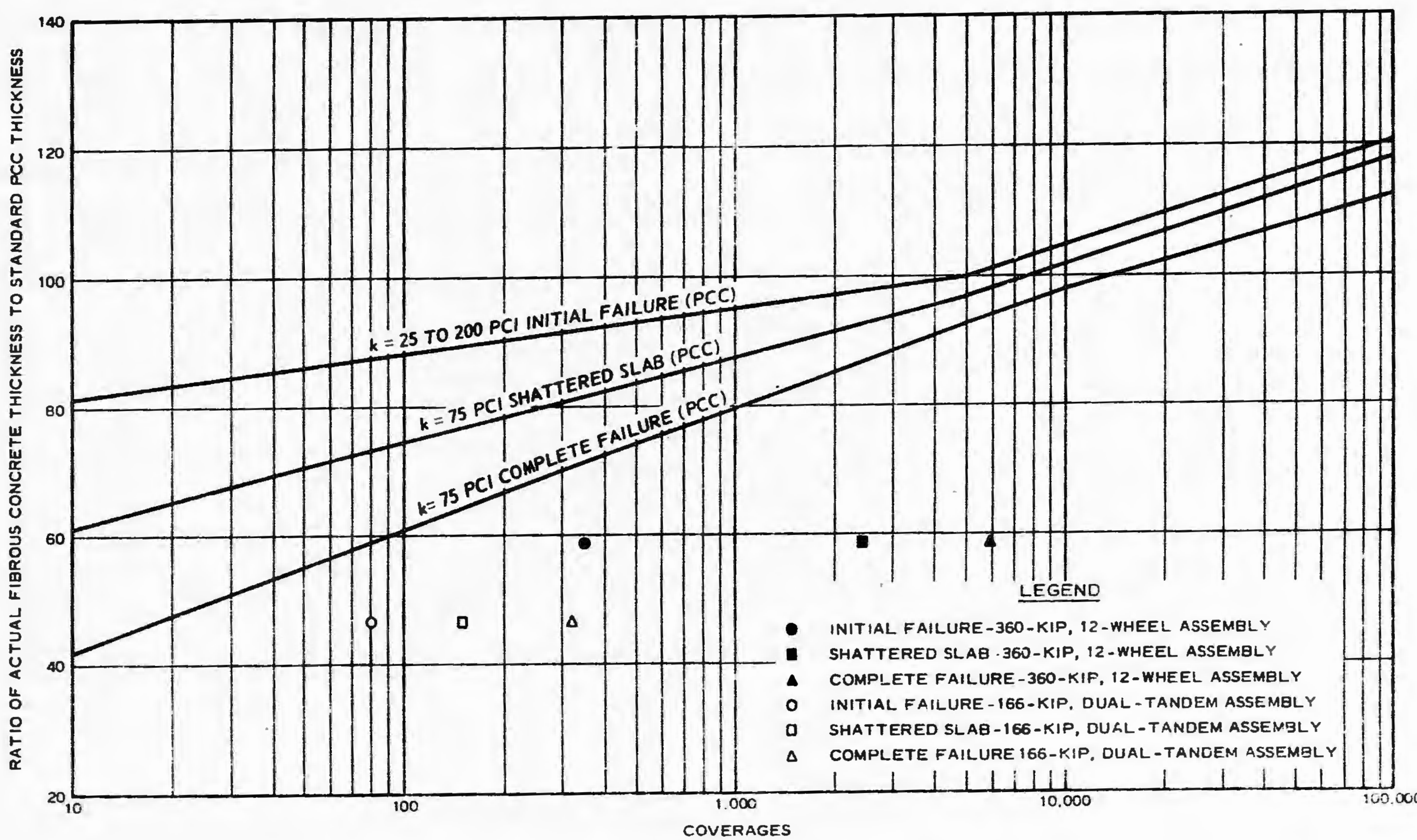

Figure 100. Comparative performance of item 5 of the keyed longitudinal joint test section

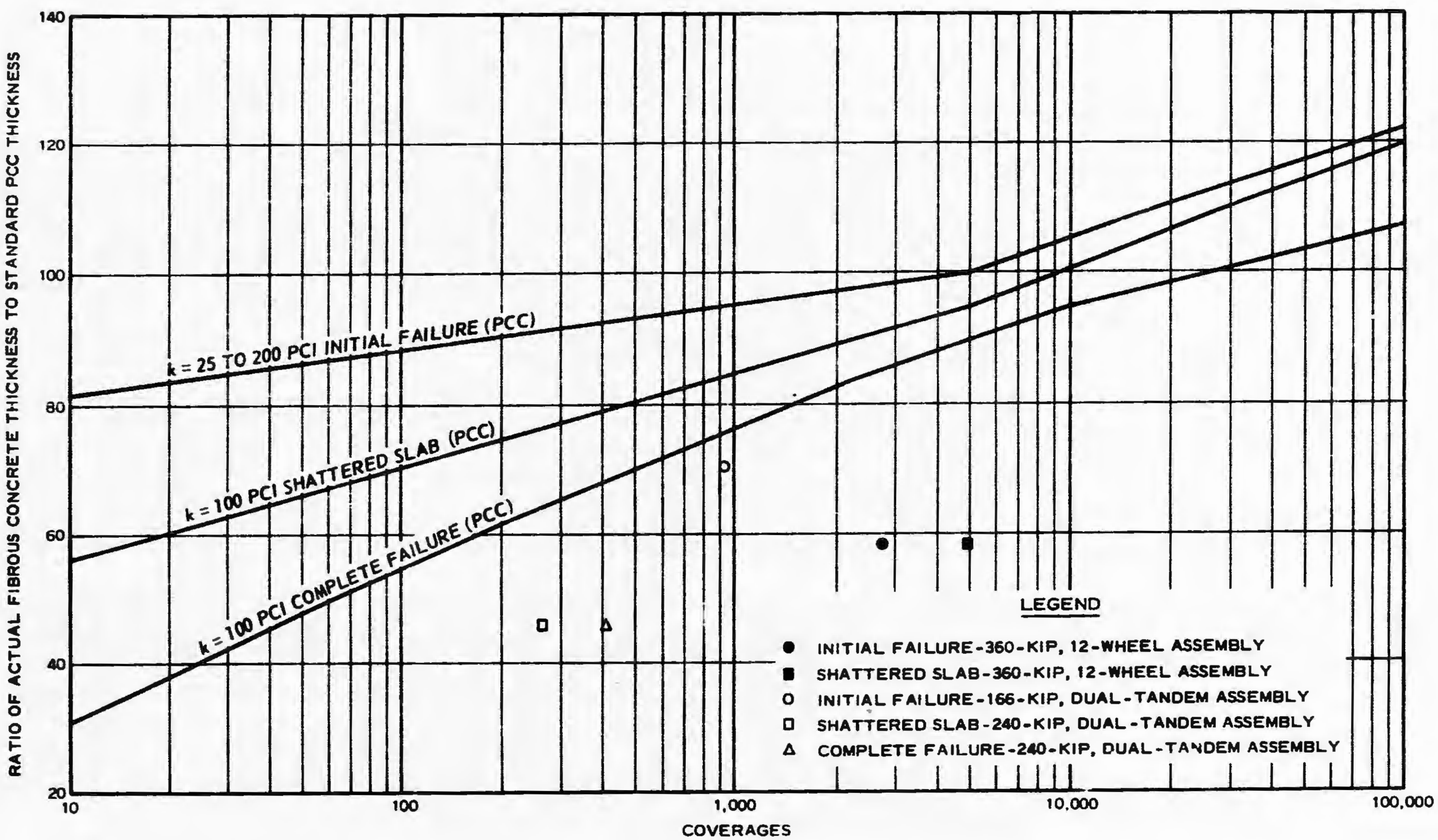

Figure 101. Comparative performance of item 3 overlay of the keyed longitudinal joint test section

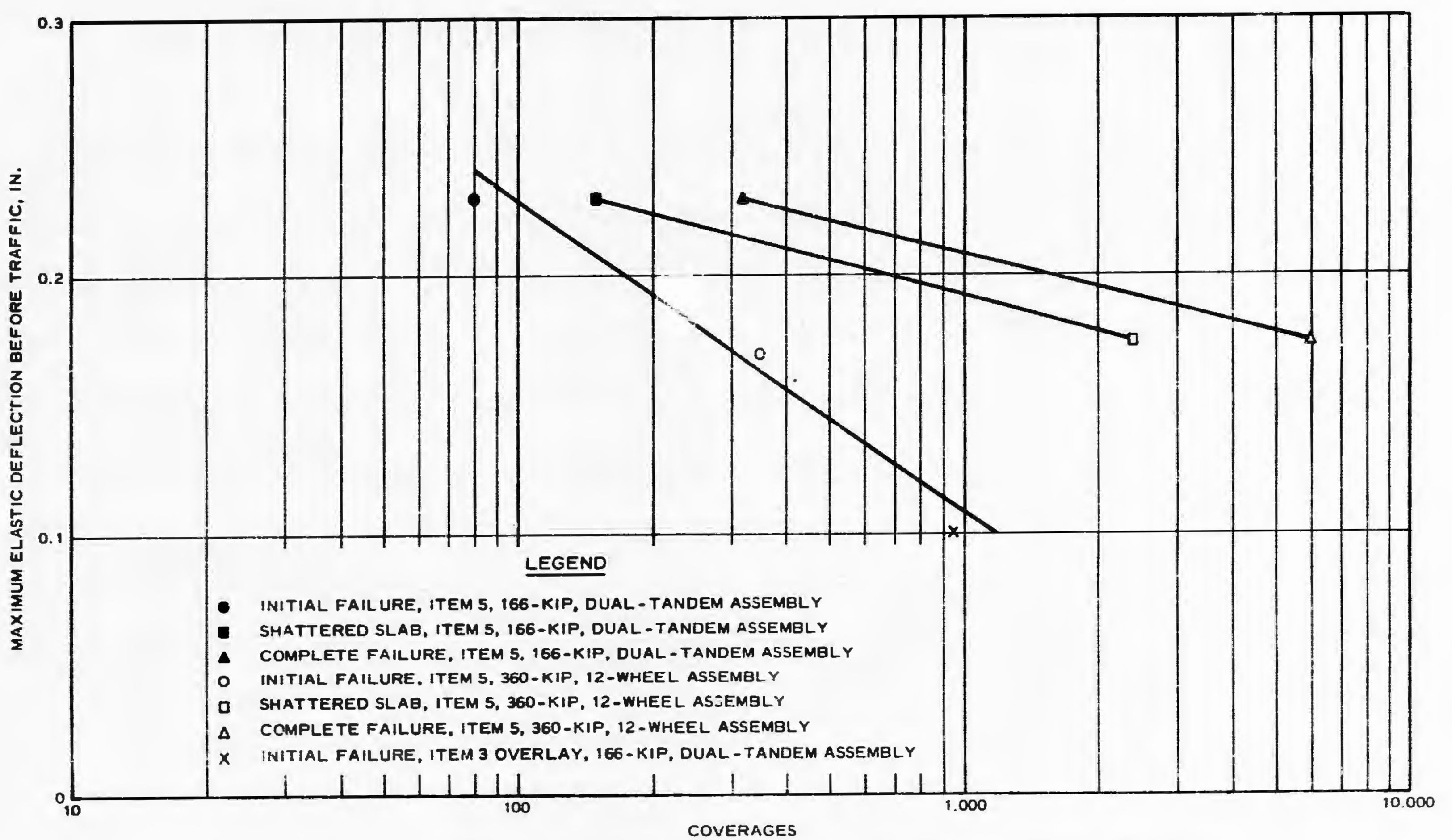

Figure 102. Pavement performance as a function of deflection for the keyed longitudinal joint test section

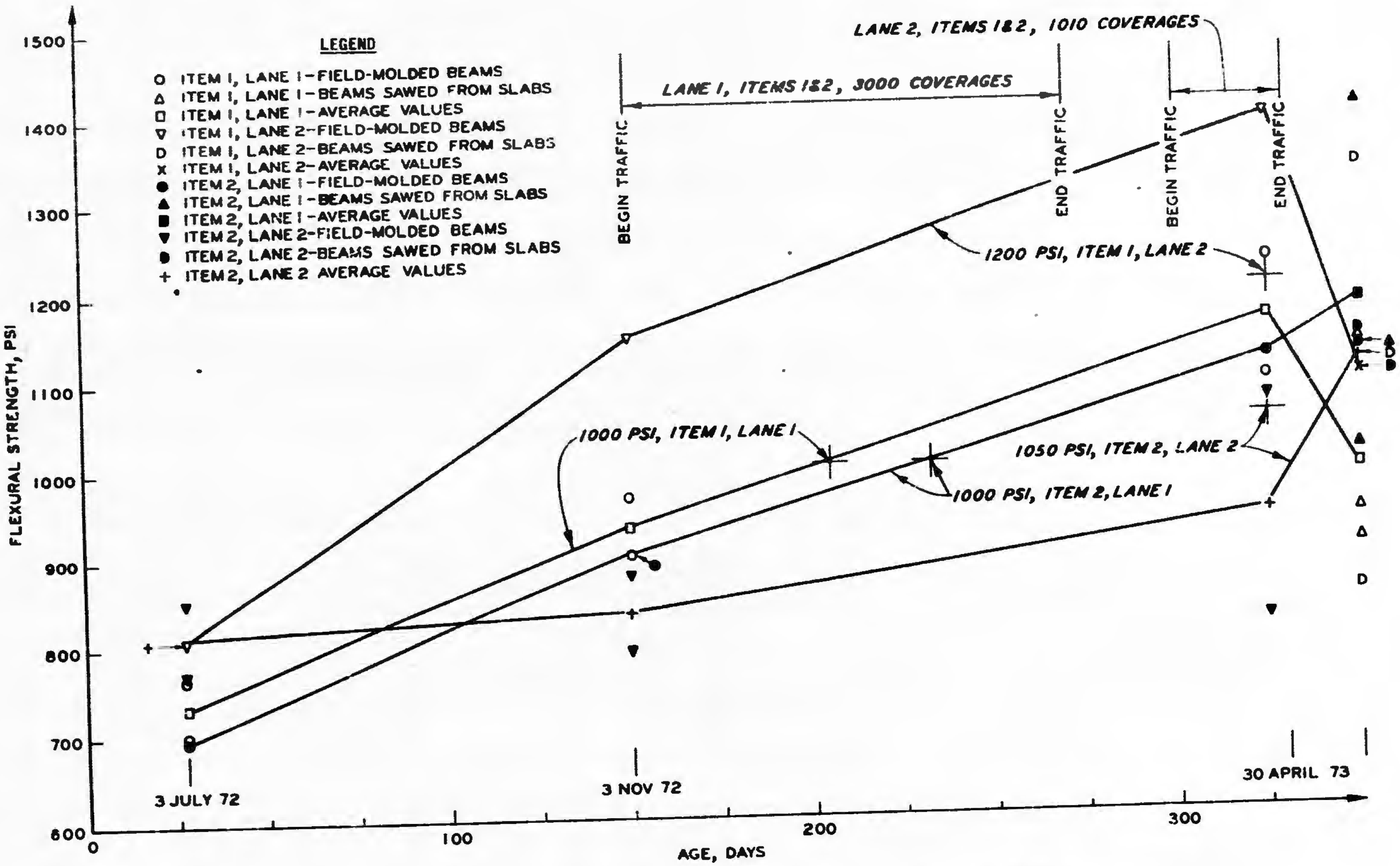

Figure 103. Flexural strength as a function of pavement age and traffic for the structural layers test section

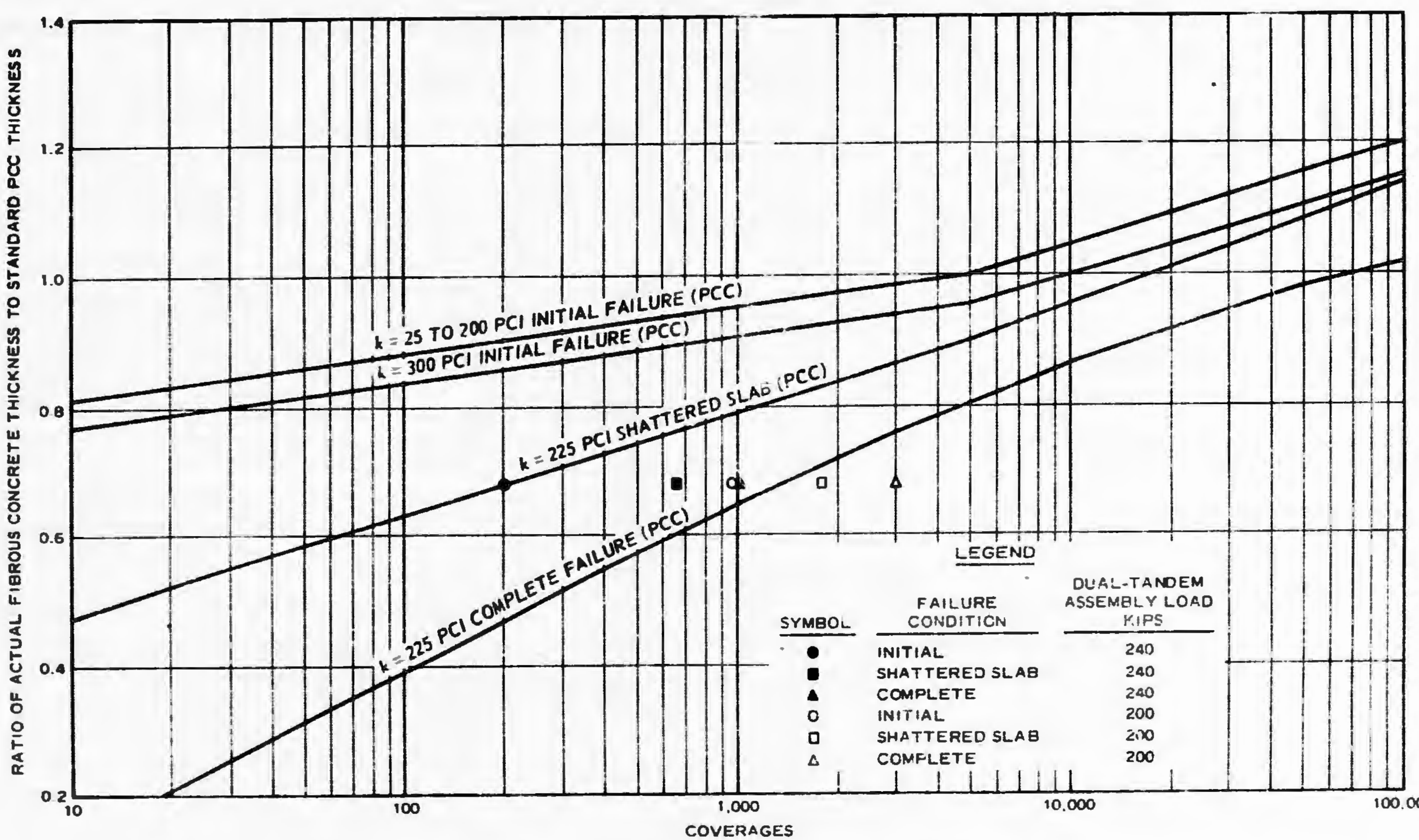

Figure 104. Comparative performance of item 1 of the structural layers test section

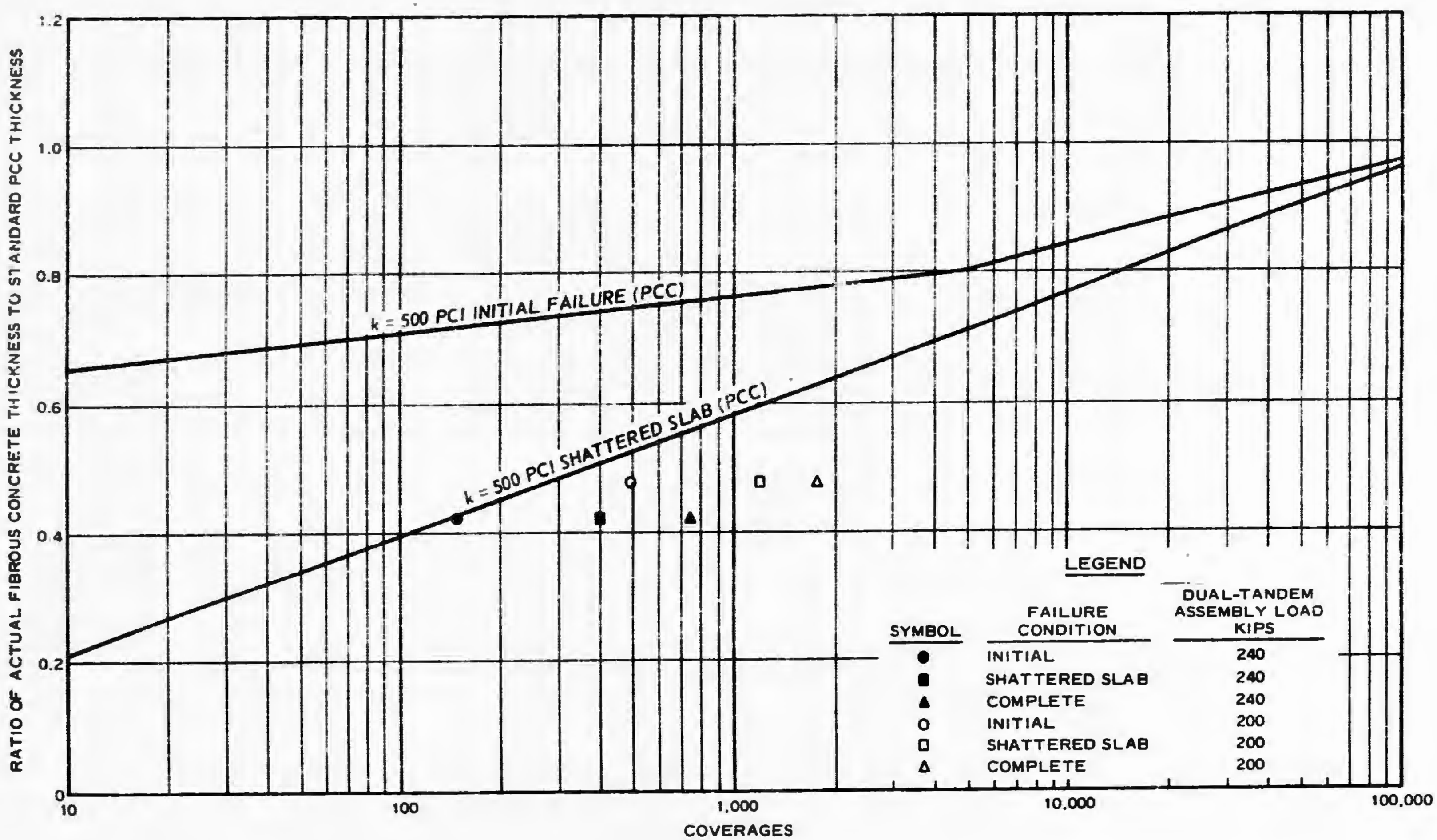

Figure 105. Comparative performance of item 2 of the structural layers test section

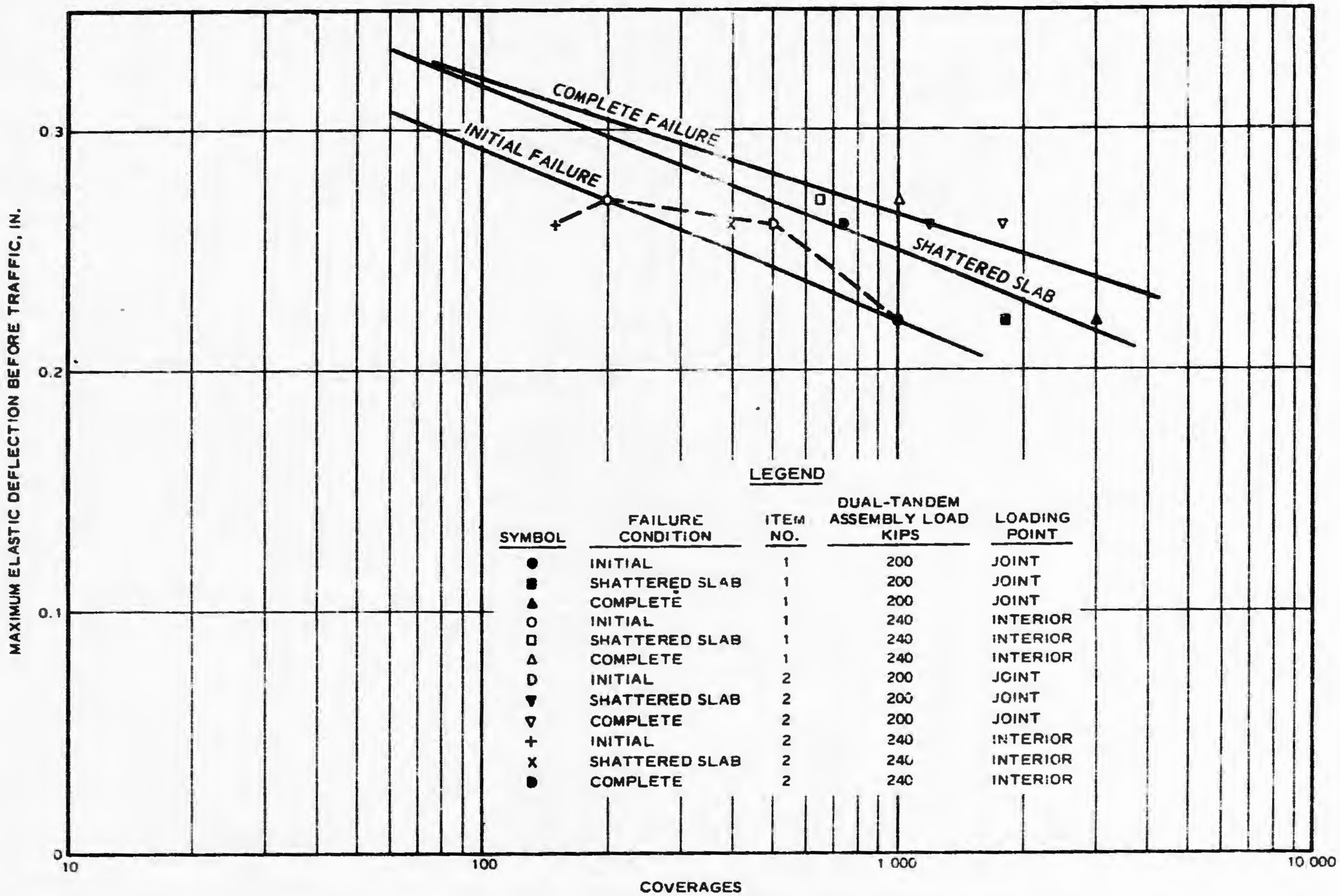

Figure 106. Pavement performance as a function of deflection for the structural layers test section

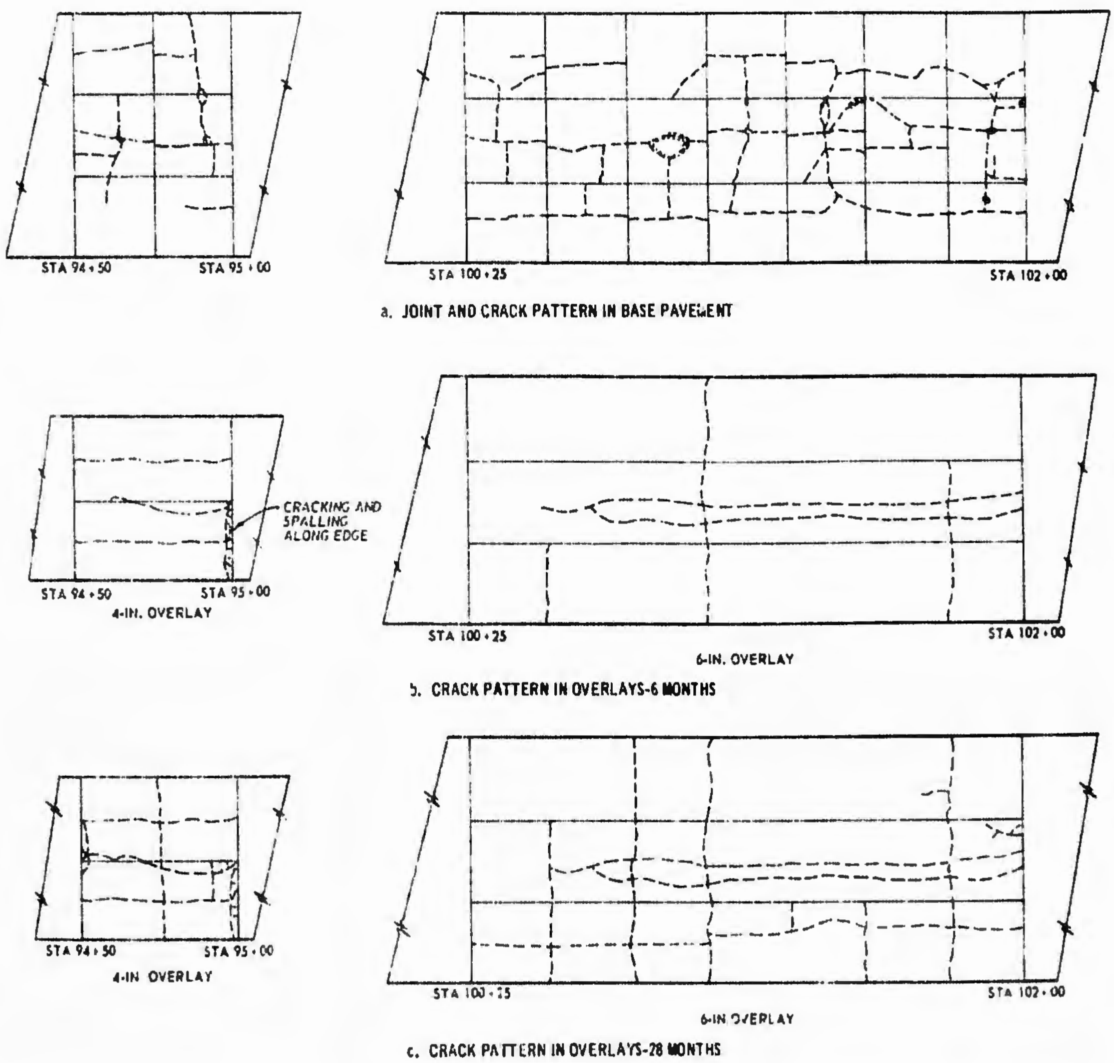

Figure 107. Joint and crack pattern in base pavement and overlays for the Tampa overlays

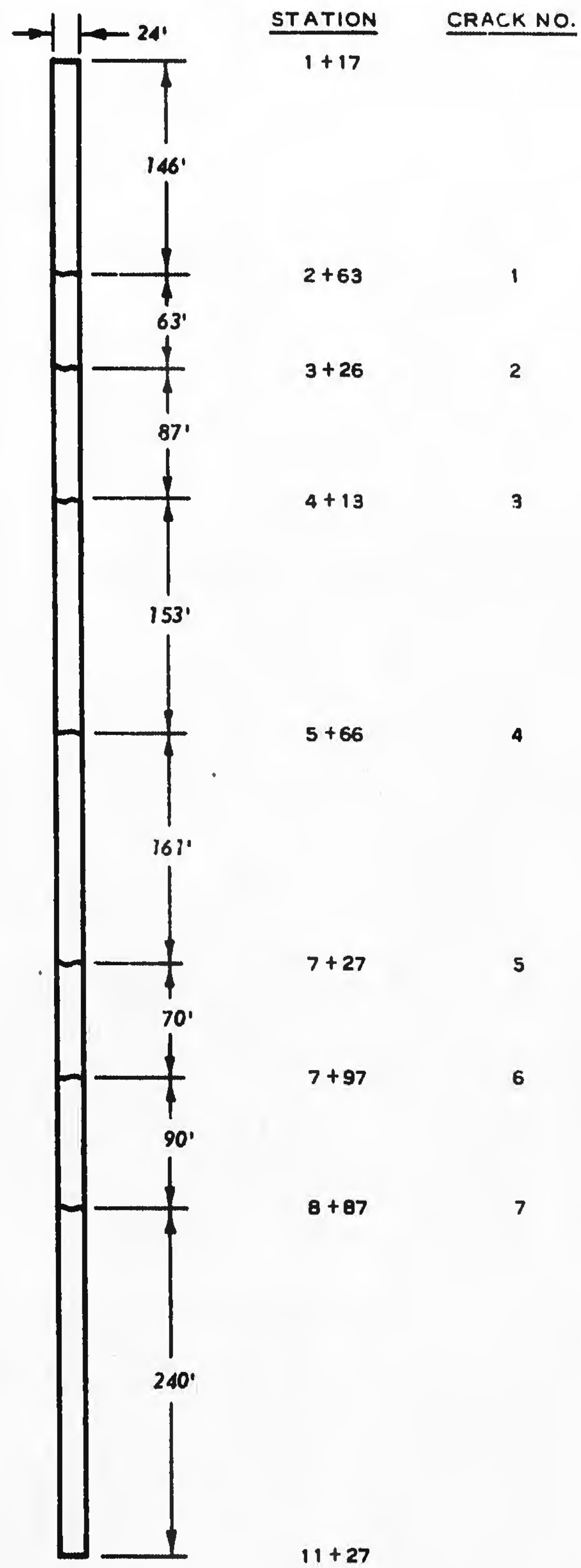

Figure 108. Crack development in the WES fibrous concrete roadway as of December 1973

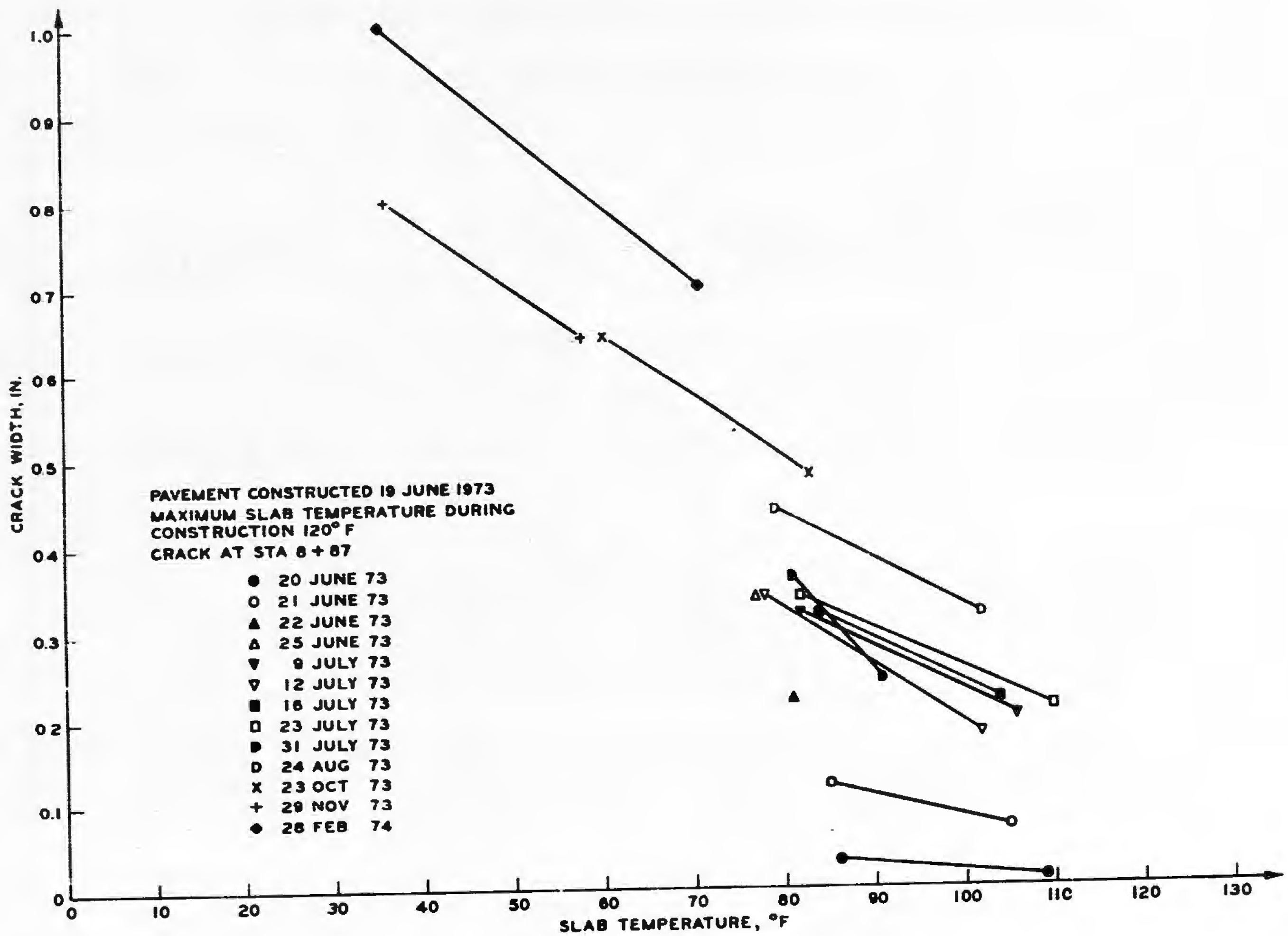

Figure 109. Crack width as a function of slab temperature

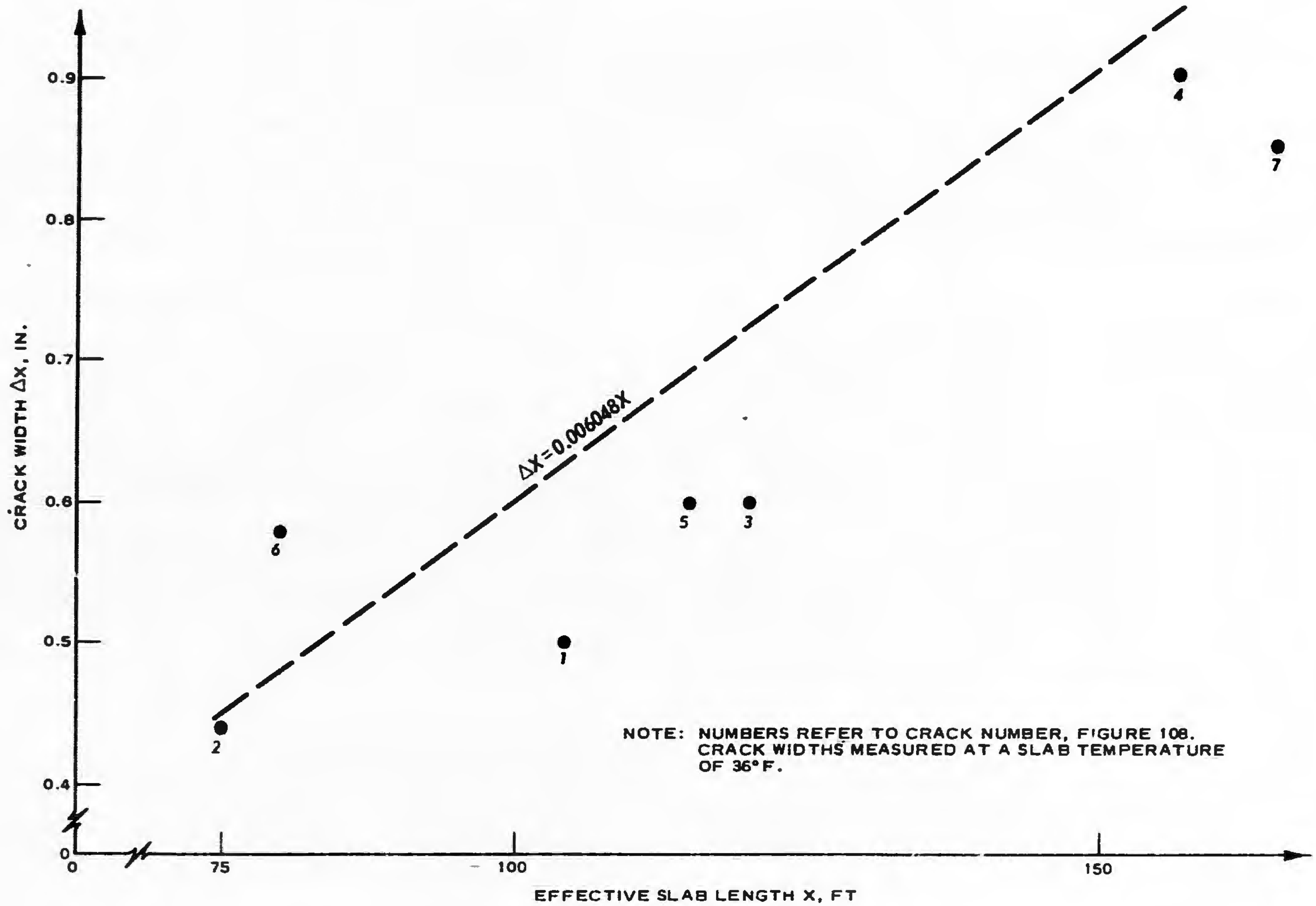

Figure 110. Crack width as a function of slab length

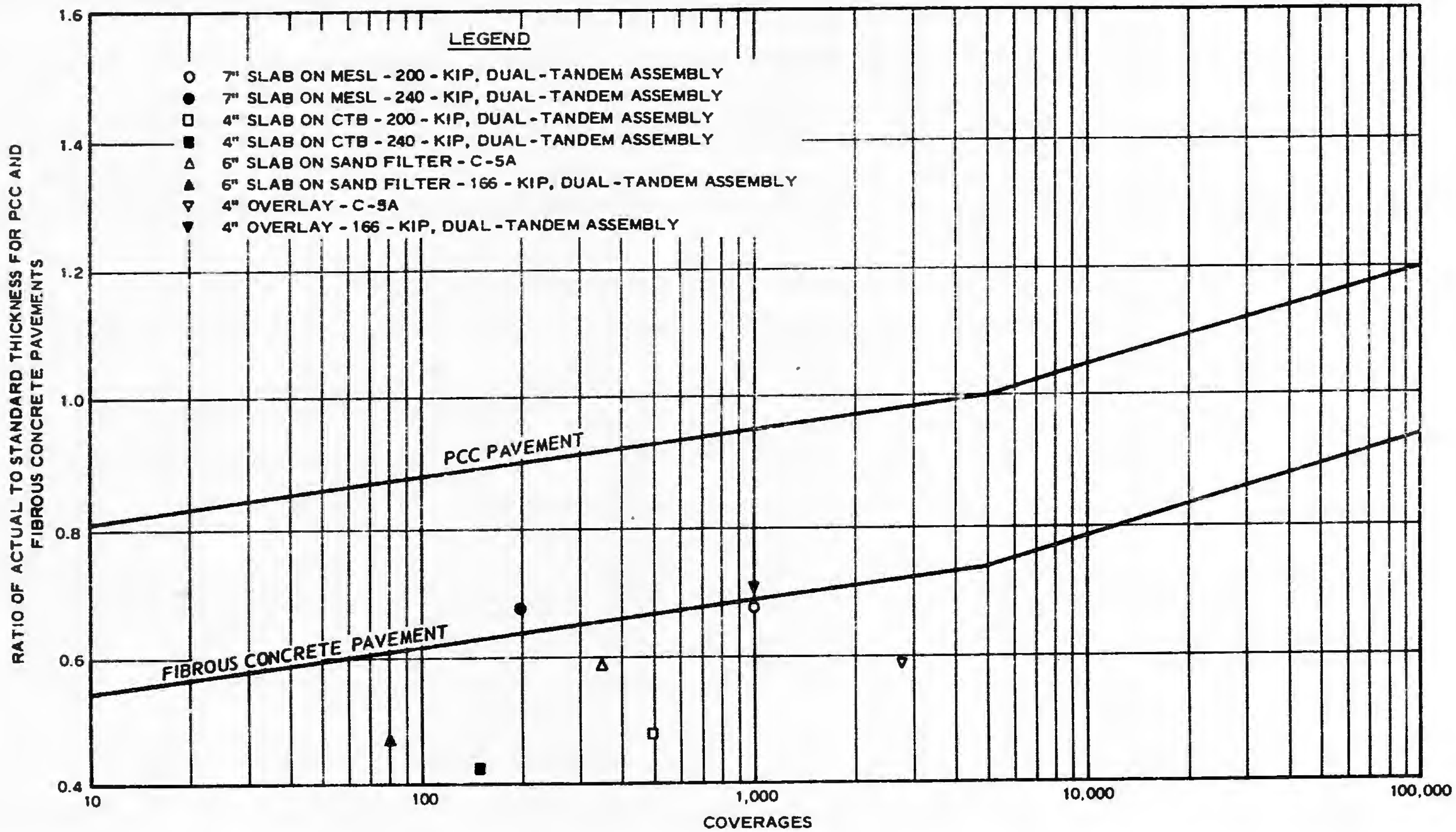

Figure 111. Performance criteria for fibrous concrete pavements based on first crack failure criterion

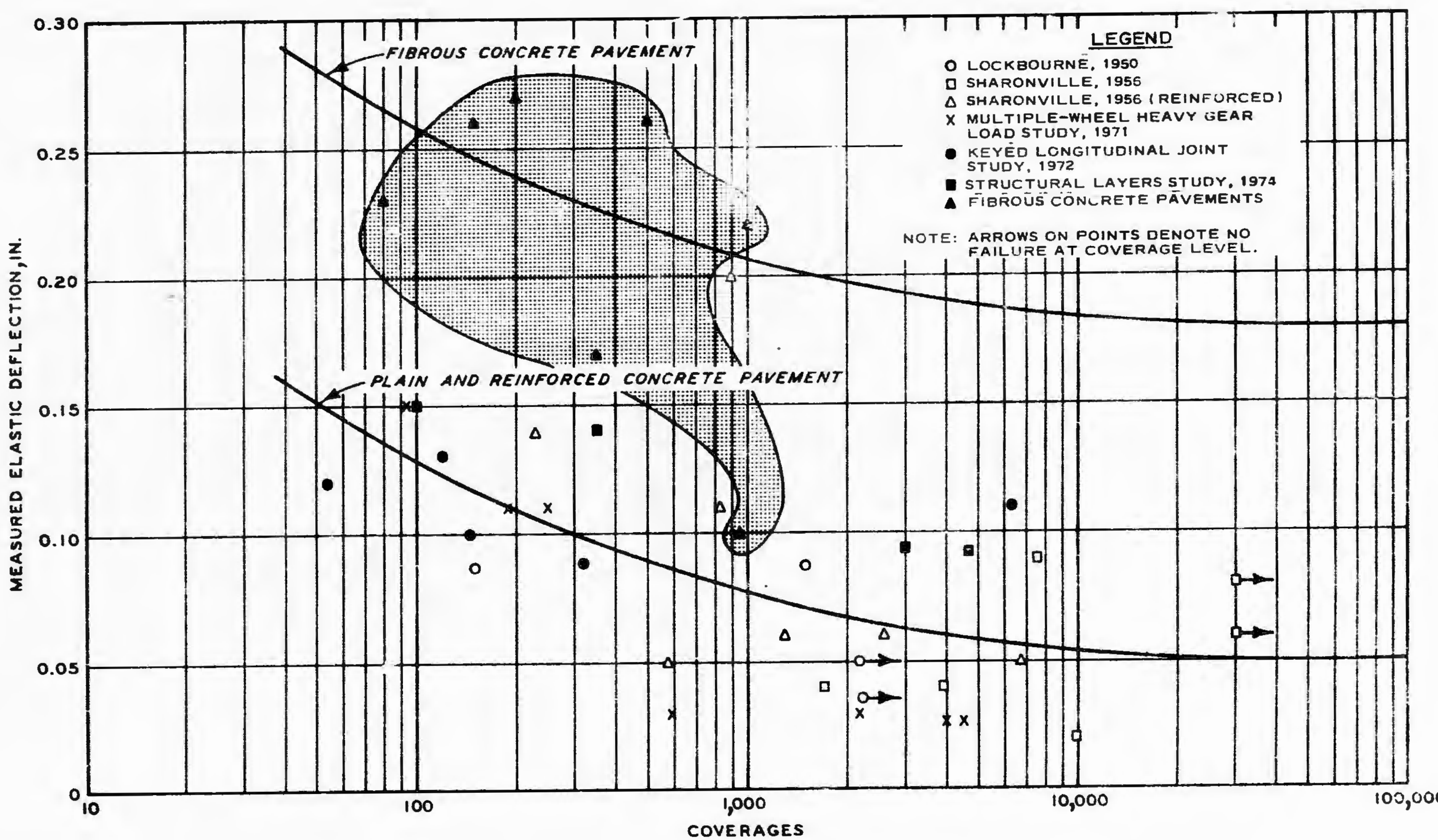

Figure 112. Relationship between measured deflection and pavement performance

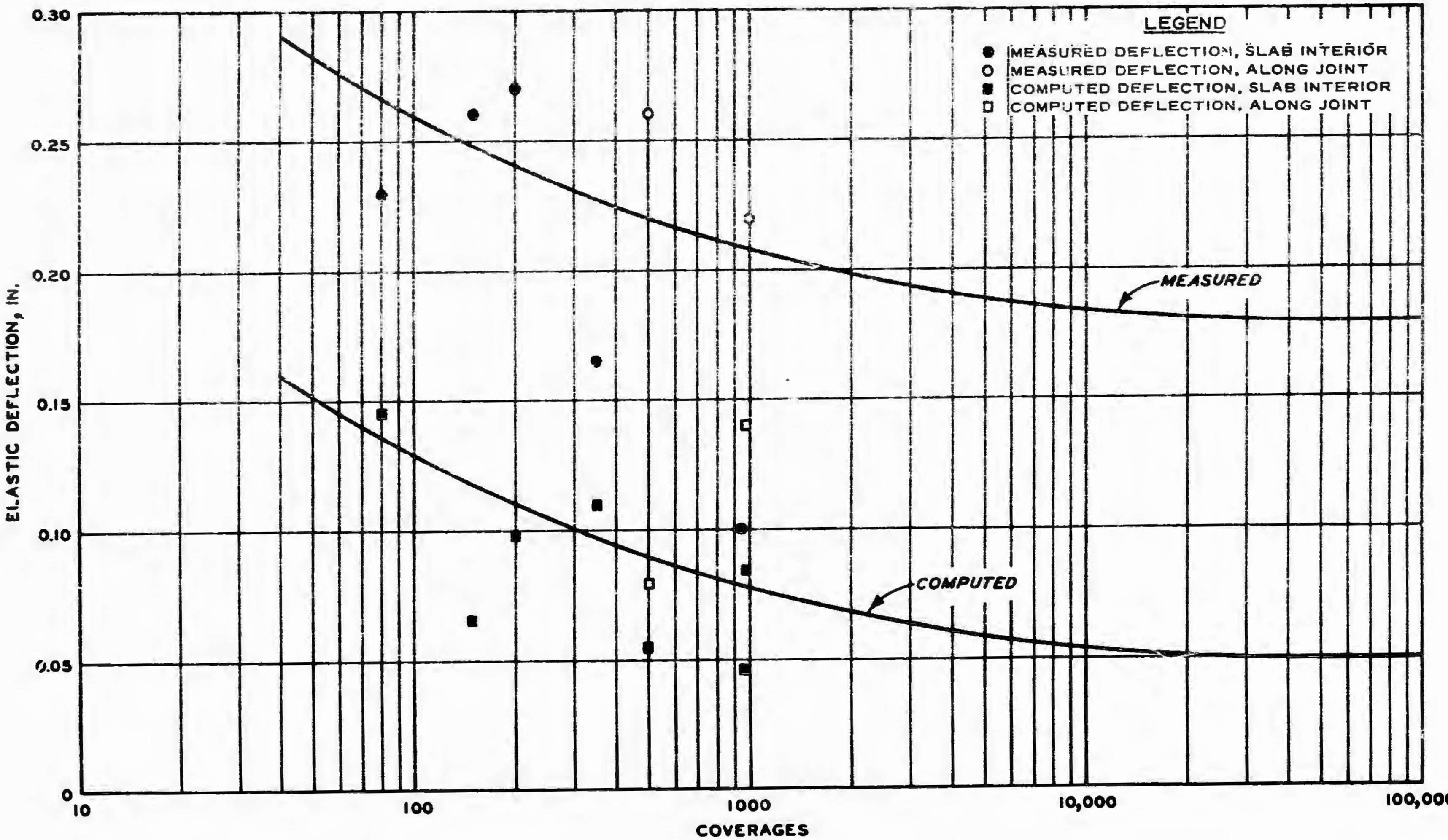

Figure 113. Limiting deflection criterion for fibrous concrete pavement

APPENDIX A: FIBROUS CONCRETE PAVEMENT PLACEMENTS

PLACEMENT 1

Location: Ohio River Division Laboratories, Cincinnati, Ohio

Date Placed: August 1967

Type of Facility: Parking lot slab (on grade)

Size: 120 by 10 ft by 6 in.

Type of Joints: None

Type of Fiber: Various steel fibers

Mix Design: Not available

Remarks: Crack developed at midslab on the day placed and opened up 3/8 to 1/2 in. wide. Cores taken on 20 April 1972 revealed that crack had developed at essentially an unplanned cold joint. Fibers at crack were completely deteriorated. Fibers in sound concrete showed no corrosion.

PLACEMENT 2 (Reported by Luke[52])

Location: Niles, Mich.

Date Placed: September 1968

Type of Facility: Left lane of entry road to industrial plant (on grade)

Size: 70 by 12 ft by 4 in.

Type of Joints: None

Type of Fiber: 3/4- by 0.012-in. round fibers and 3/4- by 0.010- by 0.020-in. rectangular fibers

Mix Design: Not available

Remarks: Direct comparison was possible with 7-1/2-in.-thick mesh-reinforced pavement in right lane. Mesh-reinforced pavement developed three full-width transverse cracks after 3 years of moderate truck traffic. Mesh-reinforced pavement was supposedly designed for a probable projected number of axles during a design life (numbers not available) to meet standard highway road construction specifications (assumed to be Michigan specifications).

PLACEMENT 3

Location: Lockbourne Air Force Base, Ohio

Preceding page blank

Date Placed: July 1970

Type of Facility: Slab 1 on parking apron (on grade); slab 2 on taxiway (on grade)

Size: Slab 1 - 35 by 46 ft by 6 in. with 4- by 5-in. leave-out in center; Slab 2 - 5 by 22 ft by 6 in. (Note: Dimensions of slabs, especially thicknesses, may not be exactly correct)

Type of Joints: None

Type of Fiber: 1-in. by 10- by 22-mil rectangular fibers

Mix Design: 180 lb of fiber per cubic yard; 752 lb of cement per cubic yard; 3/8-in. maximum-size aggregate; 0.47 water-cement ratio; 3-in. slump; and 7 percent entrained air content

Remarks: Information on slabs was rather sketchy. Slabs were 6 in. thick constructed over 9 in. of a 4-bag, lean-mix concrete and granular base course. The 6-in. fibrous concrete slabs and 9-in. lean-mix concrete were separated by 4-mil polyethylene sheeting. Cracks developed at each corner of leave-out in Slab 1 but were arrested by fibers at about 3 to 4 ft from corners. Without fibers, cracks would have propagated to free edge. There was no distress in Slab 2, but a 25- by 12-ft by 15-in. plain concrete slab adjacent to Slab 2 had developed a longitudinal crack and a number of short transverse cracks.

PLACEMENT 4 (Reported by Luke[52])

Location: Detroit, Mich.

Date Placed: July 1971

Type of Facility: Aircraft parking apron slab (on grade)

Size: 20 by 30 ft by 8 in. with leave-out for a drain box (size and shape unknown)

Type of Joints: None

Type of Fiber: 1- by 0.016-in. round fibers

Mix Design: Not available

Remarks: Adjacent slabs were 12 in. thick. Base was built up for 8-in. fibrous slab. Fibrous slab was tied to adjacent slabs with deformed rebars installed by drilling and grouting in adjacent slabs. Slab was reported to be in satisfactory condition, but no details were available.

PLACEMENT 5

Location: Ashland, Ohio

Date Placed: August 1971

Type of Facility: Entrance to truck weigh station (on grade)

Size: 500 by 16 ft by 4 in.

Type of Joints: None

Type of Fiber: 1- by 0.01- by 0.022-in. rectangular fibers

Mix Design: 265 lb of fiber per cubic yard; 9 bags of cement per cubic yard; 3/8-in. maximum-size aggregate; 30 percent coarse aggregate and 70 percent fine aggregate; 0.56 water-cement ratio; high slumps (greater than 5 in. in some batches) with considerable variation; high air content with considerable variation

Remarks: Slab was placed on a 5-in. asphaltic concrete base. Ends were tapered to 9 in. over a 7-ft length. Doweled expansion joints were installed at either end. Slab cracked at midslab on first day. Second crack developed approximately 90 ft from north end in December 1971. Both cracks appeared to be about 3/8 to 1/2 in. wide.

PLACEMENT 6

Location: Champaign, Ill.

Date Placed: November 1971

Type of Facility: Sidewalk

Size: 1140 by 6 ft by 2-3/4 in.

Type of Joints: One transverse construction joint-butt joint with no seal

Type of Fiber: 1- by 0.01- by 0.022-in. rectangular fibers

Mix Design: 200 lb of fiber per cubic yard; 5-1/3 bags of cement per cubic yard; 225 lb of fly ash per cubic yard; 3/8-in. maximum-size aggregate; 0.54 water-cement ratio; 4-in. slump; and 6 percent entrained air content

Remarks: Sidewalk was placed on graded natural soil with a thin sand layer. Construction joint opened up about 1/2 in. Two additional cracks have formed, but their exact locations are not known.

PLACEMENT 7 (Reported in ACPA Newsletter, October 1972[53])

Location: Cedar Rapids, Iowa

Date Placed: September-October 1972

Section 1: Overlay of residential street; 175 by 28 ft by 3 in.; old pavement, jointed reinforced concrete pavement; no joints; 1- by 0.016-in. round fibers

Section 2: Overlay of residential street; 200 by 24 ft by 2-1/2 in.; old pavement, asphaltic concrete; no joints; 1- by 0.016-in. round fibers

Section 3: Overlay of viaduct; 152 by 11 ft by 3 in.; placed on 2 sheets of polyethylene attached to wooden decking of viaduct; doweled expansion joints placed at either end between 152-ft-long section and a 12- by 11-ft by 3-in. fiber-reinforced concrete slab; 2-1/2- by 0.025-in. round fibers

Section 4: Overlay of airfield taxiway; 95 by 75 ft by 3 to 1 in.; old pavement, jointed plain concrete pavement; longitudinal butt-type construction joint divided section into two 95- by 37-1/2-ft slabs; 1- by 0.016-in. fibers used in one slab, and 2-1/2- by 0.025-in. round fibers in the other

Mix Design: Varied with type and quantity of fiber used; all concrete contained 9 bags of cement per cubic yard; 3/8-in. maximum-size aggregate; 75 percent coarse aggregate and 25 percent fine aggregate

Remarks: Section 4 was inspected on 5 October 1968. Section 1 was being placed on 5 October 1968. Section 2 developed transverse cracks at 80 and 110 ft from one end after being subjected to construction traffic and normal residential traffic. Section 3 had no cracks and was subjected to no traffic. Section 4 when opened to traffic had longitudinal construction and contraction joints and transverse contraction joints in base pavement that reflected through the fibrous concrete overlay.

PLACEMENT 8 (Reported in ACPA Newsletter, October 1972,[53], Arnold and Brown,[13] and Arnold[45])

Location: Detroit, Mich.

Date Placed: October 1972

Type of Facility: Overlay of urban street

Size: 1300 by 48 ft by 3 in. (slabs were 100 by 12, 50 by 24, and 50 by 24 ft)

Type of Joints: Longitudinal construction joints were butt joints; transverse contraction joints were sawed at 50- and 100-ft intervals in various sections; longitudinal contraction joints were sawed in a portion of the job

Type of Fiber: 1- by 0.010- by 0.022-in. rectangular fibers

Mix Design: Two fiber loads were used, 120 and 200 lb per cubic yard; 9 bags of type 1A cement per cubic yard; 3/8-in. maximum-size slag aggregate; 60 percent fine and 40 percent coarse aggregate; 0.37 water-cement ratio

Remarks: The concrete was batched and mixed in a central-mix plant and transported in transit-mix trucks. There were numerous fiber balls in the mix. The concrete was placed directly on old PCC pavement with a slip-form paver. There were no problems in placement. The method used for controlling grade was inadequate because several thin areas resulted. Some areas received thicknesses of about 1 in. instead of the prescribed 3-in. minimum. Several of the areas in which the concrete was thin cracked, and large pieces broke out, requiring complete removal and repair. Serious cracking has occurred in the areas in which concrete containing 120 lb of fiber per cubic yard was used, and some cracking has developed in areas in which concrete containing 200 lb of fiber per cubic yard was used. There has been a loss of bond between the overlay and the base pavement. As a result, serious curling is occurring along the slab edges. The movement of the slab is visible when vehicles pass over the joints, and signs of early deterioration are evident.

PLACEMENT 9 (Reported in ACPA Newsletter, October 1973[54])

Location: Greene County, Iowa

Date Placed: September-October 1973

Type of Facility: Overlay of county road

Size: 3.03 miles long, 22 ft wide, variable thickness (Project consists of 41 test sections of approximately 400 ft in length, including 10 duplicated sections for control. These 41 sections overlay both lanes

of an old PCC pavement built in 1921 and 1922. Since the old PCC pavement was only 18 ft wide, 2-ft widening sections of PCC 4 in. in thickness were constructed on each side of the old slab as part of the research project. The slab to be overlayed is 22 ft wide. The old 18-ft-wide slab is 8-1/2 in. thick)

Type of Fiber: 1- by 0.010- by 0.022-in. rectangular fibers, and 2-1/2- by 0.025-in. round fibers

Sections 1 and 39: 5-in.-thick partially bonded plain PCC overlays.

Section 40: 3-in.-thick partially bonded plain PCC overlay.

Sections 2 and 38: 4-in.-thick partially bonded mesh-reinforced PCC overlays.

Sections 3 and 6: 4- and 3-in.-thick, respectively, bonded continuously reinforced PCC overlays.

Sections 4 and 5: 4- and 3-in.-thick, respectively, unbonded continuously reinforced PCC overlays with "elastic" joints on 8-ft centers. This installation may be the first "elastic" jointed continuously reinforced resurfacing job in the United States.

Sections 22 and 40A: 3-in.-thick fibrous concrete overlays with fly ash and placed on grade.

Sections 12 and 21: 3-in.-thick bonded fibrous concrete overlays.

Sections 29 and 36: 2-in.-thick bonded fibrous concrete overlays.

Section 23: 2-1/4-in.-thick bonded fibrous concrete overlay of a bridge deck.

Sections 11 and 35: 3- and 2-in.-thick, respectively, unbonded fibrous concrete overlays.

Sections 7-10, 13-20, 24, 25, and 37: 3-in.-thick partially bonded fibrous concrete overlays.

Sections 26-28 and 30-34: 2-in.-thick partially bonded fibrous concrete overlays.

Mixing and Construction: Concrete was batched and mixed in a central-mix plant and transported in nonagitating end-dump trucks. Fibers were batched by dumping boxes of fibers into a front-end loader. The fibers were dumped from the front-end loader onto a vibrating

screen which dispensed the fibers onto a conveyor belt which fed onto the aggregate charging belt of the central-mix plant. The screen had diamond-shaped openings with overall dimensions of 1 by 3 in. The concrete was placed with a slip-form paver. For the unbonded sections, two sheets of polyethylene were placed between the overlay and the base slab. For the bonded sections, bond was achieved by a layer of neat cement grout. For the partially bonded sections, the surface was cleaned of debris and moistened prior to placement of the overlay.

Remarks: Inspection of the pavements after about 8 months of service revealed the following:

a. The 3-in.-thick pavements were performing significantly better than the 2-in. pavements.

b. The 2-in. pavements were tending to deteriorate along the edges and joints for all bond conditions. The deterioration was most serious in the unbonded sections and seemed to be associated with warping and curling of the thin slabs.

c. Bond was being lost in the bonded sections.

d. The 2-1/2-in.-long fibers appeared to be more effective than the 1-in.-long fibers in preventing cracks from widening.

e. For the cement contents used (600 and 750 lb per cubic yard), there was no apparent differences in performance.

f. For the range of fiber contents used (60, 100, and 160 lb per cubic yard), the sections with 160 lb of fiber per cubic yard perform significantly better than the sections with 100 or 60 lb per cubic yard.

APPENDIX B: PROPOSED DESIGN PROCEDURES

This appendix presents thickness design charts, charts for computing elastic pavement deflection, and tables of limiting elastic pavement deflection for civil and military aircraft. These charts and tables form the basis of a procedure for determining the required thickness of fibrous concrete pavement. The curves and tables were developed using criteria described in the main text of this report.

The curves and table for civil aircraft are compatible with Federal Aviation Administration (FAA) format as contained in FAA Advisory Circular AC 150/5320-6B.[26] The curves and table for military aircraft are compatible with Department of the Army format as contained in Technical Manual TM 5-823-3[49] and TM 5-824-3.[50]

Required thicknesses based on the limiting stress criterion can be determined from Figures B1-B7 for civil aircraft and from Figures B8-B11 for military aircraft. Pavement thicknesses obtained from these charts can be checked by determining the elastic pavement deflection from Figures B12-B22 for the aircraft in question, and comparing this with limiting deflections obtained from Table B1 or B2.

Table B1

Limiting Elastic Deflections for Civil Aircraft

Traffic Volume Annual Departures	Limiting Elastic Deflection in.
1,200	0.060
3,000	0.055
6,000	0.050
15,000	0.050
25,000	0.050

Figures B1-B7 are entered with the design concrete flexural strength, soil modulus, aircraft load, and traffic volume to obtain the required slab thickness for civil airports. Traffic volumes are shown

Preceding page blank

Table B2

Limiting Elastic Deflections for Military Aircraft

Traffic Passes	Limiting Deflection, in., for Cited Pavement: Light-Load Pavement	Medium-Load Pavement	Heavy-Load Pavement	Special Design Pavement
		Type A Areas		
200	--	0.145	0.125	--
1,000	--	0.100	0.085	--
5,000	--	0.075	0.065	--
15,000	--	0.060	0.055	--
25,000	--	0.055	0.055	--
50,000	--	0.055	0.050	--
100,000	--	0.050	0.050	--
		Type B Areas		
200	0.180	0.165	0.130	0.160
1,000	0.125	0.115	0.090	0.110
5,000	0.090	0.085	0.065	0.080
15,000	0.070	0.065	0.055	0.065
25,000	0.065	0.060	0.055	0.060
50,000	0.060	0.055	0.050	0.055
100,000	0.055	0.055	0.050	0.055
200,000	0.050	0.050	0.050	0.050
300,000	0.050	0.050	0.050	0.050
400,000	0.050	0.050	0.050	0.050
		Type C Areas		
200	0.210	0.165	0.130	0.185
1,000	0.150	0.115	0.090	0.130
5,000	0.100	0.085	0.065	0.090
15,000	0.080	0.065	0.055	0.075
25,000	0.075	0.060	0.055	0.060
50,000	0.065	0.055	0.050	0.055
100,000	0.060	0.055	0.050	0.050
200,000	0.055	0.050	0.050	0.050
300,000	0.050	0.050	0.050	0.050
400,000	0.050	0.050	0.050	0.050
		Type D Areas		
200	--	0.110	0.110	--

in terms of annual departures. Aircraft arrivals are neglected. The curves are based on a 20-year design life, i.e., each traffic curve represents a design for a number of aircraft departures equal to 20 times the indicated annual departure level.

Figures B8-B11 are entered with the design concrete flexural strength, soil modulus, aircraft load, traffic volume, and traffic area to obtain the required slab thickness for military airfields. Traffic volumes in terms of total aircraft passes are shown on the curves. Requirements for design loadings (light, medium, heavy, and special) and traffic areas (A, B, C, and D) are as specified in TM 5-824-1.[55]

The thickness design curves in Figures B1-B8 are entered with the design flexural strength on the vertical axis. From this point, the required thickness is obtained by proceeding through the chart as illustrated by the dashed lines. From the flexural strength scale, a horizontal line is drawn until it intersects the appropriate soil modulus curve. From this intersection, a vertical line is drawn until it intersects the appropriate load curve. From this intersection, a horizontal line is drawn until it intersects the appropriate traffic curve. Finally, a vertical line is drawn through this intersection until it intersects the horizontal thickness scale at the required thickness.

The procedures for using Figures B8-B11 are similar to the procedures for Figures B1-B7. However, one additional step is added. Once the intersection with the curve for traffic volume is found, a vertical line is drawn until it intersects the appropriate traffic area curve. From this intersection, a horizontal line is drawn until it intersects the vertical thickness scale at the required thickness.

Figures B12-B22 are entered with the slab thickness (from Figures B1-B11), soil modulus, and aircraft load, and the maximum elastic pavement deflection is obtained. The deflection thus obtained is compared with limiting values obtained from Table B1 for civil aircraft and Table B2 for military aircraft. If the computed deflection is larger than the limiting deflection, the slab thickness must be increased until the computed deflection is less than or equal to the limiting deflection,

or a new design must be initiated with different design parameters, such as concrete strength and soil modulus.

Elastic deflection is obtained from Figures B12-B22 by entering the vertical thickness scale with the slab thickness and proceeding as indicated by the dashed lines. From the thickness scale, a horizontal line is drawn until it intersects the appropriate soil modulus curve. From this intersection, a vertical line is drawn until the appropriate load curve is intersected. Finally, a horizontal line is drawn through this intersection until the vertical deflection scale is intersected at the resulting elastic vertical deflection.

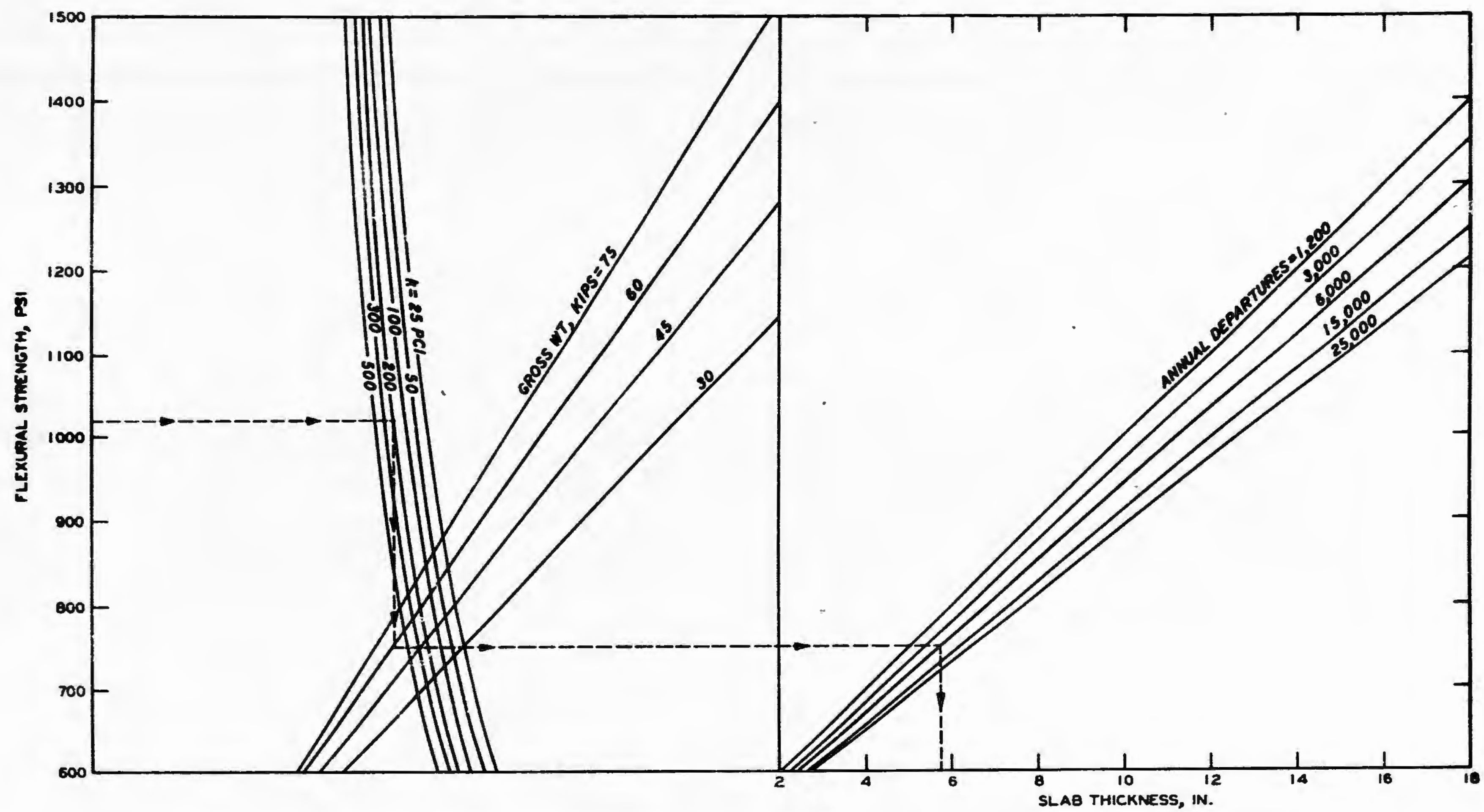

Figure B1. Fibrous concrete pavement design curves for aircraft with single-wheel gears on critical areas

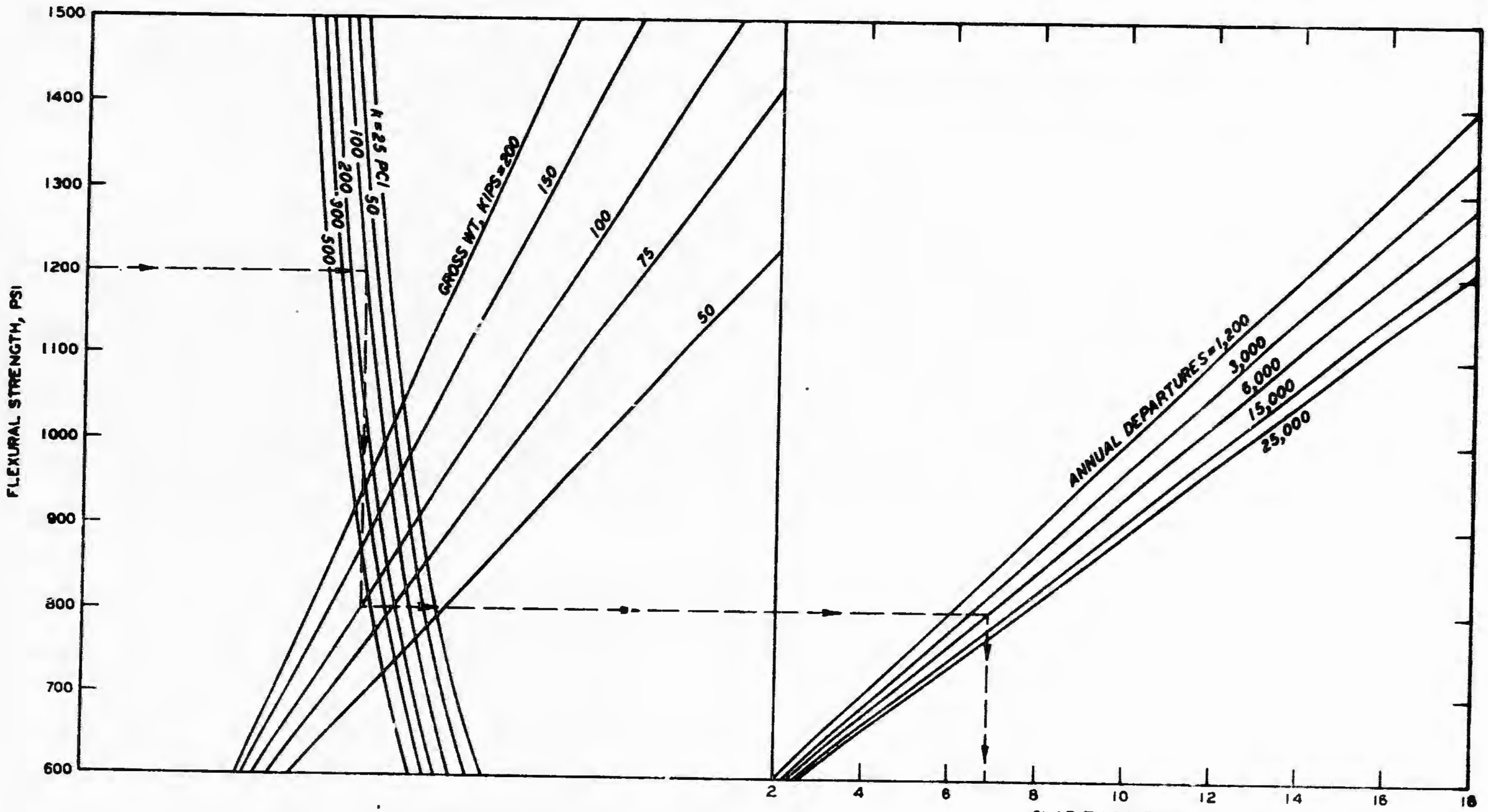

Figure B2. Fibrous concrete pavement design curves for aircraft with dual-wheel gears on critical areas

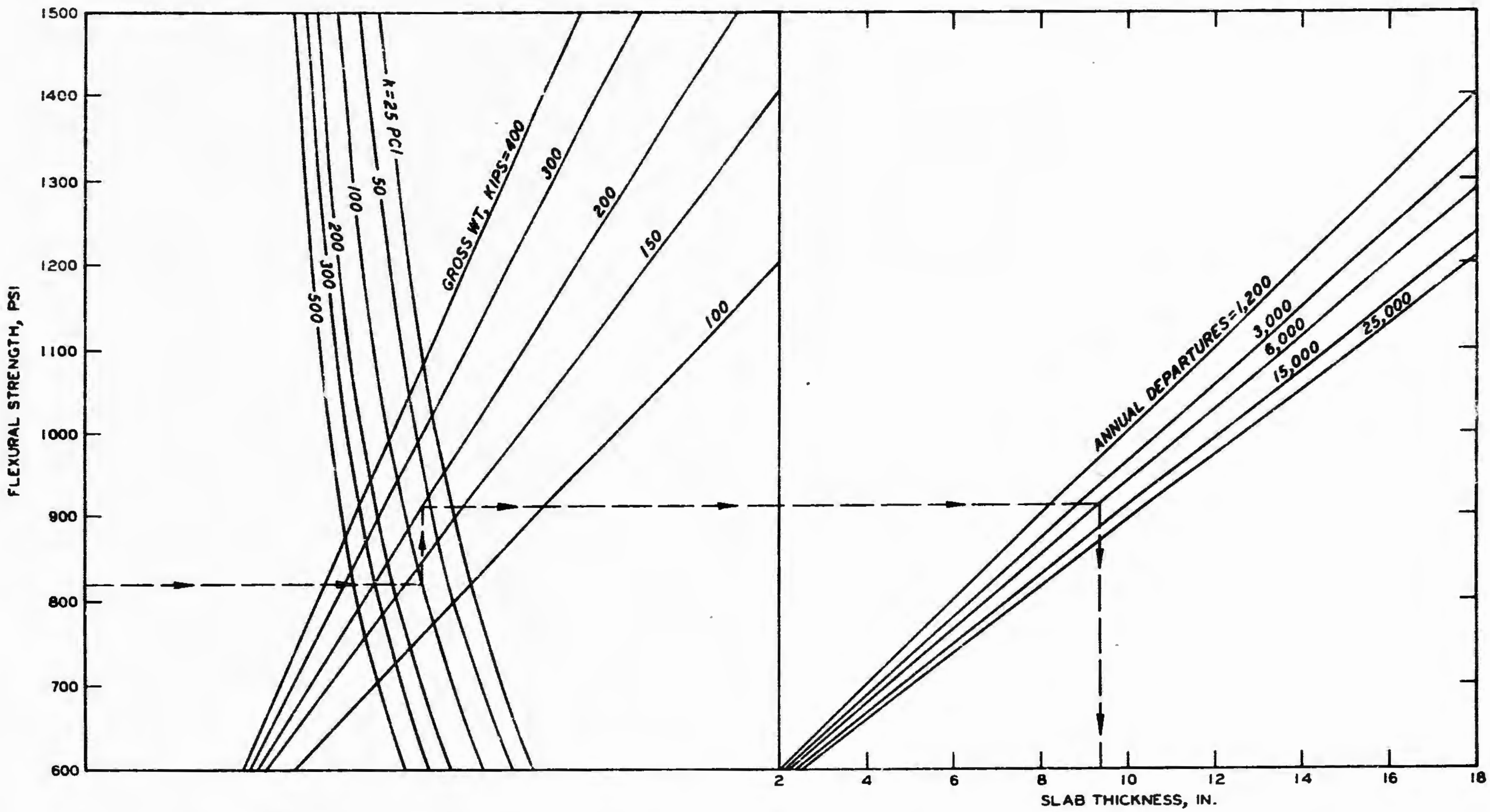

Figure B3. Fibrous concrete pavement design curves for aircraft with dual-tandem gears on critical areas

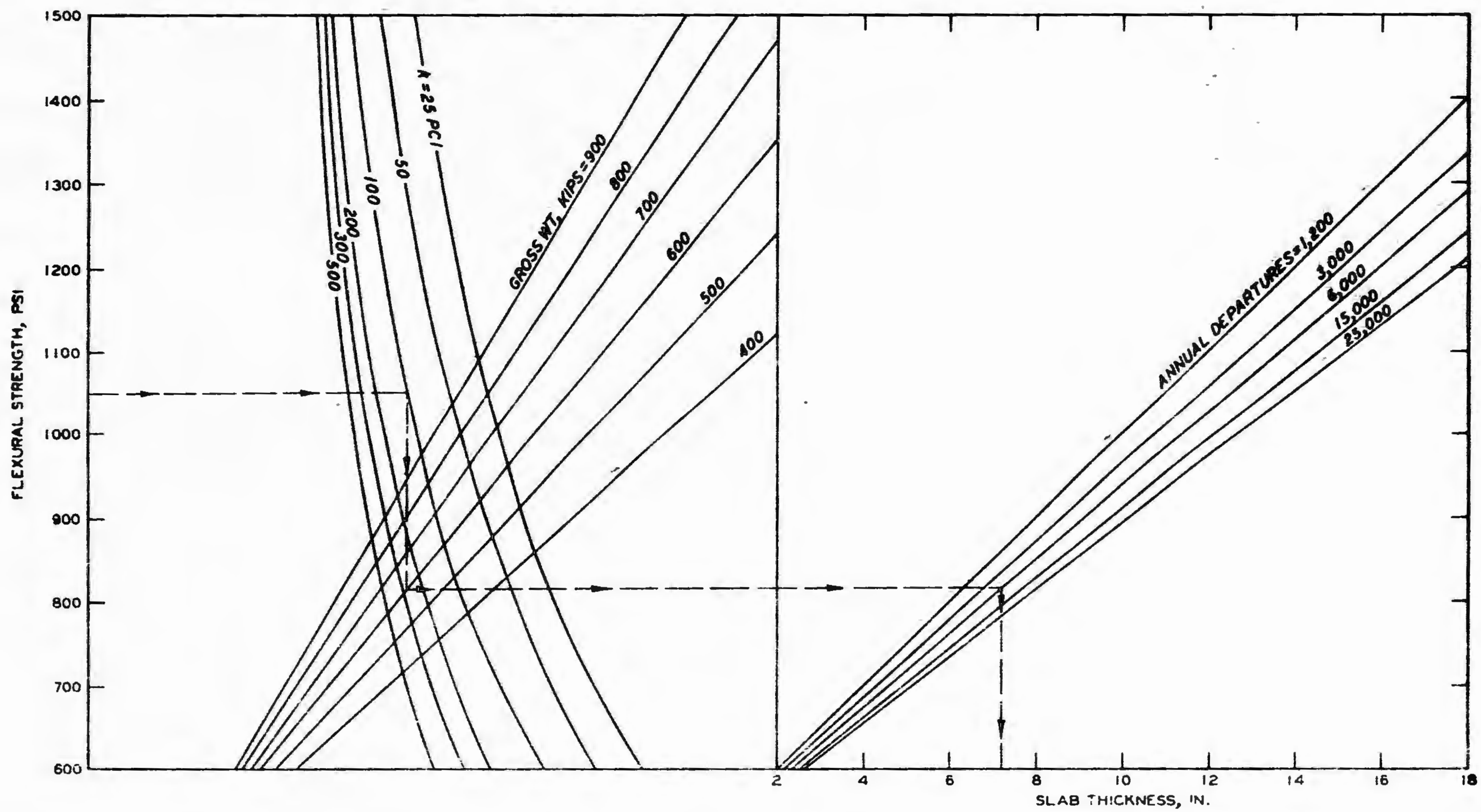

Figure B4. Fibrous concrete pavement design curves for Boeing 747 aircraft on critical areas

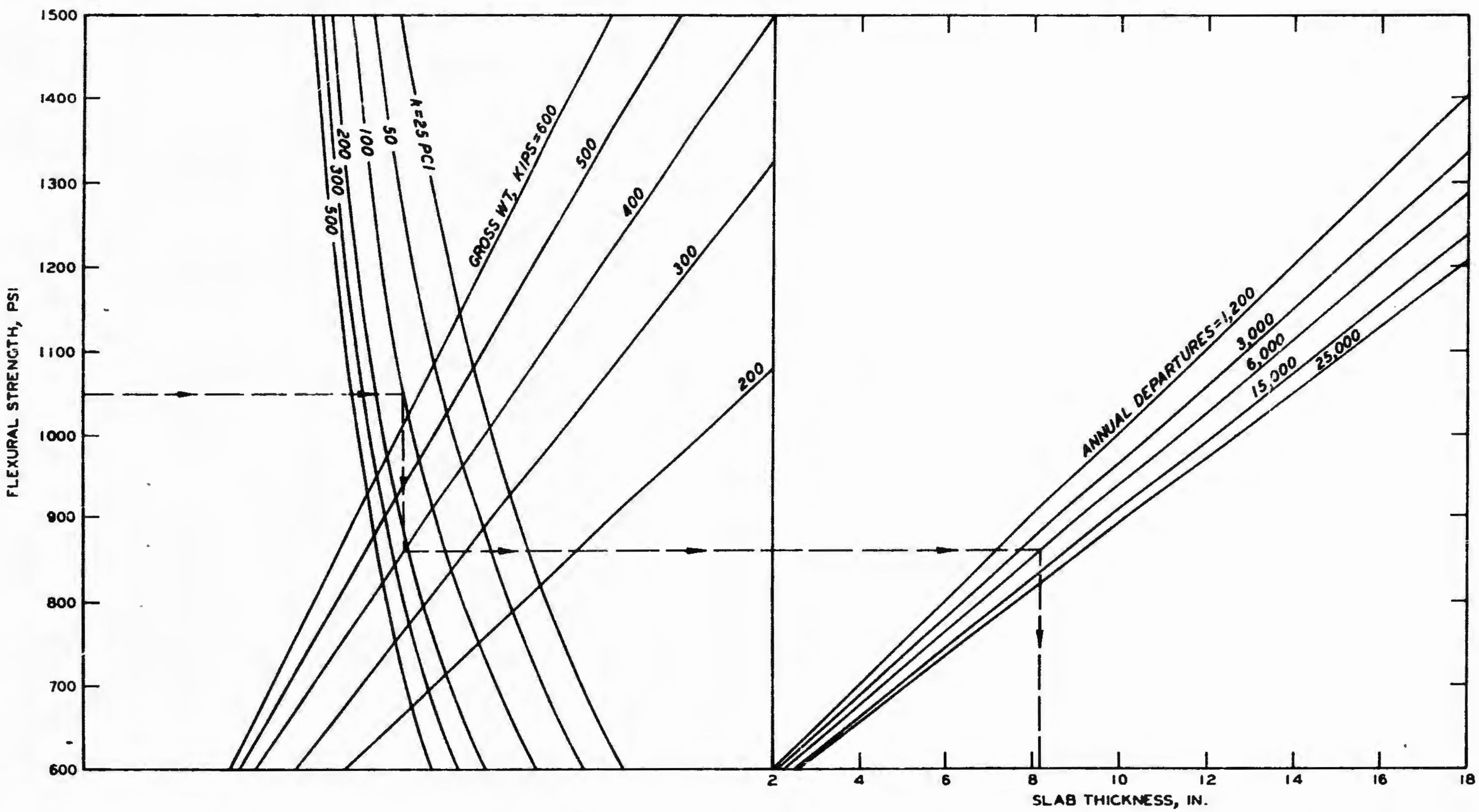

Figure B5. Fibrous concrete pavement design curves for DC-10-10 aircraft on critical areas

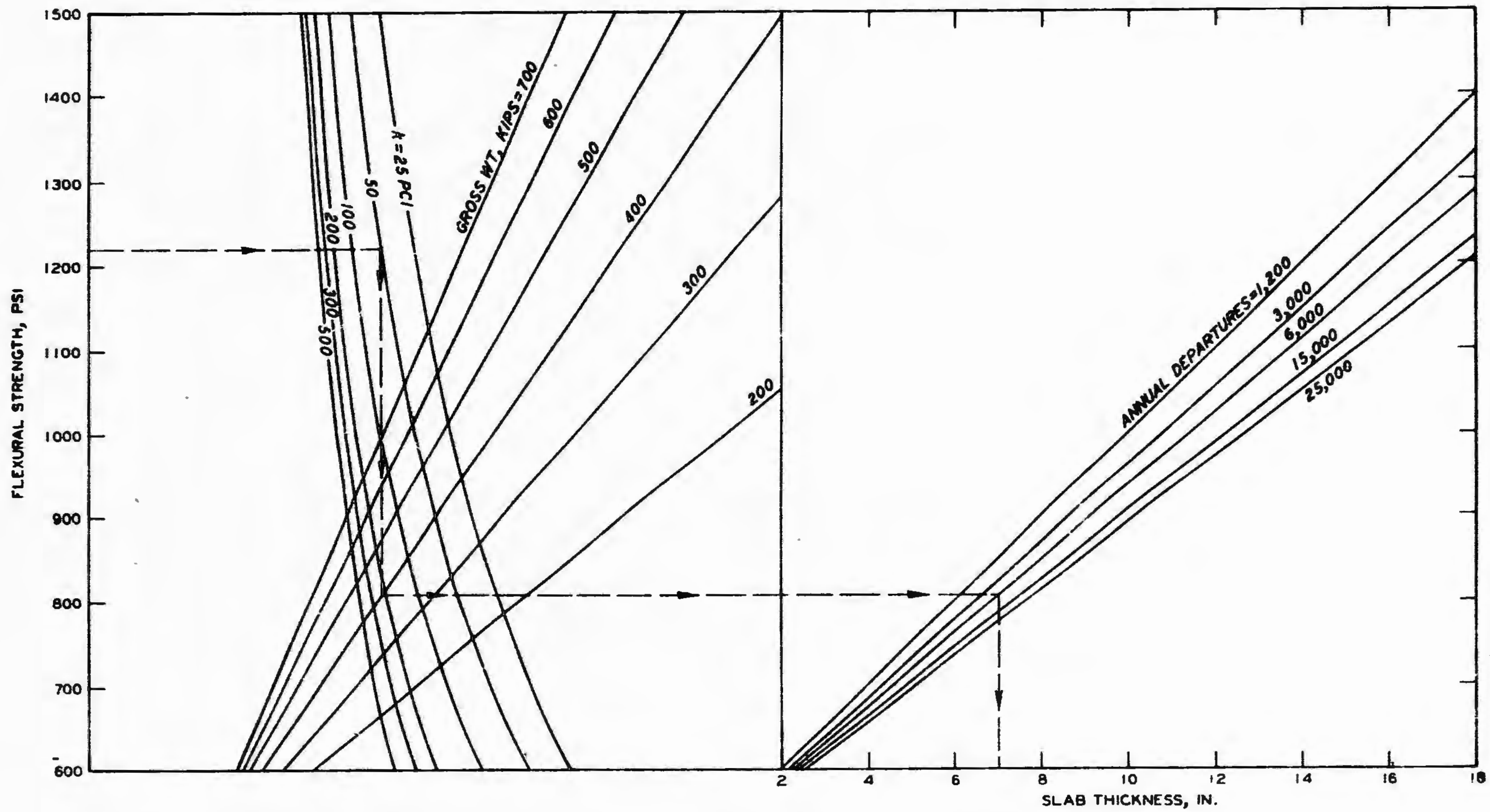

Figure B6. Fibrous concrete pavement design curves for DC-10-30 aircraft on critical areas

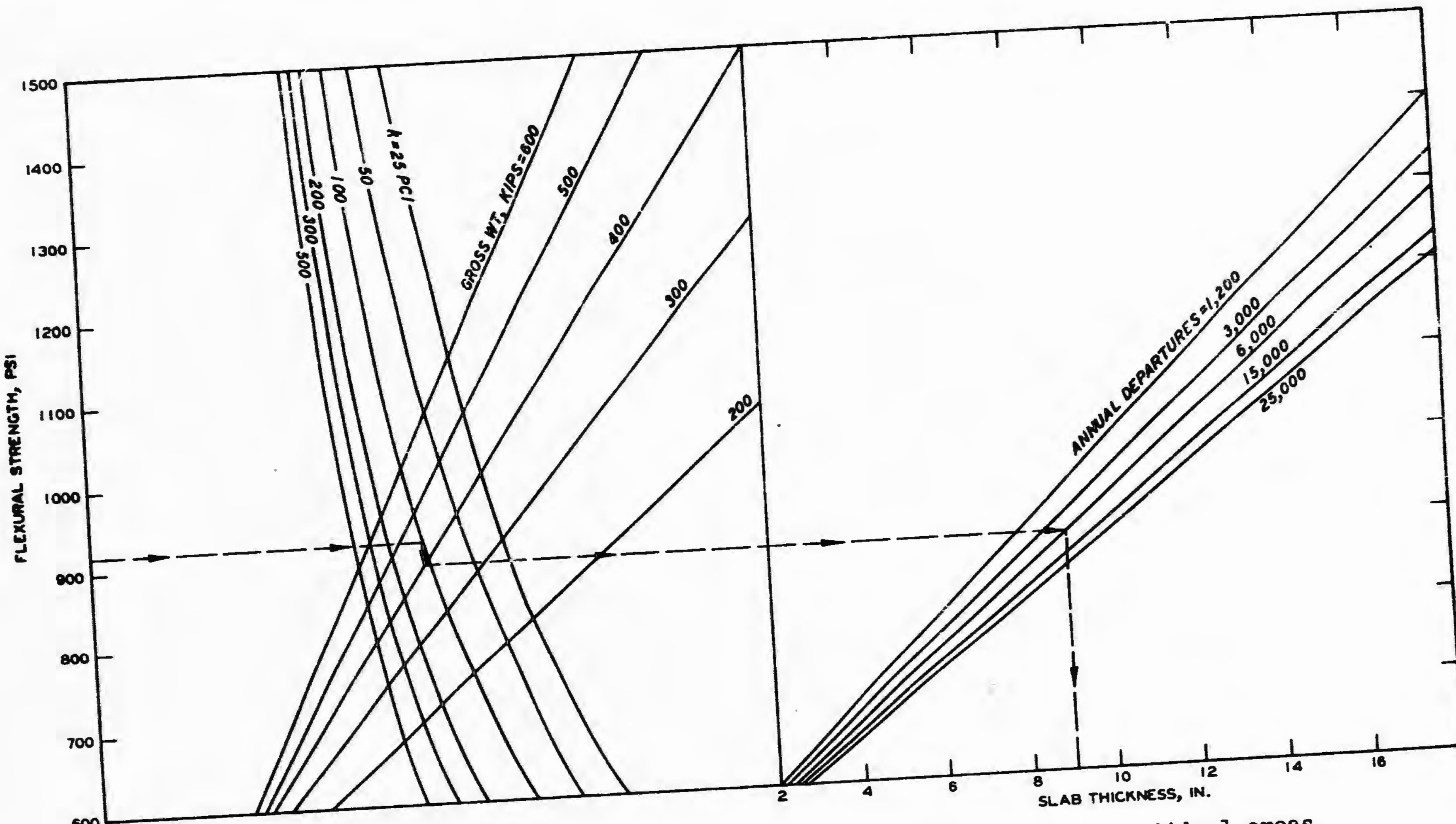

Figure B7. Fibrous concrete pavement design curves for L-1011 aircraft on critical areas

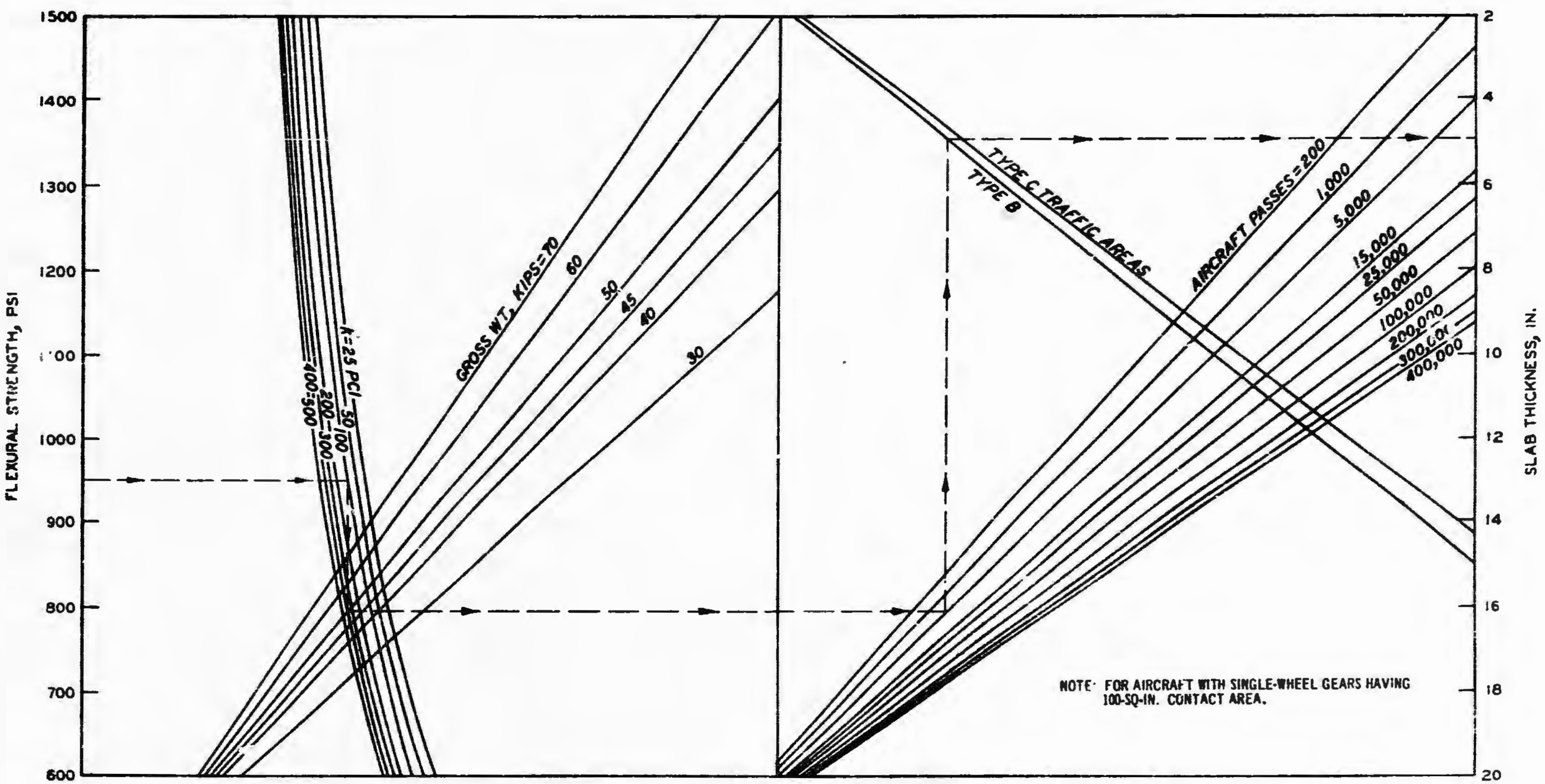

Figure B8. Fibrous concrete pavement design curves for light-load pavements

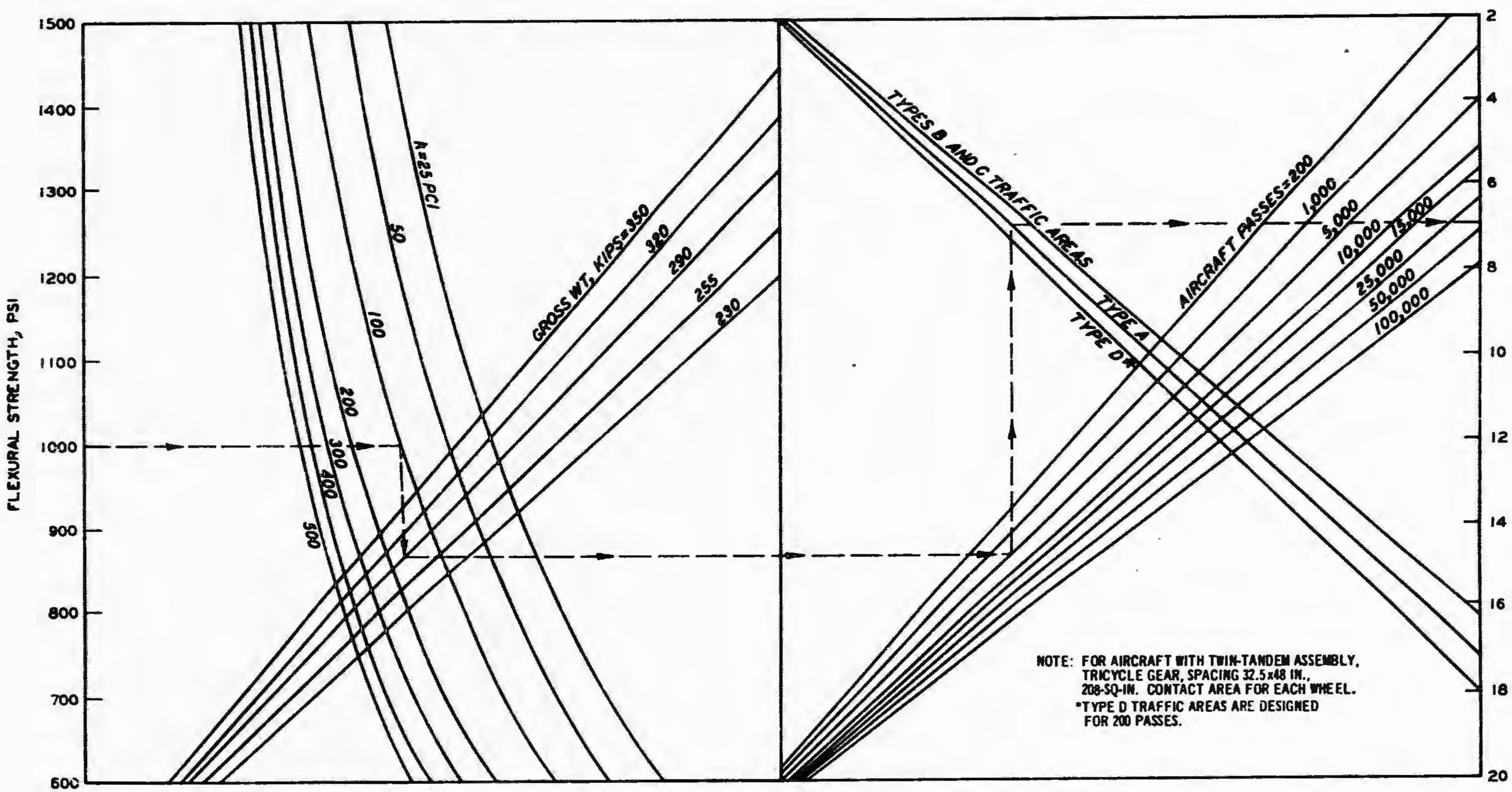

Figure B9. Fibrous concrete pavement design curves for medium-load pavements

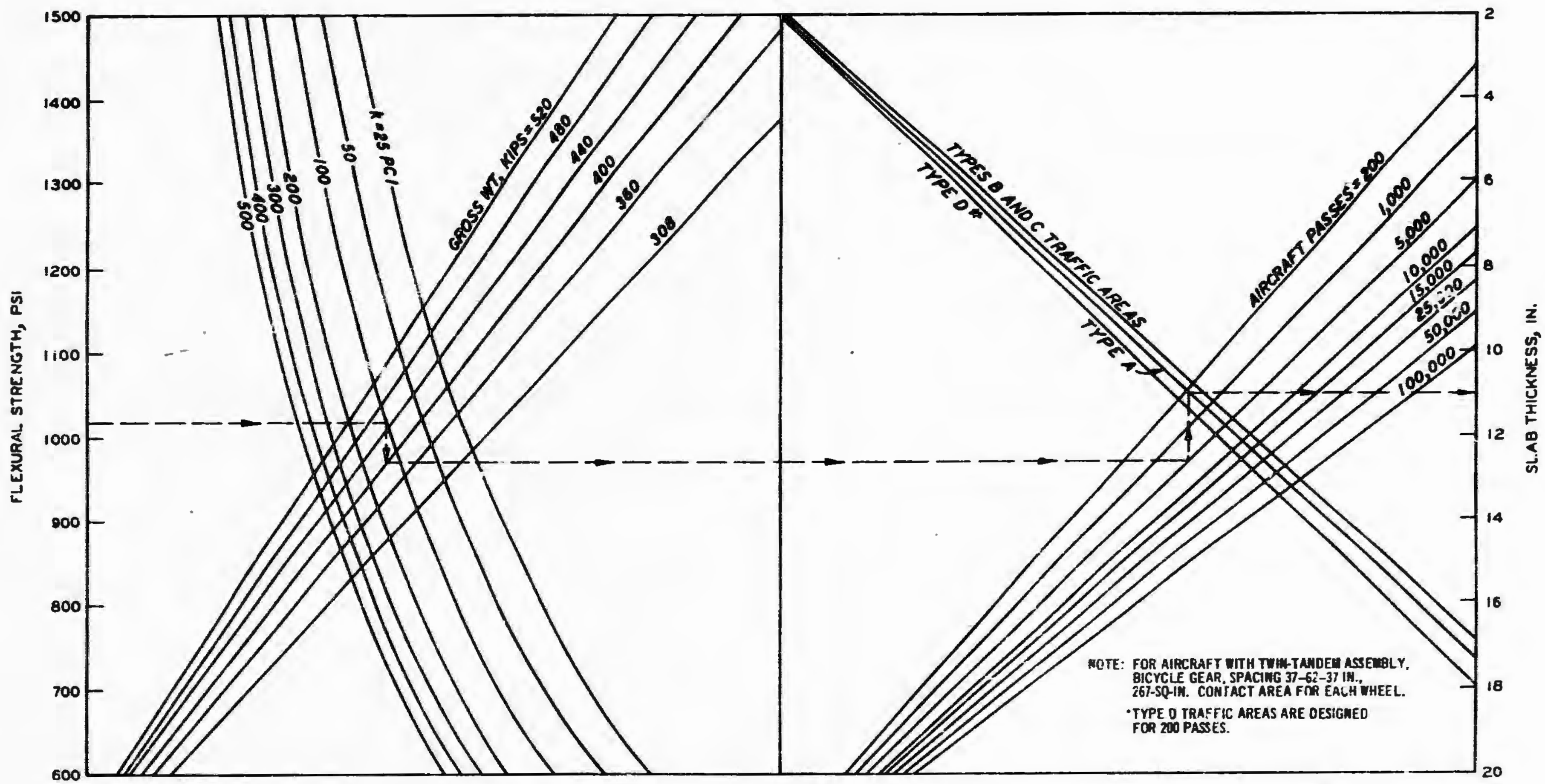

Figure B10. Fibrous concrete pavement design curves for heavy-load pavements

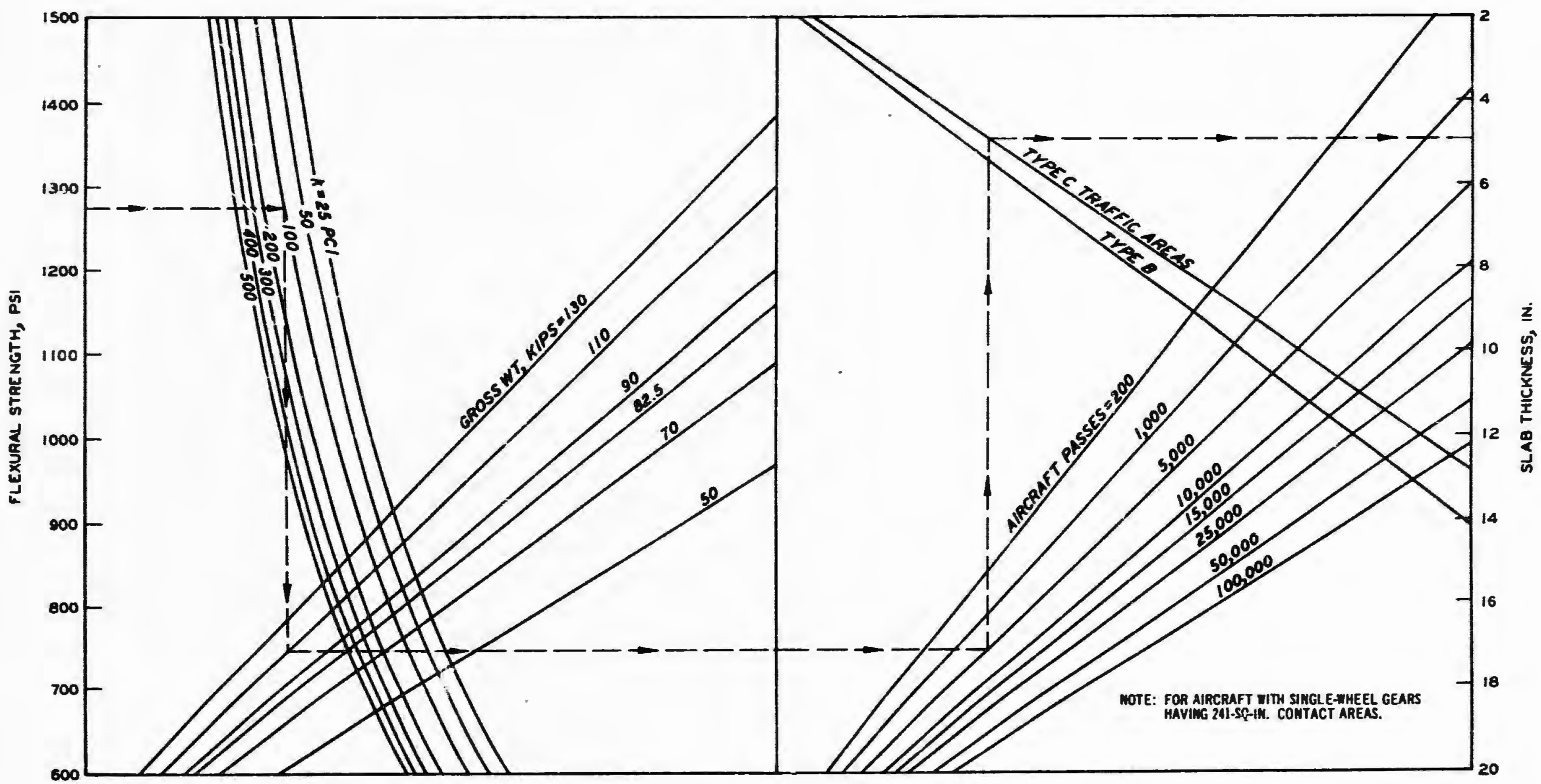

Figure B11. Fibrous concrete pavement design curves for special design pavements

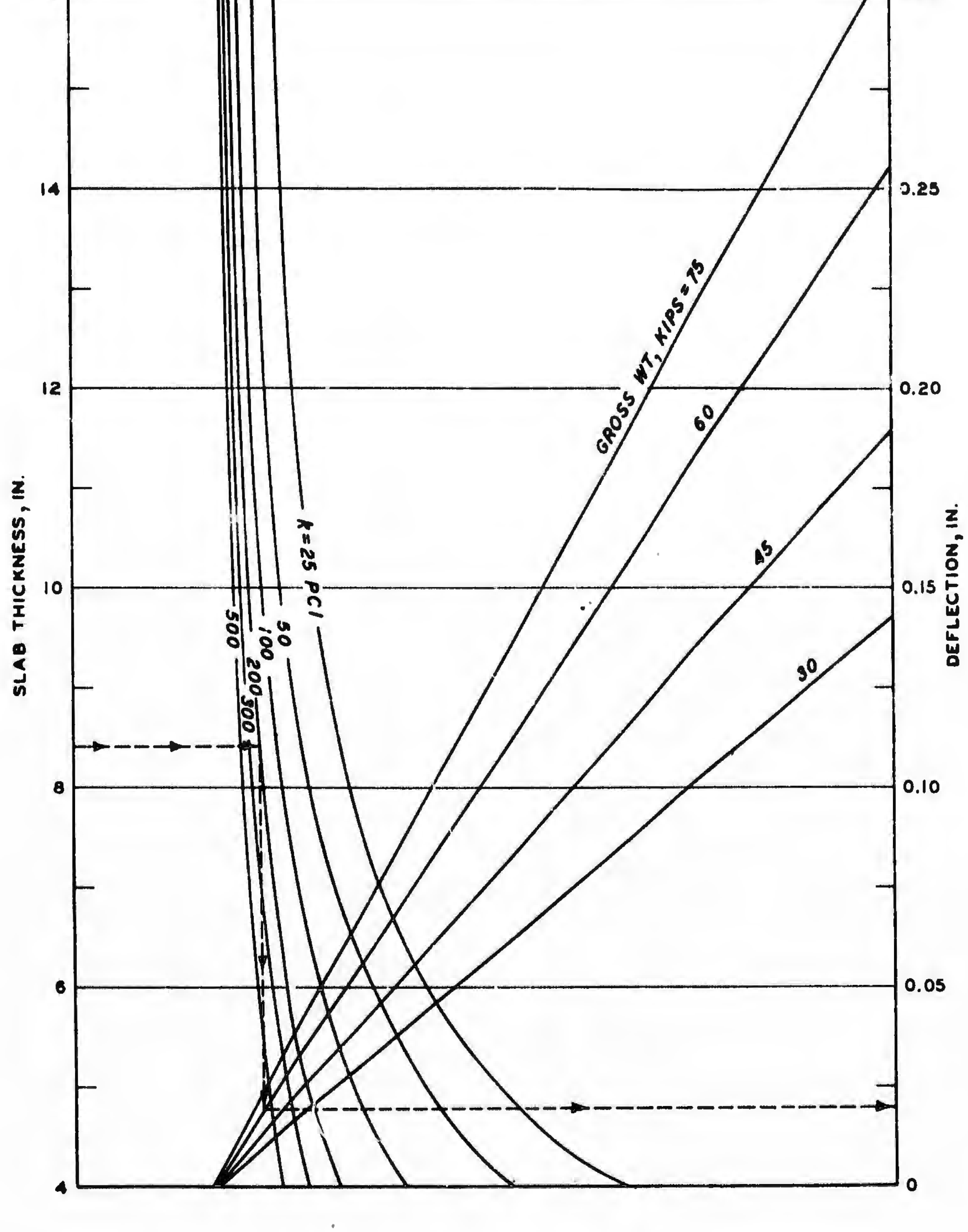

Figure B12. Curves for computation of elastic slab deflection for civil aircraft having single-wheel gears

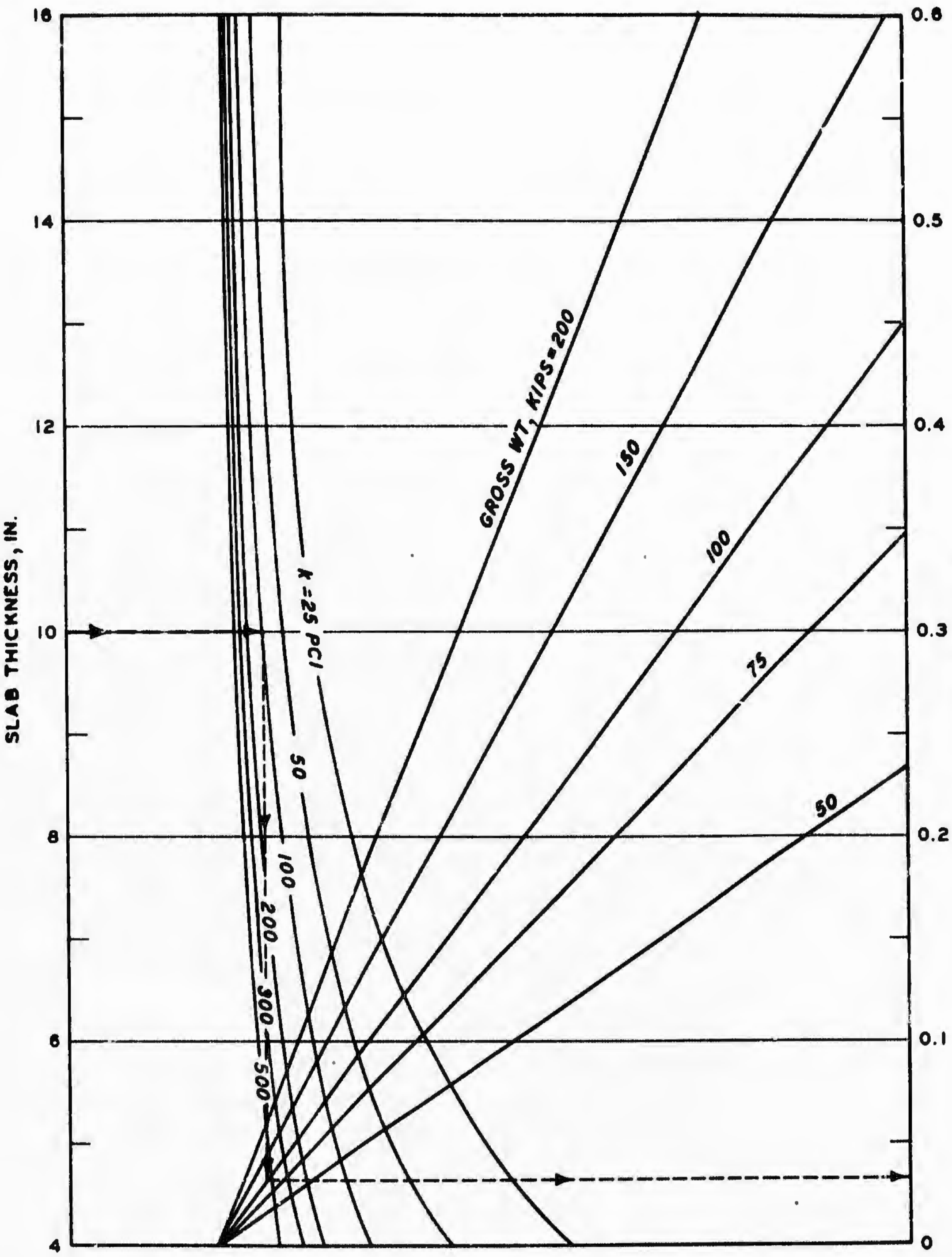

Figure B13. Curves for computation of elastic slab deflection for civil aircraft having dual-wheel gears

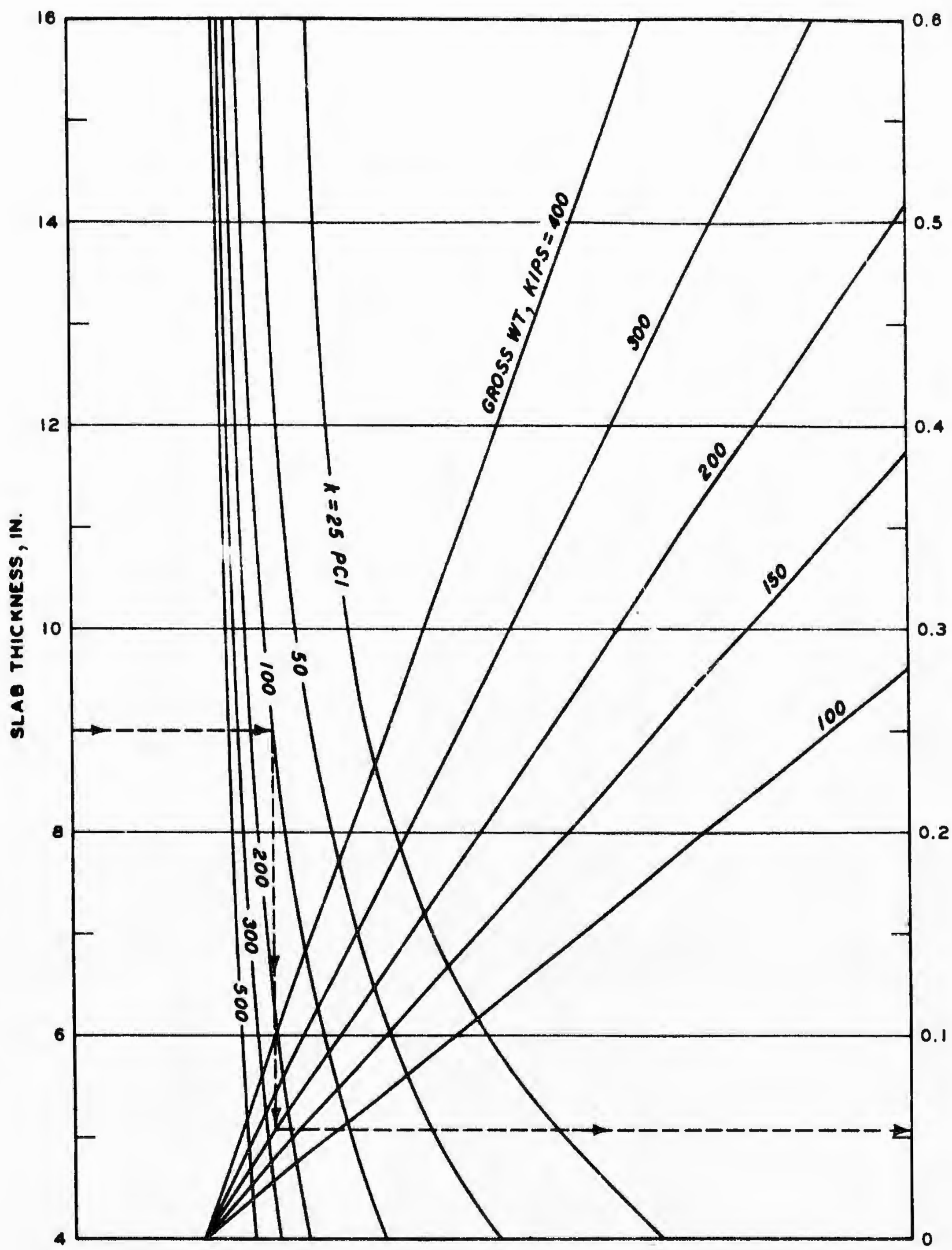

Figure B14. Curves for computation of elastic slab deflection for civil aircraft having dual-tandem gears

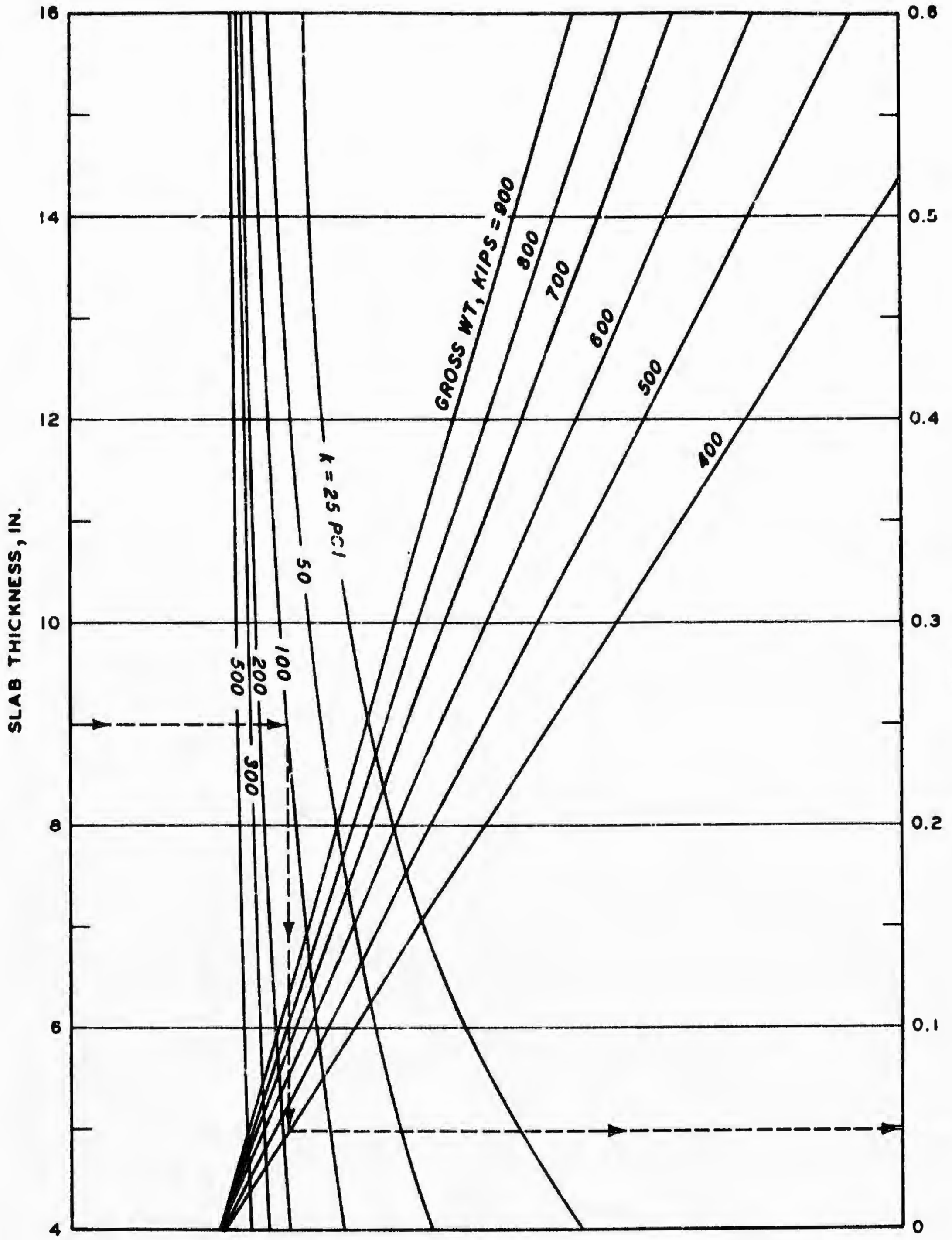

Figure B15. Curves for computation of elastic slab deflection for Boeing 747 aircraft

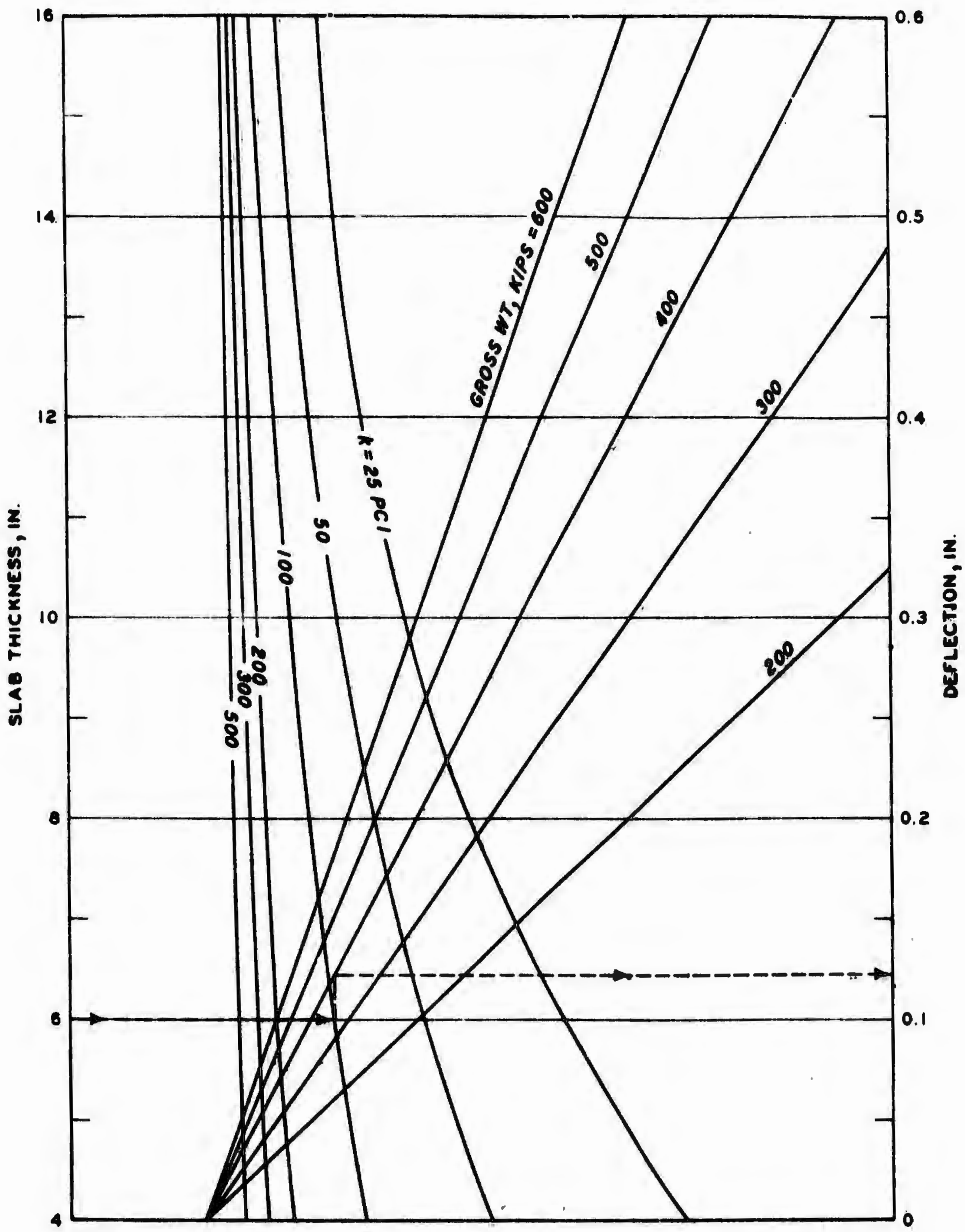

Figure B16. Curves for computation of elastic slab deflection for DC-10-10 aircraft

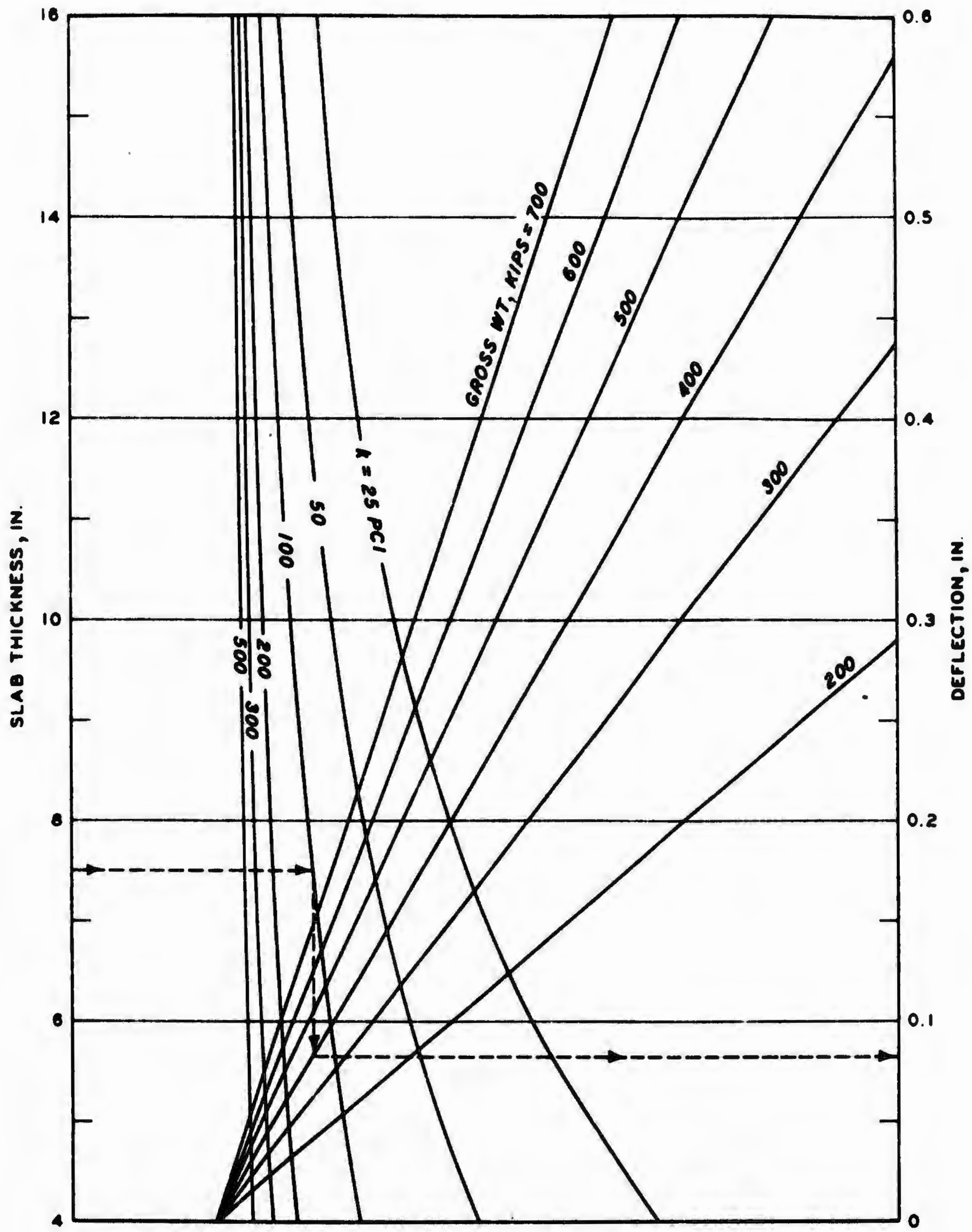

Figure B17. Curves for computation of elastic slab deflection for DC-10-30 aircraft

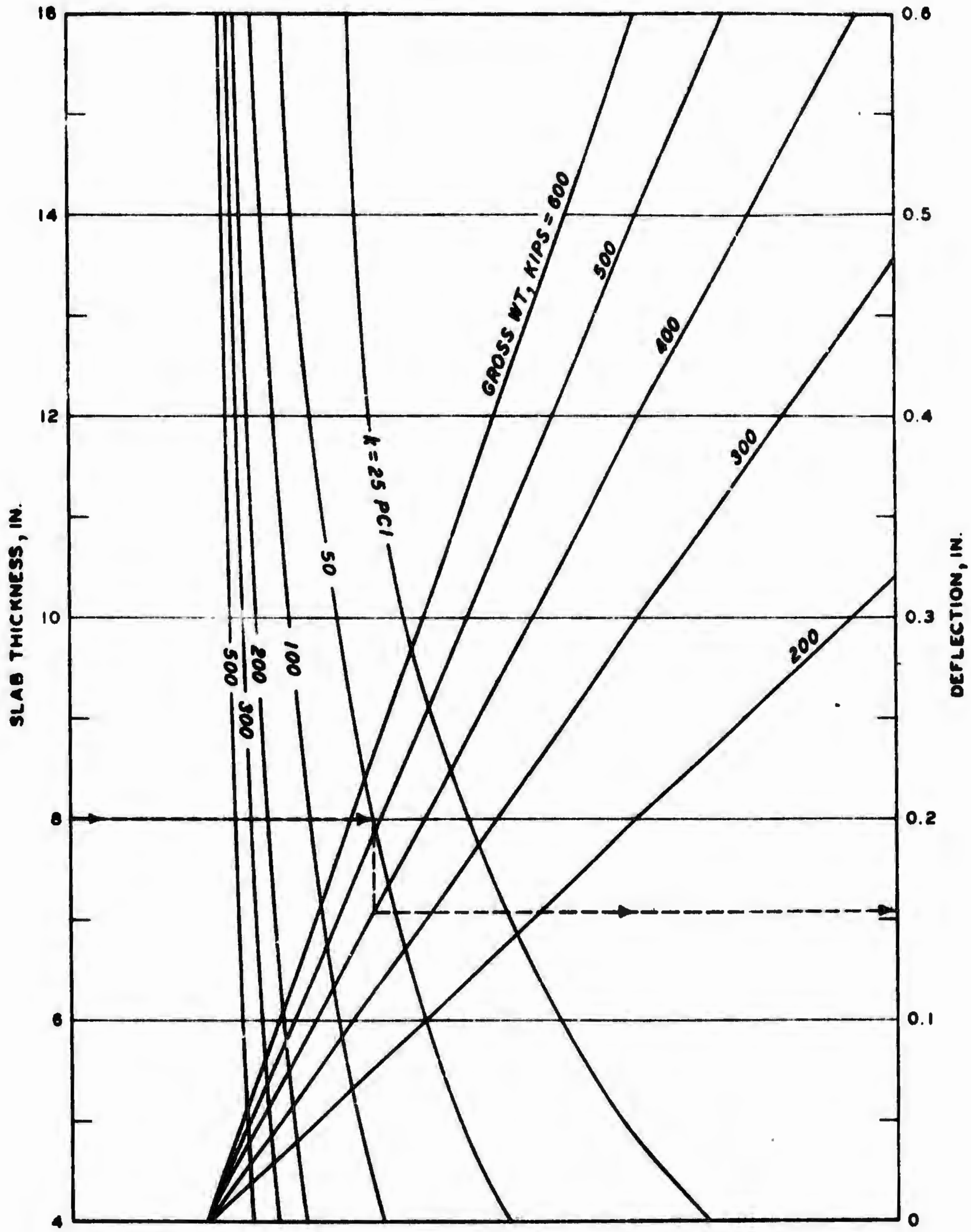

Figure B18. Curves for computation of elastic slab deflection for L-1011 aircraft

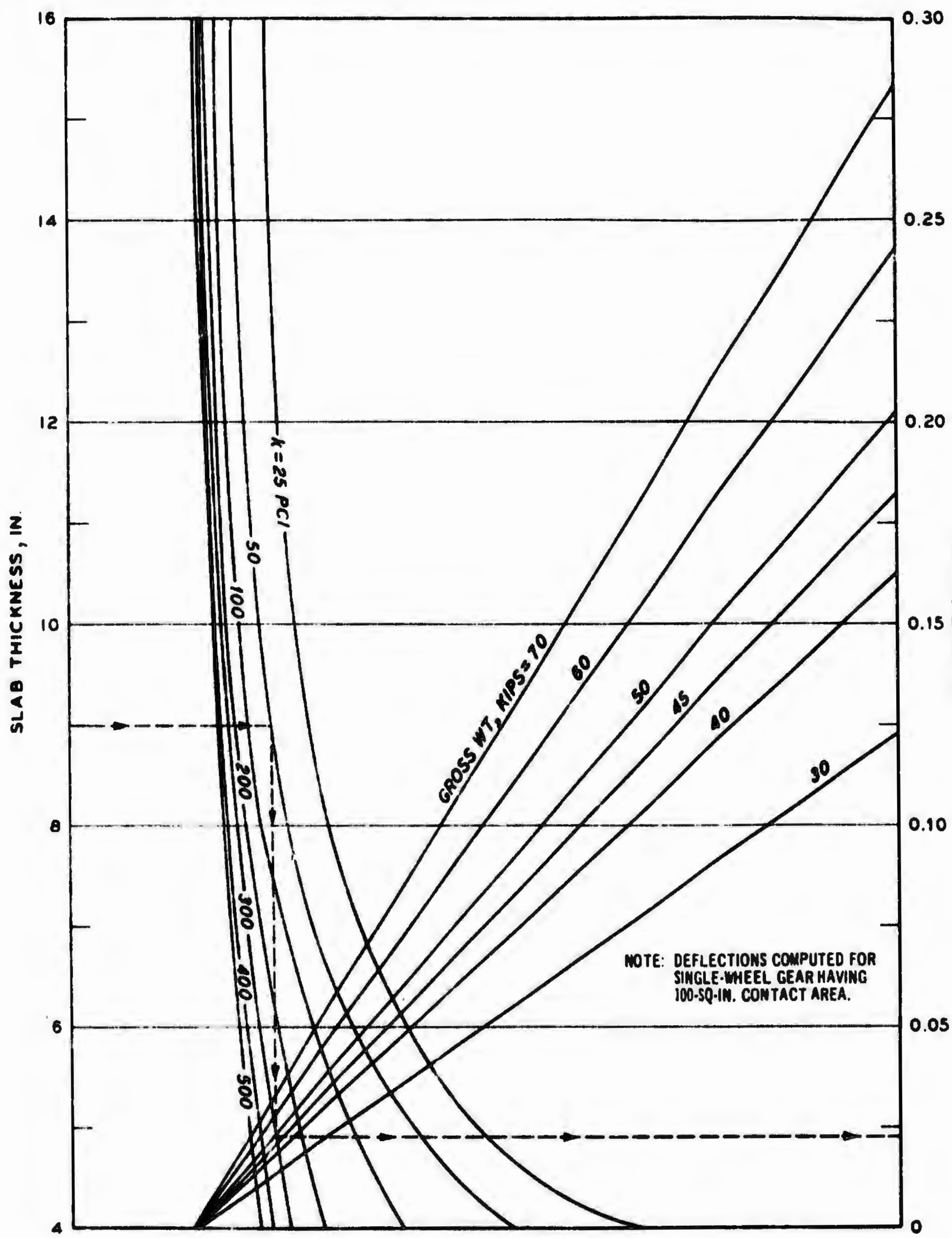

Figure B19. Curves for computation of elastic slab deflection for light-load pavements

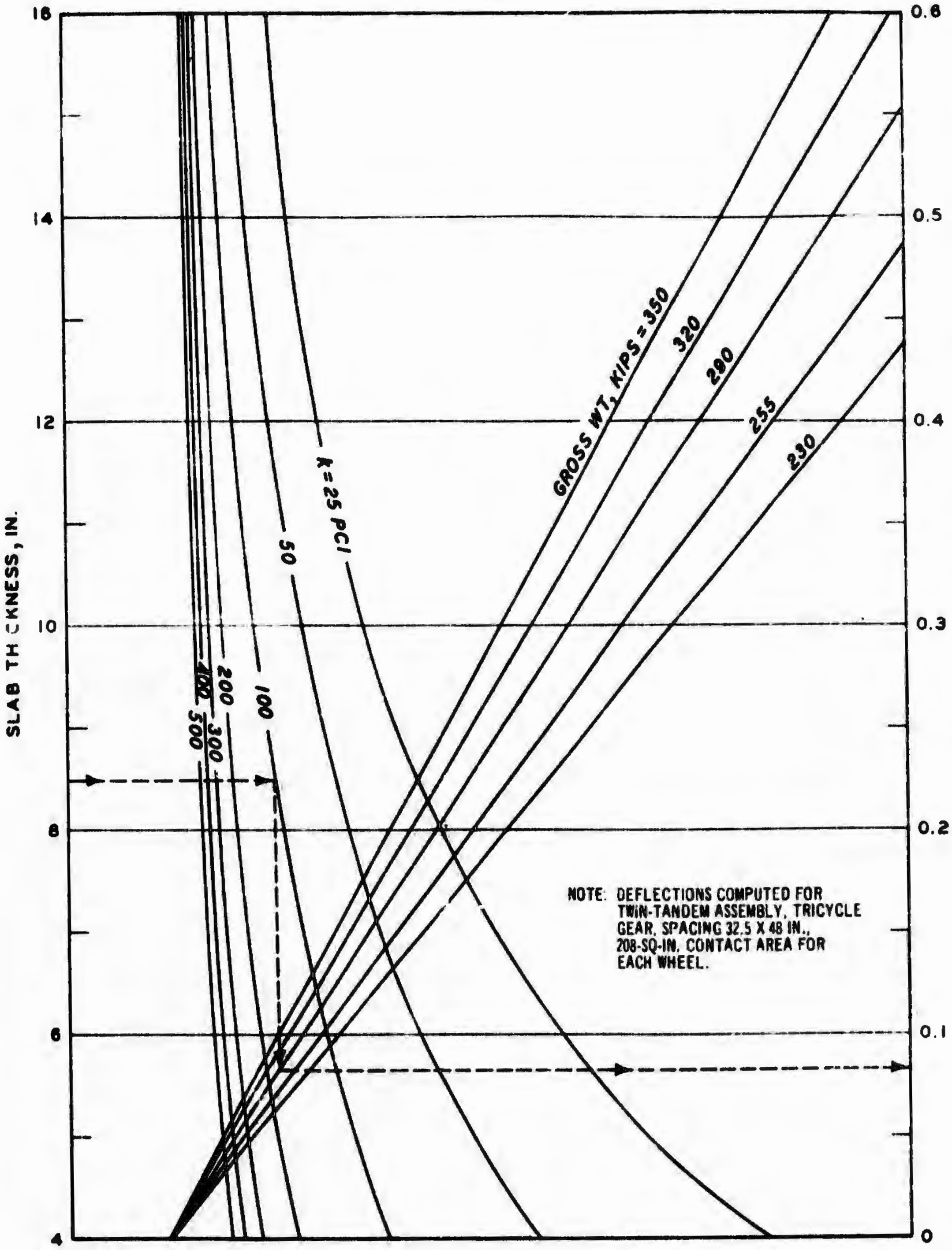

Figure B20. Curves for computation of elastic slab deflection for medium-load pavements

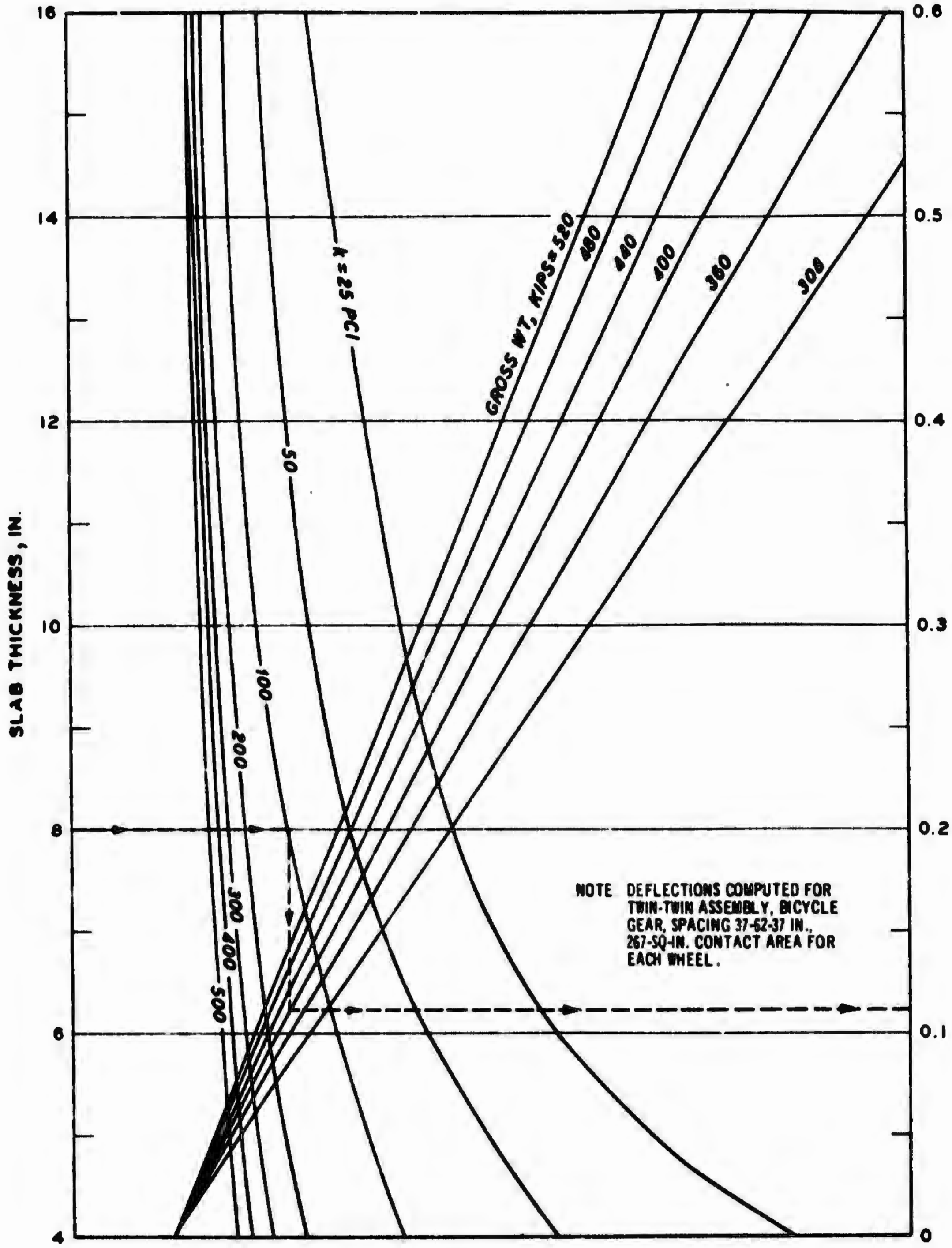

Figure B21. Curves for computation of elastic slab deflection for heavy-load pavements

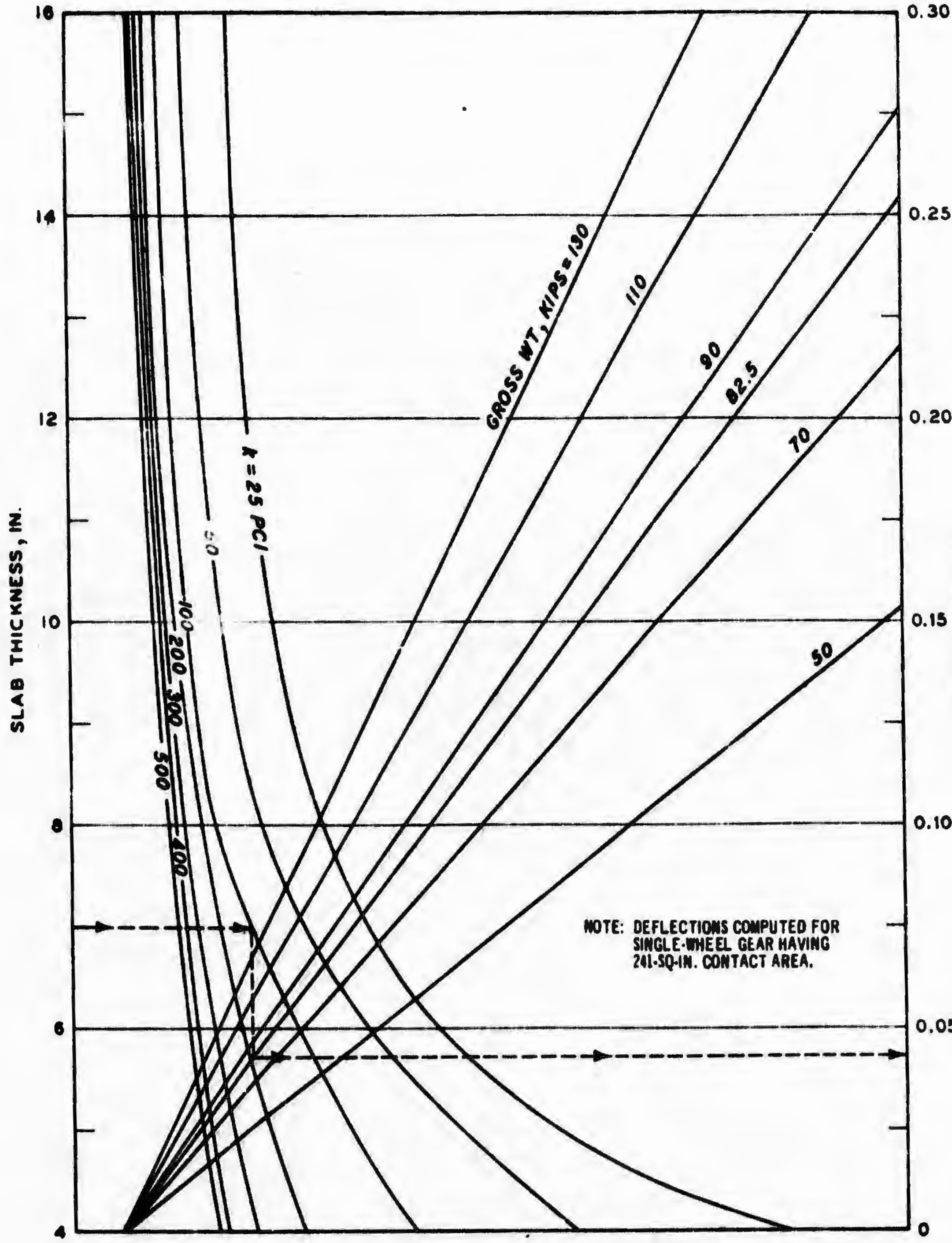

Figure B22. Curves for computation of elastic slab deflection for special design pavements

REFERENCES

1. Hsu, T. T. C. et al., "Microcracking of Plain Concrete and the Shape of the Stress-Strain Curve," Proceedings, American Concrete Institute, Vol 60, No. 2, Feb 1962, pp 209-224.

2. Romualdi, J. P. and Batson, G. B., "Behavior of Reinforced Concrete Beams with Closely Spaced Reinforcement," Proceedings, American Concrete Institute, Vol 60, No. 6, Jun 1963, pp 775-790.

3. __________, "Mechanics of Crack Arrest in Concrete," Journal of the Engineering Mechanics Division, American Society of Civil Engineers, Vol 89, EM3, Jun 1963, pp 147-168.

4. Romualdi, J. P. and Mandel, J. A., "Tensile Strength of Concrete Affected by Uniformly Distributed and Closely Spaced Short Lengths of Wire Reinforcement," Proceedings, American Concrete Institute, Vol 61, No. 6, Jun 1964, pp 657-671.

5. Snyder, M. J. and Lankard, D. R., "Factors Affecting the Flexural Strength of Steel Fibrous Concrete," Proceedings, American Concrete Institute, Vol 69, No. 2, Feb 1972, pp 96-100.

6. Waterhouse, B. L. and Luke, C. E., "Steel Fiber Optimization," Fibrous Concrete Construction Material for the Seventies, Conference Proceedings, May 1972, U. S. Army Construction Engineering Research Laboratory, CE, Champaign, Ill.

7. Batson, G. B., "Introduction to Fibrous Concrete," Fibrous Concrete Construction Material for the Seventies, Conference Proceedings, May 1972, U. S. Army Construction Engineering Research Laboratory, Champaign, Ill.

8. Gray, B. H. and Rice, J. L., "Fibrous Concrete for Pavement Applications," Preliminary Report M-13, Apr 1972, U. S. Army Construction Engineering Research Laboratory, Champaign, Ill.

9. Dixon, J. and Mayfield, B., "Concrete Reinforced with Fibrous Wire," Concrete, Vol 5, No. 3, Mar 1971, pp 73-76.

10. American Society for Testing and Materials, "Standard Method of Test for Flexural Strength of Concrete (Using Simple Beam with Third-Point Loading)," Designation: C 78-64, 1972 Annual Book of ASTM Standards, Part 10, 1972, Philadelphia, Pa.

11. Parker, F., Jr., "Construction of Fibrous Reinforced Concrete Overlay Test Slabs, Tampa International Airport, Florida," Report No. FAA-RD-72-119, Oct 1972, Department of Transportation, Federal Aviation Administration, Washington, D. C.

12. Grambling, W. L., "Steel Fiber Reinforced Concrete," Paper Presented at Highway Research Board Summer Meeting, Aug 1973, Olympia, Wash.

13. Arnold, C. U. and Brown, M. G., "Experimental Steel-Fiber Reinforced Concrete Overlay," Research Report No. R-852, Apr 1973, Michigan State Department of Highways, Lansing, Mich.

14. Williamson G. R., "Fibrous Reinforcements for Portland Cement Concrete," Technical Report No. 2-40, May 1965, U. S. Army Engineer Division Laboratories, Ohio River, CE, Cincinnati, Ohio.

15. __________, "Reponse of Fibrous-Reinforced Concrete to Explosive Loading," Technical Report No. 2-48, Jan 1966, U. S. Army Engineer Division Laboratories, Ohio River, CE, Cincinnati, Ohio.

16. Birkimer, D. L. and Hossley, J. R., "Comparison of Static and Dynamic Behavior of Plain and Fibrous-Reinforced Concrete Cylinders," Technical Report No. 4-69, Jan 1968, U. S. Army Engineer Division Laboratories, Ohio River, CE, Cincinnati, Ohio.

17. Forrest, J. B., Katona, M. G., and Griffin, D. F., "Layered Pavement Systems," Technical Report No. R-763, Apr 1972, Naval Civil Engineering Laboratory, Port Hueneme, Calif.

18. Batson, G. et al., "Flexural Fatigue Strength of Steel Fiber Reinforced Concrete Beams," Proceedings, American Concrete Institute, Vol 69, No. 11, Nov 1972, pp 673-678.

19. Ball, C. G., The Fatigue Behavior of Steel-Fiber-Reinforced Concrete, M.S. Thesis, Clarkson College of Technology, Potsdam, N. Y., Oct 1967.

20. Mikkelmeni, M. R., A Comparative Study of Fiber Reinforced Concrete and Plain Concrete Construction, M.S. Thesis, Mississippi State University, Mississippi State, Miss., 1970.

21. Shroff, J. K., The Effect of a Corrosive Environment on the Properties of Steel Fiber Reinforced Portland Cement Mortar, M.S. Thesis, Clarkson College of Technology, Potsdam, N. Y., Sep 1966.

22. Hutchinson, R. L., "Basis for Rigid Pavement Design for Military Airfields," Miscellaneous Paper No. 5-7, May 1966, U. S. Army Engineer Division Laboratories, Ohio River, CE, Cincinnati, Ohio.

23. __________, "A Method of Estimating the Life of Rigid Airfield Pavements," Technical Report No. 4-23, Mar 1962, U. S. Army Engineer Division Laboratories, Ohio River, CE, Cincinnati, Ohio.

24. Grau, R. W., "Strengthening of Keyed Longitudinal Construction Joints in Rigid Pavements," Report No. FAA-RD-72-106, Aug 1972, Department of Transportation, Federal Aviation Administration, Washington, D. C.

25. Department of Defense, "Unified Soil Classification System for Roads, Airfields, Embankments, and Foundations," Military Standard No. MIL-STD-619B, Jun 1968, Washington, D. C.

26. Department of Transportation, Federal Aviation Administration, "Airport Pavement Design and Evaluation," Advisory Circular AC 150/5320-6B, May 1974, Washington, D. C.

27. American Society for Testing and Materials, "Standard Method of Making and Curing Concrete Test Specimens in the Laboratory," Designation: C 192-69, 1972 Annual Book of ASTM Standards, Part 10, 1972, Philadelphia, Pa.

28. U. S. Army Engineer Waterways Experiment Station, CE, Handbook of Concrete and Cement, Aug 1949 (with quarterly supplements), Vicksburg, Miss.

29. American Society for Testing and Materials, "Standard Method of Test for Compressive Strength of Cylindrical Concrete Specimens," Designation: C 39-71, 1972 Annual Book of ASTM Standards, Part 10, 1972, Philadelphia, Pa.

30. __________, "Standard Method of Test for Splitting Tensile Strength of Cylindrical Concrete Specimens," Designation: C 496-71, 1972 Annual Book of ASTM Standards, Part 10, 1972, Philadelphia, Pa.

31. __________, "Standard Method of Test for Fundamental Transverse, Longitudinal, and Torsional Frequencies of Concrete Specimens," Designation: C 215-60, 1972 Annual Book of ASTM Standards, Part 10, 1972, Philadelphia, Pa.

32. __________, "Standard Method of Test for Slump of Portland Cement Concrete," Designation: C 143-71, 1972 Annual Book of ASTM Standards, Part 10, 1972, Philadelphia, Pa.

33. __________, "Tentative Method of Test for Air Content of Freshly Mixed Concrete by the Pressure Method," Designation: C 231-72T, 1972 Annual Book of ASTM Standards, Part 10, 1972, Philadelphia, Pa.

34. __________, "Standard Method of Obtaining and Testing Drilled Cores and Sawed Beams of Concrete," Designation: C 42-68, 1972 Annual Book of ASTM Standards, Part 10, 1972, Philadelphia, Pa.

35. Burns, C. D. et al., "Comparative Performance of Structural Layers in Pavement Systems; Design, Construction, and Behavior Under Traffic of Pavement Test Sections," Report No. FAA-RD-73-198, Vol I, Jun 1974, Department of Transportation, Federal Aviation Administration, Washington, D. C.

36. American Society for Testing and Materials, "Standard Method of Test for Static Modulus of Elasticity and Poisson's Ratio of Concrete in Compression," Designation: C 469-65, 1972 Annual Book of ASTM Standards, Part 10, 1972, Philadelphia, Pa.

37. __________, "Standard Method of Making and Curing Concrete Compressive and Flexural Strength Test Specimens in the Field," Designation: C 31-69, 1972 Annual Book of ASTM Standards, Part 10, 1972, Philadelphia, Pa.

38. Westergaard, H. M., "Stresses in Concrete Pavements Computed by Theoretical Analyses," Public Roads, Vol 7, No. 2, Apr 1926, pp 25-35.

39. Westergaard, H. M., "Analytical Tools for Judging Results of Structural Tests of Concrete Pavements," Public Roads, Vol 14, No. 10, Dec 1933, pp 185-138.

40. _________, "Stresses in Concrete Runways of Airports," Proceedings, 19th Annual Meeting of the Highway Research Board, Dec 1939, pp 197-202.

41. _________, "Stress Concentrations in Plates Loaded over Small Areas," Transactions, American Society of Civil Engineers, Vol 108, Paper No. 2197, 1943, pp 831-886.

42. _________, "New Formulas for Stresses in Concrete Pavements of Airfields," Transactions, American Society of Civil Engineers, Vol 113, Paper No. 2340, 1948, pp 425-444.

43. Pickett, G. et al., "Deflections, Moments and Reactive Pressures for Concrete Pavements," Bulletin No. 65, Oct 1951, Kansas State College, Manhatten, Kans.

44. Pickett, G. and Ray, G. K., "Influence Charts for Concrete Pavements," Transactions, American Society of Civil Engineers, Vol 116, Paper No. 2425, 1951, pp 49-73.

45. Arnold, C. J., "Steel-Fiber Reinforced Concrete Overlay-Progress Report," Research Report No. R-878, Aug 1973, Michigan State Department of Highways, Lansing, Mich.

46. U. S. Army Engineer Division Laboratories, Ohio River, CE, "Report of Construction; Lockbourne No. 2 - Modification, Multiple Wheel Study," May 1949, Cincinnati, Ohio.

47. Mellinger, F. M., Sale, J. P., and Wathen, T. R., "Heavy Wheel Load Traffic on Concrete Airfield Pavements," Proceedings, Highway Research Board, National Academy of Sciences - National Research Council, Vol 36, 1957, pp 175-189.

48. Ahlvin, R. G. et al., "Multiple-Wheel Heavy Gear Load Pavement Tests; Basic Report," Technical Report S-71-17, Vol 1, Nov 1971, U. S. Army Engineer Waterways Experiment Station, CE, Vicksburg, Miss.

49. Headquarters, Department of the Army, "Army Airfield and Heliport Rigid and Overlay Pavement Design," Technical Manual TM 5-823-3, Oct 1968, Washington, D. C.

50. _________, "Rigid Pavements for Airfields Other Than Army," Technical Manual TM 5-824-3 or Air Force Manual 88-6, Chapter 4, Nov 1970, Washington, D. C.

51. ACI Committee 544, "State-of-the-Art Report on Fiber Reinforced Concrete," Proceedings, American Concrete Institute, Vol 70, No. 11, Nov 1973, pp 729-744.

52. Luke, C. E., "Driveway, Road, and Airport Slabs," Fibrous Concrete Construction Material for the Seventies, Conference Proceedings, May 1972, U. S. Army Construction Engineering Research Laboratory, Champaign, Ill.

53. American Concrete Paving Association, Newsletter, Vol 8, No. 10, Oct 1972.

54. __________, Newsletter, Vol 9, No. 10, Oct 1973.

55. Headquarters, Department of the Army, "General Provisions for Airfield Design, Airfields Other Than the Army," Technical Manual TM 5-824-1, Dec 1965, Washington, D. C.

GPO 884-603